POLYMAT

eman ta zabal zazu

Universidad del País Vasco

Euskal Herriko Unibertsitatea

STUDY OF THE INTERACTIONS BETWEEN DNA AND IONIC LIQUIDS

Isabel Machado

Doctoral Thesis

Supervised by Prof. Dr.-Ing. Thomas Schäfer

Donostia – San Sebastián

2016

Acknowledgements

First of all I would like to thank to my supervisor, Prof. Dr.-Ing. Thomas Schäfer for trusting me when I joined the NanoBioSeparations (NBS) group and for his scientific guidance and all the support during my PhD studies. I would also thank Prof. Günter Mayer for giving me the opportunity to work and learn from his laboratory during my stage at LIMES - University of Bonn, Germany. I also would like to thank all the people at Mayer's lab for their help and support.

I would like to specially thank to all my colleagues who, over all these years, were part of the NBS group for their scientific and personal help and with whom I shared very good moments: Ana, Eli, Gabby, Alessandro, Cengiz, Frank, Ali and Iliane.

Also I would like to thank to all my Spanish and Portuguese friends, especially to Magui, that even being far, always showed to be there for what I needed.

I cannot finish without giving big thanks to my family, but specially to my parents, my brothers and my little niece Francisca for their love and support shown over all these years and during my life, being undoubtedly a great source of inspiration, strength and encouragement to move forward. Special mention goes to my mom for her pure and unconditional love and all the hours spent on Skype to be as close as possible. Love you mommy!

Finally, but not least important, I want to thank Jokin for being with me during all these years, for his wise advises, for the unconditional support and for all the love.

Thank you all!

Table of Contents

NOTATION/ABBREVIATIONS

A	Adenine
AA	Acrylamide
AF	Alexa fluor
ADP	Adenosine diphosphate
AMP	Adenosine monophosphate
APS	Ammonium persulfate
AFM	Atomic force microscopy
ATP	Adenosine triphosphate
BHQ	Black hole quencher
Bis	Bisacrylamide
BMIM-Br	1-Butyl-3-methylimidazolium bromide
BMIM-Cl	1-Butyl-3-methylimidazolium chloride
bp	Base pair(s)
C	Cytosine
CDHP	Choline di-hydrogen phosphate
CL	Choline lactate
CN	Choline nitrate
ct-DNA	Calf-thymus DNA
DAPI	4',6-diamidino-2-phenylindole
DES	Deep eutectic solvents
DNA	Deoxyribonucleic acid
dsDNA	double-strand DNA
EAN	Ethylammonium nitrate
EtBr	Ethydium bromide
FNA	Functional nucleic acid
G	Guanine
GMP	Guanosine monophosphate
IL(s)	Ionic liquid(s)
IR	Infra-red

Ka	Association constant
kb	Kilo-bases (1 kb = 1000 bp)
Kd	Dissociation constant
kh	Hybridization rate
MB	Molecular beacon
$MgCl_2$	Magnesium chloride
NaCl	Sodium chloride
NaDHP	Sodium di-Hydrogenphosphate
NaLac	Sodium Lactate
$NaNO_3$	Sodium Nitrate
Na_2HPO4	Sodium phosphate di-salt
NMR	Nuclear Magnetic Resonance
NTC	Negative control
NTP	Nucleoside triphosphate
PBS	Phosphate buffered solution
PCR	Polymerase chain reaction
QCM-D	Quantum crystal microbalance with dissipation
RNA	Ribonucleic acid
RT	Room temperature
SELEX	Systematic Evolution of Ligand by EXponential enrichment
sp-DNA	Salmon sperm DNA
SPR	Surface plasmon resonance
ssDNA	Single-strand DNA
T	Thymine
TAE	Tris base/acetic acid/EDTA buffer
Taq	*Thermus aquaticus polymerase*
TBE	Tris/Borate/EDTA buffer
TBS	Tris-buffered saline
TEMED	Tetramethylethylenediamine
Tm	Melting temperature
TMGL	Tetramethylguanidinium lacate
Tris	2-Amino-2-hydroxymethyl-propane-1,3-diol

UV	Ultra-violet
XNA	Xeno-nucleic acid (synthetic nucleic acids)

List of Figures, Schemes and Tables

Chapter one: General Introduction

Chapter two: Materials and Methods

Chapter three: DNA Aptamers as Functional Molecular Recognition Sensors in a Protic Ionic Liquid

Chapter four: Influence of the Ionic Liquids on Fluorescence Emission

concentrations at which F_0/F=2 occurs were also determined for each type of quenching probably occurring.

Table 4.3. Lifetime values obtained for the AF 488 in solution with different concentrations of the ILs. The standard error is ±0,2 ns.

Figure 4.4. Fluorescence lifetime of 0,8 μM of the fluorophore AF488 in pure buffer (blue line) and in buffer solution with 3M of A) EAN, B) CN, C) CDHP, D) CL, E) TMGL and F) BMIM-Cl (red lines).

Table 4.4. Dynamic quenching constants occurring to the fluorophore AF 488 during the addition of the different ILs to the solution. The respective IL (quencher) concentrations at which τ_0/τ=2 occurs were also determined.

Figure 4.5. Emission spectra of AF488 in solution with increasing concentrations of BMIM-Cl. Following the arrow the concentrations of BMIM-Cl ranged from 0% v/v (full purple line), 1% v/v, 3% v/v, 5% v/v, 10% v/v, 25% v/v and 40% v/v (medium dash red line).

Figure 4.6. FL lifetime images of AF488 in solution with 3M of A) BMIM-Cl and B) CL. Excitation wavelength was 485 nm.

Figure 4.7. Absorbance spectra of the used ILs and emission spectrum of AF 488.

Figure 4.8. Absorbance spectra of the AF 488 in solution with TBS and with the addition of 0.05 (purple line), 0.3 (blue line), 0.6 (green line), 1.5 (yellow line) and 2M (orange line) of A) CN, B) CDHP, C) CL, D) TMGL and E) BMIM-Cl.

Figure 4.9. Normalized fluorescence of AF 488 attached to the DNA oligomer 1 as function of the concentration of EAN (circles), CN (triangles), CDHP (inverted triangles), CL (diamonds), TMGL (squares) and BMIM-Cl (hexagons) in solution with TBS. Data were normalized with respect to the initial intensity (F_0) of the oligomer 1-AF in TBS. The initial concentration of the oligomer 1-AF was 17 nM. Raw data were corrected for background signal and taking into consideration the volume changes upon successive addition of IL.

Chapter five: Functional DNA in Ionic Liquids

Figure 5.6. Amount of DNA that remained hybridized with the addition of increasing concentrations of EAN (circles), CN (triangles), CDHP (inverted triangles), CL (diamonds), TMGL (squares) and BMIM-Cl (hexagons), with the zoom until 10% v/v (bottom), to the TBS solution containing the previous formed dsDNA. The concentration of the oligomers was 17 nM.

Figure 5.7. Correlation between the amount of DNA hybridized in presence of ILs and the DNA that remained hybridized after the addition of increasing concentrations of EAN (circles), TMGL (squares) and BMIM-Cl (hexagons). For illustration purposes the data of choline ILs were not included since they practically do not alter the duplex formation in IL presence neither the duplex formed before IL addition.

Figure 5.8. Circular dichroism spectrum of the dsDNA formed by oligomer 1 and oligomer 2 in TBS, with no dyes attached. The concentration of the oligos here was 5 μM.

Figure 5.9. A) Circular dichroism spectra of the dsDNA formed by oligomer 1 and oligomer 2, with no dyes attached, with the addition of 0% (solid line – purple), 1% (dotted line – dark blue), 5% (short dash line – blue), 10% (dash-dot-dot line – green), 18% (long dash line – yellow), 25% (dash-dot line – orange) and 40% v/v (medium dash line – red) of the different ILs into the TBS solution. **B)** Circular dichroism spectra of the ssDNA oligomer 1, with no dyes attached, with the addition of 0% (solid line – purple), 25% (dotted line – dark blue) and 40% (short dash line - blue) v/v of BMIMCl comparing with the dsDNA with the addition of 25% (dash-dot-dot line – green) and 40% (long dash line – yellow) v/v of BMIMCl. The concentration of the oligos here was 5 mM.

Figure 5.10. Graphic representation of the rate of DNA hybridization, k_h, as function of the increase concentration of EAN (circles), CN (triangles), CDHP (inverted triangles), CL (diamonds), TMGL (squares) and BMIM-Cl (hexagons), with the zoom until 10% v/v (bottom). The standard deviations here range from 0.012 to 1.8 (x 10^5), being the error bar smaller than the symbols.

Figure 5.11. Correlation between the hybridization rate and the melting temperature (k_h/T_m) of the ILs used respect to the same correlation specific for EAN, as an arbitrary reference. The symbols correspond to CN (triangles), CL (diamonds), TMGL (squares) and BMIMCl (hexagons). The long-dashed lines correspond to the fitting of the data.

Figure 6.6. Percentages of γ-^{32}P-DNA present in the different solutions collected in each step of the binding assay of round 1 and round 8 for **A)** buffer and **B)** CL as solvents. The bars on top of the columns represent the error bar. Every sample was measured in duplicate.

Figure 6.7. Percentages of γ-^{32}P-DNA present in the different solutions collected in each step of the binding assay of round 1 and round 8 for **A)** buffer and **B)** buffer with 2M CL as solvents, each with the addition of 1 mg/ml of salmon sperm DNA. The bars on top of the columns represent the error bar. Every sample was measured in duplicate.

Figure 6.8. Percentages of γ-^{32}P-DNA present in the different solutions collected in each step of the binding assay only with the round 1 and round 8 of buffer solution with the addition of **A)** 0,1 mg/ml and **B)** 1 mg/ml of salmon sperm DNA.

Table 6.1. Overview of experiments carried out and sample assignation in SELEX I and SELEX II with the presence of salmon sperm in the SELEX rounds.

Figure 6.9. Percentages of γ-^{32}P-DNA present in the different solutions collected in each step of the binding assay of round 1 of SELEX I and round 8' of SELEX II for **A)** buffer and **B)** buffer with 2M CL as solvents, each with the addition of 1 mg/ml of salmon sperm DNA. The bars on top of the columns represent the error bar of the measurements. Each sample was analyzed in duplicate.

Figure 6.10. Percentages of γ-^{32}P-DNA present in the different solutions collected in each step of the binding assay of **A)** R1, R4' and R8' for buffer, of **B)** R1, R4', R8' and R10' and **C)** R1, R10' and R12' for buffer with 2M CL as solvents, each with the addition of 1 mg/ml of salmon sperm DNA. The bars on top of the columns represent the error bar of the measurements. Each sample was analyzed in duplicate.

Figure 6.11. Alignments made by the bioinformatic software MUSCLE of the sequences obtained when using **A)** Tris-HCl buffer and **B)** - **C)** Tris-HCl buffer with 2M of choline lactate as solvents. The asterisk below the sequences represent the only nucleotides which are common for all the sequences in the groups.

Estudio de las interacciones entre ADN y líquidos iónicos

Resumen

Los aptameros son ácidos nucleicos de ADN o ARN de hebra simple diseñados para reconocer específicamente una diana que puede ser, como ejemplo, células, proteínas, amino ácidos, drogas o incluso pequeñas moléculas. Estos exhiben propiedades similares a los anticuerpos, pero presentan una estabilidad significativamente más elevada que estos últimos. Los aptameros son seleccionados para la diana de interés a través del procedimiento automatizado *in vitro* llamado Evolución Sistemática de un Ligando por Enriquecimiento Exponencial - "SELEX". Estos pueden ser usados en biosensores o como elementos compuerta en nanoporos para aplicaciones de liberación controlada de drogas. Los aptameros pueden ser químicamente modificados con la introducción de un ligando y un par de fluoroforo y extintor de fluorescencia dando origen a una estructura tipo horquilla comúnmente llamado de farol molecular (molecular beacon - MB). Desde que fueron desarrolladas, las sondas de MB han sido ampliamente empleadas en biosensores debido a la facilidad de la detección de la señal de fluorescencia tras la interacción con la diana. Hasta ahora, estas sondas y el SELEX se han investigado y

empleado principalmente en soluciones tampón acuosas. Sin embargo, debido a sus particulares propiedades físico-químicas, los líquidos iónicos (ILs) surgen como medio alternativo altamente interesante. Debido a que su presión de vapor es casi inexistente, esto es que prácticamente no se evaporan, los ILs tienen una gran ventaja respecto a los disolventes acuosos. La capacidad para disolver moléculas tales como los oligonucleótidos y al mismo tiempo ser capaces de experimentar interacciones electrostáticas, son también atractivas propiedades de los líquidos iónicos. Sin embargo, la información sobre las interacciones entre ADN o aptameros de ADN y líquidos iónicos es todavía limitada.

Así, el principal objetivo de esta tesis fue el estudio de las interacciones de ADN con los líquidos iónicos y de la función de un aptamero de ADN en presencia de líquidos iónicos con propiedades físico-químicas distintas. En primer lugar se estudió la capacidad de reconocimiento y la selectividad del aptamero de ATP hacía la molécula de AMP en una solución acuosa con la presencia del liquido iónico prótico nitrato de etilamonio (EAN). Demostrándose que el aptamero de ATP permanece funcional con la presencia de EAN en la solución, otros líquidos iónicos fueron utilizados para entender la influencia de líquidos ionicos con diferentes propiedades físico-químicas en la estructura y función del ADN (lactato de colina (CL), nitrato de

colina (CN), di-hidrogenofosfato de colina (CDHP), cloruro de 1-butil-3-metilimidazolio (BMIM-Cl) y lactato de 1,1,3,3-tetrametilguanidinio (TMGL)). Para eso, la hibridación y la estabilidad de una doble hebra de ADN constituida por 12 nucleótidos fueron estudiadas en solución con estos ILs. Diferentes tecnologías espectroscópicas, envolviendo la medición de la fluorescencia o el dicroísmo circular, complementadas por cálculos computacionales fueron usadas a lo largo de este trabajo. La posible influencia de estos líquidos iónicos en la emisión de la fluorescencia del fluoroforo usado, el Alexa Fluor 488, fue también investigada determinándose que cuando el AF 488 estaba libre en la solución, casi todos los líquidos iónicos disminuyeron la emisión de la fluorescencia. Por otro lado, cuando el AF 488 estaba ligado a una hebra simple de ADN, la fluorescencia se mantuvo prácticamente constante mismo con la presencia de estos ILs en solución. Estos resultados fueron entonces favorables para el uso de este sistema con AF 488 ligado al ADN en los estudios subsecuentes envolviendo líquidos iónicos en la solución. De esos estudios, se determinó que dependiendo del líquido iónico y de su concentración en solución, la función y estabilidad del ADN se mantuvieron.

La segunda parte de este trabajo envolvió el proceso de SELEX, realizado por primera vez en presencia de un liquido iónico, el lactato de colina. El objetivo aquí

era determinar hasta qué punto la introducción de un líquido iónico directamente durante el proceso de SELEX iría permitir que las secuencias de aptamero de ADN reconocieran la diana ATP y comparar la constante de reconocimiento molecular (K_d) con la obtenida usando apenas la solución tampón pura. A partir del SELEX en presencia de este líquido iónico se determinaron algunas nuevas secuencias de ADN potencialmente selectivos para el ATP, sin embargo, la medición final del K_d no pudo llevarse a cabo dentro del plazo de esta tesis.

Como conclusiones generales, esta investigación permitió determinar que el ADN permaneció funcional en presencia de un entorno no fisiológico conteniendo liquido iónico. Considerando sus propiedades físico-químicas, no se determinó ningún patrón de interacción entre los líquidos iónicos. Por lo tanto, se concluyó que cada sistema debe ser caracterizado de manera independiente, incluso si los líquidos iónicos presentan cationes o aniones comunes. Nuevas secuencias de aptamero de ADN para el ATP fueron obtenidas a través del SELEX con la presencia de CL en solución lo que demuestra que, en un principio, este procedimiento de selección puede emplearse también con una solución no convencional.

Study of the Interactions between DNA and Ionic Liquids

Abstract

Aptamers are single stranded nucleic acids of DNA and RNA, which are designed to specifically recognize desired target ligands such as whole cells, proteins, amino acids, drugs or small molecules, exhibiting properties similar to antibodies but significantly more stable. They can be select to interact with the target of interest through the *in vitro* automated selection procedure called *S*ystematic *E*volution by *L*igand *Ex*ponential Enrichment - "SELEX". Aptamers can be used in biosensors or as gating elements in nanopores, such as in controlled delivery applications. Aptamers can be chemically modified with a linker and a fluorophore/quencher pair such as to obtain a hairpin structure, the so-called “molecular beacon” (MB). Since MB probes were developed, they have been widely employed in biosensing owing to the ease of detecting the fluorescence signal upon interaction with the target.

Until now, these probes and SELEX have been mainly investigated and employed in aqueous buffer solutions. However, because of their particular physico-chemical properties, ionic liquids (ILs) arise as a highly interesting alternative medium. Because of their almost negligible vapor pressure, they practically do not

evaporate which is a great benefit over aqueous solvents. The capacity to dissolve molecules such as oligonucleotides while at the same time being capable of undergoing electrostatic interactions are also attractive properties of ILs. However information about the interactions between DNA or DNA aptamers and ionic liquids is still limited.

Thus the main propose of this thesis was the study of the interactions of DNA with ionic liquids and the function of a DNA-aptamer in presence of ILs with different physico-chemical properties. First, the ATP-molecular aptamer beacon recognition capacity and selectivity to AMP in aqueous solution in presence of the protic ionic liquid ethylammonium nitrate (EAN). After showing in how far the ATP-aptamer remains functional in presence of EAN in solution, other ILs (choline lactate (CL), choline nitrate (CN), choline dihydrogen phosphate (CDHP), 1-butyl-3-methylimidazolium chloride (BMIM-Cl) and 1,1,3,3-tetramethylguanidinium lactate (TMGL)) were investigated in order to understand how ILs of different physico-chemical properties influence the DNA structure and function. For that purpose, the hybridization and stability of a 12-mer dsDNA in solution with these ILs was studied. Different techniques, involving the fluorescence measurement and CD, complemented by computational calculations were used along this work. The

possible influence of these ILs on fluorescence emission of the fluorophore Alexa Fluor 488 was investigated and it was determined that when AF488 was free in solution nearly all ILs decreased its fluorescence emission. On the other hand, when AF488 was attached to a 12-mer ssDNA, the fluorescence remained practically constant. These results were favorable for using AF 488 attached to DNA in the subsequent studies involving ILs and it was found that depending on the IL and on the IL concentration, the DNA function and stability was maintained.

The second part of this work involved the SELEX procedure which was performed for the first time in presence of CL. The objective was to see in how far the introduction of an IL already during SELEX would yield DNA-aptamer sequences capable to recognize ATP in presence of ILs and compare the binding constant (K_d) with the one obtained in pure buffer solution. The SELEX in presence of ILs yielded some new DNA sequences potentially selective to ATP, however, the final measurement of K_d could not be conducted within the timeframe of this thesis.

As general conclusions, this research enabled to determine that DNA remained functional in the presence of a non-physiological environment containing ionic liquid. It was not possible to determine a pattern of interaction between the ionic liquids. Therefore, it was concluded that each system must be characterized

independently, even if the ILs have common cations or anions. New DNA-aptamer sequences were obtained by SELEX in presence of CL in solution showing that in principle this selection procedure might be also employed with non-conventional solution.

CHAPTER 1

General Introduction

1.1 Functional DNA

In Nature, the main function of the deoxyribonucleic acid (DNA) is to store the genetic information of living organisms and carry it from generation to generation allowing the expression of that information under physiological conditions. The information that is stored in DNA is transcribed into RNA sequences and subsequently translated into amino-acid sequences. Thus, DNA serves as a blue-print for the synthesis of proteins and is therefore of fundamental importance for living cells.[1,2]

The discovery of the double-stranded structure of DNA in 1953[3] shed light on our understanding of the significant role that nucleic acids play in life processes.

One of the strongest and most specific biomolecular recognition events is the base pairing or hybridization of nucleic acids, due to their complementarity, which forms the foundation of almost all molecular probes for nucleic acids (**Figure 1.1**).[4] Advances in molecular biology and the chemical synthesis of nucleic acids have fostered the development of nucleic acid probes, many types of which have been designed and applied in the fields of biology, medicine, and chemistry since the early 1960's.[5,6]

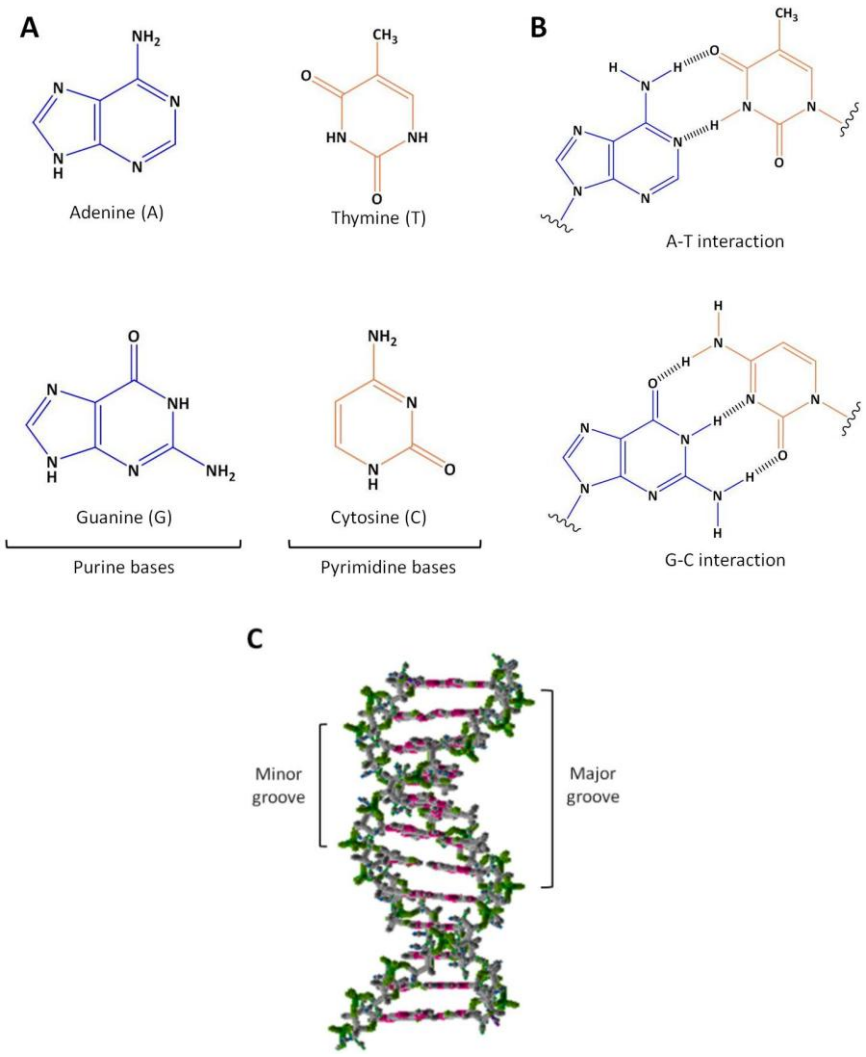

Figure 1.1. A) DNA bases: monomers that give origin to the long sequences; **B)** The DNA bases interact between them by hydrogen bonding, being adenine (A) complementary to thymine (T) and guanine (G) to cytosine (C). When DNA is in long sequences containing the sugar and the phosphate groups and two complementary sequences meet, hybridization occurs and a typical **C)** double-strand DNA is formed.

In the early 1980's, Nadrian Seeman discovered the possible use and application of nucleic acids out of a purely biological context.[7] Combined with the development of functional nucleic acids (FNAs) in the early 1990's,[8] their work is considered as the foundation of "DNA nanotechnology" and resulted in a rapid development of *in vitro* artificial constructs essentially based on DNA. Subsequently, in recent years DNA and also RNA have proven to be exceptional molecules for the design and the development of synthetic structures that can be simple, formed only by one single sequence, or complex 2D or 3D supramolecular machines with tens or even hundreds of sequences with specific functions.[2,9] The possibility of *in vitro* synthesis of nucleic acids also led to the expansion of new technologies that showed, for instance, the replication capability of DNA from just one or a few strands as a template, as occurs in the polymerase chain reaction (PCR) process with the contribution of the *Taq* polymerase enzyme.[10]

The DNA self-assembly plays a key role in the synthesis of complex structures, which is intimately related with the resulting DNA geometry (single or double-strand in A, B or Z form - **Figure 1.2**), DNA hybridization and DNA thermodynamics. The Watson-Crick base pairing through H-bonding is the core principle of DNA nanotechnology (**Figure 1.2 B**).

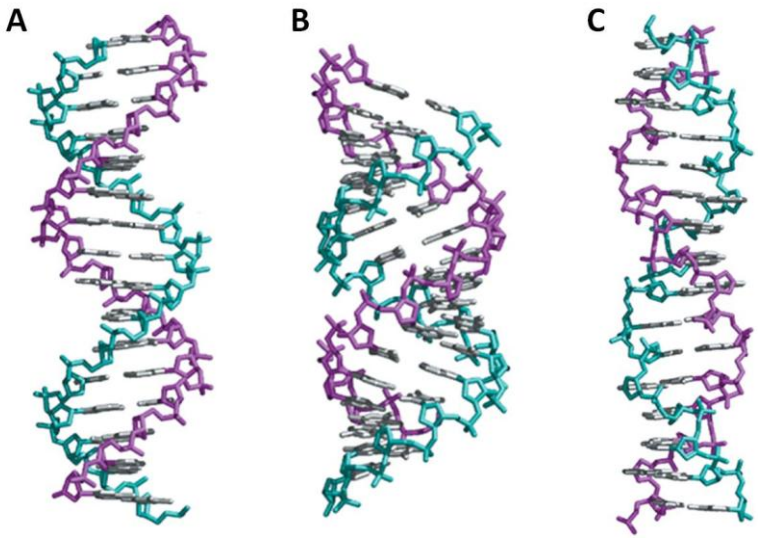

Figure 1.2. Different conformations that DNA can assume depending on the water and ions of the environment **A)** B-form DNA, **B)** A-form DNA and **C)** Z-form DNA.[11,12]

This feature, together with the double or triple-crossover by joining double helices by an exchange of strands, enabled the emergence of a tremendous number of DNA nanostructures which have been assembled by the appropriate sticky ends.[1,2] Constructs of DNA can systematically be designed mainly based on its structural versatility, which may range from: DNA double-strand in its B-conformation,[3,13] G-quadruplex,[14,15] functional DNA structures such as ribozymes,[16] aptamers,[17,18] and molecular beacons,[19,20] to DNA walkers[21–23], DNA functionalized nanoparticles[24] and DNA origami[1,25,26]. The latter structures were named following the Japanese art of

folding paper by the similar concept of folding structures, enabling nanostructures with different geometrical shapes such as a triangle, a star or a circular smiley face[25]; but also non-geometrical shapes such as maps[25], as well as 3D structures such as a nanotube[9] or a box[26]. These structures are some examples of molecular devices systematically synthesized in a bottom-up fashion from simple to more complex DNA components, reflecting the diversity of applications and the flexibility of DNA as a building block.

Understanding the underlying thermodynamics of DNA allows exploring systematically its versatility for smart applications. For example, DNA walkers consist basically in series of ingenious steps based on the complementary of DNA sequences and their consequent hybridization. Whereas hybridization reactions between structure-free DNA strands with complementary sequences occurs typically fast (with rates of order of 10^6 $M^{-1}\cdot s^{-1}$),[23] hybridization between strands with strong secondary structure, such as an hairpin structure, can become very slow.[23] Also a partially complementary DNA sequence is much easier to be detached than a totally complementary one. Then, playing with different nucleotide sequences and with the previous concepts, different authors developed systems based on the "walking capacity" of DNA.[21–23] The basis of this 'bottom up' self-assembly capacity of complex

nanostructures is the ingenious combination of interaction forces, as if selected out of a generic thermodynamic toolbox and resulting from the intrinsic properties of the functional groups of the molecules involved. In the case of DNA origami this is the basic concept applied to build-up such complex nanostructures. Despite the evident complexity, DNA origami exploits the possibility of combining bioinformatic tools and DNA engineering based on DNA hybridization, size, bending, crossovers and junctions, avoiding the electrostatic repulsion between the DNA backbones. In this way, 2D and 3D structures are obtained with manifold applications. Boxes made out of DNA can be used for drug delivery carrying the drug inside the cube, locked by a flexible lid which can be unlocked by a gene "key" monitored by fluorescence.[26] DNA functionalized gold nanoparticles (Au NPs) have become one of the most interesting sensing materials due to their selective and sensitive detection of analytes through fluorescence, colorimetric and scattering monitoring processes.[27–29] These are just a few examples of DNA nanostructures with their potential applications in sensing, therapeutics and diagnostics in nanomedicine.

Although being artificial structures prepared and used experimentally *in vitro*, deployment conditions have always been as close as possible to physiological also because of their potential application *in vivo*. This implies also the compensation of

the DNA negative charge resulting from the phosphate backbone. As a consequence, the stability of DNA constructs depends on the presence of appropriate counterions, usually being Na^+, Mg^{2+} and/or K^+, and naturally a liquid environment capable of solvating these salts.[30–32]

Hence, since the DNA function is intimately related to its structure and stability, which in turn depend on the interactions established with the surrounding molecules responsible for the balance of the forces in solution,[33] it seems obvious that DNA may not remain functional in anything but a conventional buffer medium which resembles physiological conditions. The introduction of a non-conventional solvent, such as can be an ionic liquid (IL), would presumably disturb the equilibrium of interaction forces, thereby altering the interaction between molecules, which in turn could influence the structure of DNA and finally its function.

This work aims at exploring in how far this apparent paradigm holds true. For this purpose, it investigates in how far DNA may in fact remain functional in solutions very different from physiological conditions, namely in tuneable aqueous IL solutions.

1.2. Aptamers

Nearly three decades ago, researchers started to rationally control variation of DNA nanostructures with external triggers, which further extended the area of DNA nanotechnology from structure to function. The rapid advance of DNA nanotechnology also fostered the discovery of functional nucleic acids (FNAs) such as aptamers and DNAzymes. Aptamers are a class of single-stranded nucleic acids of DNA or RNA able to specifically recognize target molecules, with antibody-like high affinity and specificity.[34–36] Aptazymes, ribozymes or DNAzymes are artificial selected nucleic acid with enzyme-like catalytic activities.[37] Both types of FNAs have the advantage over antibodies or enzymes that they can be readily chemically synthesized at low cost and high purity, apart from being more chemically stable.[1,38]

The term "aptamers" was coined from the Latin expression "aptus", meaning "fitting" or "to fit", and from the Greek word "meros" which means "particle".[8] These nucleic acid ligands of DNA or RNA have the property to adopt specific three-dimensional conformations for selectively recognizing different targets, such as inorganic compounds, small organic molecules, nucleotides and derivates, cofactors, amino acids, carbohydrates, antibiotics, peptides and proteins, enzymes, whole cells or even tissues (**Figure 1.3**).[18,39] Aptamers can bind to their target molecules

("locking" the target) with high affinity and selectivity based on a combination of common molecular interactions such as: stacking of aromatic rings; dispersion (London) and electrostatic interactions (henceforth in all chapters, "electrostatic interactions" will be used synonymous with Coulomb interactions); or hydrogen bonding.[40–42]

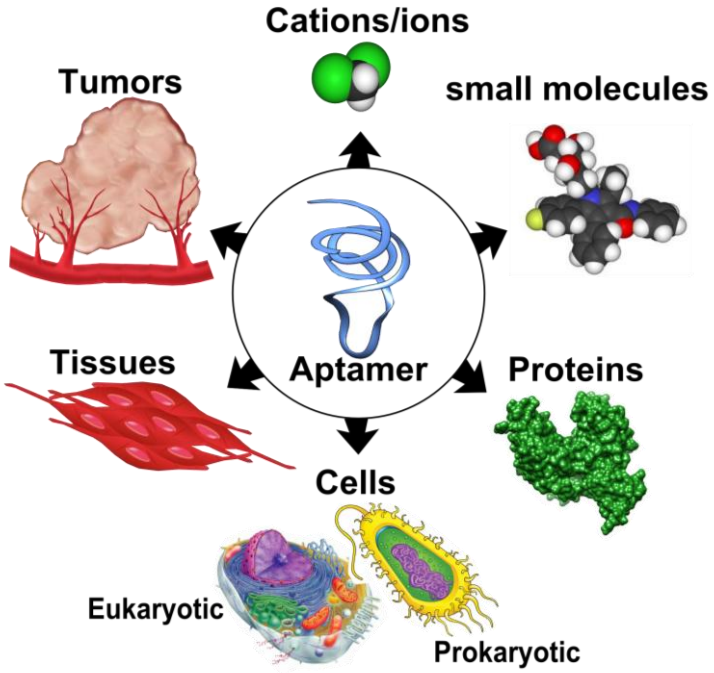

Figure 1.3. Examples of targets for aptamer selection.[18] [Copyright with permission from Ref. 18].

Normally, the size of aptamers lies between 15 to 80 bases that may fold into rather complex structures comprising stems, loops, quadruplexes, pseudoknots, bulges, or hairpins (**Figure 1.4**), such as to ensure strong interaction and high specificity to their targets. Due to their complex 3D structure, aptamers can attain binding affinities comparable or higher than those of antibodies with the advantages of being easily synthesized, and convenient to be stored for months and less prone to immunogenicity.[43] Furthermore, mainly due to their *in vitro* selection, aptamers can in principle bind to virtually any kind of target, whilst antibodies cannot be obtained for small molecules (e.g. ATP), toxic molecules (e.g. toxins) or molecules with low immunogenicity.[43,44] Moreover, in DNA nanotechnology, aptamers are ready to be engineered into DNA nanostructures.[1]

As a result, aptamers have already been employed in various diagnostic assays for detecting specific immune reactions and are routinely used in clinical analysis.[44–46]

1.2.1. Molecular beacons

The advantages of nucleic acids, particularly the aptamers, lie in the simplicity of their synthesis, their high affinity and selectivity, and their suitability for relatively

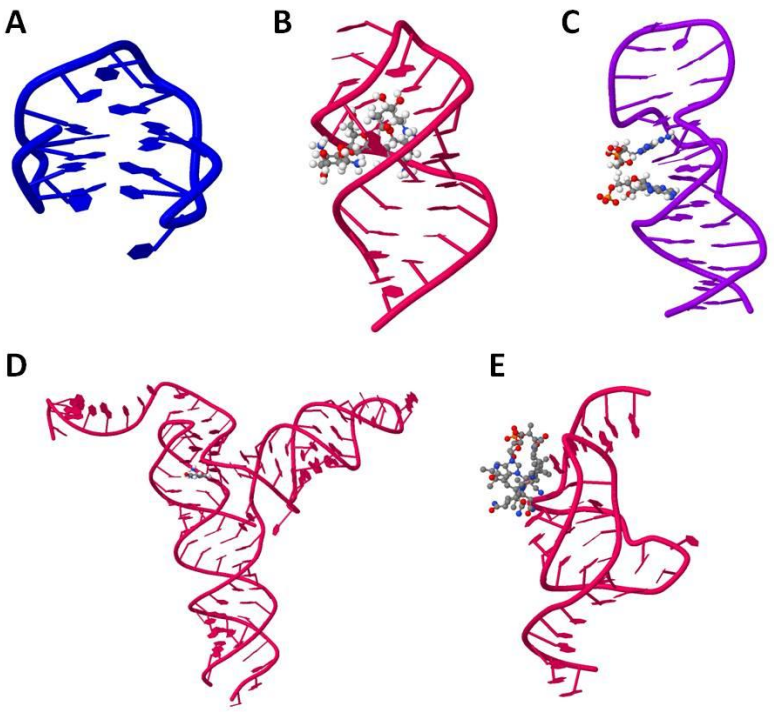

Figure 1.4. Examples of DNA aptamer structures when recognizing their specific target molecules. A) Thrombin binding aptamer (TBA) in G-quadruplex; B) Neomycin RNA aptamer; C) DNA ATP-aptamer both in hairpin conformation; D) $PreQ_1$-III RNA riboswitch with pseudoknots; and E) Vitamin B12 aptamer presenting bulge. Figures obtained from PDB web page.

straightforward structural modification. Molecular beacons (MBs) are a good example of such modifications resulting in DNA hairpin structures designed from aptamers that are widely used as fluorescent probes. MBs, first described in 1996 by

Tyagi and Kramer,[19] are DNA sequences composed of one target recognition region, flanked by two short complementary stem sequences that force the entire construct to form a stem-loop structure in the absence of the target. At the extremity of each stem sequence a fluorophore (donor) or a quencher (acceptor) are attached, respectively, forming a FRET (Fluorescent Resonance Energy Transfer) system.

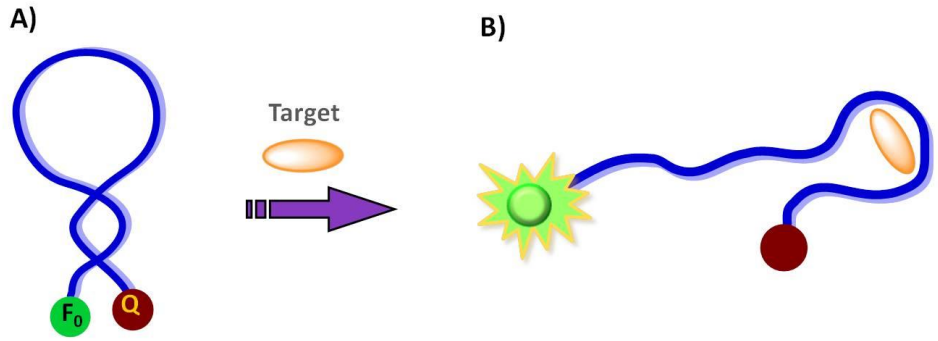

Figure 1.5. Stem-loop structure with a fluorophore and a quencher representing a molecular beacon in its **A)** close hairpin state and in its **B)** open structure, after target recognition emitting fluorescence.

Thus, when the MB is in its closed stem-loop structure, quencher and fluorophore are in close proximity, resulting in the fluorescence being quenched efficiently (**Figure 1.5 A**). Upon target recognition, thermodynamically more favorable target-aptamer interactions force the opening of the weaker stem helix. The spatial

separation of the fluorophore and the quencher then results in a detectable increase of the fluorescence (**Figure 1.5 B**). The thermodynamic stability of the hairpin structure, the highly efficient intrinsic signal switching, and the possibility of using a variety of fluorophore-quencher pairs make MBs exceptional DNA probes with excellent sensitivity and selectivity, and real-time-detection capability. MB probes can be attached to surfaces and interfaces and thus used in biosensors. Their high sensitivity and excellent selectivity make MBs effective biosensor probes on gene chips and microarrays, as well as for near-field optical and microfiber sensors.[20,47] Applications of MBs range from DNA and RNA detection,[19,48,49] the monitoring of living systems,[50,51] the investigation of enzymatic processes,[52,53] the design of biosensors,[54,55] the study of protein–DNA interactions,[56,57] and the fabrication of biochips.[54,58,59]

1.2.2. Selection of DNA-aptamers: SELEX

In order to identify the aptamers of interest, an *in vitro* selection procedure is performed on a nucleic acid library. The method was described for the first time in 1990 independently by three research groups each developing different experimental set-ups. Ellington and Szostak reported on RNA molecules that bind to

a small organic dye, and were the responsible for coining the term "aptamers" for the sequences found.[8] A second study by Tuerk and Gold defined the process as Systematic Evolution of Ligands by Exponential Enrichment (SELEX) and described the selection of RNA molecules that bind to the bacteriophage T4 DNA polymerase.[60] Finally, Robertson and Joyce described the application of *in vitro* selection for the adaptation of the group I ribozyme so that it cleaved DNA rather than single-stranded RNA.[61]

SELEX consists in the screening of a large and random library of DNA sequences against a target molecule. The process starts with a random synthetic nucleic acid library containing 10^{14} - 10^{15} sequences of ssDNA or ssRNA of a defined length (being a random part of 20 to 80 nucleotides, flanked by two known primers at 3' and 5' ends of 10 to 20 nucleotides length). This size of the random library ensures the diversity of the RNA or DNA candidate structures, increasing the probability for high affinity sequences to be detected from a pool of other lower or no-affinity sequences.[8,60,61]

Subsequently, in general the following steps are carried out (**Figure 1.6**): **0)** the target is immobilized on a support matrix, e.g. a resin, in a way such that the recognition motif is freely accessible; **1)** the library is contacted with the target of

interest to allow interaction to occur between the sequence candidates and the target molecule; **2)** separation of the candidates that did not bind to the target, or bound with low affinity, and the candidates that bound and formed a DNA-target complex (partitioning); **3)** elution of the bound candidates from the target by, for instance, increasing the temperature (heat elution) yielding the specifically binding DNA candidates. This is then followed by **4)** the amplification of the obtained DNA sequences by PCR. The SELEX procedure is then repeated with an expected continuous reduction in the variety of the DNA sequences such that the library is enriched in sequences with high affinity and specificity to the target. Finally, after several rounds of selection (6 to 20)[39] one proceeds with **5)** the cloning and sequencing of the specific DNA-aptamer sequences selected.

In this way, SELEX can be performed inexpensively *in vitro* with only routine equipment of a molecular biology laboratory. It is for these reasons that it has been gaining acceptance as a tool for the isolation of biorecognition elements of intracellular and extracellular targets.

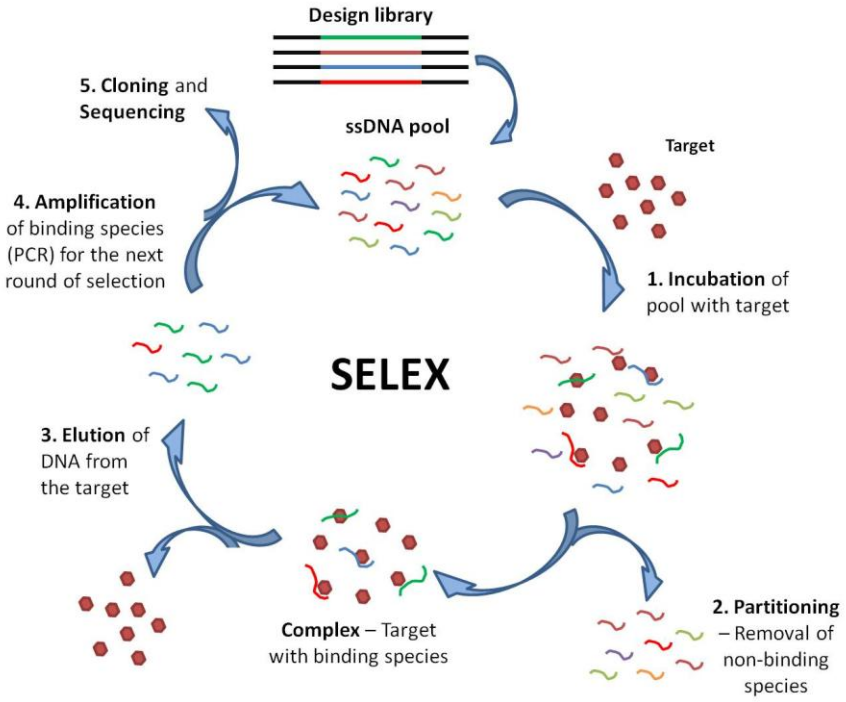

Figure 1.6. Main steps of a general SELEX procedure.

It should be noted that the SELEX procedure has hitherto been carried out under physiological conditions such as to mimic a standard *in vivo* environment for both nucleic acids and the target molecules.[39]

1.3. DNA structure: need for water and counter-cations

The secondary structure and the stability of nucleic acids depend on their interactions with their surrounding molecules, especially the ones that are ubiquitous in physiological liquid environments: water and ions. Non-covalent interactions are established in such an environment comprising electrostatic interactions due to the negative charge of nucleic acids, but also hydrogen bonding, and dispersion (London forces) interactions. The exact buffer conditions: salt concentration; size, shape, orientation and valency of the ions; physico-chemical properties (e.g. hydrophobicity) of other molecules in solution; play a crucial role in determining how DNA interacts with its liquid environment.[31,62–66]

The pioneering studies of Franklin R. and Gosling (1953) discussed for the first time the influence of water on the conformation of DNA,[67] even before Watson and Crick described the structure of nucleic acids as we know it today.[3] Later the needs of water and ions for DNA structure were confirmed by other authors using different techniques such as IR, X-ray diffraction, NMR or ultraviolet absorption.[32,68] The amount of water can profoundly influence the conformations that a duplex DNA may adopt such as B, A or Z-form, G-quadruplex, triplex or hairpin.[69] For instance, when the water content is above 85% in volume in solution, it is expected that DNA

prevails in its B-form. However, if the water content decreases to 75-80% or to 55-75% a transition from B-to-A and Z form, respectively, will occur.[69]

Owing to the significant anionic charge of DNA resulting from its phosphate backbone, the presence of cations in solution is essential to decrease the respective repulsion forces. Neutralization of these negative charges maintains the DNA sufficiently flexible to adopt, for instance, a more packed structure as occurs during the formation of DNA-protein complexes. The capacity to reach an exceptionally high packing density serves to conserve space in cells and to facilitate and organize genes for gene expression.[70] It is in fact also the motivation for considering DNA as an alternative medium for data storage.[71]

In order to achieve an efficient neutralization of the negative charge, the size and valency of the respective counter-ions play a key role in the stabilization of the DNA molecule. Both divalent and monovalent cations bind to nucleic acids but have a different effect on the resulting physical properties of the DNA. For example, both Na^+ and Mg^{2+} can stabilize a DNA duplex, facilitate its folding into the secondary and tertiary structures and thereby increase its thermal stability. Mg^{2+} is much more efficient in doing so than Na^+.[72,73] However, the Na^+ concentration used is always much higher than the used for Mg^{2+}, because Mg^{2+} is also an activator of DNA

nucleases, enzymes that catalyze the cleavage of the phosphodiester bonds of the DNA structure.[74]

The effect of the ions on a DNA structure depends also on the size of DNA itself or if the DNA is a single or double strand: because dsDNA has a higher negative charge density than ssDNA, the role of the counterions is much more pronounced in dsDNA. Moreover, interactions of counterions with dsDNA can also be more complex compared to ssDNA owing to the existence of a secondary and tertiary structure in the former.[31,72]

For the exposed reasons, nucleic acids have so far found their applications mostly under physiological conditions in which water is the primary solvent, as occurs in living cells. For studies outside living organisms it is of extreme importance to comprehend the complexity of the molecular interactions between the nucleic acids and their liquid environment, both as regards its stability as well as its capacity to undergo structural changes. Hence, when water is partially substituted by other solvents capable of dissolving DNA, such as tunable ILs, the question arises in how far this unconventional liquid environment could maintain, if not improve, DNA functionality and in this way extend the field of application of functional DNA beyond its conventional physiological context.

1.4. DNA in molecular solvents other than water

Despite the undeniable need of water and ions in living systems, water also presents some drawbacks for biomolecules. It favours hydrolytic reactions *in vivo* such as depurination of nucleic acids, responsible for mutations in purines that can generate a carcinogenic response, or deamination of 5-methylcytosine leading to the formation of G/T mismatches. Also long-term storage of DNA *in vitro* may be hindered by hydrolytic reactions causing denaturation when stored in an aqueous environment, at 4 ^{o}C or at/near room temperature, for a long period of time.[75–78] Being DNA the only data-storage medium for which real long-term data are available since ancestral times as evidenced from the archeology, the stability of DNA is currently an attractive topic in an entirely different scientific field, namely that of information storage. Very recently, it was shown that DNA can be encapsulated in an inorganic silica matrix, encoding digital information that represented two text documents.[71] After simulating accelerated aging of the DNA by increasing the temperature, decoding and restoring of the original data was conducted in a way such as to minimize errors, proving in this way the concept that DNA may be employed for storing information for very a long time despite of being outside its physiological context.[71]

The benefits of the solvation of biomolecules in solvents other than water has been shown previously, proving that water is not necessarily an irreplaceable medium for the native-like structure of biomolecules. For example, Klibanov and collaborators triggered in the late 1980s and during the 1990s the development of a whole new research field by reporting on biotransformations using enzymes in non-aqueous media.[79–83] When an enzyme is exposed to an organic solvent its denaturation should ensue. However, in their studies Klibanov and co-workers proved that an enzyme lyophilized from an aqueous solution maintains its conformation and activity. Then, when introducing this enzyme into an anhydrous organic solvent, the enzyme remained "locked" in its original conformation owing to the lack of water which would enable a conformational adaptation to the new environment. In fact, in such situation the enzyme is rather dispersed than solvated as it will not interact with the organic solvent, remaining in this way active presenting it catalytic capacity and stability.[84,85] Although the catalytic activity of some enzymes under such circumstances decreased, the efficiency of the overall biotransformation may be strongly improved when the substrate is not dissolving in an aqueous solution. In this case, the improvement of the overall catalytic process in presence of the enzyme may be due to that better dissolution of the substrate and

consequently reaction and product formation.[86,87] In other cases, conversely, the catalytic activity of the enzyme used was even improved by the addition of nucleosides to the solution from which the enzyme was lyophilized.[88] Klibanov and co-workers also studied the stability of the structure of synthetic and natural DNA in non-aqueous solvents.[64] They found that in presence of almost pure glycerol (99% wt) the stability of dsDNA, compared with dsDNA in aqueous buffer solution, decreased substantially with its melting temperature (T_m) (decreasing between 20 - 30 ^{o}C) depending on the NaCl concentration used ([NaCl] = 0.2; 100 and 500 mM). However, for the higher concentrations of NaCl used (100 and 500 mM), some duplex DNA was still detectable in solution with a T_m higher than RT (T_m = 30 and 37 ^{o}C, respectively). In solvents such as formamide, methanol or DMSO, dsDNA entirely denatured.[64] This study already indicated that non-conventional solvents might not only interact directly with DNA but that also indirect effects - such as the interaction with salts that stabilize the DNA structure - need to be taken into account.

Non-charged molecular solvents are, hence, mainly used to study compaction, aggregation and consequently the precipitation of DNA.[89] A classical example is ethanol which is employed at high concentrations (> 50% v/v) to precipitate and subsequently recover DNA for its re-use. Here, the lower dielectric constant of

ethanol as compared with water results in a stronger shielding of the DNA negative charge and consequently precipitation. At low concentrations, however, ethanol might be used as a co-solvent for the dissolution of solutes without significantly affecting DNA, such as when pyrene dye is used as a DNA intercalator in presence of 8% of ethanol apparently without disturbing DNA B-form.[89–91]

1.5. Non-molecular solvents as alternative solvation media for biomolecules

1.5.1. Ionic liquids

About 15 years ago, due to their particular physico-chemical properties ionic liquids attracted great attention for biotechnological applications. Ionic liquids are salt-like compounds consisting entirely of ions that are liquid at unusually low temperature. Using the boiling point of water as reference, one definition describes ILs as ionic materials which are liquid below 100 ^{o}C, but more preferably being liquid at or near room temperature.[92] This is why they are commonly found referred to as "room-temperature ionic liquids (RTILs)". These particular organic liquid salts possess physico-chemical properties that make them versatile alternative solvents and distinct from both molecular organic solvents (uncharged) and regular salts (solid).

Conventional salts, such as NaCl, are capable of a high packing density resulting in a highly ordered structure such that they are in the solid state at room temperature with a high thermal stability that in the case of NaCl, for instance, leads to a melting temperature of around 800 ˚C.[93] On the contrary, ILs generally consist of a bulky cation and a usually smaller anion such that ion packing cannot achieve a high degree of order (**Figure 1.7**).

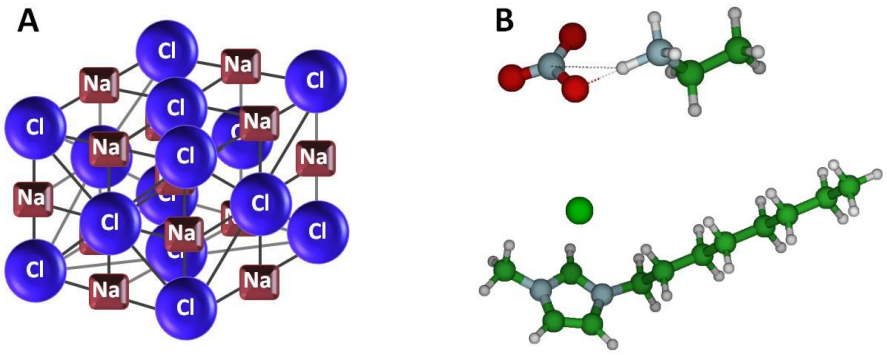

Figure 1.7. Representation of **A)** the crystalline and highly ordered structure of the solid and common salt NaCl and **B)** as representative examples, two ILs: ethylammonium nitrate, EAN (top) and 1-octyl-3-metylimidazolium chloride, OMIM-Cl (bottom). As can be seen by the structural and size differences between cation and anion of the ILs it is practically impossible to obtain the degree of order of NaCl and therefore more difficult to obtain such crystalline structure at RT.

As a consequence, even at room temperature these salts remain in a less ordered state and, therefore, liquid.

ILs are widely considered "designer solvents" because of an almost infinite set of cation-anion combinations that can be conceived. Both the cation and the anion can in theory be tuned to yield compounds of distinct physico-chemical properties. It was estimated that about 10^{18} ILs can theoretically be synthesized.[94,95] Combinations of asymmetric nitrogen-containing families of cations such as imidazolium, pyrrolidinium, pyridinium or alkylammonium, with organic or inorganic anions such as chloride, bromide, dihydrogen phosphate, hexafluorophosphate or trifluoromethanesulfonate, are some examples of the variety of ions that can be used to yield ILs.[96] This diversity is what makes ILs widely tunable with regard to their physico-chemical properties and increasingly attractive for a wide range of different areas ranging from electrochemistry, chemical synthesis, catalysis, to the life sciences.[97–99]

In the last decade, a so-called "third generation of ILs" has been designed and developed to be more biocompatible and simultaneously water-soluble. The use of readily available natural ion pairs based on molecules such as the vitamin-like choline, amino acids and naturally occurring carboxylic acids allowed the

improvement of the production of this new class of ILs. Concurrently, deep eutectic solvents (DES) were also studied as a new type of solvent.[100] Essentially, DES are based on the combination of solid salt mixtures with one of the compounds possessing a hydrogen-bond donor capability (e.g. choline chloride with urea) and whose mixture results in a significantly lower melting point than that of the pure compounds. For instance, the melting point of choline chloride (ChCl) is 302 ^{o}C and that of urea is 133 ^{o}C. Upon mixing and heating, they form an eutectic mixture with a melting temperature at 12 ^{o}C. DES have proven to be also an alternative to conventional solvents as they can be easily prepared, are biodegradable, non-toxic and relatively inexpensive, especially when compared with some ILs.[100] Some studies indicate that DNA is soluble and maintains, to some extent, long-term stability and structural conformations in presence of deep eutectic solvents.[100–102] Nevertheless, DES are not being considered ILs since part of their compounds, such as urea, are not charged and the resulting solvents are therefore not entirely ionic.

Contrary to what was initially postulated when ILs became a more intense subject of research, ILs may not always be intrinsically "green" or "benign". However, they can be designed to be environmentally benign, and being practically non-volatile they are not a source of VOCs as opposed to common organic solvents. ILs can be

recycled, and possess a certain thermal stability with some ILs maintaining their stability in a temperature range between -100 ºC to 200 ºC.[92,94] In addition, ILs present electric conductivity and the capacity of establishing a wide range of possible interactions such as electrostatic interactions due to their charge, but also hydrogen bonding, hydrophobic and/or van der Waals interactions, which make them suitable solvent media also for dissolution of various natural polymers such as cellulose[97,103,104] but also other biomolecules. Solvation of proteins in ILs avoids hydrolysis and aggregation, and enzymes thus maintain their high selectivity and stability.[105–107] This portfolio of possible interactions makes ILs so unique as compared to molecular solvents.

Owing to their electrolytic character, even the so-called hydrophobic ILs which are considered insoluble in water are somewhat hygroscopic, therefore always absorbing a certain amount of water when being in contact with humidity.[108,109] Water is, hence, an omnipresent 'impurity' in pure ILs. Since in this work solutions of ILs were used, however, water was not a relevant impurity in this context. However, water and other impurities as ions or solvent residues from IL synthesis may affect the physical properties of ILs such as viscosity, melting point and density. For instance, increasing the chloride concentration from 0,01 mol·kg^{-1} to 0,5 mol·kg^{-1} at

20 ^{o}C increases the viscosity of the IL [C_4mim][BF_4] from 154 to 201 mPa·s, respectively. If instead in a solution containing the same IL the mole fraction of water is increased from 0.12 to 0.45, the viscosity will decrease from 98 to 25 mPa·s, respectively.[110]

For the water miscibility of ILs, the anion of the ILs has a primary and the cation only a secondary effect.[103,110] Thus, depending on the system or reaction, especially when neat ILs are needed, it is of the utmost importance to assess the purity of the ILs and in the special case of water, an efficient drying and anhydrous handling has to be ensured. On the other hand, in practice it might be virtually impossible to maintain an IL totally absent of any water. Therefore, when employing ILs and study their interactions one should bear in mind that most probably one is in fact dealing with IL+water, rather than with an IL alone.

Also due to the high affinity for water and to the little explored concept of proton activity, some ILs may present intrinsic acidity or basicity. One good example is the protic ionic liquid ethylammonium nitrate (EAN) which behaves like water by transferring a proton from the proton-donor to the proton-acceptor, forming in this way an hydrogen-bond network resembling the aqueous environment.[97,111]

Therefore, when solvating pH-sensitive molecules such as proteins or DNA in

ILs and in presence of water, one needs to beware of the proton activity of the IL medium. Similarly, the addition of an IL to aqueous solutions requires pH control through buffers which might still be exceeded by the intrinsic acidity or basicity of the IL. For example, choline dihydrogenphosphate (CDHP) is a slightly acidic IL due to the acidity of the $H_2PO_4^-$ anion. Macfarlane and co-workers studied how to control its proton activity[112] using equimolar amounts of choline monohydrogen phosphate salt (CHP) and CDHP, thus establishing an equilibrium between the two phosphate species as usually done for Na_2HPO_4/NaH_2PO_4. They proved the buffering capacity of this solution by adding increasing concentrations of concentrated acid (HCl) or base (NaOH).[112]

1.6. DNA in solution with ionic liquids

1.6.1. Stability of DNA structure

In literature, the role of the ILs with regard to interactions with DNA has been considered as transiting from salts, increasing the DNA duplex stability, to solvents by decreasing the DNA melting temperature.[113] Indeed, it is not obvious whether ILs can be classified as one or another in solution, which illustrates how the solvation of DNA by ILs is complex and therefore not fully understood at a molecular level, yet.

Efforts have been made both theoretically and experimentally to elucidate the possible effect and actuation of ILs on the secondary and tertiary structure of DNA.[91,114,115] However, structural stability is only one aspect for studying the functionality of DNA in solution. When proteins denature, they lose their structure and function. However, DNA may have a function both in its single-stranded and double-stranded form. As a consequence, if a dsDNA denatures in an IL, this does not automatically mean that DNA may also lose its function. Furthermore, function of DNA in its duplex form is particular since it is a structure established through non-covalent hydrogen bonds. For example, in a hairpin structure it is the reversible hybridization/denaturing of the stem which lends the DNA construct "function" - thus, the term "stability" refers in this case to maintaining a dynamic rather than a static system.

From the aforementioned it can be seen that while IL-DNA interactions are intrinsically complex, this also opens up an opportunity. The design of DNA devices with intrinsic molecular recognition or self-assembly capacity may benefit from a liquid environment based on versatile "designer solvents" such as the ILs, yielding in this way the highest possible degree of freedom in the design of the overall system. In this context it should be recalled that some ILs such as EAN possess the capacity

to form a three-dimensional H-bond network resembling the network formed by water molecules owing to donor-acceptor capabilities of their ions.[111]

Still, the major motivation for studying DNA-IL interactions has been so far the potential of ILs as an alternative medium for long-term storage of DNA. The aim has therefore been mainly to determine in how far DNA maintains its structure in ILs, and by what molecular interactions it may be (de)stabilized. Being both DNA and ILs electrically charged, electrostatic interactions are obvious to be predominant. However, many studies also indicate that hydrophobic interactions play an important additional role as regards DNA stability in presence of ILs.[91,116–118] However, when having a closer look at the experimental protocols detecting such interactions it becomes evident that the supposed experimental or theoretical evidence can in fact not always be interpreted in a straightforward manner. For example, ILs mainly belonging to imidazolium family with partial hydrophobic character (amphiphilic) were modified by systematically increasing the alkyl chains at the cation resulting in a gradually increasing bulk hydrophobicity.[91,116–118] It was then assumed that the alkyl chain of the ILs would interact preferably with the bases of the DNA through hydrophobic interactions. For the supposed determination of such interactions, mostly spectroscopic techniques were used, in particular

fluorescence spectroscopy using DNA staining dyes such as the intercalator ethidium bromide (EtBr). The majority of such DNA staining dyes are cationic (e.g. EtBr; 4',6-diamidino-2-phenylindole, "DAPI") or neutral (e.g. pyrene) small organic molecules or metal complexes (e.g. ruthenium intercalators) which bind to DNA through the two common binding modes depending on the structure of the dye: intercalation or groove-binding.[119] Intercalation results from insertion of a planar aromatic substituent mainly through π-π stacking between DNA base pairs of the major or minor groove (classical intercalation), as occurs with EtBr, pyrene or proflavine.[120,121] There also exist intercalators carrying bulky substituents which intercalate in both the minor and major grooves of DNA simultaneously and are therefore denominated threading or bis-intercalators (threading intercalation), such as is the case for the drug nogalamycin or the agent acridine-4-carboxamide (DACA).[121–123] Independently of the type of intercalation occurring, it triggers a concomitant unwinding, stiffening and lengthening of the DNA helix.[124,125] Groove-binding, in contrast, occurs mainly through hydrogen bonding, van der Waals and hydrophobic interactions and does not disturb the duplex structure to an extent as great as intercalation.[119,121,126,127] Spermine, netropsin, DAPI or Hoechst 33258 are examples of agents that adopt an

appropriate conformation to fit the helical curvature of the groove without significant perturbation of the DNA.[120,128]

The working principle of these dyes is that they can either be non-emitting in the bulk of the solution while emitting when bound to DNA (EtBr; DAPI), or vice versa (pyrene).[129,130] The resulting DNA-dye complex is very stable and can resist even to gel electrophoresis where an electrical field is applied.[131] In presence of charged ILs, however, it is plausible that these dyes also interact with the ILs themselves, particularly when the dye is charged such as EtBr. Despite the proven preference of intercalating dyes such as EtBr for the double-stranded oligonucleotides, EtBr are strongly alike ILs in their physico-chemical nature and strong IL-EtBR interactions can be anticipated irrespective of possible interactions with DNA. This needs to be taken into account when using such intercalating dyes as a reporter molecule to elucidate DNA-IL interactions: for example, using such dyes as intercalators or groove binders for elucidating how an IL interacts with DNA, it was observed that the fluorescence intensity decreased in the case of EtBr, DAPI and Hoechst 33258 or increased in the case of pyrene, supposedly demonstrating that the dye had moved from the DNA inter-base environment into the bulk.[91,115,116] The respective authors concluded that this was due to hydrophobic interactions

established between the alkyl chains of the IL and the DNA bases, resulting in an expulsion of the dye from the inter-base environment and the subsequent compaction and restoring of the DNA to its original B-conformation. While this seems plausible, an alternative explanation may be to assume a thermodynamically more favourable interaction between the dye and the IL, as compared to the dye and DNA. Hence, EtBr might be expulsed from the DNA through direct interaction with the IL rather than an indirect action of the IL on the DNA. In fact, a recent work reported on extracting several charged DNA staining dyes (SYBR Green I (SG), ethydium bromide (EtBr), SYTO-13, PicoGreen and thiazole orange (TO) from DNA precisely using hydrophobic imidazolium-based ILs reports that while DNA remained in the aqueous phase without suffering disturbances in its structure, the DNA staining dyes moved from the water phase to the ILs phase indicating that the affinity between ILs and DNA staining dyes was stronger than that of the dyes with the DNA. Molecular solvent mixtures did not yield the same effect and did not extract the dyes form DNA, indicating that the electrostatic interactions were the main responsible for the extraction. Hence, this confirms indeed our note of caution.[132]

Other than by employing dyes, non-invasive spectroscopic techniques such as circular dichroism can circumvent these possible pitfalls and yield a fingerprint of the DNA conformation. In a system studying DNA in solution with ILs, the group of MacFarlane found that DNA was soluble and exhibited exceptional long-term stability in presence of choline lactate, nitrate and dihydrogen phosphate due to the mild H-bonding environment provided by these ILs. The authors claimed that the IL environment decreased the activity of the water present in solution, hence slowing down the rate of hydrolytic reactions and decreasing their probability of occurance.[133] A plasmid DNA also proved to be more resistant to a DNase (nuclease) degradation in presence of CDHP up to 50% w/w at room temperature over 28 days.[134] Using instead two minor groove binding probes, DAPI and Hoechst 33258, Chandran A. and co-workers also studied long-term stability of dsDNA but in 1-butyl-3-methylimidazolium chloride (BMIM-Cl). Employing CD, UV-vis absorption and fluorescent dye displacement assays, besides MD simulation, they reported that the BMIM-Cl molecules associated with the DNA structure by electrostatic and H-bond interactions to backbone and minor groove, respectively, helping then to stabilize B-DNA conformation.[135] While these studies give a glimpse on how certain ILs can

interact with dsDNA at a certain concentration, no general understanding on the dsDNA-IL interactions have been reported so far.

1.6.2. Stability of DNA function - Aptamers in non-conventional solvents

The selection of high affinity aptamers is highly dependent on the chemical properties of the ligand and, equally important, of the solvation medium in which the ligand-target binding occurs. Since the process of SELEX was firstly reported, the most used selection medium was aqueous buffer solution with the aim to mimic physiological conditions.[136,137,17] Usually, a binding buffer consists of a buffering agent (Tris, HEPES, phosphate, pH 6-8), salts (NaCl or KCl, 50-200 mM) and Mg^{2+} (1-10 mM). However, aptamers selected in aqueous buffer solution also proved to function under non-physiological conditions. An aptamer against ochratoxin-A, selected in aqueous buffer, also performed well in the presence of 20% methanol.[138] The recognition of a DNA sequence by a complementary molecular beacon was studied in presence of nine organic solvents.[139] Using concentrations up to 75% (v/v) the used solvents include ethanol, glycerol, dimethyl sulfoxide (DMSO), among others. The rate of the hybridization was significantly faster in presence of most organic solvents when compared with water, and also the beacon remained specific

discriminating single-base mismatches of the target DNA.[139] Ehrentreich-Förster E. et al. developed a fiber-optic biosensor using an aptamer that recognizes the explosive molecule trinitrotoluene (TNT). It was proven that the TNT-aptamer binds to its target in solution with concentrations of at least 50% (v/v) of acetonitrile and methanol, remaining specific when compared with the structurally similar target Tetryl.[140] An aptamer for bisphenol A was selected in 2-50% (v/v) of either one or the mixture of dioxane, dimethyl sulfoxide, N,N-dimethylformamide, tetrahydrofuran, ethanol and methanol.[141] There were also cases where the target showed a better affinity for the selected aptamer when previously treated with an organic solvent: Meng C. *et al.* showed that selected whole-cell aptamers bind preferentially to *E. coli* previously treated with methanol, ethanol, formaldehyde and glutaraldehyde solvents, rather than to the *E. coli* without any previous treatment.[142] Their results suggest that the surface properties of cells determine their binding affinity with ssDNA, which should be considered during the selection of whole-cell aptamers and their application. Very recently, Chaou T. et al. selected an aptamer specific for adenine in buffer containing 25% in volume of methanol.[143] This aptamer revealed to be more efficient for binding adenine than the previously described aptamer in pure aqueous buffer. Working in the direction of selecting an aptamer directly in a

solution different from physiological will allow enhancing the chemical diversity of aptamers and to develop aptamers directed towards poorly water-soluble chemicals.

1.7. Ionic liquids - salts or solvents?

Given the fact that ILs are both solvents and electrolytes, one may wonder whether in aqueous solution the interactions which an IL undergoes with DNA resemble more that of a salt, or a molecular solvent, or/and whether this depends on the IL concentration. Determining the DNA melting temperature (T_m) using DNA-functionalized gold nanoparticles (AuNPs) dissolved in different ILs, mainly from alkylammonium nitrate family, Menhaj A. B. and co-workers stated that at low IL concentrations (≤ 20% v/v), ILs act as salts through their cations stabilizing the DNA duplex, thus increasing its T_m.[113] At higher concentrations of the respective ILs, however, cations with hydrophobic groups tended to destabilize the DNA duplex and consequently decrease it T_m, as occurs even with small concentrations of some organic solvents in solution with DNA.

On the other hand, it is known that common salts exert their effects on the stability of biopolymers mainly through electrostatic interactions at low to moderate

salt concentrations (≤ 0.5 M), and predominantly through an indirect effect on the bulk aqueous solvent at high salt concentrations (≥ 1 M).[144] Using common salts, Tomac S. *et al.* (1996) investigated the effects of a wide range of concentrations of various sodium salts on the thermal stability of a peptide nucleic acid duplex (PNA-PNA), as well as a PNA-DNA hybrid duplex, and compared these with the effects on a common DNA duplex. The peptide nucleic acid presents no phosphate backbone and is consequently not negatively charged such as common DNA, which excludes any strong electrostatic interactions to occur. They observed that at low to moderate salt concentration the polyelectrolyte character predominates, since the T_m of PNA-DNA and DNA-DNA decreased. At high salt concentration (≥ 1 M), the electrostatic contributions are saturated and the presence of backbone charges is no longer relevant. The T_m of PNA-PNA (no charge) remained constant until ≈3M of salt in solution. Here the indirect effect of the presence of salts on the aqueous bulk as well as other type of interactions such as hydrophobic or hydrogen bonding start to play a role on the stability of the nucleic acids, irrespective of whether they are charged or not: a general decrease on the T_m of the three types of duplexes was registered irrespective of their backbone charge.[144]

Extrapolating these observations to ILs, analogous effects may be occurring with a duplex DNA. Hence, the question of whether ILs behave more like salts or more as solvents seems to lose its meaning here. Given the vast structural variety of ILs, these may exert likewise diverse effects on the structure of DNA, being undeniably the electrostatic interactions the first to be established. As much as molecular solvents can either destabilize dsDNA at low concentrations (e.g., formamide) or maintain its structure even at very high concentration (e.g. glycerol), one should therefore also differentiate between ILs based on their physico-chemical properties, rather than considering "ILs" as a general group of solvents.

1.8. Techniques used to study DNA-ILs systems and what can be introduced to better understand the system

Understanding IL-DNA interactions relies on appropriate analytical techniques. Since the earliest study involving ion conductive DNA films with ILs,[145] the methodologies found on literature to date for elucidating the interactions between DNA and ILs rely mainly on spectroscopic techniques, such as fluorescence measurement or correlation spectroscopy, UV-vis absorbance, FT-IR, or CD.[116,135,146,147] Fluorescence spectroscopy is a very common technique employed for

DNA studies due to the facility to attach fluorophore/quencher pairs to DNA sequences and exploit in this way the FRET phenomenon. However, when studying DNA in solution with ILs, care must be taken when using fluorescence techniques since ILs may interfere with the fluorescence apart from presenting auto-fluorescence. In this context, it is noteworthy that the use of dyes as signaling molecules is also not straightforward. As an example, but instead of ILs, using common salts such as NaCl and $MgCl_2$, it was observed that in a solution with DNA, EtBr and a high salt concentration, the fluorescence intensity of the solution increased. This is because with the DNA negative phosphate backbone charge being completely neutralized, EtBr tends to interact with the hydrophobic environment between the dsDNA bases. However, if the concentration of salt in solution was low or only the buffer salt concentration, two types of interactions were observed: 1) the same interaction with the double-stranded site (primary site) as at high salt concentration, which is characterized by an enhancement in fluorescence due to an intercalation of EtBr; or 2) an interaction with a second binding site (secondary site), namely the phosphate groups of DNA, resulting in low fluorescence emission.[130]

Techniques such as nuclear magnetic resonance (NMR), dynamic light scattering (DLS), capillary electrophoresis (CE), isothermal titration calorimetry (ITC)

and even microscopy were also used by different authors.[146,148,149] Regarding the latter, Ding Y. and co-workers (2010) studied a DNA-IL system by the cryogenic transmission electron microscopy (cryo-TEM).[146] Recently, Satpathi S. *et al.* (2015) employed the field emission scanning electron microscopy (FE-SEM) and TEM to probe the morphological alteration of DNA during a founded compaction process induced by a guanidinium IL.[150] Historically, electron microscopy (EM) was widely used to study various properties of DNA, enabling the imaging of the chromatin organization into cells or the fundamental property of DNA melting.[151] However, it should be noted that these microscopy based methods are appropriate for very long DNA strands only as is the case in the studies of Ding and Satpathi (calf thymus or salmon sperm DNA reaching ≥ 10 kb) as smaller DNA sequences will not be observable. Moreover, this kind of electron microscopy requires a rough sample preparation, possibly causing damage on the sample. Moreover, it yields results only from a very reduced area of the sample,[152] and it is self-evident that microscopy-based techniques do not provide any evidence on interactions on the molecular scale. The use of these microscopy techniques for systematically elucidating DNA-IL interactions is therefore strongly limited.

On the other hand, atomic force microscopy (AFM) is being increasingly improved and used to overcome the EM limitations and make possible, for instance, the detection of short sequences (as short as 25 bases) of DNA without sample damage.[152,153] AFM became a method of choice for imaging of biological specimens both in air and in solution.[154,155] One strong limitation of AFM is the need for a substrate with a surface smooth enough in the low nm-range such that the cantilever can easily detect the DNA, but one would expect that in the future work AFM will become be an appropriate technique to elucidate the influence of ILs on DNA structure and conformation.

Surface-sensitive techniques such as surface plasmon resonance (SPR) or quartz crystal microbalance with dissipation monitoring (QCM-D) are established techniques to study DNA or DNA-protein complexes. These techniques require the immobilization of the DNA on a chip surface (e.g. gold) by a common bioconjugate protocol.[156] These techniques allow then a facile change of the liquid medium and determine the resulting effect on the DNA specificity of conformational changes.[157] One possible limitation of these techniques is their sensitivity to changes in the bulk properties of the liquid, i.e., high concentrations of IL in solution would result in a

bulk response of the sensors which would mask any subtle changes occurring in the DNA.

Experimental methodologies become more and more complemented by theoretical calculations, simulating *in silico* the system under study to better understand the molecular mechanism of interactions between DNA and ILs.[91,135,147] However, this approach is still controversial since most of the times simulations are making assumptions quite far from the real, experimental system. For instance, Micaelo N. *et al.* reported a theoretical study of ct-DNA in a neat IL BMIM-Br.[114] Considering that ILs are highly hygroscopic, the term "neat" could be incorrectly used, since we will always have the presence of water in solution, even being in a residual amount. Moreover, experimentally almost all the studies used concentrations below 50% w/w of IL in a solution with DNA, especially when an imidazolium-based IL was being used,[91,132,135,146] Tateishi-Karimata and Sugimoto conducted molecular dynamic calculations to study the interaction of the choline cations of the IL choline dihydrogen phosphate (CDHP) with DNA, but discarding the anion DHP during their calculation by considering its effect on the DNA structural stability negligible from the start.[158] Nevertheless, it is expected that once simulation

studies become closer to reality, they may certainly be very helpful in elucidating DNA-IL interactions.

As can be seen, due to the fact that many analytical techniques possess significant limitations or do not even yield detailed information on the molecular interactions between DNA and ILs, and while simulations are still far from the real systems, there is a lot of room for speculations about how ILs interact with DNA. Consequently, there is a strong need for systematical studies with ILs covering a wide range of physico-chemical properties such as to be able to truly elucidate the underlying phenomena of DNA-IL interactions.

1.9. Outline

The main propose of this thesis was the study of the interactions of DNA and the function of a DNA-aptamer in presence of ILs with different physico-chemical properties. The ATP-aptamer was chosen as a probe for this study taking advantage of it previous full characterization and of the fact that the ATP or AMP target is a small molecule, reducing in this way the amount of interactions, i.e. the complexity, that could be established with the medium.

We have started with the study of the ATP-aptamer recognition capacity and selectivity in aqueous solution with the protic ionic liquid EAN. In order to use fluorescence as monitoring method, the ATP-aptamer was used in a molecular beacon structure containing a linker, as well as Alexa Fluor 488 (AF 488) and the Black Hole Quencher 1 (BHQ 1) as fluorophore-quencher pair in each extremity of the sequence (**Chapter 3**).

The number of ILs in the study was then increased to better understand how ILs presenting different physico-chemical properties influence the DNA structure and function. ILs belonging to different families presenting in some cases similar cations or anions such as to facilitate understanding the role of the ions on the DNA structure were used: CL, CN, CDHP, TMGL and BMIM-Cl. Different techniques, such as fluorescence and CD, complemented by theoretical calculations were used during this study. The possible influence of these ILs on fluorescence emission and FRET was investigated by studying AF 488 free or attached to a 12-mer DNA sequence in solution with the above mentioned ILs (**Chapter 4**). The 12-mer DNA sequence represented one arm of the stem of the hairpin molecular beacon structure described in Chapter 3.

The fundamental and unique capability of DNA to hybridize was then studied in presence of these ILs as well as the thermal stability of the dsDNA formed. The latter resembled the MB stem formed through the two complementary 12-mer oligomers (**Chapter 5**).

The final part of this work consisted, for the first time, in the SELEX procedure performed by introducing the IL choline lactate into the selection solution. The aim was to see in how far the introduction of an IL already during SELEX would yield DNA-aptamer sequences capable to recognize ATP in presence of ILs with an equal or even higher K_d than the ATP-aptamer selected in buffer solution (**Chapter 6**). Here techniques such as PCR, electrophoresis, PAGE and radioactivity labeling were used.

1.10. References

(1) Fan, C. *DNA Nanotechnology: From Structure to Function*; **2013**.

(2) Pitchiaya, S.; Krishnan, Y. First Blueprint, Now Bricks: DNA as Construction Material on the Nanoscale. *Chem. Soc. Rev.* **2006**, *35* (11), 1111–1121.

(3) Watson, J.; Crick, F. Molecular Structure of Nucleic Acids. *Nature* **1953**, *171*, 737–738.

(4) Watson, J. D.; Crick, F. H. Genetical Implications of the Structure of Deoxyribonucleic Acid. *Nature*. **1953**, 964–967.

(5) Hall, B. D.; Spiegelman, S. Sequence Complementarity of T2-DNA and T2-Specific RNA. *Proc. Natl. Acad. Sci.* **1961**, *47* (2), 137–146.

(6) Bolton, E. T.; McCarthy, B. J. A General Method for the Isolation of RNA Complementary to DNA. *Proc. Natl. Acad. Sci. U. S. A.* **1962**, *48* (1959), 1390–1397.

(7) Seeman, N. C. Nucleic Acid Junctions and Lattices. *J. Theor. Biol.* **1982**, *99* (2), 237–247.

(8) Ellington, a D.; Szostak, J. W. In Vitro Selection of RNA Molecules That Bind Specific Ligands. *Nature* **1990**, *346* (6287), 818–822.

(9) Rothemund, P. W. K.; Ekani-Nkodo, A.; Papadakis, N.; Kumar, A.; Fygenson, D. K.; Winfree, E. Design and Characterization of Programmable DNA Nanotubes. *J. Am. Chem. Soc.* **2004**, *126* (50), 16344–16352.

(10) Saiki, R. K.; Gelfand, D. H.; Stoffel, S.; Scharf, S. J.; Higuchi, R.; Horn, G. T.; Mullis, K. B.; Erlich, H. a. Primer-Directed Enzymatic Amplification of DNA with a Thermostable DNA Polymerase. *Science* **1988**, *239* (4839), 487–491.

(11) Ghosh, A.; Bansal, M. A Glossary of DNA Structures from A to Z. *Acta Crystallogr. Sect. D - Biol. Crystallogr.* **2003**, *D59*, 620–626.

(12) Arnott, S.; Chandrasekaran, R.; Birdsall, D. L.; Leslie, A. G. W.; Ratliff, R. L. Left-Handed DNA Helices. *Nature* **1980**, *283* (5749), 743–745.

(13) Search, H.; Journals, C.; Contact, A.; Iopscience, M.; Address, I. P. My IOPscience THE HELIX-COIL TRANSITION IN DNA. **1972**, *715*.

(14) Li, J. J.; Tan, W. A Single DNA Molecule Nanomotor. *Nano* **2002**, *2* (4), 315–318.

(15) Majhi, P. R.; Qi, J.; Tang, C.; Shafer, R. H. Pinaki R. Majhi, Jianying Qi, Chung-Fei Tang, Richard H. Shafer. **2008**, *89* (4), 302–309.

(16) *Functional Nucleic Acids for Analytical Applications*; Li, Y., Lu, Y., Eds.; Springer-Verlag NewYork: New York, **2009**.

(17) Huizenga, D. E.; Szostak, J. W. A DNA Aptamer That Binds Adenosine and ATP. *Biochemistry* **1995**, *34* (2), 656–665.

(18) Hernandez, L. I.; Machado, I.; Schäfer, T.; Hernandez, F. J. Aptamers Overview: Selection, Features and Applications. **2015**.

(19) Tyagi, S.; Kramer, F. R. Molecular Beacon Probes That Fluoresce on Hybridiztion. *Nat. Publ. Gr.* **1996**, *14*, 303–308.

(20) Wang, K.; Tan, W.; Wang, K.; Tang, Z.; Yang, C. J.; Kim, Y.; Fang, X.; Li, W.; Wu, Y.; Medley, C. D.; et al. Minireviews Molecular Engineering of DNA : Molecular Beacons. **2009**, 856–870.

(21) Sherman, W. B.; Seeman, N. C. A Precisely Controlled DNA Biped Walking Device. *Nano Lett.* **2004**, *4* (7), 1203–1207.

(22) Shin, J. S.; Pierce, N. A. A Synthetic DNA Walker for Molecular Transport. *J. Am. Chem. Soc.* **2004**, *126* (35), 10834–10835.

(23) Simmel, F. C. Processive Motion of Bipedal DNA Walkers. *ChemPhysChem* **2009**, *10* (15), 2593–2597.

(24) Lin, Y.-W.; Liu, C.-W.; Chang, H.-T. DNA Functionalized Gold Nanoparticles for Bioanalysis. *Anal. Methods* **2009**, *1* (July), 14.

(25) Rothemund, P. W. K. Folding DNA to Create Nanoscale Shapes and Patterns. *Nature* **2006**, *440* (7082), 297–302.

(26) Andersen, E. S.; Dong, M.; Nielsen, M. M.; Jahn, K.; Subramani, R.; Mamdouh, W.; Golas, M. M.; Sander, B.; Stark, H.; Oliveira, C. L. P.; et al. Self-Assembly of a Nanoscale DNA Box with a Controllable Lid. *Nature* **2009**, *459* (7243), 73–76.

(27) Mirkin, C. A.; Letsinger, R. L.; Mucic, R. C.; Storhoff, J. J. A DNA-Based Method for Rationally Assembling Nanoparticles into Macroscopic Materials. *Nature* **1996**, *382*, 607–609.

(28) Elghanian, R.; Storhoff, J. J.; Mucic, R. C.; Letsinger, R. L.; Mirkin, C. A. Selective Colorimetric Detection of Polynucleotides Based on the Distance-Dependent Optical Properties of Gold Nanoparticles.

(29) Lin, Y.; Liu, C.; Chang, H. DNA Functionalized Gold Nanoparticles for Bioanalysis. **2009**, No. July, 14–24.

(30) Ions, M.; Acids, N. *No Title*.

(31) Tan, Z.; Chen, S. Nucleic Acid Helix Stability : Effects of Salt Concentration , Cation Valence and Size , and Chain Length. **2006**, *90* (February).

(32) Texter, J. NUCLEIC ACID-WATER INTERACTIONS. **1978**, *33*, 83–97.

(33) Stierand, K.; Rarey, M. In Two Dimensions. **2010**, 540–545.

(34) Famulok, M.; Mayer, G.; Blind, M. Nucleic Acid Aptamers - From Selection in Vitro to Applications in Vivo. *Acc. Chem. Res.* **2000**, *33* (9), 591–599.

(35) Famulok, M.; Hartig, J. S.; Mayer, G. Functional Aptamers and Aptazymes in Biotechnology, Diagnostics, and Therapy. *Chem. Rev.* **2007**, *107* (9), 3715–3743.

(36) Mayer, G. The Chemical Biology of Aptamers. *Angew. Chemie - Int. Ed.* **2009**, *48* (15), 2672–2689.

(37) Breaker, R. R.; Joyce, G. F. A DNA Enzyme That Cleaves RNA. *Chem. Biol.* **1994**, *1* (4), 223–229.

(38) Jayasena, S. D. Aptamers: An Emering Class of Molecules That Rival Antibodies. *Clin. Chem.* **1999**, *45* (9), 1628–1650.

(39) Stoltenburg, R.; Reinemann, C.; Strehlitz, B. SELEX-A (R)evolutionary Method to Generate High-Affinity Nucleic Acid Ligands. *Biomolecular Engineering*. **2007**, pp 381–403.

(40) Patel, D. J.; Suri, A. K.; Jiang, F.; Jiang, L.; Fan, P.; Kumar, R. A.; Nonin, S. Structure , Recognition and Adaptive Binding in RNA Aptamer Complexes. **1997**.

(41) Hermann, T.; Patel, D. J. Adaptive Recognition by Nucleic Acid Aptamers. *Science* **2000**, *287* (5454), 820–825.

(42) Osborne, S. E.; Ellington, A. D. Nucleic Acid Selection and the Challenge of Combinatorial Chemistry. *Chem. Rev. (Washington, D. C.)* **1997**, *97* (2), 349–370.

(43) Lakhin, A. V.; Tarantul, V. Z.; Gening, L. V. Aptamers: Problems, Solutions and Prospects. *Acta Naturae*. **2013**, pp 34–43.

(44) Mairal, T.; Cengiz Ozalp, V.; Lozano Sanchez, P.; Mir, M.; Katakis, I.; O'Sullivan, C. K. Aptamers: Molecular Tools for Analytical Applications. *Anal. Bioanal. Chem.* **2008**, *390* (4), 989–1007.

(45) Brody, E. N.; Gold, L. Aptamers as Therapeutic and Diagnostic Agents. *J. Biotechnol.* **2000**, *74* (1), 5–13.

(46) Ng, E. W. M.; Shima, D. T.; Calias, P.; Cunningham, E. T.; Guyer, D. R.; Adamis, A. P. Pegaptanib, a Targeted Anti-VEGF Aptamer for Ocular Vascular Disease. *Nat. Rev. Drug Discov.* **2006**, *5* (2), 123–132.

(47) Krishnan, Y.; Simmel, F. C. Nucleic Acid Based Molecular Devices. *Angew. Chemie - Int. Ed.* **2011**, *50* (14), 3124–3156.

(48) Tyagi, S.; Marras, S. a; Kramer, F. R. Wavelength-Shifting Molecular Beacons. *Nat. Biotechnol.* **2000**, *18* (11), 1191–1196.

(49) Zhang, P.; Beck, T.; Tan, W. Design of a Molecular Beacon DNA Probe with Two Fluorophores. *Angew. Chemie* **2001**, *113* (2), 416–419.

(50) Bratu, D. P.; Cha, B.-J.; Mhlanga, M. M.; Kramer, F. R.; Tyagi, S. Visualizing the Distribution and Transport of mRNAs in Living Cells. *Proc. Natl. Acad. Sci. U. S. A.* **2003**, *100* (23), 13308–13313.

(51) Santangelo, P. J.; Nix, B.; Tsourkas, A.; Bao, G. Dual FRET Molecular Beacons for mRNA Detection in Living Cells. *Nucleic Acids Res.* **2004**, *32* (6), e57.

(52) Li, J. J. Using Molecular Beacons as a Sensitive Fluorescence Assay for Enzymatic Cleavage of

Single-Stranded DNA. *Nucleic Acids Res.* **2000**, *28* (11), 52e–52.

(53) Biggins, J. B.; Prudent, J. R.; Marshall, D. J.; Ruppen, M.; Thorson, J. S. A Continuous Assay for DNA Cleavage: The Application Of "break Lights" to Enediynes, Iron-Dependent Agents, and Nucleases. *Proc. Natl. Acad. Sci. U. S. A.* **2000**, *97* (25), 13537–13542.

(54) Fang, X.; Liu, X.; Schuster, S.; Tan, W. Designing a Novel Molecular Beacon for Surface-Immobilized DNA Hybridization Studies. *J. Am. Chem. Soc.* **1999**, *121* (12), 2921–2922.

(55) Li, J.; Tan, W.; Wang, K.; Xiao, D.; Yang, X.; He, X.; Tang, Z. Ultrasensitive Optical DNA Biosensor Based on Surface Immobilization of Molecular Beacon by a Bridge Structure. *Anal. Sci.* **2001**, *17* (October), 1149–1153.

(56) Fang, X.; Li, J. J.; Tan, W. Using Molecular Beacons to Probe Molecular Interactions between Lactate Dehydrogenase and Single-Stranded DNA. *Anal. Chem.* **2000**, *72* (14), 3280–3285.

(57) Tan, W. H.; Fang, X. H.; Li, J.; Liu, X. J. Molecular Beacons: A Novel DNA Probe for Nucleic Acid and Protein Studies. *Chem. Eur. J.* **2000**, *6* (7), 1107–1111.

(58) Yao, G.; Tan, W. Molecular-Beacon-Based Array for Sensitive DNA Analysis. *Anal. Biochem.* **2004**, *331* (2), 216–223.

(59) Wang, H.; Li, J.; Liu, H.; Liu, Q.; Mei, Q.; Wang, Y.; Zhu, J.; He, N.; Lu, Z. Label-Free Hybridization Detection of a Single Nucleotide Mismatch by Immobilization of Molecular Beacons on an Agarose Film. *Nucleic Acids Res.* **2002**, *30* (12), e61.

(60) Tuerk, C.; Gold, L. Systematic Evolution of Ligands by Exponential Enrichment: RNA Ligands to Bacteriophage T4 DNA Polymerase. *Science* **1990**, *249* (4968), 505–510.

(61) Robertson, D. L.; Joyce, G. F. Selection in Vitro of an RNA Enzyme That Specifically Cleaves Single-Stranded DNA. *Nature*. **1990**, pp 467–468.

(62) Hamaguchi, K.; Geiduschek, E. P. The Effect of Electrolytes on the Stability of the Deoxyribonucleate Helix. *J. Am. Chem. Soc.* **1962**, *84* (8), 1329–1338.

(63) McFail-Isom, L.; Sines, C. C.; Williams, L. D. DNA Structure: Cations in Charge? *Current Opinion in Structural Biology*. **1999**, 298–304.

(64) Bonner, G.; Klibanov, A. M. Structural Stability of DNA in Nonaqueous Solvents. **2000**, No. 617.

(65) Lerman, L. S. S. Structural Considerations in the Interaction of DNA and Acridines. *J. Mol. Biol.* **1961**, *3* (1), 18–30.

(66) Macquet, J. P.; Butour, J. L. Modifications of the DNA Secondary Structure upon Platinum

Binding: A Proposed Model. *Biochimie* **1978**, *60* (9), 901–914.

(67) Franklin, R. E.; Gosling, R. G. The Structure of Sodium Thymonucleate Fibres. I. The Influence of Water Content. *Acta Crystallogr.* **1953**, *6* (8), 673–677.

(68) Falk, M.; Hartman, K. A.; Lord, R. C. Hydration of Deoxyribonucleic Acid. II. An Infrared Study. *J. Am. Chem. Soc.* **1963**, *85* (4), 387–391.

(69) Bloomfield, V. A.; Crothers, D. M.; Tinoco Jr., I. *Nucleic Acids - Structures, Properties, and Functions*; Stiefel, J., Ed.; University Sciecne Books - Sausalito, California: Sausalito, 2000.

(70) O'Connor, C.; Adams, J. U. Essentials of Cell Biology. *Nat. Educ.* **2010**, 1–100.

(71) Grass, R. N.; Heckel, R.; Puddu, M.; Paunescu, D.; Stark, W. J. Robust Chemical Preservation of Digital Information on DNA in Silica with Error-Correcting Codes. *Angew. Chemie - Int. Ed.* **2015**, *54* (8), 2552–2555.

(72) Owczarzy, R.; Moreira, B. G.; You, Y.; Behlke, M. A.; Walder, J. A. Predicting Stability of DNA Duplexes in Solutions Containing Magnesium and Monovalent Cations. **2008**, 5336–5353.

(73) Stellwagen, E.; Muse, J. M.; Stellwagen, N. C. Monovalent Cation Size and DNA Conformational Stability. **2011**, 3084–3094.

(74) Nishino, T.; Morikawa, K. Structure and Function of Nucleases in DNA Repair: Shape, Grip and Blade of the DNA Scissors. *Oncogene* **2002**, *21* (58), 9022–9032.

(75) Lindahl, T. Instability and Decay of the Primary Structure of DNA. *Nature* **1993**, *362*, 709–715.

(76) Neddermann, P.; Gallinari, P.; Lettieri, T.; Schmid, D.; Truong, O.; Hsuan, J. J.; Wiebauer, K.; Jiricny, J. Cloning and Expression of Human G / T Mismatch-Specific Thymine-DNA Glycosylase * the Formation of G / T Mismatches . We Have Shown Previ-. **1996**, *271* (22), 12767–12774.

(77) Cavalieri, E.; Saeed, M.; Zahid, M.; Cassada, D.; Snow, D.; Miljkovic, M.; Rogan, E. Mechanism of DNA Depurination by Carcinogens in Relation to Cancer Initiation. **2012**, *64* (February), 169–179.

(78) Legoff, J.; Tanton, C.; Lecerf, M.; Bouhlal, H.; Weiss, H.; Belec, L. Influence of Storage Temperature on the Stability of HIV-1 RNA and HSV-2 DNA in Cervicovaginal Secretions Collected by Vaginal Washing. **2006**, *138*, 196–200.

(79) Klibanov, A. M. Enzymatic Catalysis in Anhydrous Organic Solvents. *Trends in Biochemical Sciences*. **1989**, 141–144.

(80) Zaks, a.; Klibanov, a. M. Enzyme-Catalyzed Processes in Organic Solvents. *Proc. Natl. Acad. Sci.*

U. S. A. **1985**, *82* (10), 3192–3196.

(81) Griebenow, K.; Klibanov, A. M. On Protein Denaturation in Aqueous-Organic Mixtures but Not in Pure Organic Solvents. *J. Am. Chem. Soc.* **1996**, *118* (47), 11695–11700.

(82) Mishra, P.; Griebenow, K.; Klibanovt, A. M. Structural Basis for the Molecular Memory of Imprinted Proteins in Anhydrous Media. **1996**, *52*, 609–614.

(83) Schmitke, J. L.; Stern, L. J.; Klibanov, a M. The Crystal Structure of Subtilisin Carlsberg in Anhydrous Dioxane and Its Comparison with Those in Water and Acetonitrile. *Proc. Natl. Acad. Sci. U. S. A.* **1997**, *94* (9), 4250–4255.

(84) Russell, A. J.; Klibanov, A. M. Inhibitor-Induced Enzyme Activation in Organic Solvents. *J. Biol. Chem.* **1988**, *263* (24), 11624–11626.

(85) Kilbanov, A. M. Improving Enzymes by Using Them in Organic Solvents. *Nature* **2001**, *409* (6817), 241–246.

(86) Griebenow, K.; Klibanov, A. M. On Protein Denaturation in Aqueous - Organic Mixtures but Not in Pure Organic Solvents. **1996**, *7863* (4), 141–144.

(87) Klibanov, A. M. In Organic Solvents. **2001**, *409* (January).

(88) Rich, J. O.; Dordick, J. S. Controlling Subtilisin Activity and Selectivity in Organic Media by Imprinting with Nucleophilic Substrates. *J. Am. Chem. Soc.* **1997**, *119* (14), 3245–3252.

(89) Piskur, J.; Rupprechtb, A. Aggregated DNA in Ethanol Solution. **1995**, *375*.

(90) Wang, H.; Wang, J.; Zhang, S. Binding Gibbs Energy of Ionic Liquids to Calf Thymus DNA : A Fluorescence Spectroscopy Study. **2011**, *1501*, 3906–3910.

(91) Jumbri, K.; Abdul Rahman, M. B.; Abdulmalek, E.; Ahmad, H.; Micaelo, N. M. An Insight into Structure and Stability of DNA in Ionic Liquids from Molecular Dynamics Simulation and Experimental Studies. *Phys. Chem. Chem. Phys.* **2014**, *16* (27), 14036–14046.

(92) Application, E. P. *ep001736542a1* (11). **2006**, No. 19, 1–24.

(93) Zhang, W.; Zhu, Q.; Boulfelfel, S. E.; Lyakhov, A. O.; Stavrou, E.; Somayazulu, M.; Prakapenka, V. B. Unexpected Stable Stoichiometries of Sodium Chlorides. **2013**, No. December.

(94) Rogers, R. D.; Seddon, K. R. Ionic Liquids - Solvents of the Future? *Science (80).* **2003**, *302* (5646), 792–793.

(95) Koel, M. Ionic Liquids in Chemical Analysis. *Crit. Rev. Anal. Chem.* **2005**, *35* (3), 177–192.

(96) Zhang, S.; Lu, X.; Zhou, Q.; Li, X.; Zhang, X.; Li, S. Chapter 1 - Database of Ionic Liquids. In *Ionic*

Liquids; **2009**; 3–20.

(97) Olivier-Bourbigou, H.; Magna, L.; Morvan, D. Ionic Liquids and Catalysis: Recent Progress from Knowledge to Applications. *Applied Catalysis A: General*. **2010**, 1–56.

(98) de María, P. D. *Ionic Liquids in Biotransformations and Organocatalysis: Solvents and Beyond*; **2012**.

(99) Baker, G. a; Baker, S. N.; Pandey, S.; Bright, F. V. An Analytical View of Ionic Liquids. *Analyst* **2005**, *130*, 800–808.

(100) Abbott, A. P.; Capper, G.; Davies, D. L.; Rasheed, R. K.; Tambyrajah, V. Novel Solvent Properties of Choline Chloride/urea Mixtures. *Chem. Commun. (Camb).* **2003**, No. 1, 70–71.

(101) Mamajanov, I.; Engelhart, A. E.; Bean, H. D.; Hud, N. V. DNA and RNA in Anhydrous Media: Duplex, Triplex, and G-Quadruplex Secondary Structures in a Deep Eutectic Solvent. *Angew. Chemie - Int. Ed.* **2010**, *49* (36), 6310–6314.

(102) Mondal, D.; Sharma, M.; Mukesh, C.; Gupta, V.; Prasad, K. Improved Solubility of DNA in Recyclable and Reusable Bio-Based Deep Eutectic Solvents with Long-Term Structural and Chemical Stability. *Chem. Commun.* **2013**, *49* (83), 9606.

(103) Ficke, L. E.; Brennecke, J. F. Interactions of Ionic Liquids and Water. *J. Phys. Chem. B* **2010**, *114* (32), 10496–10501.

(104) Liebert, T.; Heinze, T. Interaction of Ionic Liquids Wlth Polysaccharides 5. Solvents and Reaction Media for the Modification of Cellulose. *BioResources*. **2008**, 576–601.

(105) Weingärtner, H.; Cabrele, C.; Herrmann, C. How Ionic Liquids Can Help to Stabilize Native Proteins. *Phys. Chem. Chem. Phys.* **2012**, *14* (2), 415–426.

(106) Van Rantwijk, F.; Lau, R. M.; Sheldon, R. A. Biocatalytic Transformations in Ionic Liquids. *Trends in Biotechnology*. **2003**, 131–138.

(107) Lai, J.-Q.; Li, Z.; Lü, Y.-H.; Yang, Z. Specific Ion Effects of Ionic Liquids on Enzyme Activity and Stability. *Green Chem.* **2011**, *13* (7), 1860.

(108) Aki, S. N. V. K.; Brennecke, J. F.; Samanta, A. How Polar Are Room-Temperature Ionic Liquids? *Chem. Commun.* **2001**, 5, 413–414.

(109) Poole, C. F. Chromatographic and Spectroscopic Methods for the Determination of Solvent Properties of Room Temperature Ionic Liquids. *Journal of Chromatography A*. **2004**, 49–82.

(110) Seddon, K. R.; Stark, A.; Torres, M. J. Influence of Chloride, Water, and Organic Solvents on the

Physical Properties of Ionic Liquids. *Pure Appl. Chem.* **2000**, *72* (12), 2275–2287.

(111) Fumino, K.; Wulf, A.; Ludwig, R. Hydrogen Bonding in Protic Ionic Liquids: Reminiscent of Water. *Angew. Chem. Int. Ed. Engl.* **2009**, *48* (17), 3184–3186.

(112) Macfarlane, D. R.; Vijayaraghavan, R.; Ha, H. N.; Izgorodin, A.; Weaver, K. D.; Elliott, G. D. Ionic Liquid "buffers"-pH Control in Ionic Liquid Systems. *Chem. Commun. (Camb).* **2010**, *46* (c), 7703–7705.

(113) Menhaj, A. B.; Smith, B. D.; Liu, J. Exploring the Thermal Stability of DNA-Linked Gold Nanoparticles in Ionic Liquids and Molecular Solvents. *Chem. Sci.* **2012**, *3* (11), 3216.

(114) Cardoso, L.; Micaelo, N. M. DNA Molecular Solvation in Neat Ionic Liquids. *ChemPhysChem* **2011**, *12* (2), 275–277.

(115) Chandran, A.; Ghoshdastidar, D.; Senapati, S. Groove Binding Mechanism of Ionic Liquids : A Key Factor in Long- Term Stability of DNA in Hydrated Ionic Liquids ? *J. Am. Chem. Soc.* **2012**, *134*, 20330–20339.

(116) Wang, H.; Wang, J.; Zhang, S. Binding Gibbs Energy of Ionic Liquids to Calf Thymus DNA: A Fluorescence Spectroscopy Study. *Phys. Chem. Chem. Phys.* **2011**, *13*, 3906–3910.

(117) Singh, P. K.; Sujana, J.; Mora, A. K.; Nath, S. Probing the DNA-Ionic Liquid Interaction Using an Ultrafast Molecular Rotor. *J. Photochem. Photobiol. A Chem.* **2012**, *246*, 16–22.

(118) Zhou, T.; Xu, G.; Ao, M.; Yang, Y.; Wang, C. DNA Compaction to Multi-Molecular DNA Condensation Induced by Cationic Imidazolium Gemini Surfactants. *Colloids Surfaces A Physicochem. Eng. Asp.* **2012**, *414*, 33–40.

(119) Chaires, J. B. Drug-DNA Interactions. *Current Opinion in Structural Biology*. 1998, pp 314–320.

(120) Strekowski, L.; Wilson, B. Noncovalent Interactions with DNA: An Overview. *Mutat. Res.* **2007**, *623* (1–2), 3–13.

(121) Rescifina, A.; Zagni, C.; Varrica, M. G.; Pistar??, V.; Corsaro, A. Recent Advances in Small Organic Molecules as DNA Intercalating Agents: Synthesis, Activity, and Modeling. *European Journal of Medicinal Chemistry*. **2014**, 95–115.

(122) Egli, M.; Williams, L. D.; Frederick, C. a; Rich, A. DNA-Nogalamycin Interactions. *Biochemistry* **1991**, *30* (5), 1364–1372.

(123) Howell, L. A.; Gulam, R.; Mueller, A.; O'Connell, M. A.; Searcey, M. Design and Synthesis of Threading Intercalators to Target DNA. *Bioorganic Med. Chem. Lett.* **2010**, *20* (23), 6956–

6959.

(124) Zeglis, B. M.; Pierre, V. C.; Barton, J. K. Metallo-Intercalators and Metallo-Insertors. *Chem. Commun.* **2007**, *7345* (44), 4565–4579.

(125) Liu, H.-K.; Sadler, P. J. Metal Complexes as DNA Intercalators. *Acc. Chem. Res.* **2011**, *44* (5), 349–359.

(126) Kwon, Y.-W.; Lee, C. H.; Choi, D.-H.; Jin, J.-I. Materials Science of DNA. *J. Mater. Chem.* **2009**, *19* (10), 1353.

(127) Neto, B. a D.; Lapis, A. a M. Recent Developments in the Chemistry of Deoxyribonucleic Acid (DNA) Intercalators: Principles, Design, Synthesis, Applications and Trends. *Molecules* **2009**, *14* (5), 1725–1746.

(128) Mishra, K.; Bhardwaj, R.; Chaudhury, N. K. Netropsin, a Minor Groove Binding Ligand: A Potential Radioprotective Agent. *Radiat. Res.* **2009**, *172* (6), 698–705.

(129) Waring, M. J. Complex Formation between Ethidium Bromide and Nucleic Acids. *J. Mol. Biol* **1965**, *13*, 269–282.

(130) LePecq, J. B.; Paoletti, C. A Fluorescent Complex between Ethidium Bromide and Nucleic Acids. Physical-Chemical Characterization. *J. Mol. Biol.* **1967**, *27* (1), 87–106.

(131) Sigmon, J.; Larcom, L. L. The Effect of Ethidium Bromide on Mobility of DNA Fragments in Agarose Gel Electrophoresis. *Electrophoresis* **1996**, *17* (10), 1524–1527.

(132) Khimji, I.; Doan, K.; Bruggeman, K.; Huang, P.-J. J.; Vajha, P.; Liu, J. Extraction of DNA Staining Dyes from DNA Using Hydrophobic Ionic Liquids. *Chem. Commun. (Camb).* **2013**, *49*, 4537–4539.

(133) Vijayaraghavan, R.; Izgorodin, A.; Ganesh, V.; Surianarayanan, M.; MacFarlane, D. R. Long-Term Structural and Chemical Stability of DNA in Hydrated Ionic Liquids. *Angew. Chemie - Int. Ed.* **2010**, *49* (9), 1631–1633.

(134) Mazid, R. R.; Cooper, A.; Zhang, Y.; Vijayaraghavan, R.; MacFarlane, D. R.; Cortez-Jugo, C.; Cheng, W. Enhanced Enzymatic Degradation Resistance of Plasmid DNA in Ionic Liquids. *RSC Adv.* **2015**, *5* (54), 43839–43844.

(135) Chandran, A.; Ghoshdastidar, D.; Senapati, S. Groove Binding Mechanism of Ionic Liquids: A Key Factor in Long-Term Stability of DNA in Hydrated Ionic Liquids? *J. Am. Chem. Soc.* **2012**, *134* (50), 20330–20339.

(136) Stanlis, K. K.; McIntosh, J. R. Single-Strand DNA Aptamers as Probes for Protein Localization in Cells. *J. Histochem. Cytochem.* **2003**, *51* (6), 797–808.

(137) Ueyama, H.; Takagi, M.; Takenaka, S. A Novel Potassium Sensing in Aqueous Media with a Synthetic Oligonucleotide Derivative. Fluorescence Resonance Energy Transfer Associated with Guanine Quartet-Potassium Ion Complex Formation. *J. Am. Chem. Soc.* **2002**, *124* (48), 14286–14287.

(138) Cruz-Aguado, J. A.; Penner, G. Determination of Ochratoxin A with a DNA Aptamer. *J. Agric. Food Chem.* **2008**, *56* (22), 10456–10461.

(139) Dave, N.; Liu, J. Fast Molecular Beacon Hybridization in Organic Solvents with Improved Target Specificity. *J. Phys. Chem. B* **2010**, *114* (47), 15694–15699.

(140) Ehrentreich-Forster, E.; Orgel, D.; Krause-Griep, A.; Cech, B.; Erdmann, V. A.; Bier, F.; Scheller, F. W.; Rimmele, M. Biosensor-Based on-Site Explosives Detection Using Aptamers as Recognition Elements. *Anal. Bioanal. Chem.* **2008**, *391* (5), 1793–1800.

(141) Keisaku Okada, I. ; S.; Senda, I. ; A.; Kobayashi, T. ; E.; Fukusaki, S. ; I.; Yanagihara, S. ; T.; Nakanishi, Y. Aptamer Capable of Specifically Adsorbing to Bisphenol A and Method for Obtaining the Aptamer, **2005**.

(142) Meng, C.; Zhao, X.; Qu, F.; Mei, F.; Gu, L. Interaction Evaluation of Bacteria and Protoplasts with Single-Stranded Deoxyribonucleic Acid Library Based on Capillary Electrophoresis. *J. Chromatogr. A* **2014**, *1358*, 269–276.

(143) Chaou, T.; Vialet, B.; Azéma, L. DNA Aptamer Selection in Methanolic Media: Adenine-Aptamer as Proof-of-Concept. *Methods* **2016**, *97*, 11–19.

(144) Tomac, S.; Sarkar, M.; Ratilainen, T.; Wittung, P.; Nielsen, P. E.; Norde, B.; Gra, A.; Nordén, B.; Gräslund, a. Ionic Effects on the Stability and Conformation of Peptide Nucleic Acid Complexes. *J. Am. Chem. Soc.* **1996**, *118* (96), 5544–5552.

(145) Nishimura, N.; Ohno, H. Design of Successive Ion Conduction Paths in DNA Films with Ionic Liquids. *J. Mater. Chem.* **2002**, *12* (8), 2299–2304.

(146) Ding, Y.; Zhang, L.; Xie, J.; Guo, R. Binding Characteristics and Molecular Mechanism of Interaction between Ionic Liquid and DNA. *J. Phys. Chem. B* **2010**, *114* (5), 2033–2043.

(147) Pabbathi, A.; Samanta, A. Spectroscopic and Molecular Docking Study of the Interaction of DNA with a Morpholinium Ionic Liquid. *J. Phys. Chem. B* **2015**, *119* (34), 11099–11105.

(148) Marusic, M.; Tateishi-Karimata, H.; Sugimoto, N.; Plavec, J. Structural Foundation for DNA Behavior in Hydrated Ionic Liquid: An NMR Study. *Biochimie* **2015**, *108*, 169–177.

(149) Qin, W.; Li, S. F. Y. Electrophoresis of DNA in Ionic Liquid Coated Capillary. *Analyst* **2003**, *128* (1), 37–41.

(150) Satpathi, S.; Sengupta, A.; Hridya, V. M.; Gavvala, K.; Koninti, R. K.; Roy, B.; Hazra, P. A Green Solvent Induced DNA Package. *Sci. Rep.* **2015**, *5*, 9137.

(151) Lyubchenko, Y. L. AFM Imaging in Liquid of DNA and Protein-DNA Complexes. In *Atomic Force Microscopy in Liquid*; Baró, A. M., Reifenberger, R. G., Eds.; Wiley, **2012**; 231–258.

(152) Pang, D.; Thierry, A. R.; Dritschilo, A. DNA Studies Using Atomic Force Microscopy: Capabilities for Measurement of Short DNA Fragments. *Front. Mol. Biosci.* **2015**, *2* (January), 1.

(153) Hansma, H. G.; Revenko, I.; Kim, K.; Laney, D. E. Atomic Force Microscopy of Long and Short Double-Stranded, Single-Stranded and Triple-Stranded Nucleic Acids. *Nucleic Acids Res.* **1996**, *24* (4), 713–720.

(154) Hansma, H. G.; Bezanilla, M.; Zenhausern, F.; Adrian, M.; Sinsheimer, R. L. Atomic Force Microscopy of DNA in Aqueous Solutions. *Nucleic Acids Res.* **1993**, *21* (3), 505–512.

(155) Liu, Z.; Li, Z.; Zhou, H.; Wei, G.; Song, Y.; Wang, L. Imaging DNA Molecules on Mica Surface by Atomic Force Microscopy in Air and in Liquid. *Microsc. Res. Tech.* **2005**, *66* (4), 179–185.

(156) Nguyen, H. H.; Park, J.; Kang, S.; Kim, M. Surface Plasmon Resonance: A Versatile Technique for Biosensor Applications. *Sensors (Switzerland)*. **2015**, 10481–10510.

(157) Serrano-Santos, M. B.; Llobet, E.; Özalp, V. C.; Schäfer, T. Characterization of Structural Changes in Aptamer Films for Controlled Release Nanodevices. *Chem. Commun. (Camb).* **2012**, *48* (81), 10087–10089.

(158) Tateishi-Karimata, H.; Sugimoto, N. A-T Base Pairs Are More Stable than G-C Base Pairs in a Hydrated Ionic Liquid. *Angew. Chemie - Int. Ed.* **2012**, *51* (6), 1416–1419.

CHAPTER 2

Materials and Methods

2.1. Experimental Methods (Chapter 3 to Chapter 5)

2.1.1. Reagents

2.1.1.1. Buffer

Tris Buffered Saline (TBS) buffer was prepared in 1L of ultra-pure water consisting of 50 mM Tris, 138 mM NaCl, 2.7 mM KCl, 5 mM $MgCl_2$ and adjusted to pH 8.0 at 25 ˚C. All aforementioned reagents were purchased from Sigma-Aldrich, Spain. All solutions were prepared with ultra-pure water (18 MΩ) produced with the Ultra Clear TWF with EI-Ion CEDI electro deionization system from Inycom, Spain.

2.1.1.2. ATP DNA aptamer, molecular beacon and oligomers

The ATP-DNA-aptamer, the ATP-DNA-molecular aptamer beacon and the DNA-oligonucleotides were purchased from Eurofins (mwg | operon), biomers or VBC biotech, all purified by HPLC. Their sequences are listed below.

ATP DNA Aptamer:[1,2]

5'-ACC TGG GGG AGT ATT GCG GAG GAA GGT-3'

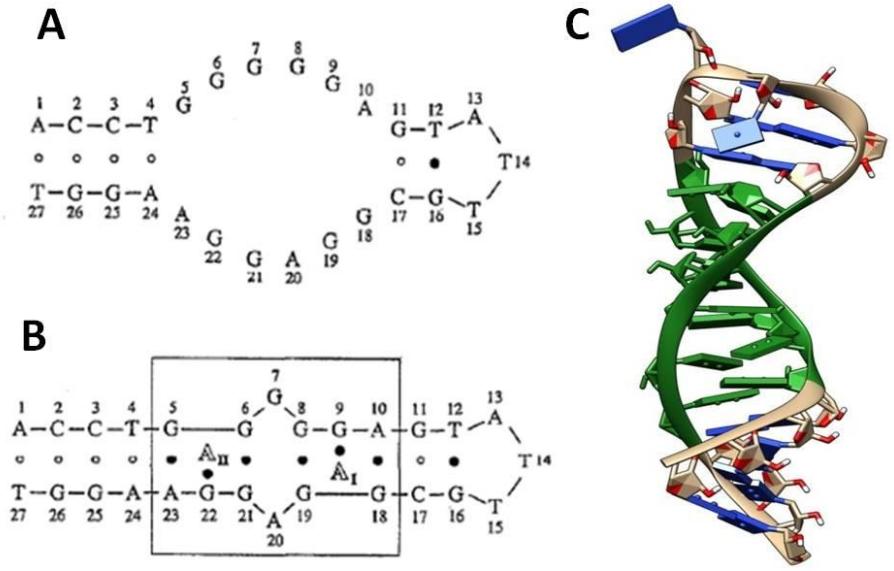

Figure 2.1. ATP-aptamer structure and conformation determined by **a)** Huizenga and Szostak, **b)** Lin and Patel and **c)** by the Chimera software.

ATP DNA Aptamer Molecular Beacon (MB):

5'-CAC CTG GGG GAG TAT TGC GGA GGA AGG TTX XXX XXC CAG GTG-3'

The 5' and 3' ends of the sequence were labeled with Alexa Fluor 488 (AF488) and a black hole quencher 1 (BHQ1), respectively. The "X"-sequence represents an alkyl chain of 18 carbons used as a linker to provide the DNA aptamer beacon with a

flexible loop which warrants its reversible opening/closing function. Besides, this linker also keeps the fluorophore far enough from the quencher when the MB is open (according to the Förster distance), allowing then a correct fluorescence emission upon recognition of ATP. The MB was designed by Prof. Veli Cengiz Özalp.

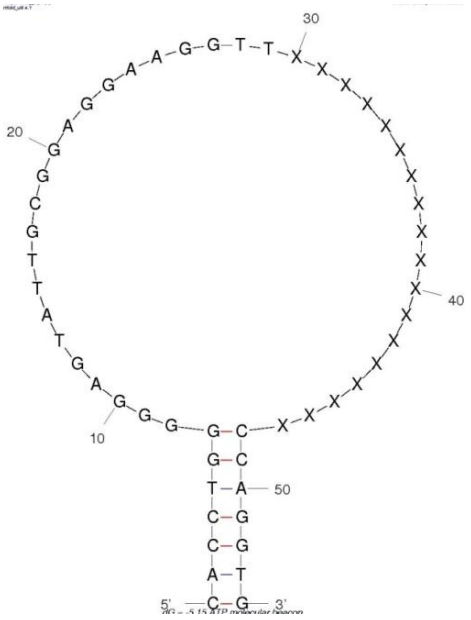

Figure 2.2. ATP-molecular aptamer beacon predicted structure by the mfold software. Even not represented, to the 5' end and to the 3' end are linked the Alexa Fluor 488 and the Black Hole Quencher, respectively. The prediction was performed by mfold software.

DNA-oligonucleotides (oligos):

Oligomer 1: 5’-AGG TTC CAG GTG-3’

Oligomer 2: 5’-CAC CTG GAA CCT-3’

Containing 7 nucleobases identical to one strand of the MB stem, the oligomer 2 used was a GC-rich 12-mer (GC content 58.3%) for better stability, and was also modified with a covalently labeled BHQ1 (**Figure 2.3 up**) at its 3’ extremity. Oligomer 1 was the complementary strand of oligomer 2 and was also modified with a covalently labeled AF488 (**Figure 2.3 bottom**) at its 5’ end.

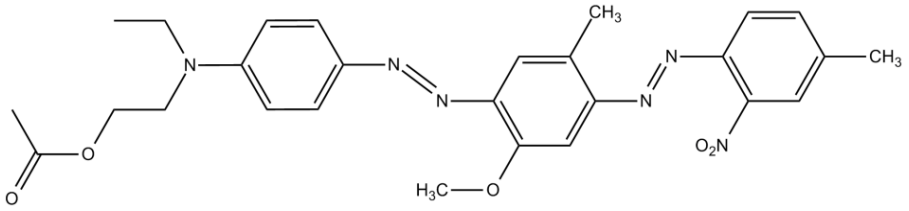

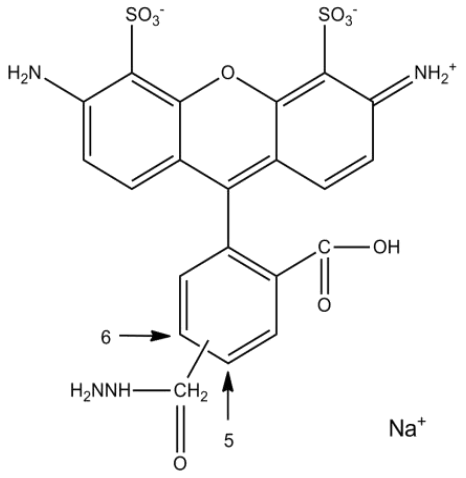

Figure 2.3. Chemical structure of the black hole quencher 1 (top) and the Alexa Fluor 488 dye (bottom).

2.1.1.3. Molecular Targets

Adenosine 5'-monophosphate (5'-AMP), adenosine (99%) and guanosine 5'-monophosphate (5'-GMP) targets - **Figure 2.4** - were purchased from Sigma-Aldrich. For each one a stock solution was prepared with TBS buffer from which further dilutions were made. The pH of each solution was adjusted to 8.0.

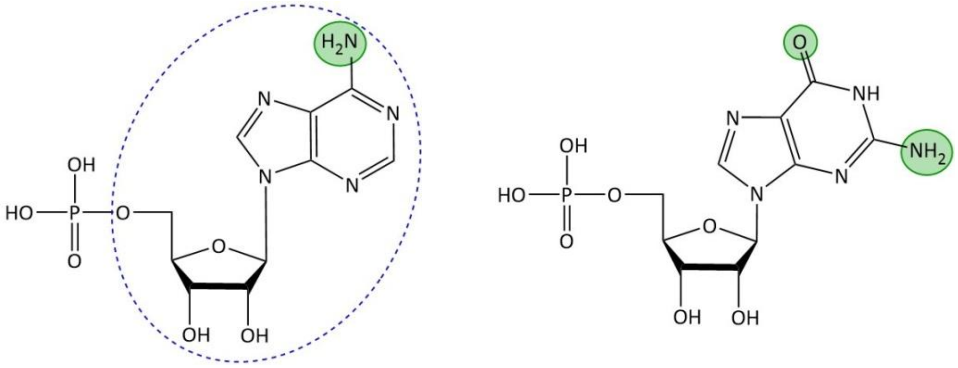

Figure 2.4. Chemical structure of 5'-AMP (left) and 5'-GMP (right). The structural differences between the two targets are highlighted in green. The adenosine structure is surrounded by the blue dashed circle.

2.1.1.4. Ionic Liquids

The ionic liquid ethylammonium nitrate (EAN) used in Chapter 3 was synthesized in the lab according to Werzer O., et al., 2010.[3] The details of the preparation are described in the next section of methods. For the experiments in

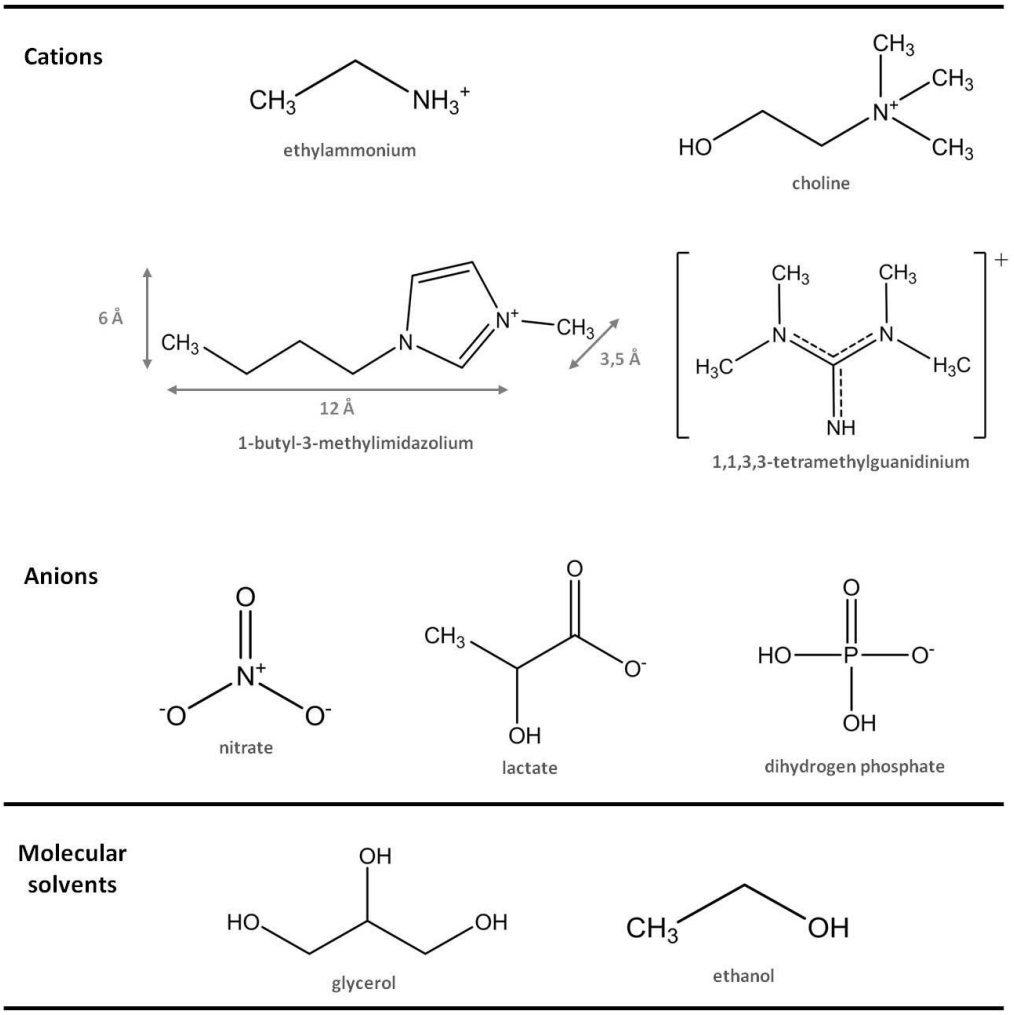

Figure 2.5. Chemical structure of the ionic liquids and organic solvents used. Dimensions of BMIM-Cl from Ref. 4.

Chapter 4 and Chapter 5, EAN was purchased from Solvionic, France, and used as received. EAN is liquid at room temperature (melting point 12 ^{o}C).

The ionic liquids choline lactate (CL), choline nitrate (CN), choline dihydrogen phosphate (CDHP), 1,1,3,3-tetramethylguanidinium lactate (TMGL) and 1-butyl-3-methylimidazolium chloride (BMIM-Cl) were purchased from Solvionic, France and were used as received.

2.1.1.5. Salts and Molecular Solvents

The salts NaCl, NaDHP, NaLac and $NaNO_3$ and the organic solvent glycerol were purchased from Sigma-Aldrich and used as received. Concentrated stock-solutions of each salt and solvent were prepared with ultra-pure water and then diluted further. Ethanol (absolute, 99,9% v/v) was purchased from Panreac and directly added to TBS buffer during the experiments.

2.1.2. Methods

*2.1.2.1. Synthesis of ethylammonium nitrate (EAN) and analysis of the obtained product (**Chapter 3**)*

The reaction between ethylamine and nitric acid to origin ethylammonium nitrate is represented in scheme 2.1 and was conducted according to Werzer O., et al., 2011.[3] Thus, an equimolar amount of the Brønsted base ethylamine (C_2H_7N; Sigma–Aldrich, 70% w/w) and the Brønsted acid nitric acid (HNO_3) (Panreac, ≥ 69% w/w) were mixed to react in excess water. The mixing was done carefully while purging with nitrogen and maintaining the solution at 8 - 10 ^oC to prevent the formation of oxide impurities. Water was later on removed by rotary evaporation at 50 - 55 ^oC and under vacuum. Finally, the solution was heated to 105 - 110 ^oC over a oil bath for 12h to remove any possible remaining volatile impurities including water. Hereby the solution was also purged with nitrogen.

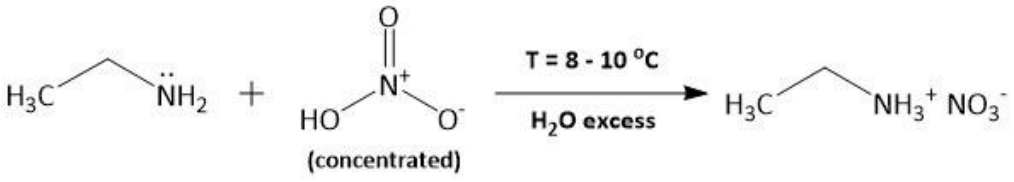

Scheme 2.1. Ethylamine reacting with concentrated nitric acid at low temperature to yield ethylammonium nitrate ($C_2H_8N_2O_3$).

2.1.2.1.1. Water content analysis by Karl Fisher

The water content in EAN was determined using a Metrohm 831 Karl Fisher coulometer and a percentage of 1.5% of water was found under constant reference storage conditions (room temperature conditions) of EAN, conducting periodic measurements in triplicate.

2.1.2.1.2. Elemental Analysis

To confirm the structure of the EAN synthesized, we resorted to elemental analysis. The content of carbon (C), hydrogen (H), nitrogen (N) and oxygen (O) was determined. Oxygen was determined by the difference between the total percentage and the sum of the percentages of the other elements. The results presented in **Table 2.1** list the values measured for each element, as well as the theoretical values expected.

Table 2.1 Experimental and theoretical percentage values of the atoms that consist EAN, determined by elemental analysis.

	theory, %				measured, %			
	C	**H**	**N**	**O**	**C**	**H**	**N**	**O**
EAN	22.2	7.4	25.9	44.5	20.4	7.8	25.5	46.2
					20.8	7.8	25.4	46.0

2.1.2.1.3. FT-IR and NMR

Fourier Transform Infrared spectroscopy (FT-IR) and Nuclear Magnetic Resonance spectroscopy (NMR) were employed to confirm the structure of the EAN synthesized.

For FTIR, a small drop of EAN was placed in a KBr pellet and the IR-spectrum determined. The FT-IR equipment was operated with a resolution of 4 cm^{-1} and scanning range from 4000 to 400 cm^{-1}. The FT-IR spectrum in **Figure 2.6** shows the characteristic peaks of EAN, each indicated by an arrow: -N-H, 3430-3450 cm^{-1}; -CH_2, 3030 cm^{-1}; -CH_3, 2880 cm^{-1}; NO_3, 1590 cm^{-1}; -C-N-, 1200 cm^{-1}. The peak at 3290 cm^{-1} corresponds to O-H bonds, probably due to the ambient water present in the system. The FT-IR spectrum confirmed the structure of EAN.

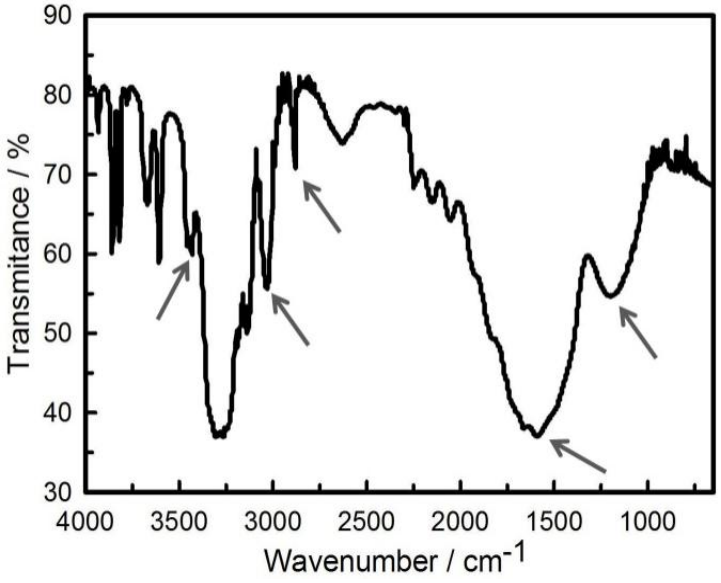

Figure 2.6. FTIR spectrum of the synthesized EAN.

The ^{1}H-NMR spectrum of EAN was obtained by dissolving the latter in an appropriate deuterated solvent (DSS was used for reference signal), with a final volume of 500 μl. The chemical shifts (δ) expressed in parts per million (ppm) were: δ = 4.68 (NH_3), 2.94, 2.92, 2.90, 2.88 (-CH_2) and 1.13, 1.11, 1.09 (-CH_3). Data analysis was carried out with MesteNova software package.

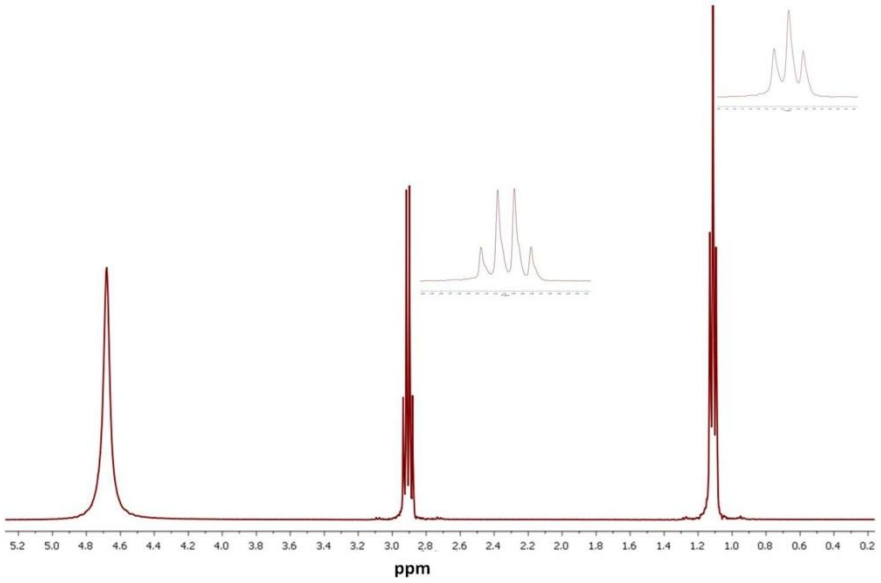

Figure 2.7. NMR spectrum of the synthesized EAN, with the zoom of the multiplex peaks.

2.1.2.2. Other ionic liquids

CN, CDHP and BMIM-Cl are solid at room temperature (melting points 34 ^{o}C, 185 ^{o}C, 70 ^{o}C, respectively), while TMGL (melting point C) presents a jelly-like texture and CL is liquid but very viscous (melting point C). Nevertheless, dissolved in a very small amount of water, each of these ILs becomes a clear and fluid liquid at room temperature.[5] In consequence, stock solutions of 70% w/w (CL), 75% w/w (CDHP, BMIM-Cl) and 80% w/w (CN and TMGL) were prepared to be used in the

experiments and stored at room temperature. By mixing ILs with water, some of them presented intrinsic acidity (EAN, CL, CDHP and TMGL). When preparing the samples with the TBS buffer, the buffering capacity was maintained when using EAN, but the pH decreased when mixing CL, CDHP and TMGL. In order to adjust the pH of these samples to the same as the buffer (pH 8.0) necessary amounts of 5 M of NaOH were added (**Table 2.2**). Since the pH of CDHP samples was more difficult to adjust, 10 M of NaOH was used for adjustment for the higher concentrations of CDHP in solution. The addition of NaOH resulted in an overall increase of the Na^+ cation in solution. Apparently, the results were not affected by this increased amount and, even with the highest concentrations of ILs, the amount of Na^+ in solution never reached the highest amounts of NaCl used (**Table 2.2**).

Despite adjusting previously the pH, the influence of the pH change in the DNA hybridization amount and rate was tested in a pH range between 4 and 9 (see Figure A1 and Figure A2 in the **Annex** for the results), by mixing different amounts of 0,5M of sodium phosphate monosalt (NaH_2PO_4) solution with 0,5M sodium phosphate di-salt (Na_2HPO_4) solution. It was determined that the rate of hybridization decreases below pH 7 and above pH 8,5. However, the amount of DNA that hybridizes do not changes significantly between pH 5 and 8,5.

Table 2.2. Total concentration of NaOH added to the IL-buffer solutions to adjust the pH to 8.0. Then, total Na^+ concentration present in each solution from the TBS buffer and from the added NaOH. On the last column is the total Na^+ concentration obtained when to the TBS buffer NaCl was added (**Chapter 5**).

	5 or 10 M [NaOH] added (mM)			Total [Na^+] (mM) (NaCl buffer + NaOH added)			Total [Na^+] (mM) (NaCl buffer + NaCl added)
[IL] (% v/v)	**CL**	**CDHP**	**TMGL**	**CL**	**CDHP**	**TMGL**	**NaCl**
0	0	0	0	138	138	138	138
1	0	50	0	138	188	138	188
3	15	100	0	153	238	138	288
5	33	213*	33	171	351	171	388
8	33	407*	35	171	545	173	538
10	33	433*	43	171	571	181	638
25	67	583*	107	205	721	245	1421
40	167	667*	153	305	805	291	2190

*In these samples 10 M of NaOH to adjust the pH were used.

2.1.2.3. Preparation of solutions of AMP, adenosine and GMP

A stock solution of the targets used for the studies with the ATP-aptamer or with molecular aptamer beacon were prepared by dissolving 350 mg of AMP, adenosine or GMP in 1.5 ml of 1M NaOH. Then 1.0 ml of ultra-pure water was added to the previous mixture. Subsequently, the pH was adjusted with 5M of NaOH to

obtain a final pH of 8, similar to the pH of TBS. Finally, the volume was adjusted with ultra-pure water to obtain a final concentration of 330 mM of AMP, adenosine or GMP and a total volume of 3 ml.

2.1.2.4. Fluorescence measurements

For **Chapters 3**, **4** and **5**, the fluorescence measurements were conducted employing a FS920 single photon counting spectrofluorimeter from Edinburgh Instruments (Edinburgh, Scotland, UK) equipped with a 450 W xenon arc lamp. Since the fluorophore used during the experiments was Alexa Fluor 488, using the kinetic scan setup fluorescence versus time the excitation was measured at 480 nm with an emission at 520 nm, and a monochromator bandwidth at 3 and 6 nm, respectively. During measurements, the temperature was controlled by the T-App Temperature Control Application software to be 25 ˚C.

For molecular recognition studies of **Chapters 3** and **5**, samples were prepared stepwise by: introducing the concentration of ionic liquid intended with TBS buffer into a quartz cuvette of 10 mm light path; adding the molecular beacon; and finally adding the molecular target to yield the different concentrations of AMP or GMP

(50, 250, 500, 750, 1000, 1500, 2000 and 2500 μM) or adenosine (50, 250, 500, 750, 1000 and 1500 μM).

The hybridization studies of **Chapters 3** and **5** consisted in: introducing the concentration of ionic liquid intended with TBS buffer into a quartz cuvette of 10 mm light path; adding then the oligomer 1 (25 μM), followed by the oligomer 2 (25 μM) and finally rising the temperature from 25 to 70 ˚C to obtain the *Tm* of the double-strand previously formed.

In **Chapter 5**, the reverse method was carried out to check whether there was any difference between the formation of dsDNA in presence of ILs or the formation of dsDNA in pure buffer followed by addition of ILs. In the latter case the oligomers were added together in pure TBS buffer at 25 ^{o}C into a quartz cuvette of 10 mm light path to hybridize; subsequently the intended concentrations of ionic liquids were added to this solution. The fluorescence was registered in each step.

Figures 2.8, **2.9** and **2.10** illustrate a typical time-dependent measurement in pure aqueous buffer for studying the molecular recognition (**Chapters 3** and **5**), the hybridization and melting (**Chapters 3** and **5**), and the melting of the dsDNA by the addition of ILs (**Chapter 5**), respectively. Together with the concurrently acquired

temperature data, step 4 in **Figure 2.9** allowed determining the melting temperature of double-stranded oligomers.

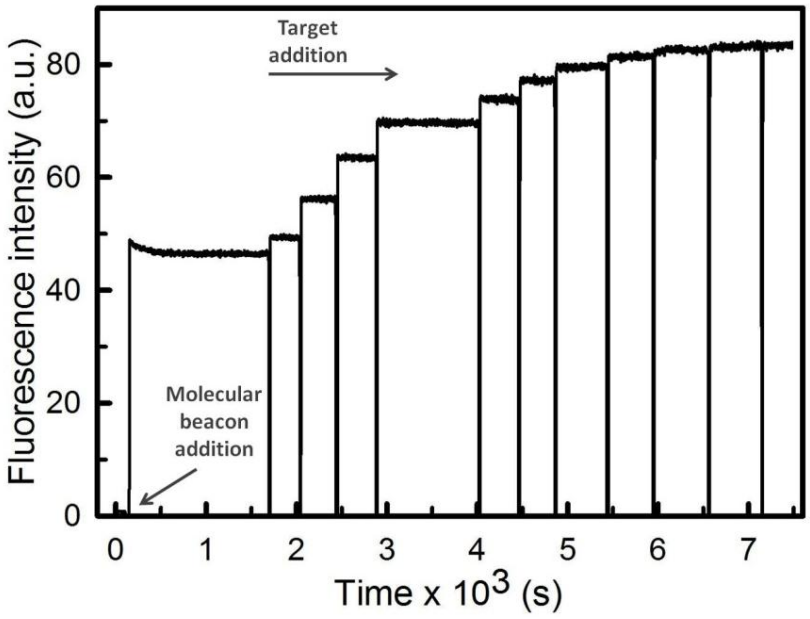

Figure 2.8. Real time measurement of the fluorescence intensity increase resulting from the opening of the MB after target recognition.

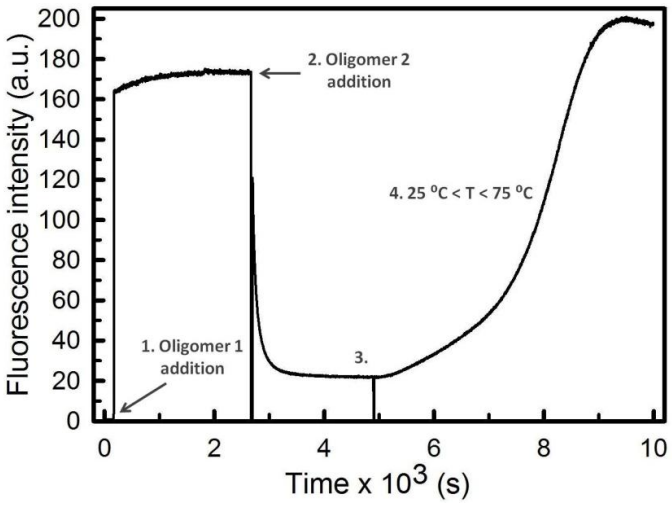
Fluorescence intensity (a.u.)
200
180
160
140
120
100
80
60
40
20
0
0
2
4
6
8
10
Time x 10^3 (s)
1. Oligomer 1 addition
2. Oligomer 2 addition
3.
4. 25 °C < T < 75 °C

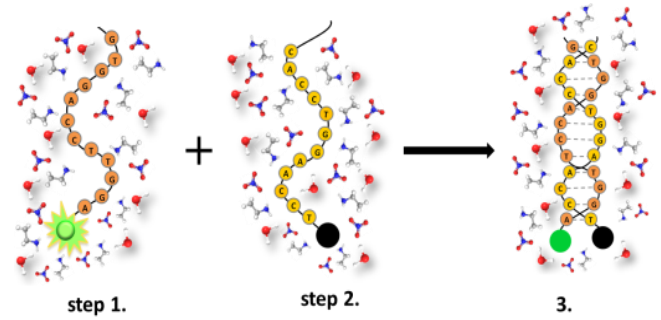
step 1.
step 2.
3.

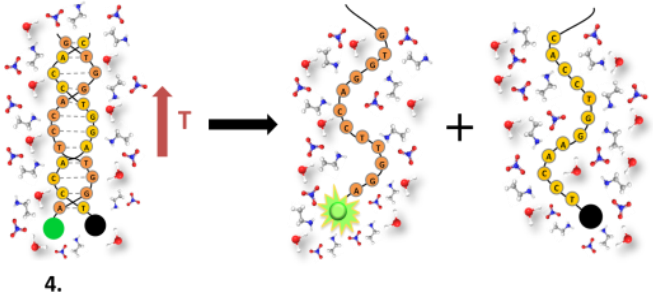
T
4.

Figure 2.9 Real time change in fluorescence signal resulting from the hybridization and the melting of the oligomers in solution. **1.** Fluorescence background of the TBS or TBS/IL solution followed by the oligomer 1 addition; **2.** Maximum fluorescence obtained after the addition of oligomer 1 to the solution. For the determination of the amount of DNA that subsequently hybridizes we consider this plateau 100% of fluorescence; Addition of oligomer 2; **3.** After the addition of oligomer 2 hybridization occurs reaching its equilibrium value. From these time-dependant data we determine the hybridization rate. The difference between plateau 2 and 3 represents the quantity of DNA hybridized; **4.** DNA melting curve with the temperature values being recorded with time in parallel to calculate the T_m.

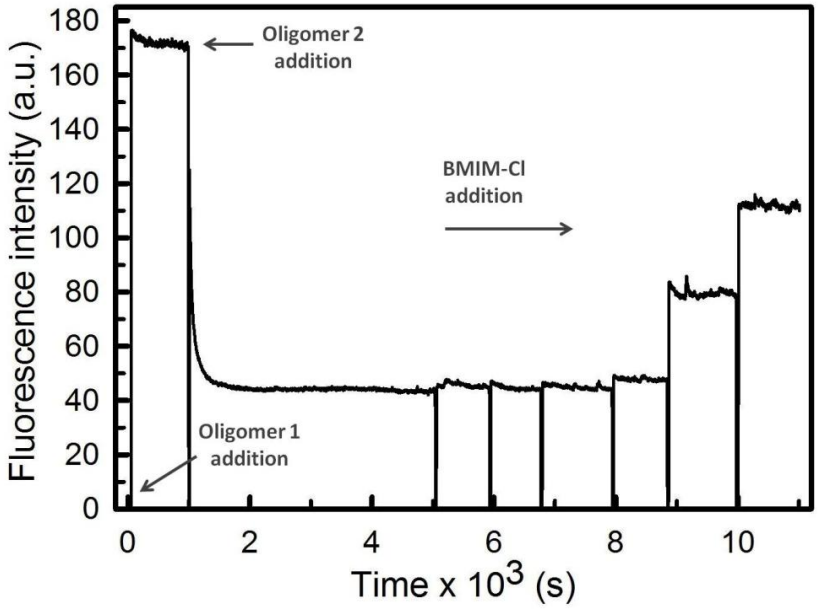

Figure 2.10. Real time change in fluorescence signal resulting from the hybridization of the oligomers in solution with TBS and the subsequent melting by the addition of (in this particular case) BMIM-Cl.

During the experiments leading to the results presented in **Chapter 4**, Alexa Fluor 488 or the oligomer 1 were added to the solution in a 10 mm light path cuvette at 25 ^{o}C to yield a final concentration of 25 nM or 17 nM, respectively. The measurements were done at an excitation wavelength of 480 nm and an emission at wavelength of 520 nm.

For FRET, the emission of the AF488 was measured exciting and emitting at the same wavelengths, but with a concentration of AF488 of 1 μM in order to obtain a more perfect emission spectrum.

2.1.2.5. Calculation of the dissociation constant, K_d

The dissociation constant K_d was calculated from mathematical fitting of the normalized raw data of **Figure 2.8**.

The normalization of the data was made following the equation 2.1:

$$F\left([AMP]\right)_N = \frac{F\left([AMP]\right)}{F_0} - 1 \qquad \text{(equation 2.1)}$$

where, *F([AMP])* is the mean value of the raw fluorescence obtained upon the

addition of the different concentrations of AMP target in solution with the AMP-molecular aptamer beacon; F_0 is the initial raw fluorescence obtained when [AMP] = 0 μM, just due to the introduction of the molecular beacon in solution and then $F([AMP])_N$ is the normalized fluorescence at each different concentration of AMP target in solution.

With this normalization we force all set of data starting from zero. The data obtained from this equation are represented in **Figure 3.1**.

Using the Sigma-Plot ligand binding fitting for one site binding saturation, equation 2.2, we determined the K_d value as for the AMP-molecular aptamer beacon in TBS as with 2 M of EAN in solution. Since this aptamer is specific for AMP independently if we have EAN in solution or not, we were not able to calculate the K_d values for GMP.

$$F\left([AMP]\right)_N = \frac{B_{máx.} \times [AMP]}{K_d + [AMP]}$$

(equation 2.2)

2.1.2.6. Calculation of the hybridization rate, k_h

The hybridization rate k_h was calculated from mathematical fitting of the raw data following the work of Tsuruoka M., et al.[6] According to their work we used the following equations to fit our fluorescence data and determine k_h:

$$F(t) = F_0 + a \cdot e^{-b \cdot t} \quad \text{(equation 2.3)}$$

where *F(t)* is the fluorescence at time *t*, F_0 is the initial fluorescence when the hybridization between the two oligomers starts, and *a* and *b* are constants obtained through curve fitting, with

$$b = [oligo2]_0 \cdot k_h \quad \text{(equation 2.4)}$$

Thus, knowing constant *b* and the initial concentration of the oligomer 2 we can calculate the hybridization rate k_h between the two oligomers.

2.1.2.7. Calculation of percentage of DNA hybridized

As a reference condition, the amount of DNA hybridized in TBS buffer solution was considered to be 100% as a maximum reference value. The quantity of hybridized DNA in TBS/EAN solution was calculated relative to this value by subtracting (Figure 2.9) plateau value 3 from plateau value 2. The auto-fluorescence of TBS or TBS/IL solution did hereby not need to be accounted for, since it is considered in both plateau values.

2.1.2.8. Calculation of the melting temperature T_m

After the hybridization of the two oligomers resulting in of the double-strand, the temperature of the system was increased from 25˚C to 70˚C at a rate of 0.5˚C/min to determine the melting temperature, T_m. T_m was determined at the point of inflection when recording fluorescence as a function of the temperature, as can be seen in Figure 2.9.

2.1.2.9. Calculation of the fluorescence correction of Figure 3.6

The fluorescence values represented in Figure 3.6 were firstly corrected by the auto-fluorescence of EAN and by the dilution factor caused by the addition of EAN to the dsDNA+TBS solution. The influence of EAN in the emission of fluorescence by the Alexa Fluor fluorophore of the oligomer 1 was also accounted for. By adding increasing concentrations of EAN to a solution with only oligomer 1 in TBS, a calibration curve was determined and used to correct the above mentioned values as follows:

$$F = Fi \times (-0{,}00055 \cdot [EAN]^2 + 0{,}04398 \cdot [EAN] + 1{,}09188)$$

(equation 2.5)

where, *F* is the corrected fluorescence that we pretended; *Fi* the measured fluorescence after subtracting the auto-fluorescence of EAN and accounting for the dilution factor of EAN addition; and *[EAN]* is the corresponding concentration of EAN.

All calculations were carried out using the SigmaPlot 11.0 and 12.0 suite of programs.

2.1.2.10. Circular Dichroism (CD)

The CD spectrum of the ATP-aptamer was recorded from 350 to 200 nm; the data gathered per spectrum were the average of 36 time scans at a scanning rate of 200 nm/min and a bandwidth of 5 nm to minimize the noise and to smooth the signal. The scan of 2 M of EAN alone recorded at room temperature was subtracted from the average scan for the ATP-aptamer to see the real influence of the ionic liquid on the conformational change of the aptamer. The data were collected in milidegrees versus wavelength.

2.1.2.11. Theoretical Calculations

The theoretical calculations presented in this thesis were performed by Prof. Elixabete Rezabal, expert in the field part of the research group when the corresponding experimental work was being carried out.

Density Functional Theory (DFT) geometry optimizations and frequency calculations were performed at the B3LYP/TZVP,[7–11] theory level, as implemented in the Gaussian09 program.[12]

The binding energy between EAN and the nucleobases was defined as the enthalpy balance of the reaction

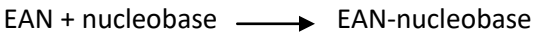

Harmonic frequency calculations were carried out, ensuring that there were no imaginary modes; enthalpy values were obtained by performing a thermo-chemistry analysis using the standard expressions for an ideal gas in the canonical ensemble.

2.2. Experimental Methods (Chapter 4)

To understand whether the ionic liquids affect the emission of the fluorophore Alexa Fluor 488 used in our studies, we divided this part of the work in two situations where the fluorophore was present:

- **Situation 1:** Alexa Fluor 488 free in TBS solution with increasing concentrations of ILs;

- **Situation 2:** oligomer 1 labelled with Alexa Fluor 488 in TBS solution with increasing concentrations of ILs.

In both situations the steady state fluorescence emission was measured as detailed above.

In addition the following methods were also used to carrid the work of **Chapter 4** out.

2.2.1. Viscosity measurements

The viscosity measurements were carried out by Dr. Mercedes Fernández. A controlled stress rheometer (AR-G2, TA Instruments) was employed to analyze ILs viscosities using cone and plate geometry with 4 mm diameter and 2 cone angle. This rheometer is especially suitable for testing ILs as it only requires a very small amount of sample (1–2 mL) to wet the whole cone surface. Samples were initially equilibrated for 5 min, then the shear rate was exponentially increased from 10 to 8000 s^{-1} via stress controlled feedback over 5 min recording 10 points per decade. Since these ILs are highly hydrophilic and the solution measured contained already

water, each measurement was performed with a new sample. Repetitiveness was very good with root-mean square deviations (RMSD) less than 5% in all series. The temperature of viscosity measurement was always assessed at 293 K employing a Peltier plate to set the temperature. All measurements were performed at atmospheric pressure.

2.2.2. Emission measurements

The fluorescence emission measurements of 25 nM of AF488 (same concentration as used with oligomers) were conducted in a quartz cuvette 10 mm light path, employing a FS920 single photon counting spectrofluorimeter from Edinburgh Instruments (Edinburgh, Scotland, UK) equipped with a 450 W xenon arc lamp. The excitation was at 480 nm. The temperature was controlled by the T-App Temperature Control Application software to be 25 ˚C.

2.2.3. UV-vis absorbance measurements

The UV-vis absorbance measurements were conducted with the cuvette option of a NanoDrop 2000c UV-Vis spectrophotometer (Thermo Scientific) using a

10 mm light path cuvette at 25 ^{o}C: for FRET measurements (**section 4.2.1.3. - Chapter 4**), a sample of each stock-solution of the ILs was measured, to obtain the maximum absorbance with the maximum concentration of each IL (EAN pure; CN and TMGL 80% w/w; CDHP and BMIM-Cl 75% w/w; CL 70% w/w); for the absorbance spectra of the fluorophore with increasing concentration of ILs (**section 4.2.1.4. - Chapter 4**), the Alexa Fluor 488 final concentration was 0.8 μM, and the ILs were adding step-by-step to reach the required concentration. The AF488 concentration here was higher than in the fluorescence measurements due to the differences in the sensitivity of the devices. The pure TBS solution was considered as the baseline directly in the device the for all measurements. Then separately the absorbance values for TBS+IL were determined for each concentration by triplicate and the average was subtracted to the absorbance values of TBS+AF488+IL. The obtained values were finally multiplied by the dilution factor. Each spectra represent the mean absorbance values obtained from 3 measurements.

2.2.4. Fluorescence lifetime measurements

The time resolved photoluminescence (PL) decays were recorded using a PicoQuant Microtime200 time resolved confocal microscope system, equipped with an Olympus IX71 inverted microscope. Each sample was prepared with TBS buffer and containing 0.8 μM of AF488 and the different ILs used with concentrations of 0.25M, 1M and 3M, separately. The samples were excited by a 485 nm picosecond laser pulse (PicoQuant DH-485 laser heads controlled by Sepia II driver). The system has an overall resolution of 200 ps. PL lifetime maps (two-dimensional in-plane variations of the PL decay times) were calculated on a per pixel basis by fitting the lifetime of each pixel to the logarithm of the intensity.

2.3. Experimental Methods (Chapter 6 - SELEX)

2.3.1. DNA SELEX Library

The SELEX method starts with the library design. This particular library, called D3, was designed by the group of Professor Günter Mayer in the Life & Medical

Science (LIMES) Institute - Universität Bonn, in Bonn, Germany. A 80-mer single DNA was designed with 18 and 19 nucleotides primer flanking known sequences at the 5' and 3' ends, respectively, and a randomized 43 nucleotide internal sequence represented by "N" (**Figure 2.10**). In addition, two primer sequences were designed according with the library primers template to use in the PCR procedure. The reverse primer was 5'-phosphate labelled to make possible the later digestion of dsDNA into ssDNA by the lambda exonuclease.

The sequences of the library and the primers were as follows:

5’-GCT GTG TGA CTC CTG CAA - N43 - GCA GCT GTA TCT TGT CTC C-3’

or

5’-GCT GTG TGA CTC CTG CAA (AGCT) GCA GCT GTA TCT TGT CTC C-3’

Forward primer (Fw):

5'-GCT GTG TGA CTC CTG CAA-3'

Reverse primer (5'-Pho-Rv):

5'-Phos-GGA GAC AAG ATA CAG CTG C-3'

Figure 2.10. Design and prediction of the SELEX library. The prediction was performed by mfold software.

2.3.2. Target molecule

The target molecule used was purchased from Jena Bioscience as adenosine triphosphate (ATP) immobilized at the C8 of the purine ring through a 9 atom spacer to agarose to yield 8-Amino-hexyl-ATP-Agarose (**Figure 2.11**).

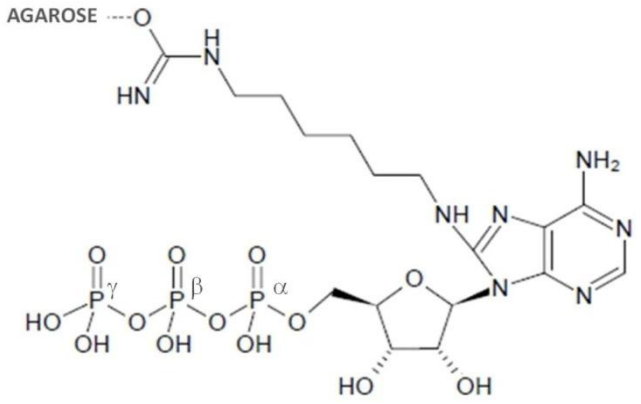

Figure 2.11. Structural formula of the immobilized 8-Amino-hexyl-ATP. The ATP molecule is linked to agarose through the C8 of the purine ring through a 9 atom spacer, exposing in this way the purine for molecular recognition.

2.3.3. Buffer and ionic liquid

Tris-HCl buffer was used in the SELEX procedure and prepared according to Huizenga and Szostak, 1995, consisting of 20 mM Tris, 300 mM NaCl, 5 mM $MgCl_2$ and the pH was adjusted to 7.6 with HCl at room temperature.[1]

The ionic liquid used was choline lactate and was used as explained above.

2.3.4. SELEX procedure

The strategy of the SELEX started with the initial D3 DNA library being incubated with the ATP target immobilized on agarose beads (**Figure 6.1 - step 1**). For this incubation and for all the other SELEX steps bio-spin chromatography columns from Bio-Rad with a porous 30 μm polyethylene bed support and 1,2 ml bed volume were used (**Figure 2.12**).

Figure 2.12. Bio-spin chromatography columns from Bio-Rad used during the SELEX procedure.

In each round, 100 μL of the suspension with the target beads (≈5 μM) were introduced in the column and washed with the 200 μl of Tris-HCl buffer for five times. Then, 200 μL of a solution containing the desired concentration of the DNA pool were added to the column for interaction with the target by incubating in a thermomixer at a constant temperature of 25 ^{o}C. The solvent consisted of Tris-HCl buffer, representing the positive control, and in parallel the selection matrix of Tris-HCl with 2M of choline lactate as the new solvent that we wanted to introduce in the system. After the incubation time, which as selection pressure step was being

decreased along with SELEX rounds (**Table 2.3**), both incubation solutions were let to pass by gravity and the flow through obtained was discarded.

Unbound or weakly bound DNA was washed off the column using buffer or buffer with 2M of choline lactate, respectively, to maintain the same conditions as during incubation. The DNA that specifically bound to the ATP in solution was then eluted by heat denaturation with 200 μL of previously heated water (95 ˚C) and by placing the columns at 95 ˚C for 2 minutes. The sample from the elution step was then used for amplification by PCR. By eluting with water, the amount of IL remaining in this solution from the previous step was then diluted and became residual. As a consequence, the ILs would not interfere with the subsequent PCR procedure used to amplify the number of binding DNA sequences for the next round.

Each PCR reaction was then carried out in presence of 200 μM of dNTPs (deoxynucleotides triphosphate - A, G, T, C), 2mM of $MgCl_2$ and 2,5 units of *Taq* polymerase per 100 μL of reaction. The primer concentrations were 1 μM for both the forward and the reverse primer. The thermal cycling was 95 ˚C for 60 s, 64 ˚C for

30 s, 72 ˚C for 45 s, for as many cycles as needed depending on the reaction, and 72 ˚C for 120 s for final extension.

After amplification of the obtained sequences from the elution step, an agarose electrophoresis gel 4% (2g agarose; 50 ml TBE buffer) was performed to confirm that the double-stranded DNA had formed properly. Ethidium bromide was added to each sample of the running gel. The electrophoresis of each gel was carried out at 130-150 V by 10-15 min. As a reference we used a Gene Ruler Ultra Low Range DNA Ladder 10-300 bp from Thermo-Fisher Scientific (**Figure 2.13**). The ladder is a mixture of chromatography-purified individual DNA fragments.

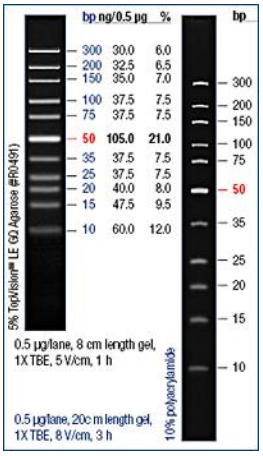

Figure 2.13. Gene Ruler Ultra Low Range DNA Ladder 10-300 bp used in the agarose gel as reference control.

After confirmation of the success of PCR by the agarose gel, the samples were purified using the NucleoSpin Gel and PCR Clean-up kit form Macherey-Nagel, Germany.

To convert the dsDNA from the PCR process into ssDNA again, we used λ-exonuclease. λ-exonuclease is a 5′ to 3′ exodeoxyribonuclease that selectively digests the 5′-phosphorylated strand of dsDNA at 37 ^{o}C. For this purpose, a 5′-phosphate group is introduced into one strand of dsDNA by performing PCR where only one of the two primers is 5′-phosphorylated. The phosphorylated strand is then removed by digestion with λ-exonuclease and the sequence that remains is the one used for the next SELEX round. Before proceeding with the latter, and after the confirmation of the digestion into ssDNA by another agarose gel 4% (**Figure 6.3**), the samples were purified to eliminate the λ-exonuclease. This was done through deactivating the samples at 80 ^{o}C first, followed by using the NucleoSpin Gel and PCR Clean-up kit.

The sequences of interest were then used in the next round of SELEX and all the previous steps were repeated for all rounds. Consecutive rounds of SELEX were performed until completing the 8th round of selection, based on the results

reported by Huizenga and Szostak.[1] Finally, we verified whether the enrichment of the pool had in fact been achieved.

During the SELEX procedure the parameters of the pool concentration, incubation time and the number of washing steps of the formed complex were changed in order to increase the stringency of the process (**Table 2.3**). In this manner the specificity of the DNA pool to the ATP target may be increased and, hence, the enrichment of the pool is more likely to be reached.

Table 2.3. Parameters changed along the selection process, SELEX "pressure".

SELEX round	D3 DNA pool (pmol)	Incubation time (min.)	Nº washing steps
1	500	30	5
2-3	50	30	5
4	25	30	8
5	25	30	10
6-7	25	20	10
8-12	25	15	10

2.3.4.1. Evolution monitoring of the SELEX method (enrichment of the pool)

2.3.4.1.1. Kinasation

In order to determine the enrichment of the sequences during the SELEX process, the ssDNA sequences of the rounds of interest were labelled with the radioisotope γ-^{32}P-ATP. The labelling was performed using 10 U/μl T4 Polynucleotide Kinase (T4 PNK) which catalyzes the transfer of the γ-^{32}phosphate from ATP to the free 5' hydroxyl terminus of the polynucleotides. Recall that with the use of λ-exonuclease during the selection process we guaranteed that the sequence with the 5'-phosphate was digested. Hence, the ssDNA sequences that were obtained during the kinasation possessed an OH- group at the 5' end, the one to which the kinase will attach the γ-^{32}P. The ssDNA sequences of interest were incubated with T4 PNK enzyme, 10x T4 PNK buffer (New England Biolabs), γ-^{32}P-ATP and ultrapure water in a total volume of 20 μl for 1h at 37 ^{o}C. Thereafter, 30 μl of ultrapure water were added to complete a volume of 50 μl and the solution was purified in the Illustra MicroSpin G25 columns (GE Healthcare Life Sciences) centrifuging at 720 rcf for 2 min. This purification step removes all the free γ-^{32}P-ATP still in solution.

2.3.4.1.2. PAGE-Gel

To assure that the samples of the previous section were properly labelled with the γ-^{32}P-ATP, 30 ml of a polyacrilamide gel 15% were prepared and PAGE gel performed.

After assembling the plates, spacers and clamps, the PAGE gel was prepared and it was proceeded following the next protocol: mix 18 ml of 25% Bis / Acrylamide containing 8.3 M urea; 9 ml of 8.3 M urea in water; 3 ml of 8.3 M urea in 10x TBE-buffer (TBE = 89 mM Tris, pH 8.0, 89 mM boric acid and 2 mM EDTA); 240 μl of 10% APS and 12 μl of TEMED, which should be the last to be added since it is the initiator of the polymerization. Pour the mixture into the space between the two glass plates previously assembled and insert the comb. Let it polymerize for at least 30 min. Carefully remove the comb and the spacer at the bottom of the glass plates. Assemble the gel-running unit. Fill the lower chamber with running buffer and remove any air bubbles between gel and buffer. Afterwards, fill the upper chamber with buffer and rinse the wells with running buffer using a syringe. Mix 50 μL of radioactively labeled DNA sample from the previous section of kinasation, with 17 μL 4× PAGE-gel loading buffer (9M Urea, 50 mM EDTA, pH 8.0), heat it for 3 min at 80

°C and load onto the gel immediately. Run the gel with 300 V, 25 mA for ≈1h or until the used dye xylene cyanol band has migrated through 2/3 of the gel. Remove the gel from the gel-running unit and the glass plates and wrap it in plastic foil. Put the gel into an irradiation cassette and place an imaging plate on top, close the cassette and expose the screen for 10 min. Read the screen using a phosphorimager. Print the image at 100 % scale.

2.3.4.1.3. Liquid scintillation counting (LSC)

The radioactively labelled samples were incubated with ATP immobilized on agarose beads, and a run similar to a single SELEX round was performed (**Figure 6.5**). For this purpose, all supernatants collected during the process were kept for further measurement in a liquid scintillator using the Cherenkov counting. With the Cherenkov counting we yield the activity of a radioactive sample in a liquid solution by counting the resultant photon emissions. The results obtained from the scintillation counter were in counts per minute (CPM). Considering that the sum of the CPM of the collected solutions plus the beads corresponded to 100% of the radioactivity that we introduced in each column with the incubation sample, we

could calculate the percentage of DNA that specifically bound to the ATP target. All measurements were made in duplicate.

2.3.4.2. Cloning procedure

The cloning procedure was carried out by the Ph.D student Anna Maria Pyka in the laboratory of Prof. Günter Mayer in the Life & Medical Science (LIMES) Institute - Universität Bonn, in Bonn, Germany.

TOPO TA Cloning® kit was selected in order to perform the cloning procedure of final SELEX samples. TOPO Cloning provides a highly efficient, and one-step cloning strategy ("TOPO® Cloning) for the direct insertion of *Taq* polymerase-amplified PCR products into a plasmid vector. The plasmid vector pCR2.1-TOPO TA is supplied linearized with: a) Single 3´-thymidine (T) overhangs for TA Cloning®; b) Topoisomerase I covalently bound to the vector (referred to as "activated" vector).

Taq polymerase has a non template-dependent terminal transferase activity that adds a single deoxyadenosine (A) to the 3´ ends of PCR products. The linearized vector supplied in this kit has single, overhanging 3´ deoxythymidine (T) residues. This allows PCR inserts to ligate efficiently with the vector.

Topoisomerase I from *Vaccinia* virus binds to duplex DNA at specific sites and cleaves the phosphodiester backbone after 5'-CCCTT in one strand.[13] The energy from the broken phosphodiester backbone is conserved by formation of a covalent bond between the 3' phosphate of the cleaved strand and a tyrosyl residue (Tyr-274) of topoisomerase I. The phospho-tyrosyl bond between the DNA and enzyme can subsequently be attacked by the 5' hydroxyl of the original cleaved strand, reversing the reaction and releasing topoisomerase.[14]

In order to complete the procedure, the steps described in the next section have been carried out.

2.3.4.2.1. Preparation of LB-agar plates / LB-medium

20 g of LB-powder were added with 15 g of agar and both to an 1 L of distilled water. The medium was then autoclaved (121 ^{o}C, 20 min.). After cool LB agar solution until it was possible to safely handle (to around 60 ^{o}C), ampicillin was added (final: 50 µg/mL). Then the LB agar solution was poured on plates and let them cool. The plates were stored bottom up at 4 ^{o}C. The remained medium was also stored at 4 ^{o}C.

2.3.4.2.2. PCR with Taq-polymerase

Prepare one 100 µl of PCR reaction for each SELEX round to be cloned (+ one NTC) according **Table 2.4**. Use Go-*Taq* polymerase (3' A addition needed).

Table 2.4. PCR reaction components.

Substance	Volume	Stock Conc.	Final Conc.
Buffer	20 µL	5x	1x
$MgCl_2$	8 µl	25 mM	2 mM (+1.5 mM)
dNTPs	1 µL	25 mM	250 µM
fw-Primer	1 µL	100 µM	0.5 µM
rev-Primer (without 5'-P)	1 µL	100 µM	0.5 µM
***Taq*-polymerase**	1 µL	5 U/µL	0.025 U/µL
ddH_2O	67 µL		
Template / water	1 µl		

The thermal cycling of PCR consisted in 95 ^{o}C for 2 min., then a repetition of 7 cycles of 95 ^{o}C for 30s, 62 ^{o}C for 30s, 72 ^{o}C for 1 min. and finally at 72 ^{o}C for 5 min. for final extension. The PCR outcome was checked by an 4% agarose gel.

2.3.4.2.3. Cloning

After cloning TOPO TA reaction, prepare one sample with 2 μl of each PCR product (and one with NTC as negative control) and add 2 μL of water, 1 μl salt-solution and 1 μl of the vector (that come with the kit). The reaction was mixed gently and incubated at 23 ^{o}C, 300 rpm for 30 min. Then the cloning reaction was placed on ice. The TOP10-cells (*E.* coli) were then carefully thawed on ice for 5 minutes. 2 μl of the cloning sample were added and gently mixed and incubated 10 min. on ice. Heat-shocking step (30 seconds at 42 ^{o}C without shaking) is required before immediately transferring the tubes to ice again for 2 min.

2.3.4.2.4. Inoculation on media-LB agar plates

a) Add 250 μL SOC-Medium at room temperature and incubate at 37°C, 300 rpm, for 1h;

b) Plate 20/50/100 μl from each sample on pre-warmed LB-plates (Amp) prepared on section *2.2.4.2.1.*

c) Incubate at 37°C overnight.

2.3.4.2.5. Clone picking for overnight culture

Prepare 50 Falcons of 15 ml with 5 ml of LB-Amp-Medium (50 µg/ml Amp) for each sample. Pick 50x ONE colony with a white pipette tip and dip it into the medium. Incubate overnight at 37°C in the incubator.

2.3.4.2.6. Plasmid extraction

The plasmid extraction procedure was performed by the NucleoSpin Plasmid DNA Purification kit (Macherey-Nagel) by follow the next steps:

a) Use 2 ml *E. coli* LB culture and centrifuge at 11000 x g for 60 sec. Discard supernatant;

b) Add 250 µL Buffer A1, resuspend cell pellet by vortexing;

c) Add 250 µL Buffer A2 and invert tube gently 6 – 8x. Do not vortex;

d) Incubate at room temperature for 5 min. until lysate is clear;

e) Add 300 µL Buffer A3 and invert tube gently 6 – 8x. Do not vortex;

f) Centrifuge 5 min. at 11000 x g at room temperature;

g) Repeat this step in case the supernatant is not clear;

h) Place column in a 2 ml collection tube, load supernatant onto column.

Centrifuge 1 min at 11000 x g. Discard flow-through and add 500 µL AW-Buffer. Centrifuge 1 min at 11000 x g;

i) Add 600 µL Buffer A4. Centrifuge 1 min at 11000 x g;

j) Discard flow-through and centrifuge 2 min. Discard collection tube;

l) Place column in a fresh 1.5 ml tube;

m) Add 50 µL water, incubate 1 min. at RT, centrifuge 1 min. at 11000 x g.

2.3.4.3. Sequencing

Before starting with the sequencing method, the concentration of the plasmid solution was measured. For sequencing, 20 µl of 30-100 ng/µl of plasmid solution are required. A simple confirmation of the purification of the plasmid was carried out by standard PCR for control. The PCR was performed using 1 µl of each plasmid solution and the commercial M13 primers. Then, the band (around 300 bp) that corresponds to the specific plasmid segment was observed by gel electrophoresis. The sequencing of the final obtained SELEX sequences were carried out by GATC biotech company.

2.4. References

(1) Huizenga, D. E.; Szostak, J. W. A DNA Aptamer That Binds Adenosine and ATP. *Biochemistry* **1995**, *34* (2), 656–665.

(2) Lin, C. H.; Patel, D. J. Structural Basis of DNA Folding and Recognition in an AMP-DNA Aptamer Complex: Distinct Architectures but Common Recognition Motifs for DNA and RNA Aptamers Complexed to AMP. *Chem. Biol.* **1997**, *4* (11), 817–832.

(3) Werzer, O.; Warr, G. G.; Atkin, R. Conformation of Poly(ethylene Oxide) Dissolved in Ethylammonium Nitrate. *J. Phys. Chem. B* **2011**, *115* (4), 648–652.

(4) Gebbie, M. a; Valtiner, M.; Banquy, X.; Fox, E. T.; Henderson, W. a; Israelachvili, J. N. Ionic Liquids Behave as Dilute Electrolyte Solutions. *Proc. Natl. Acad. Sci. U. S. A.* **2013**, *110* (24), 9674–9679.

(5) Vijayaraghavan, R.; Izgorodin, A.; Ganesh, V.; Surianarayanan, M.; MacFarlane, D. R. Long-Term Structural and Chemical Stability of DNA in Hydrated Ionic Liquids. *Angew. Chemie - Int. Ed.* **2010**, *49* (9), 1631–1633.

(6) Tsuruoka, M.; Yano, K.; Ikebukuro, K.; Nakayama, H.; Masuda, Y.; Karube, I. Optimization of the Rate of DNA Hybridization and Rapid Detection of Methicillin Resistant Staphylococcus Aureus DNA Using Fluorescence Polarization. *J. Biotechnol.* **1996**, *48* (3), 201–208.

(7) Becke, A. D. Density-Functional Exchange-Energy Approximation with Correct Asymptotic Behavior. *Phys. Rev. A* **1988**, *38* (6), 3098–3100.

(8) Lee, C.; Yang, W.; Parr, R. G. Development of the Colle-Salvetti Correlation-Energy Formula into a Functional of the Electron Density. *Phys. Rev. B* **1988**, *37* (2), 785–789.

(9) Stephens, P. J.; Devlin, F. J.; Chabalowski, C. F.; Frisch, M. J. Ab Initio Calculation of Vibrational Absorption and Circular Dichroism Spectra Using Density Functional Force Fields. *J. Phys. Chem.* **1994**, *98* (45), 11623–11627.

(10) Schäfer, A.; Horn, H.; Ahlrichs, R. Fully Optimized Contracted Gaussian-Basis Sets for Atoms Li to Kr. *J. Chem. Phys.* **1992**, *97* (4), 2571–2577.

(11) Schäfer, A.; Huber, C.; Ahlrichs, R. Fully Optimized Contracted Gaussian Basis Sets of Triple Zeta Valence Quality for Atoms Li to Kr. *J. Chem. Phys.* **1994**, *100* (8), 5829.

(12) Frisch, M. J.; Trucks, G. W.; Schlegel, H. B.; Scuseria, G. E.; Robb, M. A.; Cheeseman, J. R.; Scalmani, G.; Barone, V.; Mennucci, B.; Petersson, G. A.; et al. Gaussian 09, Revision D.01. *Gaussian Inc.* 2009, p Wallingford CT.

(13) Shuman, S. Recombination Mediated by Vaccinia Virus DNA Topoisomerase I in Escherichia Coli Is Sequence Specific. *Proc Natl Acad Sci U S A* **1991**, *88* (22), 10104–10108.

(14) Shuman, S. Novel Approach to Molecular Cloning and Polynucleotide Synthesis Using Vaccinia DNA Topoisomerase. *J. Biol. Chem.* **1994**, *269* (51), 32678–32684.

CHAPTER 3

DNA Aptamers as Functional Molecular Recognition Sensors in a Protic Ionic Liquid

3.1. Introduction

The multifunctionality of a complex macromolecule such as DNA, from storing and processing genetic information to specifically recognizing other molecules, is strongly associated to its solvation in an aqueous medium. Recently, XNA has been reported as an artificial nucleic acid, which does not occur in Nature but which still is capable of performing similar functions as conventional DNA in aqueous solutions,[1,2] giving rise to what has been coined “synthetic genetics”, and possibly augmenting the degree of freedom in designing the properties of synthetic genetic material. In view of this context, we wondered in how far it would be feasible to increase the degree of freedom even further through substituting, in turn, the aqueous medium by liquids that possess a high degree of tuneability while warranting the functionality of DNA. Such solvents may be ionic liquids (ILs), which are long known as designer solvents and the physicochemical properties of which may be adjusted by selecting the appropriate cations and anions.[3–5] They have been studied as solvents or additives in enzymatic processes,[6,7] and as solvation medium for proteins.[8–10] DNA films with high ionic conductivity were one of the early works involving ionic liquids and DNA, reported by Nishimura and Ohno,[11] and since then the stability of dsDNA

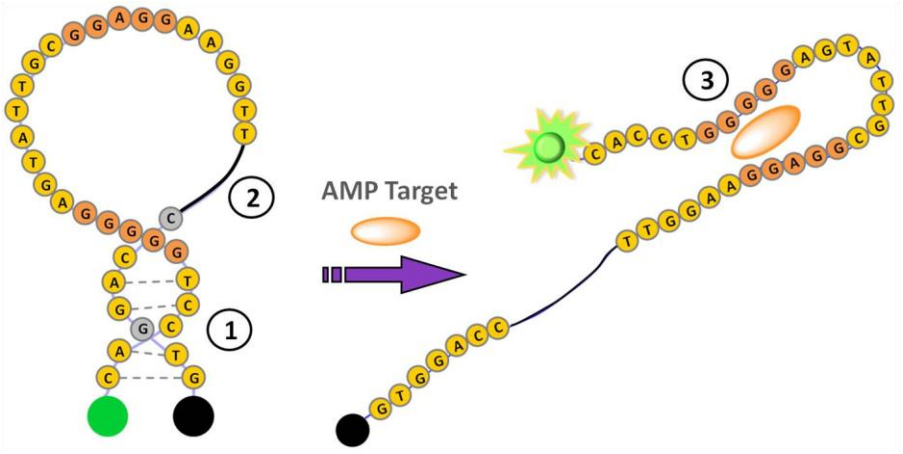

Scheme 3.1. Representation of the target recognition by a DNA molecular beacon probe and its main structural parts: 1) stem of hybridized strands; 2) loop (with a C18 linker represented by the black line); 3) recognition binding pocket.

in ionic liquids has been investigated in several works.[12–15] However, to the best of our knowledge, none of these works has systematically correlated so far the structural changes of DNA occurring in ionic liquids with their molecular recognition function, such as it occurs in DNA-molecular beacons. Aptamers are single stranded nucleic acids (ssDNA or RNA), which specifically recognize their desired targets such as proteins, amino acids, antibiotics or even small molecules.[16–20] They can conveniently be modified chemically by introducing a linker, as well as a fluorophore/quencher couple giving rise to the so-called molecular beacon (**Scheme**

3.1). In the absence of the target, the MB prevails in a stem–loop or "hairpin" design formed by dsDNA, thereby keeping the fluorophore and quencher in close proximity (about 7–10 nm)[21] such that an overall low emission of fluorescence occurs owing to fluorescence resonance energy transfer (FRET). Upon selective interaction of the MB with its target, however, the hairpin stem denatures and opens through breaking the respective hydrogen bonds of the dsDNA, resulting in the fluorophore to move away from the quencher and hence emitting a measurable increase of fluorescence (**Scheme 3.1**). In this way, MBs lend DNA the functionality of a molecular-recognition machine combined with a reversible conformational change. Hence, the concept of "stability" goes beyond that known from dsDNA or ssDNA as it refers to maintaining a reversible "function" rather than only a stable conformation. In fact, structural stability is to some extent unwanted for MBs as their function relies precisely on a reversibility of their structure depending on the presence of a target. This highly interesting feature has prompted DNA-molecular beacons (DNA-MBs) to be studied as "nanogates" in mesoporous devices.[22–24] Since MB probes were developed,[25] they have found applications in in vitro RNA and DNA monitoring, biosensors and biochips, nucleic-acid amplification, enzymatic studies, as well as gene typing and

mutation detection,[26–30] mainly because their molecular interaction with targets can conveniently be measured by spectrofluorimetry.

In our study, we used an AMP aptamer molecular beacon to investigate its molecular recognition capacity of AMP in a protic ionic liquid, ethylammonium nitrate (EAN). The latter shares with water the capacity to form a hydrogen-bond network.[31,32] It was also previously found to interfere least with the conformation of TMR (C102)-cyt c (tetramethylrhodamine-labeled yeast cytochrome c) when compared with aprotic imidazolium-based ILs,[8] a finding which served as a starting point for our studies, although bearing in mind that proteins and oligonucleic acids are in general two entirely different systems.

3.2. Results and Discussion

Henceforth, throughout all work, the denomination "AMP-aptamer" is used synonymous with "ATP-aptamer" since the respective DNA sequence is specific for both AMP and ATP.[33,34]

3.2.1. Affinity and specificity of the ATP-aptamer in EAN solution

Figure 3.1 displays the molecular recognition of AMP by the AMP molecular aptamer beacon both in Tris buffer solution (TBS) and in a 2M solution of EAN in TBS

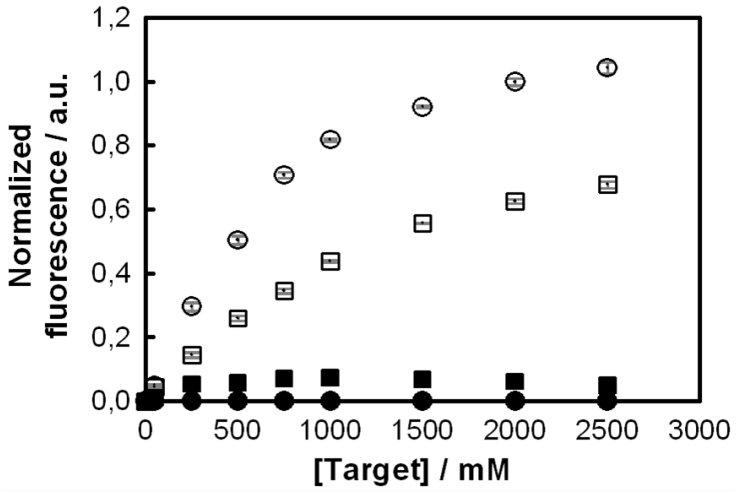

Figure 3.1. Normalized fluorescence obtained by the recognition of AMP-molecular aptamer beacon of increasing concentrations of AMP in 0 M (open circles) and 2 M (open squares) of EAN with the respective error bars and GMP in 0 M (filled circles) or 2 M (filled squares) of EAN in TBS solution at 25 ˚C.

corresponding to ≈17% (v/v) of EAN. In the latter, the EAN concentration was tenfold more concentrated than all the other salts in the TBS buffer (see **Chapter 2**). It should be noted that the aptamer beacon was initially selected in total absence of EAN, so that addition of the ionic liquid at such a high concentration means a significant perturbation of the standard working conditions. Based on the normalized fluorescence data (**Equation 2.1** in **Chapter 2**) it can be seen that with 2M of EAN in TBS solution the aptamer was still capable of recognizing AMP. A dissociation constant (K_d) of 1654 μM in 2M EAN/TBS solution compared favorably to a K_d of 834 μM in pure TBS solution, indicating a slight decrease in sensitivity. However, the recognition specificity of the aptamer was perfectly maintained as verified in both solutions against guanosine monophosphate (GMP), a structurally very similar target (see structures of targets in **Figure 2.2** - **Chapter 2**) but which is not recognized by the AMP-aptamer. While the decrease in sensitivity might seem significant, it should be emphasized that the AMP aptamer had initially been selected through SELEX[33] to be selective for AMP in TBS solution only, and in entire absence of EAN. The functioning of the aptamer MB at such a high concentration of EAN is therefore remarkable, although further addition of EAN inevitably deteriorated aptamer performance also detected by a considerable increase of the

K_d (Table in **Figure 3.2**). While running a SELEX procedure with an EAN-containing buffer solution would possibly yield an optimized aptamer sequence - detailed later in **Chapter 6** - the macroscopic observations noted above evidenced that DNA-based molecular recognition might be feasible even in unusual non-molecular solvents, such as ILs. This is surprising given that the functionality of DNA-MBs is based on a very subtle interplay between forces which would be

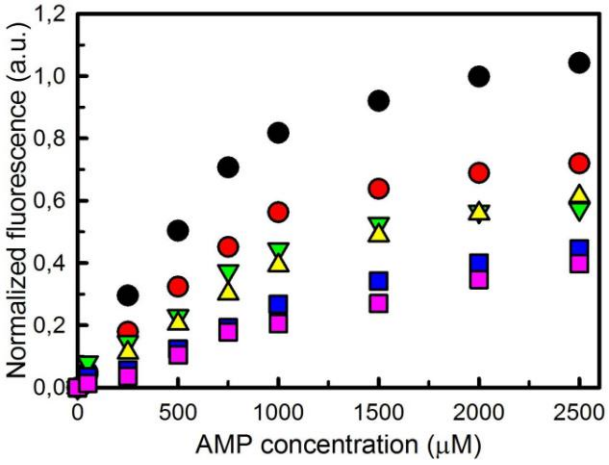

[EAN] (M)	*Kd* (μM)
0,00	834
0,12	998
0,58	1034
2,00	1654
2,92	3115
4,00	4554

Figure 3.2. Normalized fluorescence obtained by the recognition of AMP-molecular aptamer beacon of increasing concentrations of AMP in 0 M (black), 0.12 M (red), 0.58 M (green), 2 M (yellow), 2.92 M (blue) and 4 M (pink) and the respective K_d values obtained for each concentration of EAN in TBS solution at 25 ˚C.

expected to be strongly imbalanced by the presence of a fully charged solvent such as an ionic liquid. We, therefore, investigated in more detail how an ionic liquid such as EAN interacts and affects the functionality of DNA-MBs on the molecular level with the aim of exploring to what extent DNA may be used in liquid environments that are not conventional molecular solvents but rather media of tunable physico-chemical properties.

3.2.2. Structural DNA effects due to the presence of EAN in solution

Three principal sites of interaction between EAN and the DNA-aptamer MB were identified and are depicted in **Scheme 3.1**: **1)** interaction of EAN with the nucleotides and/or the phosphate groups of the stem zone in either dsDNA or ssDNA; **2)** interaction with the, guanine binding pocket of the selective aptamer sequence (inbox and green part of **Figure 2.1 - Chapter 2**), so as to impede interaction with the target. According to Huizenga and Szostak model,[33] the ATP-binding pocket is centered forming two bulges containing adenine residues flanked by a G-tetrad and helical stems that emanate from a G-quadruplex platform; on the other hand, according to Lin and Patel,[34] the structural architecture of the pocket contains pairs of related G·G and G·A mismatches and two G·AMP recognition sites

(see **Figure 2.1**); **3)** electrostatic interaction of EAN with the AMP target possibly hindering its recognition by the guanine pocket. These three steps represent different degrees of significance during this study.

Step 1 refers to the general interaction of an ionic liquid with DNA of a mixed nucleotide sequence, and the stem zone of a DNA-MB is an excellent probe to study this interaction; step 2 is related to a specific sequence but of general importance given the relevance of guanine-rich regions as recognition elements; step 3 is independent of the aforementioned two but requires attention as it may strongly affect the recognition capacity of the DNA-MB.

In absence of any target and in solution, a DNA-MB will be mostly closed, meaning that its stem sequence is hybridized. The opening of the structure would then only be due to the recognition of the target when introduced into the solution. We therefore monitored first the interaction of the two 12-mer forming the stem sequence (see **Chapter 2**) from single to double strand in buffer only, and in presence of increasing concentrations of EAN in solution. As in the DNA-MB, a fluorophore (AF 488) and a black hole quencher (BHQ) were attached to oligomers 1 and 2, respectively. Hybridization could thereby be monitored over time through a decrease in fluorescence as the juxtaposition of the two labels in the duplex formed

resulted in a strong quenching of the fluorescence emission. In this manner, we found the hybridization rate, k_h (**Figure 3.3 A**), that is, the rate at which the association-dissociation between oligomers reaches its equilibrium,[35] as well as the overall degree of hybridization (**Figure 3.3 B**) at equilibrium (for experimental details and calculations, see **Chapter 2**, **section 2.4** and **2.5**, respectively). Once the duplex had been obtained we determined its melting temperature (T_m) through increasing the solution temperature and monitoring the increase in fluorescence (**Figure 3.3 C**). The T_m of the DNA duplex represents the temperature at which half of the dsDNA is unpaired; it is hence an indicator for the stability and the strength of the dsDNA formed. This is opposed to the information provided in **Figure 3.3 A** and **B**, which refer to the stability of ssDNA and how far it can hybridize, at all, in the presence of EAN.

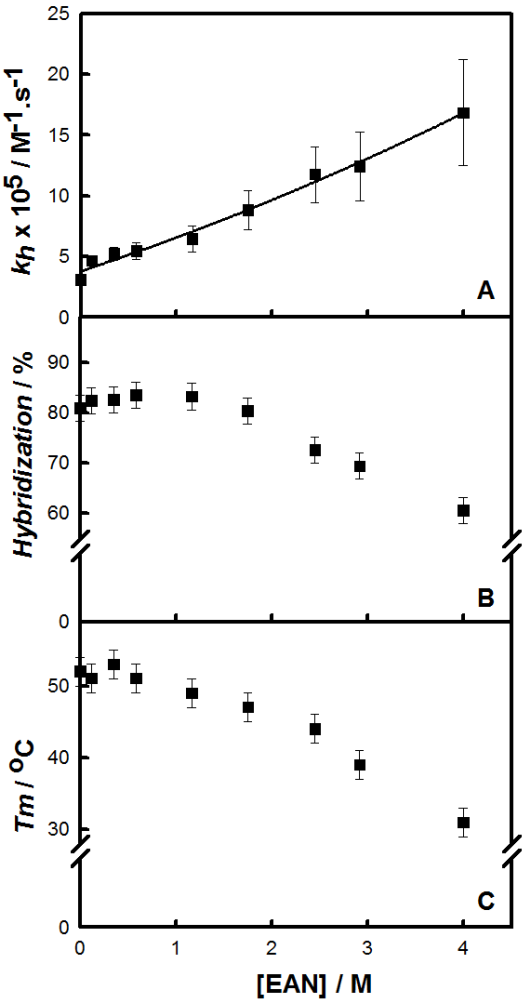

Figure 3.3. Graphic representation of the: A) hybridization rates, k_h, B) amount of DNA hybridized (in %), and C) melting temperatures, T_m, as function of the increase of EAN concentration in TBS solution.

As can be inferred from **Figure 3.3 A**, the rate of hybridization, k_h, increased more than fivefold until 4 M of EAN in TBS, thus increasing strongly the rate of formation of dsDNA. Similar results were observed by Dave and Liu studying the hybridization of a molecular beacon with its DNA target, but here using increasing concentrations of nine organic solvents. They justify this effect of organic solvents on the DNA hybridization rate simply as a decrease in activation energy needed for the hybridization and the melting reactions of DNA. In our system, a possible explanation is an increasing alignment of ssDNA in solution[36,37] similarly to what has been observed with carbon nanotubes where the ionic liquid had a shielding effect.[38] When exchanging Na^+ counterions of DNA with the cations of EAN a shielding of charges takes place resulting thereby in a higher probability of duplex formation with time.[39]

The degree of hybridized DNA, however, decreases from about 85% in TBS to 61% in 4 M of EAN in TBS-solution, as depicted in **Figure 3.3 B**. Also the stability of the duplex formed decreased with rising EAN concentration in solution (**Figure 3.3 C**). The duplex form of DNA relies mainly on hydrogen bonds established between bases. At high concentrations of EAN in solution, less activation energy is apparently needed to denature dsDNA. Menhaj et al. made a similar observation when using

functionalized gold nanoparticles modified with thiolated DNA in solution, although at significantly higher concentrations of EAN (60% (v/v), 7 M approx.) which may be explained by the different experimental system.[40] Tateishi-Karimata and Sugimoto also observed the stability of a GC-rich DNA duplex decreased in presence of up to 4 M of choline dihydrogenphosphate in solution,[14] a finding which contrasted, however, with the long-term structural stability of dsDNA detected in solutions of up to 80% (w/w) of choline based ionic liquids through circular dichroism.[15] Our study evidences that the kinetics of DNA hybridization is greatly enhanced in presence of high amounts of EAN, however, the resulting duplex formed appears to be less and less stable. The percentage of dsDNA actually hybridized in presence of EAN was found linearly correlated with its T_m (**Figure 3.4**). This indicated that, at least in the case of EAN, both parameters can be investigated synonymously with regard to the stability of DNA duplexes.

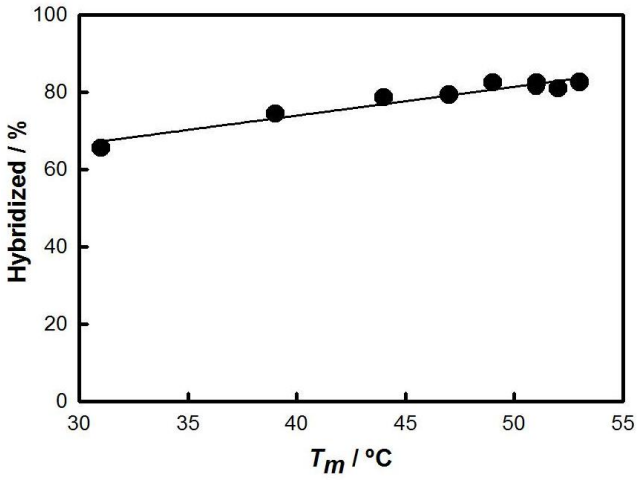

Figure 3.4. Relation between the percentage of DNA that hybridized and the respective T_m.

3.2.2.1. NMR

The weakened hydrogen bonds may be explained by hydrophobic interactions of the ethyl groups of EA^+ interacting with the bases of DNA strands as have been postulated before for both DNA,[41] and also proteins,[10] interacting with ionic liquids in general, but also a deshielding of the base protons in the presence of the protic EAN. Indeed, ^{1}H-NMR spectra in the range of the amino-hydrogen atoms as well as the C6 and C8 hydrogen atoms, between 6-9 ppm,[42] reveal changes in peaks between DNA in TBS solution on one hand, and DNA in TBS solution with 2.65% (w/w) of EAN added on the other (**Figure 3.5**). The interaction between the

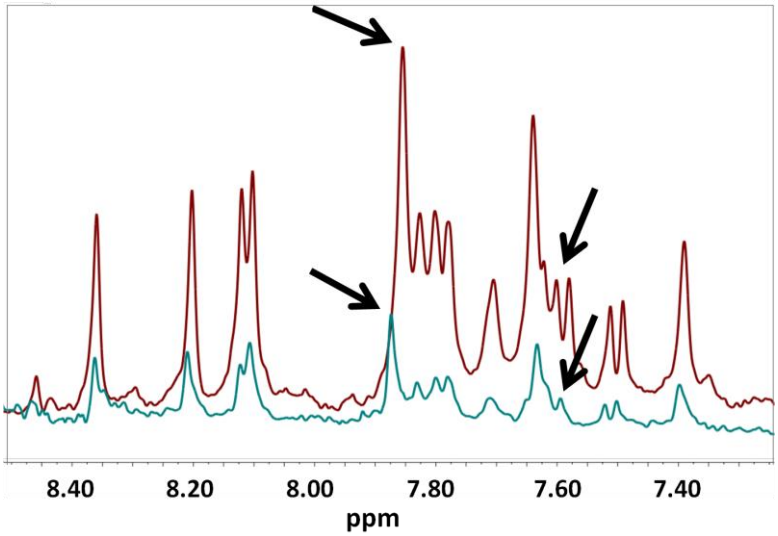

Figure 3.5. ^{1}H NMR spectrum of free DNA (red upper line) and DNA with 2.65 % (w/w) of EAN (green bottom line).

single stranded oligomer and EAN, even at small concentrations of the latter, becomes apparent through an important change from a duplex to a simplex peak at 7.6 ppm, as well as a chemical shift of the peak at 7.85 ppm downfield to 7.87 ppm indicating a deshielding of the respective protons. It can, hence, be concluded that hybridization of ssDNA is significantly accelerated in presence of EAN, although at the cost of the overall amount of dsDNA formed. Transferred to DNA molecular beacons and their molecular recognition capacity, this would suggest a significantly

improved response time during recognition at the expense of a smaller signaling population.

3.2.2.2. Addition of EAN to the dsDNA already formed

It must be pointed out, however, that the aforementioned studies on the stability of dsDNA were conducted with EAN already present during the hybridization. This might pose a potentially different situation than conducting stability studies with dsDNA which first formed in buffer solution and then is contacted with EAN, and it could possibly explain some of the contradictory findings encountered in literature. The aforementioned 12-mer dsDNA was therefore equilibrated in TBS buffer solution and then aliquots of buffer with increasing amounts of EAN were added. **Figure 3.6** depicts the corrected fluorescence values obtained for the duplex DNA in different concentrations of EAN (for calculations, see **Chapter 2**). It can be seen that until approximately 2 M of EAN in solution the DNA structure remains hybridized. Increasing the EAN concentration further, an increase in fluorescence emission is observed, indicating the gradual separation of the two oligomers. This indeed confirmed our previous findings and also evidences that apparently duplex stability in an ionic liquid, here EAN, is independent of whether

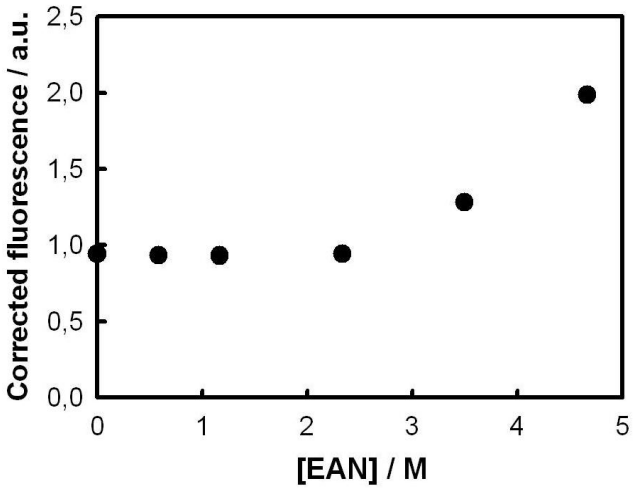

Figure 3.6. Representation of the corrected fluorescence values obtained for the duplex DNA in solution as a function of increasing concentrations of EAN in TBS solution at 25 ^{o}C.

the ionic liquid is present during hybridization of the single strands, or only added thereafter (studies with other ILs will be presented in **Chapter 5**). As a consequence, one may argue that an ionic liquid does not interfere with the hybridization itself, as also corroborated by the increased hybridization rates which we observed, but that it rather destabilizes DNA as a whole by weakening hydrogen bonds, which EAN itself can also establish. Apparently, 2 M of EAN is the concentration at which such interactions between EAN and dsDNA structure start to be noticeable.

Extrapolating these results to the function of the DNA-MB can apparently explain the slightly higher K_d determined in 2 M EAN solution when compared with

the aqueous buffer, as well as confirm that the DNA-MB keeps its capacity to reversibly open and close rather than "freeze" in a stable conformation owing to the presence of the ionic liquid.

However, in solution, the phosphate group of the target itself, AMP, may in fact also interact with EAN via the positively charged ethylammonium group, EA^+, and the adenosine group via the nitrate anion, NO^{3-}. As a consequence, part of the target would not be available for binding to the DNA aptamer recognition pocket, resulting in an apparently higher dissociation constant, K_d, which would also explain the findings presented in **Figure 3.1**.

3.2.3. Interaction between EAN and the AMP charged phosphate

To verify this previous hypothesis, we determined the K_d of the DNA aptamer beacon for the uncharged adenosine differing from AMP in the absence of the phosphate group, only. Notably, it is known that the phosphate group of AMP is practically irrelevant for the recognition through an AMP aptamer as it is directed away from the DNA-binding pocket (**Figure 1.3 C**),[34] such that binding constants between the AMP aptamer and adenosine, AMP, ADP and ATP, respectively, have been found to be quite similar.[24] Indeed, the recognition of adenosine in presence of

2 M of EAN using the same DNA aptamer beacon as in **Figure 3.1** yielded a similar dissociation constant, K_d, as AMP, namely 285 μM in TBS and 634 μM in 2M EAN, **Figure 3.7**. This means that the hypothesis of a significant interaction of the ionic liquid with the target itself can be dismissed. Still the question remained as to how far interactions particularly occurring around the DNA aptamer binding pocket could be the responsible for modulating the molecular recognition capacity of DNA aptamer beacons in presence of ILs.

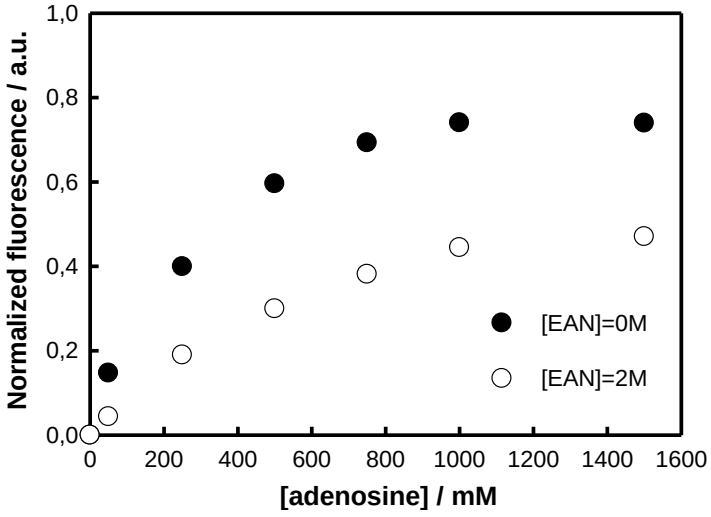

Figure 3.7. Representation of normalized fluorescence obtained as a response to the recognition of increasing concentrations of adenosine by AMP-molecular aptamer beacon in 0 M and 2 M of EAN, respectively.

3.2.4. Circular dichroism of the ATP-aptamer in solution with EAN

We therefore studied the structure of the AMP-aptamer spectrum both in TBS solution and in 2 M EAN in TBS using circular dichroism. The CD spectrum of the aptamer in TBS (**Figure 3.8**) depicts the characteristic two positive bands at 206 nm and 262 nm and a negative band at 240 nm, representing a typical AMP aptamer fingerprint.

In 2 M EAN/TBS solution, however, the bands at 206 and 240 nm, respectively, were lost and a shift of the positive band at 262 nm to 268 nm was observed, along with a decrease in its intensity.

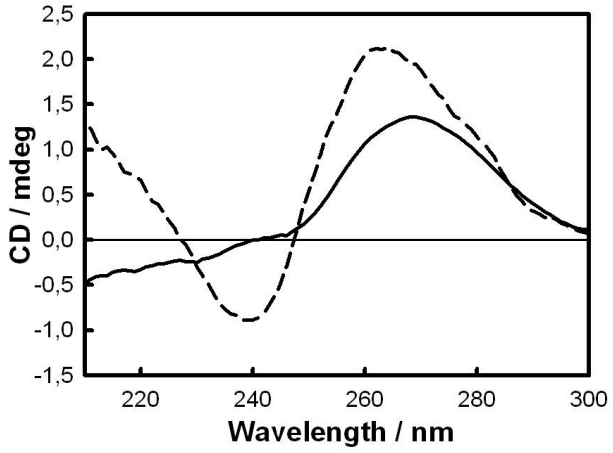

Figure 3.8. The CD spectra of the 5 μM of AMP aptamer with 0 (dashed line) and 2M (solid line) of EAN in solution, at 25 ^{o}C.

This clearly revealed that the addition of EAN indeed altered the structure of the AMP aptamer and as a consequence most probably also the binding pocket responsible for the target recognition.

3.2.5. Theoretical calculations

To corroborate these experimental findings, we explored the possible interference of EAN with the molecular recognition of AMP by the AMP aptamer employing theoretical quantum chemistry calculations (see **Chapter 2** for further details) during which we first strived to understand the distribution of the IL molecules around the oligonucleic acids.

Due to the charged nature of the IL, we can expect that it will interact with the negatively charged phosphates. The negatively charged phosphates will interact with the cations of the IL, the anions of which will be repelled and prefer to interact with the adenine nucleobase of the target (AMP-EAN). Regarding the nucleobase, we could see that both the cation and the anion of the IL interact with the polar groups of the nucleotides, and similarly in guanine (G-EAN) and adenine (A-EAN), respectively (**Figure 3.9**, right). Each of the ions of the IL provides three atoms to bind to the nucleobase (the oxygen atoms in the case of the anion, and the amine

hydrogen atoms in the case of the cation), which we found to enable a very flexible coordination of the system. Using more sophisticated calculations, a similar observation was reported in literature.[43] As a consequence, upon perturbation of this system no large energy penalty is to be expected for the reorganization of the IL ions around the nucleobase, thus allowing the interaction between guanine and adenine to take place mainly unhindered. In fact, we found that the ionic liquid shows a very similar affinity for the AG base pair (-9.3 kcal/mol, **Figure 3.9**) as compared to the non-interacting nucleobases G-EAN and A-EAN (-7.1 kcal/mol and -3.8 kcal/mol, respectively). Despite of its limitation and simplicity, these findings entirely agree with the experimental data. We observe that the strongest interaction which would require most energy to alter by the ionic liquid takes place in the phosphate group (-61.6 kcal/mol as compared to -7.1 kcal/mol or -3.8 kcal/mol with the nucleobases), however, it is widely irrelevant with regard to the target AMP as its phosphates do not interfere with its recognition by the DNA-aptamer beacon. With regard to the phosphates of the DNA aptamer beacon, however, such a strong interaction around the phosphates could originate a structural destabilization of the dsDNA, precisely as it is indeed observed at higher concentrations of EAN in solution.

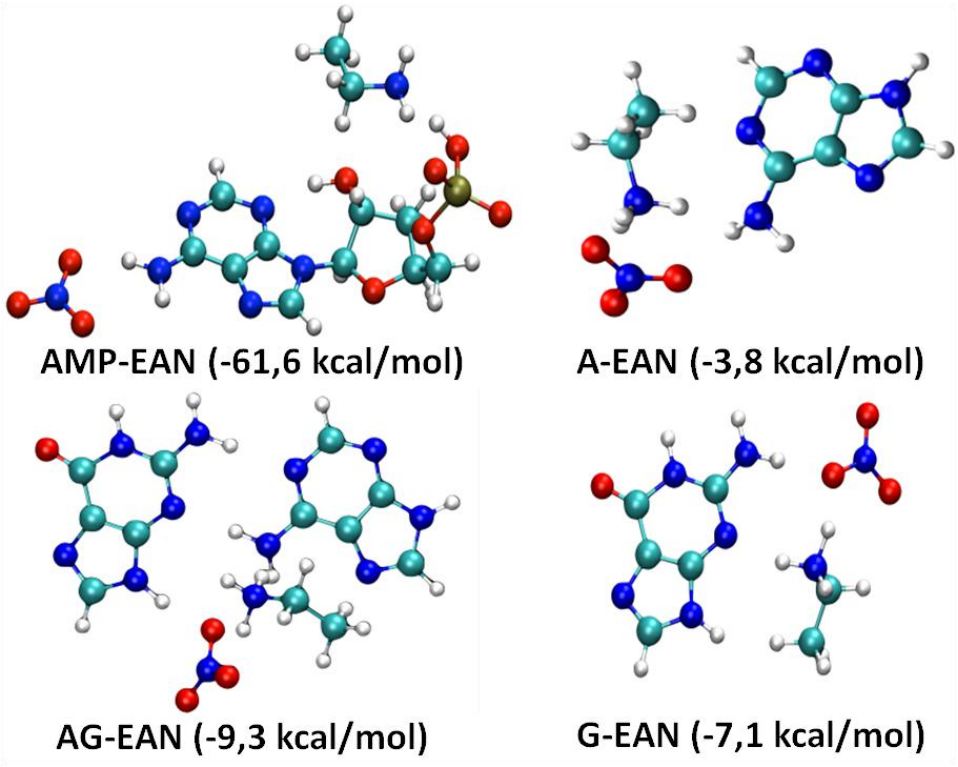

Figure 3.9. Representation of the molecular interactions as considered in the theoretical studies between: AMP-EAN; adenine-EAN; adenine-guanine-EAN; and guanine-EAN. The stick-dots model representing the structure of the interacting molecules follow the color code of: dark-blue dots for nitrogen (N); light blue dots for carbon (C), red dots for oxygen (O); and white dots for hydrogen (H).

Finally, the coordination flexibility of the EAN around the nucleobases revealed by our a priori calculations agree with the experimental evidence that molecular recognition of AMP through the DNA aptamer beacon is possible even at

higher concentrations of EAN, but with a decreasing efficiency. Naturally, the observed coordination flexibility is specific for EAN and may not be transferred to any IL in general, as theoretical studies with different ionic liquids in other systems,[43] also highlight.

3.3 Conclusions

In conclusion, we have proven that molecular recognition events that trigger the reversible actuation of DNA-based nanovalves or DNA-based nanodevices, such as DNA-aptamers in gating systems, may be possible even in the presence of a non-molecular solvent which possess entirely different physico-chemical properties than aqueous systems, and which cannot be considered common salt, either. The study of such intricate systems is not straightforward given the subtle interplay of interaction forces which determine the function of the DNA. Our findings suggest that artificial DNA-based sensing and actuation systems, in which both functional oligonucleotides and solvent are unconventional, are conceivable. However, from our results it also became clear that for such applications a selection from the scratch of respective DNA aptamers in ionic liquid solutions is indispensable. This procedure will be detailed and discussed in **Chapter 6**.

3.4. References

(1) Pinheiro, V. B.; Holliger, P. The XNA World: Progress towards Replication and Evolution of Synthetic Genetic Polymers. *Current Opinion in Chemical Biology*. **2012**, 245–252.

(2) Pinheiro, V.; Taylor, A.; Cozens, C. Synthetic Genetic Polymers Capable of Heredity and Evolution. *Science (80-.).* **2012**, *336* (6079), 341–344.

(3) Seddon, K. R. Ionic Liquids: A Taste of the Future. *Nat. Mater.* **2003**, *2*, 363.

(4) Kumar, V.; Parmar, V. S.; Malhotra, S. V. Structural Modifications of Nucleosides in Ionic Liquids. *Biochimie*. **2010**, 1260–1265.

(5) Welton, T. Room-Temperature Ionic Liquids . Solvents for Synthesis and Catalysis Room-Temperature Ionic Liquids . Solvents for Synthesis and Catalysis. *Chem. Rev.* **1999**, *99*, 2071–2084.

(6) Bagheri, M.; Rodríguez, H.; Swatloski, R. P.; Spear, S. K.; Daly, D. T.; Rogers, R. D. Ionic Liquid-Based Preparation of Cellulose-Dendrimer Films as Solid Supports for Enzyme Immobilization. *Biomacromolecules* **2008**, *9* (1), 381–387.

(7) Moniruzzaman, M.; Kamiya, N.; Goto, M. Activation and Stabilization of Enzymes in Ionic Liquids. *Org. Biomol. Chem.* **2010**, *8* (13), 2887–2899.

(8) Baker, S. N.; Zhao, H.; Pandey, S.; Heller, W. T.; Bright, F. V; Baker, G. a. Fluorescence Energy Transfer Efficiency in Labeled Yeast Cytochrome c: A Rapid Screen for Ion Biocompatibility in Aqueous Ionic Liquids. *Phys. Chem. Chem. Phys.* **2011**, *13*, 3642–3644.

(9) Byrne, N.; Angell, C. A. Protein Unfolding, and the "Tuning In" of Reversible Intermediate States, in Protic Ionic Liquid Media. *J. Mol. Biol.* **2008**, *378* (3), 707–714.

(10) Summers, C. A.; Flowers, R. A. Protein Renaturation by the Liquid Organic Salt Ethylammonium Nitrate. *Protein Sci.* **2000**, *9* (10), 2001–2008.

(11) Nishimura, N.; Ohno, H. Design of Successive Ion Conduction Paths in DNA Films with Ionic Liquids. *J. Mater. Chem.* **2002**, *12* (8), 2299–2304.

(12) Chandran, A.; Ghoshdastidar, D.; Senapati, S. Groove Binding Mechanism of Ionic Liquids : A Key Factor in Long- Term Stability of DNA in Hydrated Ionic Liquids ? *J. Am. Chem. Soc.* **2012**, *134*, 20330–20339.

(13) Nakano, M.; Tateishi-Karimata, H.; Tanaka, S.; Sugimoto, N. Choline Ion Interactions with DNA Atoms Explain Unique Stabilization of A-T Base Pairs in DNA Duplexes: A Microscopic View. *J. Phys. Chem. B* **2014**, *118* (2), 379–389.

(14) Tateishi-Karimata, H.; Sugimoto, N. A-T Base Pairs Are More Stable than G-C Base Pairs in a Hydrated Ionic Liquid. *Angew. Chemie - Int. Ed.* **2012**, *51* (6), 1416–1419.

(15) Vijayaraghavan, R.; Izgorodin, A.; Ganesh, V.; Surianarayanan, M.; MacFarlane, D. R. Long-Term Structural and Chemical Stability of DNA in Hydrated Ionic Liquids. *Angew. Chemie - Int. Ed.* **2010**, *49* (9), 1631–1633.

(16) You, K.; Lee, S.; Im, a; Lee, S. Aptamers as Functional Nucleic Acids: In Vitro Selection and Biotechnological Applications. *Biotechnol. Bioprocess Eng.* **2003**, *8*, 64–75.

(17) Bock, L. C.; Griffin, L. C.; Latham, J. a; Vermaas, E. H.; Toole, J. J. Selection of Single-Stranded DNA Molecules That Bind and Inhibit Human Thrombin. *Nature* **1992**, *355*, 564–566.

(18) Geiger, A.; Burgstaller, P.; Von der Eltz, H.; Roeder, A.; Famulok, M. RNA Aptamers That Bind L-Arginine with Sub-Micromolar Dissociation Constants and High Enantioselectivity. *Nucleic Acids Res.* **1996**, *24* (6), 1029–1036.

(19) Wallace, S. T.; Schroeder, R. In Vitro Selection and Characterization of Streptomycin-Binding RNAs: Recognition Discrimination between Antibiotics. *RNA* **1998**, *4* (1), 112–123.

(20) Jenison, R.; Gill, S.; Pardi, A.; Polisky, B. High-Resolution Molecular Discrimination by RNA. *Science (80).* **1994**, *263* (5152), 1425–1429.

(21) Li, Y.; Zhou, X.; Ye, D. Molecular Beacons: An Optimal Multifunctional Biological Probe. *Biochemical and Biophysical Research Communications*. **2008**, 457–461.

(22) Hernandez, F. J.; Hernandez, L. I.; Pinto, A.; Schafer, T.; Ozalp, V. C. Targeting Cancer Cells with Controlled Release Nanocapsules Based on a Single Aptamer. *Chem Commun* **2013**, *49* (13), 1285–1287.

(23) Schafer, T.; Ozalp, V. C. DNA-Aptamer Gating Membranes. *Chem. Commun.* **2015**, *51* (25), 5471–5474.

(24) Serrano-Santos, M. B.; Llobet, E.; Ozalp, V. C.; Schafer, T. Characterization of Structural Changes in Aptamer Films for Controlled Release Nanodevices. *Chem Commun* **2012**, *48* (81), 10087–10089.

(25) Tyagi, S.; Kramer, F. R. Molecular Beacons: Probes That Fluoresce upon Hybridization. *Nat.*

Biotechnol. **1996**, *14* (3), 303–308.

(26) Culha, M.; Stokes, D. L.; Griffin, G. D.; Vo-Dinh, T. Application of a Miniature Biochip Using the Molecular Beacon Probe in Breast Cancer Gene BRCA1 Detection. *Biosens. Bioelectron.* **2004**, *19* (9), 1007–1012.

(27) Leone, G.; Van Schijndel, H.; Van Gemen, B.; Kramer, F. R.; Schoen, C. D. Molecular Beacon Probes Combined with Amplification by NASBA Enable Homogeneous, Real-Time Detection of RNA. *Nucleic Acids Res.* **1998**, *26* (9), 2150–2155.

(28) Marras, S. A. E.; Tyagi, S.; Kramer, F. R. Real-Time Assays with Molecular Beacons and Other Fluorescent Nucleic Acid Hybridization Probes. *Clinica Chimica Acta*. **2006**, 48–60.

(29) Tan, W.; Wang, K.; Drake, T. J. Molecular Beacons. *Current Opinion in Chemical Biology*. **2004**, 547–553.

(30) Yamamoto, R.; Kumar, P. K. R. Molecular Beacon Aptamer Fluoresces in the Presence of Tat Protein of HIV-1. *Genes to Cells* **2000**, *5* (5), 389–396.

(31) Evans, D. F.; Yamauchi, A.; Jason Wei, G.; Bloomfield, V. A. Micelle Size in Ethylammonium Nitrate as Determined by Classical and Quasi-Elastic Light Scattering. *J. Phys. Chem.* **1983**, *87*, 3537–3541.

(32) Fumino, K.; Wulf, A.; Ludwig, R. Hydrogen Bonding in Protic Ionic Liquids: Reminiscent of Water. *Angew. Chem. Int. Ed. Engl.* **2009**, *48* (17), 3184–3186.

(33) Huizenga, D. E.; Szostak, J. W. A DNA Aptamer That Binds Adenosine and ATP. *Biochemistry* **1995**, *34* (2), 656–665.

(34) Lin, C. H.; Patel, D. J. Structural Basis of DNA Folding and Recognition in an AMP-DNA Aptamer Complex: Distinct Architectures but Common Recognition Motifs for DNA and RNA Aptamers Complexed to AMP. *Chem. Biol.* **1997**, *4* (11), 817–832.

(35) Tsuruoka, M.; Yano, K.; Ikebukuro, K.; Nakayama, H.; Masuda, Y.; Karube, I. Optimization of the Rate of DNA Hybridization and Rapid Detection of Methicillin Resistant Staphylococcus Aureus DNA Using Fluorescence Polarization. *J. Biotechnol.* **1996**, *48* (3), 201–208.

(36) Okahata, Y.; Kobayashi, T.; Tanaka, K.; Shimomura, M. Anisotropic Electric Conductivity in an Aligned DNA Cast Film. *J. Am. Chem. Soc.* **1998**, *120* (24), 6165–6166.

(37) Tanaka, K.; Okahata, Y. A DNA-Lipid Complex in Organic Media and Formation of an Aligned Cast Film. *J. Am. Chem. Soc.* **1996**, *118* (44), 10679–10683.

(38) Wang, J.; Chu, H.; Li, Y. Why Single-Walled Carbon Nanotubes Can Be Dispersed in Imidazolium-Based Ionic Liquids. *ACS Nano* **2008**, *2* (12), 2540–2546.

(39) Stellwagen, E.; Dong, Q.; Stellwagen, N. C. Quantitative Analysis of Monovalent Counterion Binding to Random-Sequence, Double-Stranded DNA Using the Replacement Ion Method. *Biochemistry* **2007**, *46* (7), 2050–2058.

(40) Menhaj, A. B.; Smith, B. D.; Liu, J. Exploring the Thermal Stability of DNA-Linked Gold Nanoparticles in Ionic Liquids and Molecular Solvents. *Chem. Sci.* **2012**, *3* (11), 3216.

(41) Ding, Y.; Zhang, L.; Xie, J.; Guo, R. Binding Characteristics and Molecular Mechanism of Interaction between Ionic Liquid and DNA. *J. Phys. Chem. B* **2010**, *114* (5), 2033–2043.

(42) Address, K. J.; Feigon, J. *Bioorganic Chemistry: Nucleic Acids*; Hecht, S. M., Ed.; Oxford University Press: New York, **1996**.

(43) Rezabal, E.; Schäfer, T. First Principle Approach to Solvation by Methylimidazolium-Based Ionic Liquids. *J. Phys. Chem. B* **2013**, *117* (2), 553–562.

CHAPTER 4

Influence of the Ionic Liquids on Fluorescence Emission

4.1 Introduction

Owing to the possibility of designing ionic liquids (ILs) with low toxicity and high capacity to dissolve biomolecules like proteins, enzymes or nucleic acids, they have also been widely investigated as solvation media for enzymatic catalysis, as well as solvation media for conformational studies and interaction sites with proteins and DNA.[1–5] In recent years, various authors furthermore studied nucleic acids in non-conventional environments, reducing the presence of water in solution, with the aim of achieving long-term stability of DNA[6] as well as develop DNA nanodevices.[7–9] During these studies, the function of the DNA nanodevice must be characterized and monitored for which various spectroscopic techniques involving absorbance, fluorescence or circular dichroism are applied.[4,5,10] In particular, intra-molecular stain binders or dyes covalently bound to the ends of the DNA structure can be used to monitor DNA structural and stability changes by fluorescence.[10–13] Dyes can have a neutral charge, but also be either cationic or anionic, and have different excitation and emission wavelengths depending on their chemical structure.

Three classes of dyes are generally used to stain nucleic acids: the intercalating dyes, such as ethidium bromide (EtBr) or propidium iodide; groove binders, such as DAPI or the Hoechst dyes that bind to the minor groove; and other types of nucleic acid binders, binding to the external part of DNA or intercalating in two parts of the DNA structure (bi-intercalators), such as oxazole yellow homodimer (YOYO) and thiazole orange homodimer (TOTO) (**Figure 4.1 A**). Since these dyes emit fluorescence when they interact with DNA forming a dye-DNA

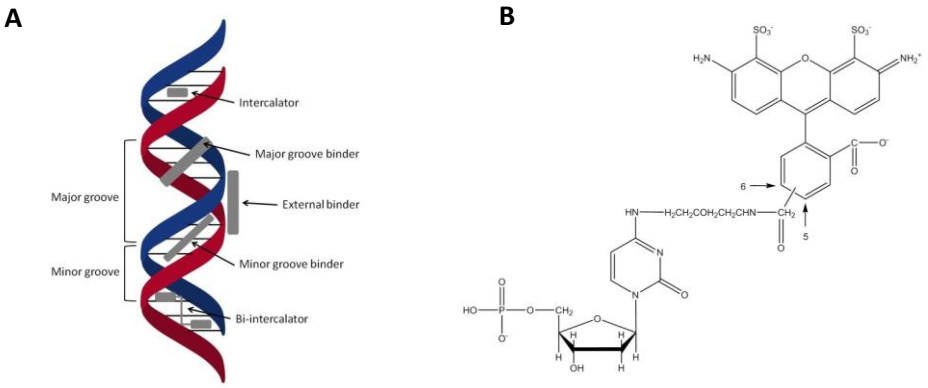

Figure 4.1. A) Schematic diagram showing the different binding modes of DNA intercalators (dyes or other ligands) to the duplex DNA structure. **B)** Example of a DNA labeling dye: Alexa Fluor 488 attached via a spacer to the DNA base, in this particular case deoxycytidine triphosphate (dCTP). (From Chapter 8 of Ref. [14])

complex, their use enables the detection and quantification of DNA, oligonucleotides and RNA in solution or in electrophoresis gels, as applied in genetics or molecular biology.[11,15,16]

Depending on the system used and on what information is being sought, the nucleic acids may also be labeled with fluorophores that are covalently attached to the nucleic acid, as it is usually done with Alexa Fluor (AF) (**Figure 4.1 B).** This method is normally used for FISH (fluorescence *in situ* hybridization), DNA arrays/microarrays and other hybridization techniques sometimes conjugated with other fluorophores or a quencher for a switch-like on/off system.[17–20]

The AF "family" of dyes stands out in quantum yield and photostability of the conjugates, with longer lifetimes than traditional fluorophores (e.g. fluorescein, rhodamine, Cy3, Cy5). Most of these fluorophores also stand out for being insensitive to pH over a broad range (from 4 to 10) within which they maintain a high fluorescence intensity,[21] while it is well-known that the pH of the aqueous phase commonly affects the degree of ionization of a dye molecule and hence its emmision.[22] Alexa Fluor dyes are, hence, widely used to study conformational changes of biomolecules, proteins and nucleic acids upon perturbations of the

system.[9,23–25] With regard to studies in IL media as is our case, the use of an AF dye which is widely pH-insensitive is a strong advantage as some ILs when mixed in aqueous solution cause a slight change in the pH of the medium (non published results - **Chapter 5**).

Still, the use of fluorophores as reporter molecules in IL media of varying concentrations might not be straightforward. Several ILs contain aromatic rings with a similar structure as the majority of fluorophores and DNA bases. Therefore, hydrophobic, π-π or even electrostatic interactions in the case of electrically charged fluorophores are possible between ILs and fluorophores. As a consequence, there is a possibility that the ILs influence the fluorescence emission of a dye probe when both are present in solution, or, in other words, that the IL quenches the fluorescence. During experiments where the concentration of an IL is used to study its effect on DNA conformation or structure, as is our case, changes in fluorescence may hence not be straightforwardly be interpreted.

Still, this aspect has been widely ignored in studies reported in literature. FRET is a very common technique used in studies of nucleic acids by detecting conformational changes upon the introduction of a stimulus into the solution by using two

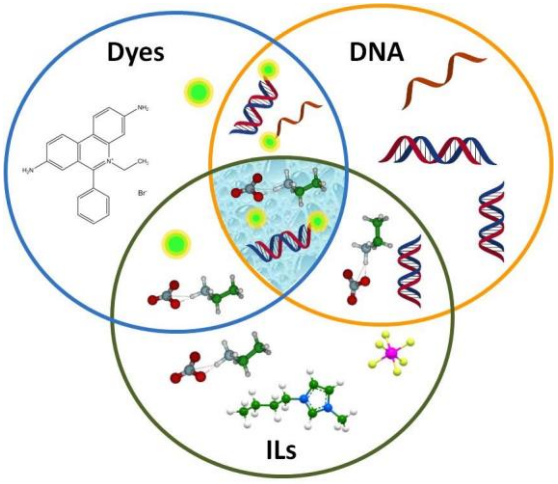

Scheme 4.1. Representation of the systems subject of study in this work.

fluorophores or a fluorophore-quencher pair attached to the nucleic acids sequences extremities.[26–28] Other studies attempting to understand where ILs could possibly interact with the DNA structure employed staining dyes that interacted to the different regions of DNA such as to the minor or major grooves or by bases intercalation.[4,10,29–32] Competitive interactions between the dye and the DNA on one side, and the dye and ILs on the other, have been widely neglected in literature although this is extremely important to be considered in order to avoid pitfalls during the interpretation of experimental results. For example, using the intercalator ethydium bromide (EtBr) it was studied how ILs could possibly cause perturbations

on the DNA structure. A decrease of fluorescence stemming from the intercalator EtBr was interpreted as this dye being driven out of the DNA interbase region by the IL which would establish supposedly favourable hydrophobic interactions with this very same region of the DNA.[4] Apparently, in these works[4,10,29–32] the high possibility of electrostatic interaction between the IL and the dye was not taken into consideration. However, in the case of the dyes being electrically charged, it would be precisely the electrostatic interaction between IL and dye that would prevail rather than any hydrophobic interaction between the dye and the DNA bases. Hence, if a charged intercalator dye such as EtBr moves out of the DNA interbase region in presence of ILs in solution, it could possibly be due to a favourable IL-dye interaction rather than a competitive one of the IL with DNA.

Regarding the effect of ILs on the fluorescence of dye probes, different groups explored the influence of the ILs as solvation medium of dyes free in solution.[33–35] To the best of our knowledge, the influence of ILs on the fluorescence emission of a fluorescent probe covalently labeled to the end of a DNA sequence has not been investigated so far. In this context, we studied here the effect of ILs on the fluorescent dye when it is free in solution as compared to when it is covalently bound to an ssDNA oligomer.

4.2. Results and Discussion

4.2.1. Alexa Fluor 488 in TBS solution with increasing concentrations of ILs

4.2.1.1. Fluorescence measurements

Figure 4.2 depicts how the normalized fluorescence (F/F_0) decreases with increasing concentrations of different ILs when Alexa Fluor 488 (AF488) is free in TBS solution. With the exception of EAN, in presence of which the fluorescence remained almost constant, it is clear that in general all ILs quenched the fluorescence of the dye as a function of their respective concentration in solution. At ≈50% (v/v) in solution, BMIM-Cl and TMGL were the ILs that quenched the fluorescent probe emission more than the other ILs, reaching half the fluorescence emission when comparing with the total absence of these ILs in solution.

The quenching may occur in the excited state or in the ground state of the fluorophore, being the latter denoted as static quenching. During static quenching, a formation of a complex between the fluorophore and the quencher occurs, inhibiting the fluorophore excitation and subsequently the emission of fluorescence. Since the formation of this non-fluorescent complex occurs in the ground-state, it is considered that the fluorophore has been statically quenched and that this process is independent of the diffusion or the collision of the molecules.

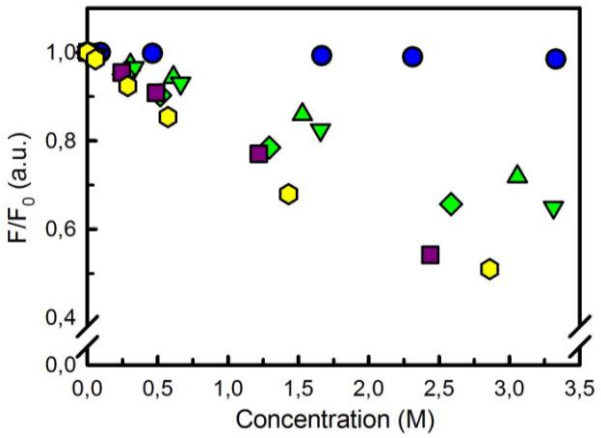

Figure 4.2. Normalized fluorescence changes of free AF488 dye as function of EAN (circles), CN (triangles), CDHP (inverted triangles), CL (diamonds), TMGL (squares) and BMIM-Cl (hexagons) concentration in solution with TBS. Data were normalized respect to the fluorescence intensity of the AF 488 dye in the absence of IL in the TBS solution (F_0). The concentration of the dye was 25 nM. Raw data were corrected for the background signal.

On the other hand, in the excited state the quenching depends entirely on the diffusion and contact (collision) between the molecules. Collisional or dynamic quenching occurs then when the fluorophore in an excited-state contacts with an atom or molecule, the quencher, which deactivates the fluorophore emission. The fluorophore returns then to the ground state non-emitting fluorescence. This can

occur due to electron exchange, molecular rearrangements or resonance energy transfer (RET).

AF and ILs are charged (**Figure 2.3 bottom** and **Figure 2.5**, respectively) which will generate electrostatic interactions between them. This may then be occurring in the ground-state or in an excited state of the fluorophore, avoiding or stopping, respectively, the excitation of the fluorophore and subsequently the emission of the fluorescence.

ILs are known to possess a significantly higher viscosity than a buffer solution. According to Wang et al., a higher viscosity which slows down the diffusion of the molecules will hinder in part the collision between fluorophore and quencher in case of dynamic quenching. In our case, however, no clear correlation was found between the quenching of fluorescence at 2,5M of each IL in solution and the ILs viscosity, as can be seen in **Table 4.1**.

Table 4.1. Viscosity of the stock solutions prepared for the different ILs with water and the decrease F/F_0 generated at 2,5M of each IL in solution.

	[IL]% w/w	Viscosity (mPa.s)	F/F_0 at [IL]=2.5M
TMGL	80	78,5	0,530
CDHP	75	76,9	0,735
CL	70	26,9	0,662
BMIM-Cl	75	19,1	0,538
CN	80	18,5	0,771
EAN	80	7,5	0,989

Therefore, we could in the following exclude the role of viscosity when determining whether the quenching occurring to AF 488 by the ILs was static in the ground state, or collisional (dynamic) in the excited state.

In order to do so, we should consider that the same population of the fluorophore can be quenched both by complex formation and, once excited, by collisions with the same quencher, and a combination of both types of quenching by the ILs may also be occurring.

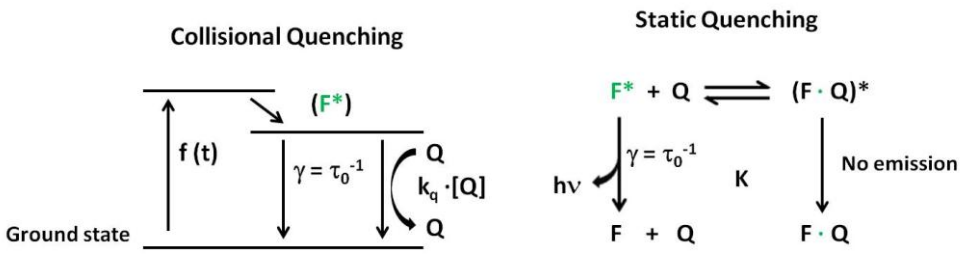

Scheme 4.2. Comparison of dynamic and static quenching.[36]

This can be verified by the Stern-Volmer plot or the Stern-Volmer (S-V) equation:

$$F_0/F = 1 + K_{SV}\cdot[Q] = 1 + k_q\cdot\tau_0\cdot[Q] \qquad \textbf{(equation 4.1)}$$

where F_0 and F are the fluorescence intensities observed in the absence and in the presence, respectively, of the quencher Q; K_{SV} is the Stern-Volmer quenching constant, k_q is the bimolecular quenching constant, τ_0 is the unquenched lifetime, and $[Q]$ is the quencher concentration. The Stern-Volmer plot consists in the representation of F_0/F versus $[Q]$, with the interception on the y-axis at unity and being the slope equal to K_D. In a linear Stern-Volmer plot, K_D^{-1} corresponds to the quencher concentration at which $F_0/F = 2$ or at which 50% of the fluorescence intensity is quenched.[36] This linear type of plot indicates that all the fluorophores are

equally accessible to be quenched and only one type of quenching is occurring, either collisional or static. If a non-linear plot is obtained, this reveals a combination of both types of quenching, static and dynamic.

The Stern-Volmer plots from the steady-state emission data of the AF 488 as donor in solution with the different ILs as acceptors are depicted in **Figure 4.3** for different concentration of all ILs (potential quenchers). For the solution with EAN the plot is nearly constant at unity, revealing that no quenching occurs and as was already observed in **Figure 4.2**. For the solutions with CL or BMIM-Cl, a linear Stern-Volmer plot with a constant slope was obtained, indicating that quenching is purely dynamic or static. For the ILs CN, CDHP and TMGL in solution, a clear ascendant concave Stern-Volmer curve was obtained confirming that a combination of static and dynamic quenching was likely occurring when these ILs were in solution.

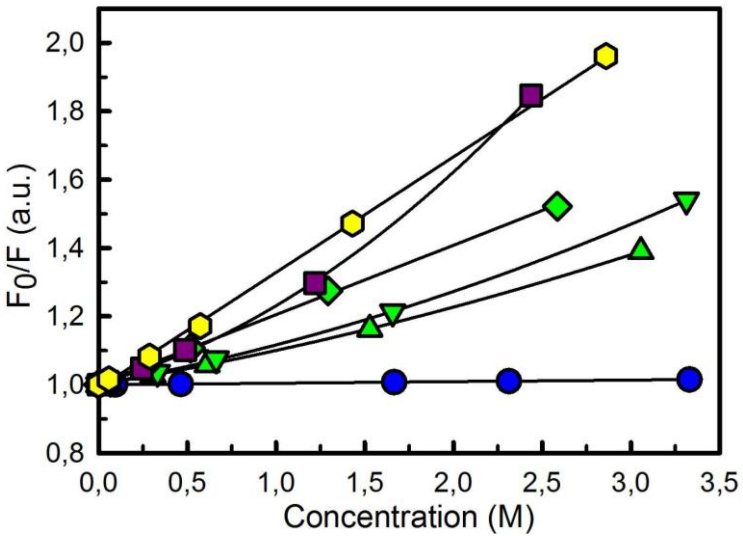

Figure 4.3. Stern-Volmer plot representing the quenching of the AF 488 by EAN (circles), CN (triangles), CDHP (inverted triangles), CL (diamonds), TMGL (squares) and BMIM-Cl (hexagons) increasing concentration in solution with TBS. The black lines represent the fitting curves of the data.

When both kinds of quenching are present for the same fluorophore, the Stern-Volmer equation (**equation 4.1**) is modified, becoming a second order equation in *[Q]* (**equation 4.2**), which here corresponds to the concentration of the ILs:

$$F_0/F = (1+ K_D\cdot[Q])\cdot(1+ K_S\cdot[Q]) \qquad \textbf{(equation 4.2)}$$

The quenching constants corresponding to static (K_S) and dynamic (K_D) fractions of quenching were then determined by the fit of Stern-Volmer plots and are presented in **Table 4.2**.

Table 4.2. Static and dynamic quenching constants occurring to the fluorophore AF 488 during the addition of the different ILs to the solution. The respective IL (quencher) concentrations at which F_0/F=2 occurs were also determined for each type of quenching probably occurring.

	K_S (M^{-1})	Std. error	K_D (M^{-1})	Std. error	[Q] (M)	[Q] (M)
EAN	-	-	-		-	-
CN	0,057	*	0,057	*	17,54	-
CDHP	0,0704	**	0,0704	**	14,20	-
CL	0,2032	0,0026	0,0	-	4,92	-
TMGL	0,1409	*	0,1409	*	7,10	-
BMIM-Cl	0,0328	0,0146	0,2779	0,023	30,49	3,60

Note: standard error *10^3 and **10^4

With the identical values obtained for the two quenching constants for CN, CDHP and TMGL, despite the high values of error, we could confirm the presence of both types of quenching when these ILs are in solution with free AF 488. However, in the case of CL and BMIM-Cl two clearly different constants were obtained, revealing one type of quenching prevailing. E**quation 4.2.** alone does not allow to attribute either constant to a certain type of quenching. Therefore, and in order to identify

the degree of static and dynamic quenching, respectively, fluorescence lifetime measurements were conducted.

4.2.1.2. Fluorescence lifetime measurements

Dynamic quenching results in a decrease in the lifetime of the fluorophore. Therefore, the excited state lifetime in the absence of quencher (τ_0) divided by the lifetime measured with increasing concentrations of ILs in solution will depend on the concentration of IL similar to the fluorescence correlation: $F_0/F = \tau_0/\tau$. Consequently, the Stern-Volmer equation will be similar as the one represented in **equation 4.1**:

$$\tau_0/\tau = 1 + K_D \cdot [Q] \qquad \textbf{(equation 4.3)}$$

In the case of a complex formation between fluorophore and quencher, the quenching will be static and the lifetime of the sample will remain constant, $\tau = \tau_0$, so $\tau_0/\tau = 1$. Unless the concentration of the fluorophore is very high, which is not the case in this work, the fluorescence lifetime is independent of the fluorophore concentration.

Table 4.3 presents the lifetimes measured with τ_1 denoting the long lifetime component, for the highest fluorescence amplitudes obtained (majority of the fluorophore population) and τ_2 representing the short lifetime component of the fluorophore population. According to **Table 4.3**, up to 1M of all the used ILs the lifetime of AF 488 remained practically constant and quenching should, hence, be

Table 4.3. Lifetime values obtained for the AF 488 in solution with different concentrations of the ILs. The standard error is ±0,2 ns.

	EAN		CN		CDHP		CL		TMGL		BMIM-Cl	
[IL] (M)	**τ_1 (ns)**	**τ_2 (ns)**	**τ_1 (ns)**	**τ_2 (ns)**	**τ_1 (ns)**	**τ_2 (ns)**	**τ_1 (ns)**	**τ_2 (ns)**	**τ_1 (ns)**	**τ_2 (ns)**	**τ_1 (ns)**	**τ_2 (ns)**
0	3,98	-	3,98	-	3,98	-	3,98	-	3,98	-	3,98	-
0,25	n.d.	-	4,10	-	n.d.	-	n.d.	-	n.d.	-	4,00	-
1	4,14	3,33	3,94	3,09	3,87	-	4,01	-	4,00	-	3,92	-
3	3,99	-	3,66	-	3,57	1,5	3,89	0,97	3,82	1,95	2,31	4,07

n.d. = not determined; τ_1 = lifetime at higher fluorescence emission; τ_2 = lifetime at lower fluorescence emission

only static. At 1M, for EAN and CN two lifetimes were determined, which could mean that the fluorophore population was heterogeneous. However, for both ILs, the differences between the two lifetimes are not that significant, besides that this corresponds to a small part of the AF 488 population that was apparently suffering

dynamic quenching at a residual level and for EAN not detected by the steady-state fluorescence measurements (**Figure 4.2**).

When increasing the concentration of the ILs up to 3M, the lifetime of AF 488 remained constant for EAN as expected since no quenching had been observed. It decreased in presence of CN, CDHP and slightly for TMGL, respectively, revealing that dynamic quenching occurred (**Figure 4.4**). With 3M of CL in solution practically no changes in the lifetime were observed within the experimental error, indicating that probably a complex between the fluorophore and IL formed in the ground state and causing only static quenching even at this high concentration. This is in agreement with the linear Stern-Volmer plot and with the quenching constants presented in **Table 4.2**. The most significant decrease in the lifetime was observed for 3M of BMIM-Cl, where the majority of the fluorophore population presented a lower lifetime, τ_1 = 2.31 ns, decreasing nealy 1.70 ns with respect to the lifetime of AF 488 in pure buffer. This indicates that at this concentration dynamic quenching was occurring. The short lifetime component remained at 4 ns, revealing that a small part of AF488 population was apparently not accessible to the quenching effect of BMIM-Cl. Thus, apparently, at this concentration BMIM-Cl is probably causing different effects on the AF488 leading to the determination of different lifetimes and

consequently to a dynamic quenching. This apparent dependency of the type of quenching on the concentration of BMIM-Cl was not obvious from the Stern-Volmer plot. However, it also must be noted that 3M BMIM-Cl, at which dynamic quenching started to be observed, was the highest concentration measured. At this concentration two lifetimes were also found for CDHP, CL and TMGL, meaning that the influence of the IL on the fluorophore population was not totally homogeneous.

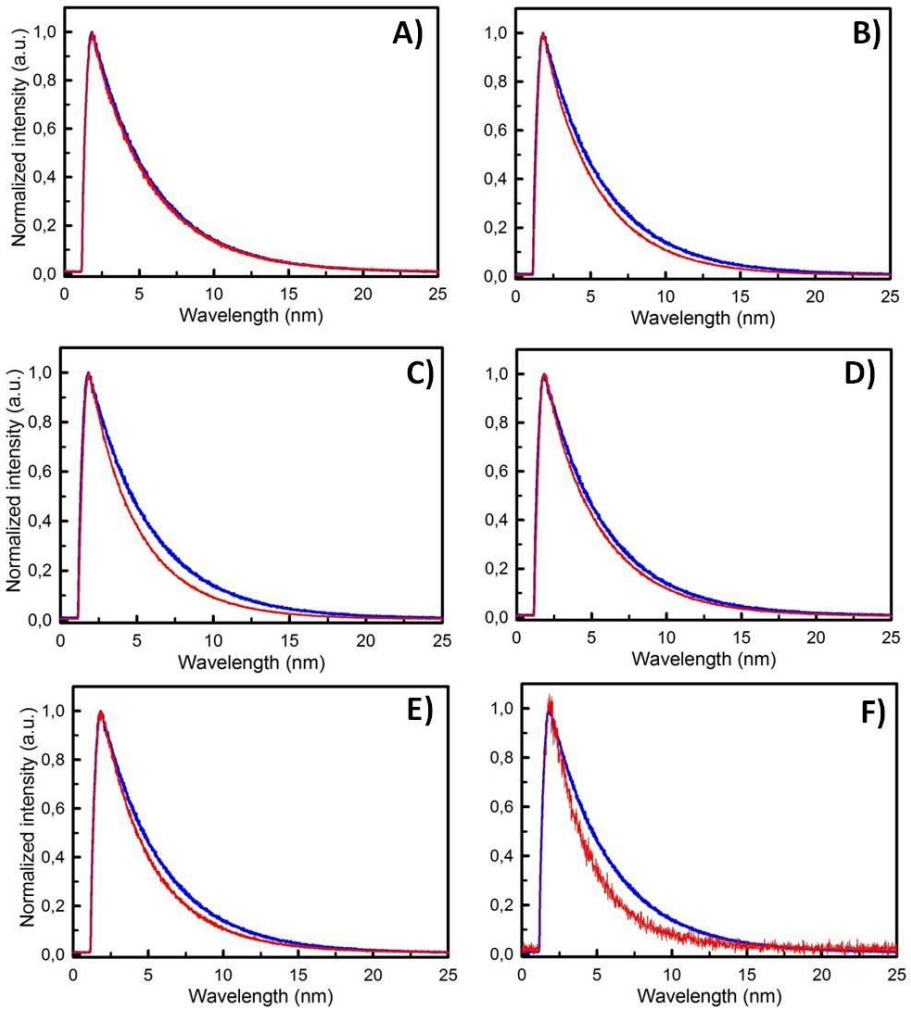

Figure 4.4. Fluorescence lifetime of 0,8 μM of the fluorophore AF488 in pure buffer (blue line) and in buffer solution with 3M of **A)** EAN, **B)** CN, **C)** CDHP, **D)** CL, **E)** TMGL and **F)** BMIM-Cl (red lines).

Using **equation 4.3** and comparing with the values of **Table 4.2** we determined the dynamic quenching constant (K_D) by calculating and fitting the plots of τ_0/τ (**Table 4.4**).

Table 4.4. Dynamic quenching constants occurring to the fluorophore AF 488 during the addition of the different ILs to the solution. The respective IL (quencher) concentrations at which τ_0/τ=2 occurs were also determined.

	K_D (M^{-1})	Std. Error	[Q] (M)
EAN	-	-	-
CN	0,0263	0,0073	38,02
CDHP	0,0373	0,0021	26,81
CL	0,0062	0,0032	161,29
TMGL	0,0121	0,0040	82,64
BMIM-Cl	0,2169	0,0404	4,61

The K_D values obtained here are in agreement with the values of K_D of **Table 4.2**. With regard to CL, the low K_D value confirms that the quenching is purely static. But also TMGL exhibits a relatively low K_D. For BMIM-Cl, the quenching seems to be mainly dynamic, however, care must be taken with this value since using **eq. 4.3** to fit the data resulted in a less accurate fitting than the standard error might suggest (Figure I. - Annex I). On the other hand, the concentration obtained in both methods for BMIM-Cl at which F_0/F or τ_0/τ = 2 or 50% (right column of **Table 4.2** and **Table**

4.4, respectively) was very similar and slightly above the used of 3M. The slight differences observed between the K_D values in general may be due to the different number of concentrations used in each experiment and the different methods used to calculate the values of steady-state fluorescence and fluorescence lifetime.

The presence of two lifetimes may be due to an equilibrium occurring between the formation of AF 488 dimers and monomers[37a] or the possible formation of aggregates. Then the aggregates here can take place between the IL molecules[37b] or between the IL and the fluorophore, which here seems more logical to be occurring. Molecular aggregates are macroscopic clusters of molecules with sizes intermediate between crystals and isolated molecules.[38] Aggregation of dye molecules was previously reported in water and other solvents at concentrations ranging from 1 to 100 μM.[39,40] Considering the low concentration of the AF488 used in this work, the formation of aggregates by the fluorophore can be dismissed. On the other hand, studying the system DNA, EtBr and BMIM-Cl, Ding et al. reported the formation of small micelle-like aggregates of BMIM-Cl when the concentration of this IL in solution was above 0,5 M (in our study this corresponds approximately to 8% v/v).[4] We therefore verified whether in our system any aggregation would take place through dye-IL interactions or through IL self-aggregates. A spectral shift of the

emission spectra maximum of AF 488 relative to the maximum in buffer solution at ±520 nm should then be observed.

Figure 4.5 shows the emission spectra of AF 488 with increasing concentration of BMIM-Cl. As expected from the steady-state fluorescence measurements, the emission intensity of AF488 decreased from the lowest to the highest concentrations of BMIM-Cl added to the solution. For concentrations until 10% v/v no shift in the maximum of the emission peak was observed remaining at 520 ± 1 nm (**Figure 4.5** - from the full purple line until long dash yellow line). Nevertheless, when adding 25% or 40% v/v of BMIM-Cl in the AF solution the peak suffered a red shift toward 524 nm (**Figure 4.5** - medium dash dot orange line and medium dash red line, respectively).

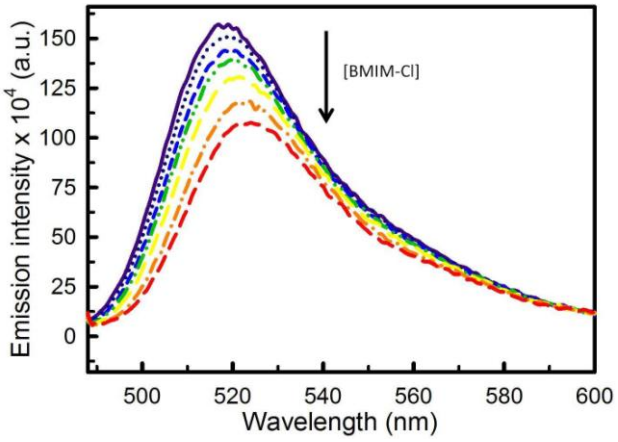

Figure 4.5. Emission spectra of AF488 in solution with increasing concentrations of BMIM-Cl. Following the arrow the concentrations of BMIM-Cl ranged from 0% v/v (full purple line), 1% v/v, 3% v/v, 5% v/v, 10% v/v, 25% v/v and 40% v/v (medium dash red line).

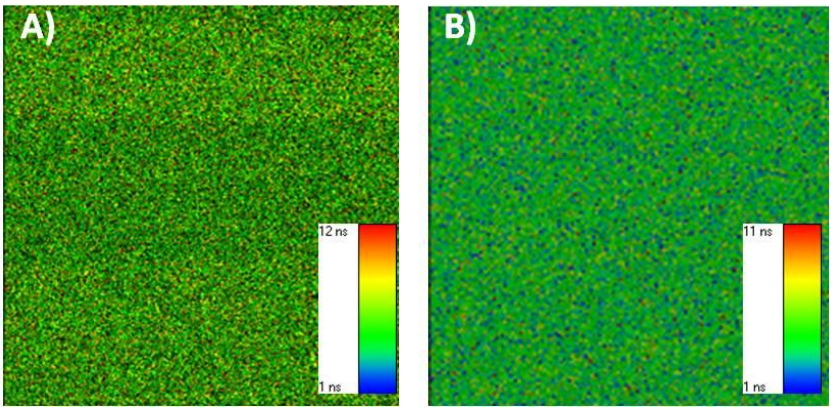

Figure 4.6. FL lifetime images of AF488 in solution with 3M of **A)** BMIM-Cl and **B)** CL. Excitation wavelength was 485 nm.

This means that at these concentrations aggregation of BMIM-Cl molecules[37b] or of BMIM-Cl with the fluorophore may be occurring. An attempt was made to detect potential aggregates through fluorescence lifetime (FL) using a confocal microscope.

The FL maps depicted in **Figure 4.6** were determined for AF 488 with 3M of BMIM-Cl and for comparison with 3M of CL in solution. The FL lifetime images for both ILs did not show any detectable aggregates with the fluorophore under the experimental conditions. However, for BMIM-Cl aggregates may be occurring at this high concentration, but they are not entrapping the AF488 in the micelles, thus it is not possible to see the aggregates with the FL images. Even being green the predominant color, representing the AF 488 lifetime of around 4 ns, it is possible to detect longer and shorter lifetimes through the color scale for BMIM-Cl and CL, respectively. For CL the detected blue dots correspond to the small fluorophore population presenting τ_2 lifetime, registered in **Table 4.3**.

4.2.1.3. Förster resonance energy transfer (FRET)

In order to verify whether the photophysical process of the Förster Resonance Energy Transfer (FRET) was occurring in our system, we determined the emission spectrum of the donor AF 488 and the absorption spectrum of the six ILs as potential acceptors (**Figure 4.7**).

This type of quenching may occur in the excited state, but without collisions between the molecules. In this particular case, the energy is transferred between a donor and an acceptor that are nearby. The distance between the donor and the acceptor determines the extent of energy that is transferred and the extent of emission-absorption spectral overlap. RET occurs when, after being excited, an electron of the donor when trying to return to the ground state **is transferred** to the acceptor. Immediately an electron of the ground-state of the acceptor passes to a higher excited-state orbital. Then, if the acceptor is fluorescent,

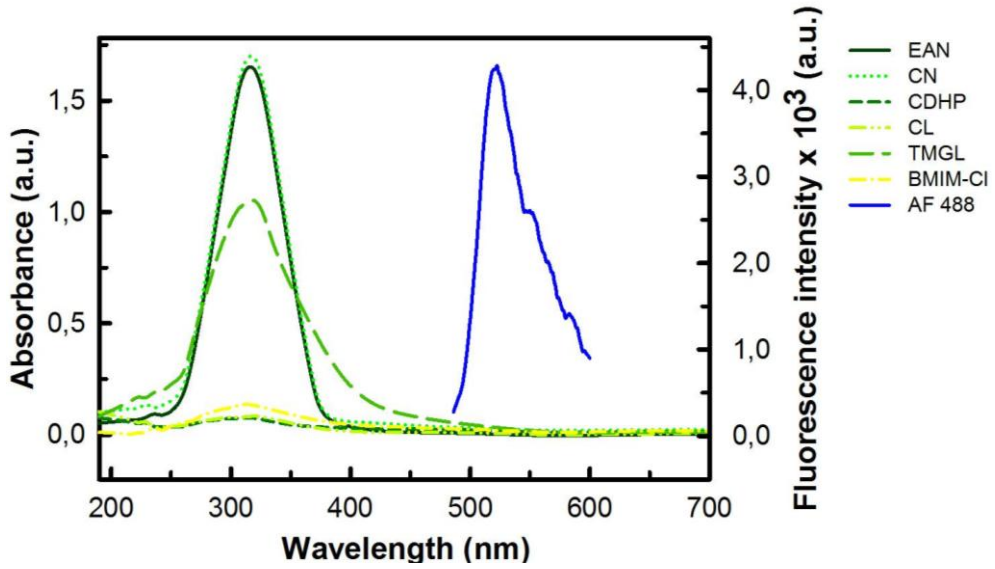

Figure 4.7. Absorbance spectra of the used ILs and emission spectrum of AF 488 (25 nM). The absorbance spectra were obtained from the ILs stock-solutions (see Chapter 2 for more details).

this electron emits fluorescence when it returns to the ground-state in a different wavelength. However, if the acceptor is a non-fluorescent molecule, a quencher, the energy is released by internal convention (instead by fluorescence), dissipating as heat.[35,36] This type of quenching cannot be evaluated by the S-V plot. However, it can be revealed by a possible overlap between emission and absorption spectra of the donor and the acceptor, respectively. RET does not require molecular contact between the donor and the acceptor, but a distance at which RET is 50% efficient,

the Förster distance, R_0. For this reason RET is not sensitive to steric factors or electrostatic interactions.[36,41]

In **Figure 4.7** EAN and CN presented the highest absorbance near 1.7 a.u. at 317 nm. TMGL also presented absorbance near this wavelength but with a lower intensity than EAN and CN (≈ 1.0 a.u.). The other ILs studied presented almost no absorbance within the wavelength range considered. For comparison, AF has its maximum fluorescence emission at 520 nm after excitation at 480 nm. As can be clearly seen in **Figure 4.7**, no overlap of emission spectrum of the donor and absorption spectrum of acceptors was observed. As a consequence, it can be inferred that any fluorescence quenching of AF 488 by the ILs did not result from energy transfer (FRET) between them in the excited state.

4.2.1.4. Absorption measurement

Finally, absorption spectra of the fluorophore in presence or in absence of the ILs are also a manner to distinguish/confirm whether the quenching occurring between the molecules involved is static or dynamic. If the quenching is dynamic, it only affects the excited states of the fluorophore and thus no changes in the absorption spectra would be registered. On the other hand, if the formation of a

complex between dye and quencher occurs in the ground-state, then it will result in a change of the absorption spectra of the fluorophore.[36] Shifts of the absorption spectra may also provide hints on the formation of aggregates. To verify this, the absorption spectra of AF 488 were acquired with the addition of increasing concentrations of the ILs. The results are depicted in **Figure 4.6**.

It could be seen that with increasing concentrations of any of the ILs to the solution, the absorption intensity of AF 488 at 494 ± 1 nm remained practically constant. These results confirm then the dynamic quenching part detected by Stern-Volmer plots for CN, CDHP and TMGL. For CL, changes in the spectra were expected revealing the pure static quenching, but the obtained spectra were very similar independently of the concentration and similar to the other cholines.

In general, all the ILs maintained the peak wavelength with no shifts. An exception was detected for AF488 with BMIM-Cl that caused a red-shift of 4 and 5 nm when the concentrations in solution were 1,5 and 2M respectively, regarding the previous concentration peaks. This also reveals the possible formation of BMIM-Cl aggregates at these concentrations as already mentioned in the lifetime and emission measurements.

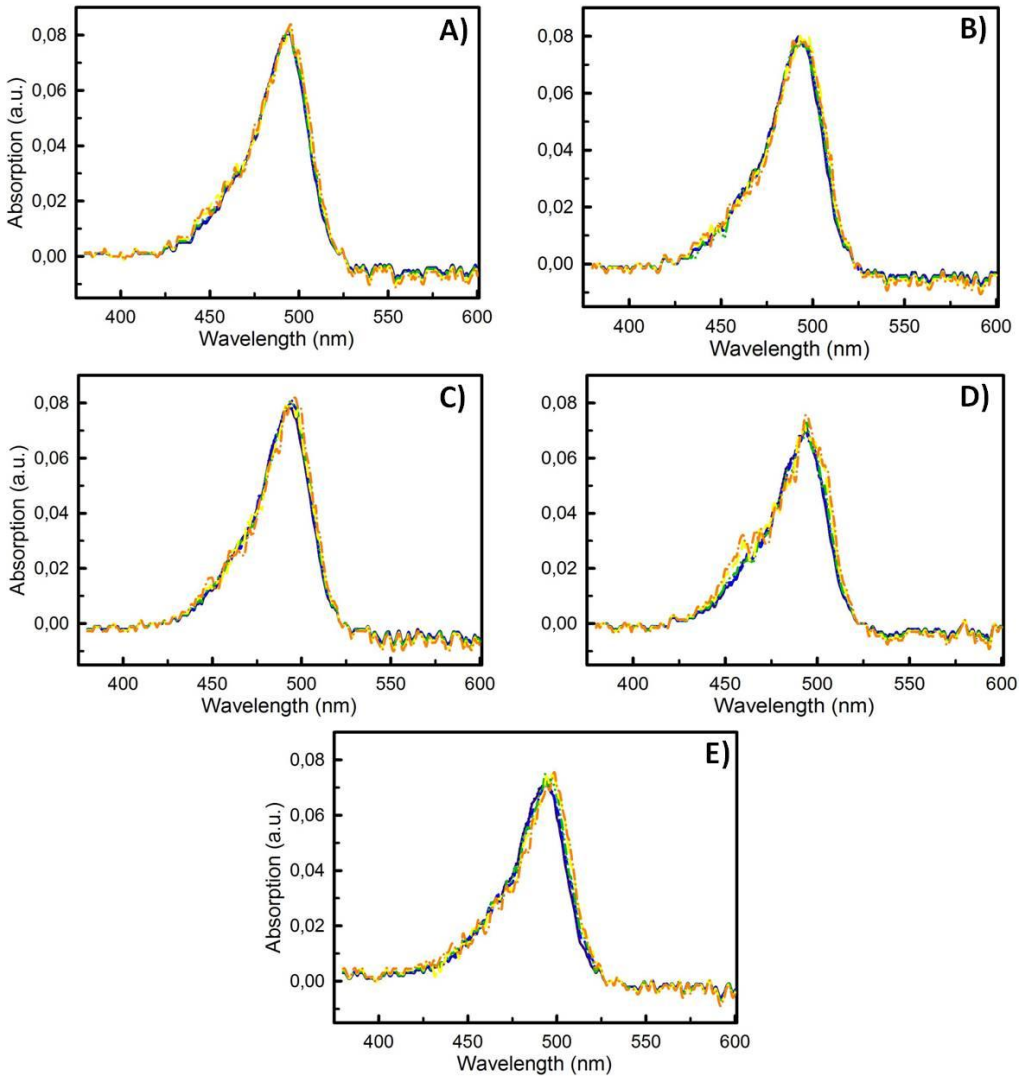

Figure 4.6. Absorbance spectra of the AF 488 in solution with TBS and with the addition of 0.05 (purple line), 0.3 (blue line), 0.6 (green line), 1.5 (yellow line) and 2M (orange line) of **A)** CN, **B)** CDHP, **C)** CL, **D)** TMGL and **E)** BMIM-Cl.

In accordance with our results, Wang H. et al. (2012) observed that the fluorescence intensity of free 4-tert-octylphenol (4-t-OP) decreased with increasing concentrations of ILs belonging to the imidazolium family, with BF_4^- and PF_6^- as anions. Their observations suggest that the quencher role of ILs in the process of steady-state fluorescence of a free fluorophore in solution is a combination of static and dynamic quenching mechanism. They determined that the ILs with PF_6^- as anion had a weaker quenching effect than with BF_4^- due to the stronger viscosity of PF_6^-, reducing in this way the collision probability of fluorophores.[34] Here we found that CN, CDHP and TMGL exerted a combination of static and dynamic quenching. On the other hand, CL shared that same cation with CN and CDHP but caused a purely static quenching, only. Finally, the type of quenching observed for BMIM-Cl seemed to depend on its concentration in solution.

From these results and from the literature we may assert that there is no a pattern that allows to predict the influence of ILs on the fluorescence emission of a fluorophore, in this particular case of AF 488. Although we studied only a small sample of ILs, it became clear that even presenting structural similarities by cations or anions do not allow predicting the quenching effect of ILs on AF 488.

4.2.2. AF488 attached to ssDNA oligomer 1 in solution with increasing concentrations of ILs

When measuring the fluorescence intensity of AF 488 attached to a 12-mer DNA oligomer in presence of increasing concentrations of ILs, the results were surprisingly different from having the fluorophore free in solution: the fluorescence remained practically stable irrespective of the increasing IL concentration (**Figure 4.7**). Only BMIM-Cl and TMGL exhibited a slight increase and decrease, respectively, of the fluorescence intensity of the fluorophore for highest IL concentrations studied. Again, the alteration of the viscosity of the solution (see **Table 4.1.**) did not seem to have any effect, either.

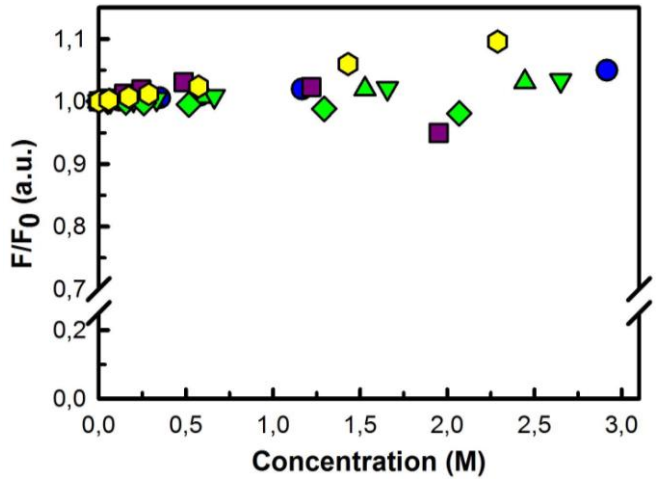

Figure 4.7. Normalized fluorescence of AF 488 attached to the DNA oligomer 1 as function of the concentration of EAN (circles), CN (triangles), CDHP (inverted triangles), CL (diamonds), TMGL (squares) and BMIM-Cl (hexagons) in solution with TBS. Data were normalized with respect to the initial intensity (F_0) of the oligomer 1-AF in TBS. The initial concentration of the oligomer 1-AF was 17 nM. Raw data were corrected for background signal and taking into consideration the volume changes upon successive addition of IL.

A possible explanation for this observation could be that the fluorescent probe is somehow "protected" from the quenching IL, as has been observed when dyes were "buried" in the secondary or tertiary structure of a macromolecule. When a stimulus causes an alteration in the conformation of the macromolecule, the dye

will be exposed to quenching to a different degree, consequently generating a "light-on" or a "light-off" situation depending on the dye and system used.[36,43–45]

In our case, however, AF 488 was covalently attached to the 5' end of a single-stranded 12-mer. With a normal salt concentration in solution, the structure of ssDNA is not so rigid as a double-strand and may fluctuate, assuming an equilibrium between different conformations.[46] However, in **Chapter 3** and as will be discussed in detail in **Chapter 5**, especially the ILs containing bulky cations such as BMIM-Cl and TMGL seem to induce a stretching of the DNA at high IL concentrations, increasing in this way the stiffness of DNA and the possibility of exposing the fluorophore to possible quenching.[9] Indeed, this seems to start to occur for the highest concentrations of BMIM-Cl and TMGL as can be seen in **Figure 4.7**.

Similarly, when the steroid dihydroequilenin (DHE) as fluorophore is free in solution it was quenched when surrounded by acrylamide as solvent. However, when DHE was bonded to a steroid-binding protein (SBP) much less quenching occurred. The modest amount of quenching that occurs was attributed to dissociation of DHE from the protein.[36] Levitus M. and co-workers found similar results when using Cy3 dye free and attached to sequences of single and double stranded DNA through the determination of fluorescence quantum yields, emission

lifetimes and fluorescence anisotropy decays. They reported that the quantum yield and lifetime of Cy3 covalently attached to the 5' terminus of a ssDNA was higher when compared with the free dye in solution. The increase in fluorescence efficiency was related to interactions between the dye and the DNA structure, strongly depending on temperature, DNA structure and dye labeling location, be it internal or to the end of the DNA strand.[47–49]

Apparently, the nucleic acids labeled with the AF dyes do not aggregate or precipitate, even at high-salt conditions.[50] We observed that this statement may not be entirely correct. **Figure 4.8** depicts the average lifetime and intensity images obtained for DNA-AF 488 with the addition of 3M of BMIM-Cl and TMGL, respectively, and compared with the images of DNA-AF 488 in pure TBS solution. In contrast to what was observed with the free fluorophore in solution, at 3M of BMIM-Cl in solution aggregates were clearly detected both through lifetime and intensity images. Brighter zones, presenting shorter lifetimes, can easily be identified in the FL lifetime and intensity images.

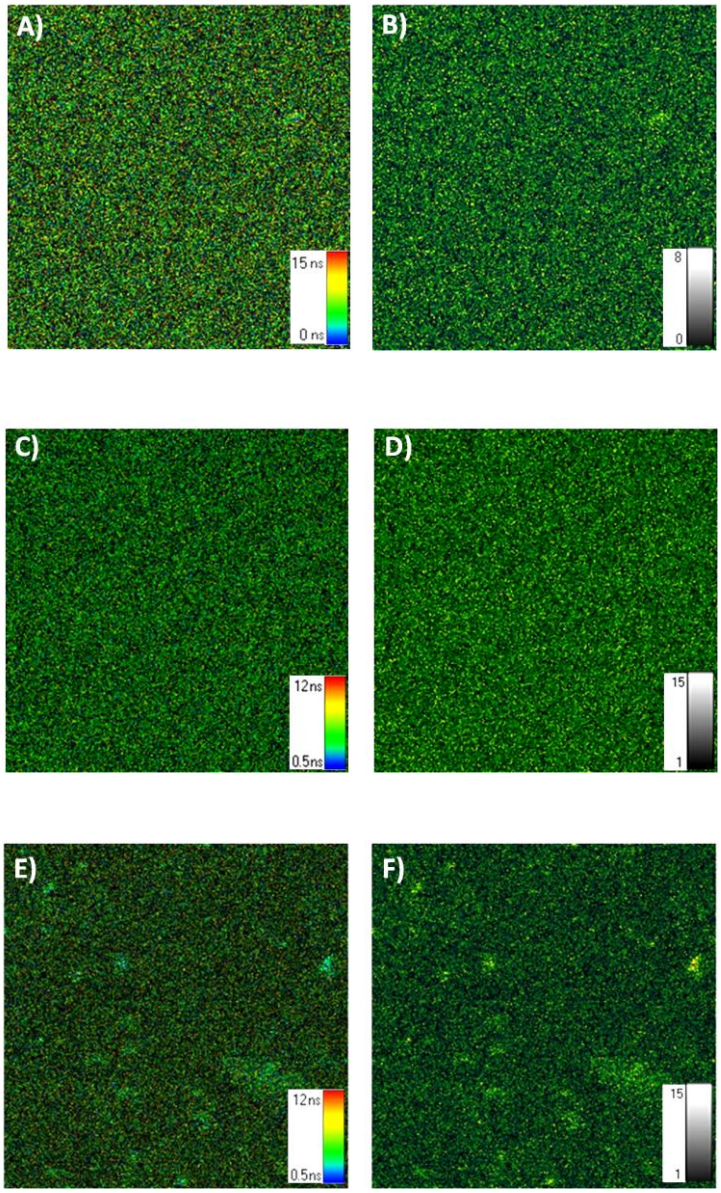
A)
15 ns
0 ns
B)
8
0
C)
12ns
0.5ns
D)
15
1
E)
12ns
0.5ns
F)
15
1

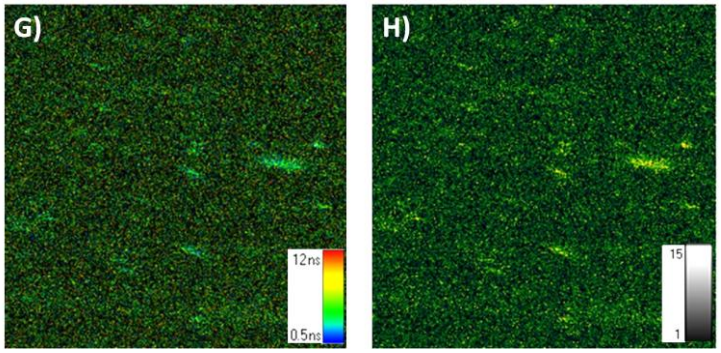

Figure 4.8. FL lifetime (**A**, **C**, **E** and **G**) and FL intensity images (**B**, **D**, **F** and **H**) of the AF 488 attached to the oligomer 1 (17 nM) in solution with **A)** and **B)** TBS buffer, **C)** and **D)** 3M of TMGL and **E)** - **H)** 3M of BMIM-Cl. The images **E)** to **H)** are images of the same sample but corresponding to different zones. The excitation wavelength was 485 nm.

In pure buffer or at 3M of TMGL, however, no aggregates were observed. Despite the formation of these aggregates, they did not seem not to interfere significantly with the fluorescence emission intensity since it only slightly increased in presence of 2,5 M of BMIM-Cl and when in fact no quenching was observed (**Figure 4.7**).

4.3. Conclusions

In conclusion, we showed that the steady-state fluorescence emission intensity of the AF 488 free in solution decreases with the rising concentrations of the ILs CN, CDHP, CL, TMGL and BMIM-Cl. When the IL used was EAN, no significant decrease in the fluorescence was registered.

Different kinds of quenching were identified depending on the ILs employed. From the Stern-Volmer plot it was determined that CN, CDHP and TMGL exerted a combination of static and dynamic quenching of the AF 488 fluorophore, confirmed by the absorption spectra and the fluorescence lifetime with the respective FL images. For CL the quenching was purely static. In the case of BMIM-Cl the type of quenching changed depending on the concentration of the IL in solution: according to lifetime measurements, at low concentrations BMIM-Cl exerts static quenching, whilst at higher concentration (3M BMIM-Cl) quenching becomes dynamic, as detected by the strong decrease of the lifetime. These two types of quenching that BMIM-Cl exhibited could not be detected from absorbance spectra or the Stern-Volmer plot. Furthermore, it was in general found that when AF 488 is free in solution the quenching observed in the presence of an IL was not due to FRET, because no overlap of the emission spectrum of AF488 with the absorption spectra

of the respective IL occurred. No aggregates of free AF 488 were detected in presence of the ILs.

On the other hand, when attached to a 12-mer DNA, AF 488 fluorescence emission was practically not affected by the presence of any of the six ILs studied. This was explained by the fact that the AF 488 covalently attached to DNA is less exposed to quenching of the IL. Only for the highest concentrations of TMGL and BMIM-Cl used a slight decrease and increase of the normalized fluorescence was detected, respectively, attributed to the stretching of the DNA sequences. Formation of aggregates of AF 488 was observed for 3M of BMIM-Cl in solution by taking FL images. This may indicate that BMIM-Cl causes DNA aggregation at this high concentration. On the contrary, with 3M of TMGL the formation of DNA-AF488 aggregates were not detected by the FL images.

As an overall conclusion, even using a reduced number of ILs and only one fluorophore, we can claim that we could not find a pattern that allows to predict the influence of ILs on the fluorescence emission of a fluorophore, in this case AF 488. Therefore, the possible influence of the ILs on the fluorescence must always be taken into account when using fluorophores as reporter molecules that should evidence possible conformational changes of hybridization events in DNA systems.

Here it was evidenced that even containing structural similarities by cations or anions, each IL has a particular effect on the fluorescence depending on their particular physico-chemical properties.

4.4. References

(1) Constantinescu, D.; Herrmann, C.; Weingärtner, H. Protein Denaturation by Ionic Liquids and the Hofmeister Series. In *Ionic Liquids: From Knowledge to Application*; Plechkova, N. V., Rogers, R. D., Seddon, K. R., Eds.; American Chemical Society, **2009**; 107–117.

(2) de María, P. D. *Ionic Liquids in Biotransformations and Organocatalysis: Solvents and Beyond*; **2012**.

(3) Baker, G. a; Baker, S. N.; Pandey, S.; Bright, F. V. An Analytical View of Ionic Liquids. *Analyst* **2005**, *130*, 800–808.

(4) Ding, Y.; Zhang, L.; Xie, J.; Guo, R. Binding Characteristics and Molecular Mechanism of Interaction between Ionic Liquid and DNA. *J. Phys. Chem. B* **2010**, *114* (5), 2033–2043.

(5) Chandran, A.; Ghoshdastidar, D.; Senapati, S. Groove Binding Mechanism of Ionic Liquids: A Key Factor in Long-Term Stability of DNA in Hydrated Ionic Liquids? *J. Am. Chem. Soc.* **2012**, *134* (50), 20330–20339.

(6) Vijayaraghavan, R.; Izgorodin, A.; Ganesh, V.; Surianarayanan, M.; MacFarlane, D. R. Long-Term Structural and Chemical Stability of DNA in Hydrated Ionic Liquids. *Angew. Chemie - Int. Ed.* **2010**, *49* (9), 1631–1633.

(7) Krishnan, Y.; Simmel, F. C. Nucleic Acid Based Molecular Devices. *Angew. Chemie - Int. Ed.* **2011**, *50* (14), 3124–3156.

(8) Serrano-Santos, M. B.; Llobet, E.; Özalp, V. C.; Schäfer, T. Characterization of Structural Changes in Aptamer Films for Controlled Release Nanodevices. *Chem. Commun. (Camb).* **2012**, *48* (81), 10087–10089.

(9) Machado, I.; Özalp, V. C.; Rezabal, E.; Schäfer, T. DNA Aptamers Are Functional Molecular Recognition Sensors in Protic Ionic Liquids. *Chemistry* **2014**, *20* (37), 11820–11825.

(10) Wang, H.; Wang, J.; Zhang, S. Binding Gibbs Energy of Ionic Liquids to Calf Thymus DNA: A Fluorescence Spectroscopy Study. *Phys. Chem. Chem. Phys.* **2011**, *13*, 3906–3910.

(11) Glazer, A. N.; Rye, H. S. Stable Dye-DNA Intercalation Complexes as Reagents for High-Sensitivity Fluorescence Detection. *Nature* **1992**, *359* (6398), 859–861.

(12) LePecq, J. B.; Paoletti, C. A Fluorescent Complex between Ethidium Bromide and Nucleic Acids. Physical-Chemical Characterization. *J. Mol. Biol.* **1967**, *27* (1), 87–106.

(13) Tang, Z.; Mallikaratchy, P.; Yang, R.; Kim, Y.; Zhu, Z.; Wang, H.; Tan, W. Aptamer Switch Probe Based on Intramolecular Displacement. *J. Am. Chem. Soc.* **2008**, *130* (34), 11268–11269.

(14) Wiederschain, G. Y. The Molecular Probes Handbook. A Guide to Fluorescent Probes and Labeling Technologies. *Biochem.* **2011**, *76* (11), 1276–1276.

(15) Glazer, a N.; Peck, K.; Mathies, R. a. A Stable Double-Stranded DNA-Ethidium Homodimer Complex: Application to Picogram Fluorescence Detection of DNA in Agarose Gels. *Proc. Natl. Acad. Sci. U. S. A.* **1990**, *87* (10), 3851–3855.

(16) Rye, H. S.; Yue, S.; Wemmer, D. E.; Quesada, M. a; Haugland, R. P.; Mathies, R. a; Glazer, a N. Stable Fluorescent Complexes of Double-Stranded DNA with Bis-Intercalating Asymmetric Cyanine Dyes: Properties and Applications. *Nucleic Acids Res.* **1992**, *20* (11), 2803–2812.

(17) O'connor Claire. Fluorescence in Situ Hydribation. *Nat. Educ.* **2008**, *1* (1), 171.

(18) Li, Y.; Zhou, X.; Ye, D. Molecular Beacons: An Optimal Multifunctional Biological Probe. *Biochemical and Biophysical Research Communications*. **2008**, 457–461.

(19) Hacia, J. G.; Fan, J. B.; Ryder, O.; Jin, L.; Edgemon, K.; Ghandour, G.; Mayer, R. a; Sun, B.; Hsie, L.; Robbins, C. M.; et al. Determination of Ancestral Alleles for Human Single-Nucleotide Polymorphisms Using High-Density Oligonucleotide Arrays. *Nat. Genet.* **1999**, *22* (2), 164–167.

(20) Pollack, J. R.; Perou, C. M.; Alizadeh, A. A.; Eisen, M. B.; Pergamenschikov, A.; Williams, C. F.; Jeffrey, S. S.; Botstein, D.; Brown, P. O. Genome-Wide Analysis of DNA Copy-Number Changes Using cDNA Microarrays. *Nat. Genet.* **1999**, *23* (1), 41–46.

(21) Panchuk-Voloshina, N.; Haugland, R. P.; Bishop-Stewart, J.; Bhalgat, M. K.; Millard, P. J.; Mao, F.; Leung, W. Y.; Haugland, R. P. Alexa Dyes, a Series of New Fluorescent Dyes That Yield Exceptionally Bright, Photostable Conjugates. *J. Histochem. Cytochem.* **1999**, *47* (9), 1179–

1188.

(22) Yuan, C. P.; Jian, J. W.; Xiao, P. X.; Fan, J.; Fan, M. Factors Affecting Ionic Liquids Based Removal of Anionic Dyes from Water. *Environ. Sci. Technol.* **2007**, *41* (14), 5090–5095.

(23) Mojumdar, S. Sen; Chowdhury, R.; Chattoraj, S.; Bhattacharyya, K. Role of Ionic Liquid on the Conformational Dynamics in the Native, Molten Globule, and Unfolded States of Cytochrome C: A Fluorescence Correlation Spectroscopy Study. *J. Phys. Chem. B* **2012**, *116* (40), 12189–12198.

(24) Huang, J.; Wu, J.; Li, Z. Biosensing Using Hairpin DNA Probes. *Reviews in Analytical Chemistry*. **2015**, 1–27.

(25) Su, X.; Zhu, X.; Zhang, C.; Xiao, X.; Zhao, M. In Situ, Real-Time Monitoring of the 3′ to 5′ Exonucleases Secreted by Living Cells. *Anal. Chem.* **2012**, *84* (11), 5059–5065.

(26) Jockusch, S.; Martí, A. a; Turro, N. J.; Li, Z.; Li, X.; Ju, J.; Stevens, N.; Akins, D. L. Spectroscopic Investigation of a FRET Molecular Beacon Containing Two Fluorophores for Probing DNA/RNA Sequences. *Photochem. Photobiol. Sci.* **2006**, *5* (5), 493–498.

(27) Santangelo, P. J.; Nix, B.; Tsourkas, A.; Bao, G. Dual FRET Molecular Beacons for mRNA Detection in Living Cells. *Nucleic Acids Res.* **2004**, *32* (6), e57.

(28) Tan, W.; Wang, K.; Drake, T. J. Molecular Beacons. *Current Opinion in Chemical Biology*. **2004**, 547–553.

(29) Cheng, D. H.; Chen, X. W.; Wang, J. H.; Fang, Z. L. An Abnormal Resonance Light Scattering Arising from Ionic-liquid/DNA/ Ethidium Interactions. *Chem. - A Eur. J.* **2007**, *13* (17), 4833–4839.

(30) Singh, P. K.; Sujana, J.; Mora, A. K.; Nath, S. Probing the DNA-Ionic Liquid Interaction Using an Ultrafast Molecular Rotor. *J. Photochem. Photobiol. A Chem.* **2012**, *246*, 16–22.

(31) Khimji, I.; Doan, K.; Bruggeman, K.; Huang, P.-J. J.; Vajha, P.; Liu, J. Extraction of DNA Staining Dyes from DNA Using Hydrophobic Ionic Liquids. *Chem. Commun. (Camb).* **2013**, *49* (40), 4537–4539.

(32) Pabbathi, A.; Samanta, A. Spectroscopic and Molecular Docking Study of the Interaction of DNA with a Morpholinium Ionic Liquid. *J. Phys. Chem. B* **2015**, *119* (34), 11099–11105.

(33) Mandal, P. K.; Samanta, A. Fluorescence Studies in a Pyrrolidinium Ionic Liquid: Polarity of the Medium and Solvation Dynamics. *J. Phys. Chem. B* **2005**, *109* (31), 15172–15177.

(34) Wang, H.; Mao, J.; Duan, A.; Che, B.; Wang, W.; Ma, M.; Wang, X. Fluorescence Quenching of 4-Tert-Octylphenol by Room Temperature Ionic Liquids and Its Application. *J. Fluoresc.* **2013**, *23* (2), 323–331.

(35) Ghosh, A.; De, C. K.; Chatterjee, T.; Mandal, P. K. What Type of Nanoscopic Environment Does a Cationic Fluorophore Experience in Room Temperature Ionic Liquids? *Phys. Chem. Chem. Phys.* **2015**, *17* (25), 16587–16593.

(36) Lakowicz, J. R. *Principles of Fluorescence Spectroscopy*; **2006**.

(37a) Blackman, M. J.; Corrie, J. E. T.; Croney, J. C.; Kelly, G.; Eccleston, J. F.; Jameson, D. M. Structural and Biochemical Characterization of a Fluorogenic Rhodamine-Labeled Malarial Protease Substrate. *Biochemistry* **2002**, *41* (40), 12244–12252.

(37b) Singh T., Kumar A. Aggregation Behaviour of Ionic Liquids in Aqueous Solutions: Effect of Alkyl Chain Length Cations and Anions, *J. Phys. Chem. B* **2007**, 111, 7843-7851

(38) Sauer, M.; Hofkens, J.; Enderlein, J. *Handbook of Fluorescence Spectroscopy and Imaging*; **2011**.

(39) Talap, P. D.; Appl, A.; Res, S. Self - Aggregation of Rhodamine-6G in Aqueous Medium and Aqueous Solution of Urea Dm Mole ε ε θ. **2012**, *4* (2), 826–830.

(40) Hihara, T.; Okada, Y.; Morita, Z. The Aggregation of Triphenodioxazine Reactive Dyes in Aqueous Solution and on Cellulosic and Nylon Substrates. *Dye. Pigment.* **2000**, *45* (2), 131–143.

(41) Skoog, D. A.; Holler, F. J.; Crouch, S. R. *Principles of Instrumental Analysis Sixth Edition*; **1998**.

(42) Sauer, M.; Hofkens, J.; Enderlein, J. Basic Principles of Fluorescence Spectroscopy. In *Handbook of fluorescence spectroscopy and imaging*; **2011**; 1–30.

(43) Baker, S. N.; Zhao, H.; Pandey, S.; Heller, W. T.; Bright, F. V; Baker, G. a. Fluorescence Energy Transfer Efficiency in Labeled Yeast Cytochrome c: A Rapid Screen for Ion Biocompatibility in Aqueous Ionic Liquids. *Phys. Chem. Chem. Phys.* **2011**, *13*, 3642–3644.

(44) Chowdhury, R.; Mojumdar, S. Sen; Chattoraj, S.; Bhattacharyya, K. Effect of Ionic Liquid on the Native and Denatured State of a Protein Covalently Attached to a Probe: Solvation Dynamics Study. *J. Chem. Phys.* **2012**, *137* (5).

(45) Ogoshi, T.; Harada, A. Chemical Sensors Based on Cyclodextrin Derivatives. *Sensors* **2008**, *8* (8), 4961–4982.

(46) Murphy, M. C.; Rasnik, I.; Cheng, W.; Lohman, T. M.; Ha, T. Probing Single-Stranded DNA

Conformational Flexibility Using Fluorescence Spectroscopy. *Biophys. J.* **2004**, *86* (4), 2530–2537.

(47) Stennett, E. M. S.; Ciuba, M. A.; Levitus, M. Photophysical Processes in Single Molecule Organic Fluorescent Probes. *Chem. Soc. Rev.* **2014**, *43* (4), 1057–1075.

(48) Harvey, B. J.; Perez, C.; Levitus, M. DNA Sequence-Dependent Enhancement of Cy3 Fluorescence. *Photochem. Photobiol. Sci.* **2009**, *8* (8), 1105–1110.

(49) Sanborn, M. E.; Connolly, B. K.; Gurunathan, K.; Levitus, M. Fluorescence Properties and Photophysics of the Sulfoindocyanine Cy3 Linked Covalently to DNA. *J. Phys. Chem. B* **2007**, *111* (37), 11064–11074.

(50) Invitrogen. Alexa Fluor Dyes - Simply the Best and Brightest Fluorescent Dyes and Conjugates. *Mol. Probes, Inc.* **2005**, 1–36.

(51) So, P. T. C.; Dong, C. Y. Fluorescence Spectrophotometry. *Encycl. Life Sci.* **2002**, 1–4.

CHAPTER 5

Functional DNA in Ionic Liquids

5.1 Introduction

The structure and function of nucleic acids are defined to a large extent by interactions between the bases through hydrogen bonds, but also with the molecules surrounding them. As documented by Privé et al. "…DNA is built from five structural elements rather than three: the familiar bases, sugars and phosphate groups, but also ordered water molecules and bound counterions."[1] As many other so-called "biomolecules", nucleic acids mostly find their applications under physiological conditions in which water is the primary solvent. However, on one hand water also presents some drawbacks for nucleic acids as it favours hydrolytic reactions such as depurination or deamination.[2–4] On the other, the benefits of the solvation of "biomolecules" in solvents other than water have been shown previously: the study of biotransformations using enzymes in non-aqueous media reported by Klibanov triggered the development of a whole new research field enhancing significantly the degree of freedom in designing enzyme-based catalysis.[5–8] Later, ILs proved to avoid hydrolysis and aggregation when solvating proteins, and in certain cases enzymes exhibited a higher selectivity and stability when dissolved in ILs.[9–11] Hence, considering the function of "biomolecules" associated with and limited to aqueous environments is not necessarily justified. With DNA being a

functional molecule of unique characteristics and possibilities for self-assembled materials,[12] it seems an attractive perspective to be able to reproduce the success enzymatic functions exhibited in tunable non-aqueous solvents such as ILs, and have systems at disposal in which DNA is able to function at water concentrations far lower than usual or even becoming residual.

DNA-aptamers are one example of systematically designing DNA nanostructures responsive to external molecular triggers, which extended the area of DNA nanotechnology from mere structure to also function[13,14] and has enabled its use as reversible and smart building blocks of nanodevices.[15–17] The design of such devices benefits from the highest possible degree of freedom and the use of functional elements with an intrinsic molecular recognition or self-assembly capacity. Substituting water in part or entirely by versatile "designer solvents" such as ILs could therefore give rise to a whole new range of applications.

ILs entirely consisting of cations and anions have been considered "clean solvents" owing to their negligible vapor pressure, as much as this evaluation needs to be made on a case-to-case basis and cannot be generalized. However, one doubtless and unique asset of ILs is their capability of undergoing a whole range of interactions, which in addition to those of conventional molecular solvents comprise

electrostatic interactions. This results in a high degree of tuneability of their physico-chemical properties which make ILs extremely attractive (co-)solvents particularly for DNA-based functional elements.

Considering the high number of ILs already available, the solvation of DNA by ILs has been studied to a reduced number of ILs and a reduced number of DNA structures.[18,19] Experimental and theoretical efforts have been made to elucidate the possible effect of ILs on the secondary and tertiary structure of DNA with the aim of increase the DNA structure stability for a long-term storage and resistance to nucleases.[20–22] Supposed displacement of DNA staining dyes like the intercalators ethidium bromide or pyrene from DNA by imidazolium ILs was investigated as a means of elucidating interactions between IL and DNA[3,23,24] not accounting, however, for the possibly stronger electrostatic interactions between the dye and the IL. Molecular dynamics (MD) simulations have attempted elucidating interactions taking place between the ions of an IL and DNA[3,25] and while these were able to shed light on the complexity of the system under study, it must be emphasized that currently, the parameterized force fields required for MD simulations of such innovative systems may still not exactly reflect those of practical

validation experiments and conclusions drawn on their basis need to be pondered carefully.

Interactions of ILs with DNA become a particularly challenging task when DNA function is envisaged, such as the reversible molecular recognition function exhibited by DNA-aptamers. With aptamers being nucleic acids that can undergo facile site-directed structural modifications, such as for instance in order to create hairpin structures such as molecular beacons (MB),[26] they have been widely studied for biosensors[27,28] or as reversible gating elements capable of modulating flow across nanopores in stimuli-responsive controlled release nanodevices.[15–17] The reversible dynamic actuation of DNA-aptamer hairpins involves a combination of molecular interactions strongly influenced by the composition of the surrounding liquid, and in particular as regards surrounding ions.[29,30] Hence, when it comes to functional DNA which reversibly switches from one conformation to another, the challenge is to stabilize its function rather than a defined structure which, however, has so far been the primary objective of studies reported in literature. In the past we have shown that DNA-aptamers may maintain their function even at high concentrations of one particular protic IL, ethylammonium nitrate (EAN) (**Chapter 3**).[31] To the best of our knowledge, no systematic study has been reported so far on how DNA-aptamer

hairpins may remain functional in other non-conventional IL environments. It therefore is the aim of this work to show not only that depending on the nature of the IL this may indeed be feasible, but also to systematically elucidate the underlying IL-DNA interactions in the quest for conceiving functional DNA-based nanodevices operating in liquids of low or residual water content.

5.2. Results and Discussion

Molecular beacons consist of an hairpin structure with a loop and a stem which is a double stranded DNA reversibly changing between dsDNA and ssDNA depending on the presence of the target, which lends the beacon its reversible signaling function of a molecular recognition event (**Scheme 3.1 - Chapter 3 and Figure 2.2 - Chapter 2**). A high stability of both states is, hence, not desired. In this context, “stability” rather refers to maintaining a reversible recognition function, which goes beyond the concept of characterizing dsDNA in IL solutions, where “stability” refers to maintaining a fixed structure.

5.2.1. dsDNA formation and stability

Since the reversible signaling function of the DNA-aptamer beacon strongly depends on the dynamics of its stem region, we first investigated (for experimental details and calculations, see **Chapter 2**) on how it would preserve its function in the presence of ILs of different physico-chemical properties (**Figure 2.5** - **Chapter 2**).

At equilibrium and for concentrations up to 10% v/v (≤ 1M), we observed that none of the ILs used detrimentally affected the duplex formation when compared with pure TBS buffer solution (**Figure 5.1 bottom**). However, further increasing the concentration of ILs up to 40% v/v (≈2-3M, depending on the IL) in solution, some ILs caused a dramatic decrease of the amount of duplex formed while the presence of others remained widely without any effect. All choline-based ILs, bearing the same cation, roughly maintained the amount of dsDNA formed with only a very slight decrease toward highest IL concentrations (**Figure 5.1 up**). On the contrary, BMIM-Cl and TMGL were the two ILs which strongly affected the hybridization of the oligomers in the same concentration range. At a concentration of 40% v/v the

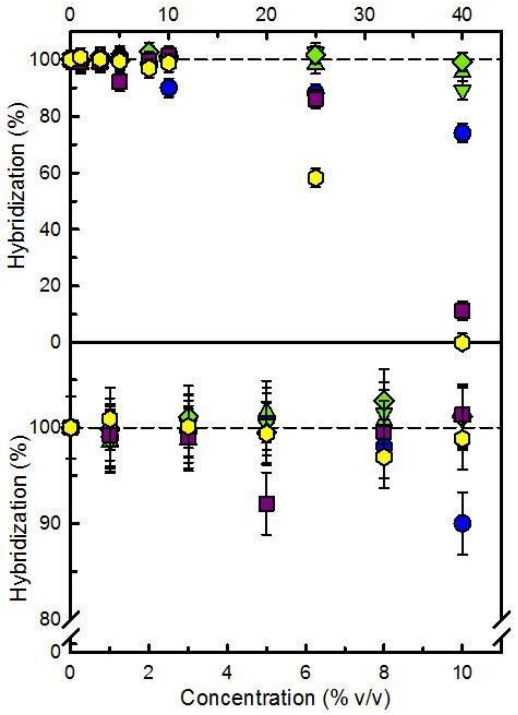

Figure 5.1. Graphic representation of the amount of DNA hybridized, in percentage (%), as function of the increase concentration of **A)** EAN (circles), CN (triangles), CDHP (inverted triangles), CL (diamonds), TMGL (squares), BMIM-Cl (hexagons), with the zoom until 10% v/v (bottom).

hybridization between the two oligomers decreased almost 90% for TMGL and was no longer observed for BMIM-Cl (**Figure 5.1 up**). Recalling the FL images results for oligomer 1 attached with AF 488 in solution with 3M of BMIM-Cl of **Chapter 4** (**Figure 4.8 E-H**), aggregation of the fluorophore, meaning aggregation of the ssDNA

sequence was observed. Here we did not reach such a high concentration, but apparently the effects of BMIM-Cl preventing DNA hybridization could be in part also related to this aggregation phenomenon.

On the other hand, these results suggest that the IL cation plays a key role in the interaction with DNA, rather than the anion. While this seems at first sight obvious in view of the negative charge of the phosphate backbone of DNA, it should be recalled that the IL anions have a greater effect on the surrounding water structure than do the IL cations, and differences between monovalent cations are generally less significant than the differences between the monovalent anions.[32] Using different salts, Stellwagen E. et al., 2011 concluded that the ion concentration, charge and/or size are the properties of the cations determining the interaction with DNA.[30] However, amongst these features they pointed to the size of the monovalent cations as being most responsible for the changes in the stability of DNA, affecting the relative electrostatic shielding of the phosphates in hairpin structure and random coil conformations. The underlying reasoning would be that these cations cannot physically approach the phosphate residues as much or as densely as smaller cations, establishing therefore less efficient electrostatic interactions,[19,30] favouring the random coil conformation and disadvantaging the formation of dsDNA. This is in

line with our experimental observation at high concentrations of ILs (> 1M), where indeed the ILs with cations of largest electronic spatial extent (ESE), BMIM-Cl and TMGL (see **Figure 2.5** and **Table 5.1**), caused a significant decrease of the amount of DNA hybridized as opposed to the other ILs used.

Table 5.1. Comparison of the radius of the monovalent common cation Na^+ present in the TBS buffer with the electronic spatial extent of the monovalent cations of the used ILs.

IL cation	R**2 (a.u.)
$BMIM^+$	2347
TMG^+	1088
$choline^+$	846
EA^+	208
Na^+	1

A word of caution must be added, however, with respect to the concentrations of the constituents used. While the concentration of ILs was in the molar range, DNA was added at a nanomolar level, i.e. at eight to nine orders of magnitude less a concentration. At low concentrations of ILs, competition between the counterions present in the buffer (Na^+, $Tris^+$ and K^+) and the cations of ILs is expected to occur around DNA.[33,34] Apart from prevailing electrostatic interactions, ILs are also capable of forming dispersion and H-bond interactions.[35,36] Hence, with

increasing concentration of ILs in solution, it may be anticipated that the IL will further interact through dispersion (London interactions), H-bonding and/or charge dipole interactions with parts of the DNA other than the phosphates, especially the bases. This may explain why an IL might affect the DNA duplex formation differently at high molar concentrations as compared to its interaction in dilute solution.

In order to understand in how far theoretical chemistry calculations could further elucidate the experimental observations, we analyzed first the affinity of the different ILs used in the experiments for the DNA bases considering those sites participating in the Watson-Crick hybridization. All ILs studied showed significant affinity for the bases with binding energies ranging from -36,6 to -13.7 kcal/mol. Interestingly, gas phase calculations (solid symbols in **Figure 5.2**) did not reveal any significant affinity differences arising from the physico-chemical nature of the IL; this was further confirmed by solvent phase calculations instead gas phase, considering the influence of the solvent on the affinity. The interaction of two ILs yielding different experimental results, CN and BMIM-Cl, with the DNA bases were estimated theoretically (hollow symbols in **Figure 5.2**), obtaining very similar results. This suggests that with regard to the interaction with the DNA-bases, the particular

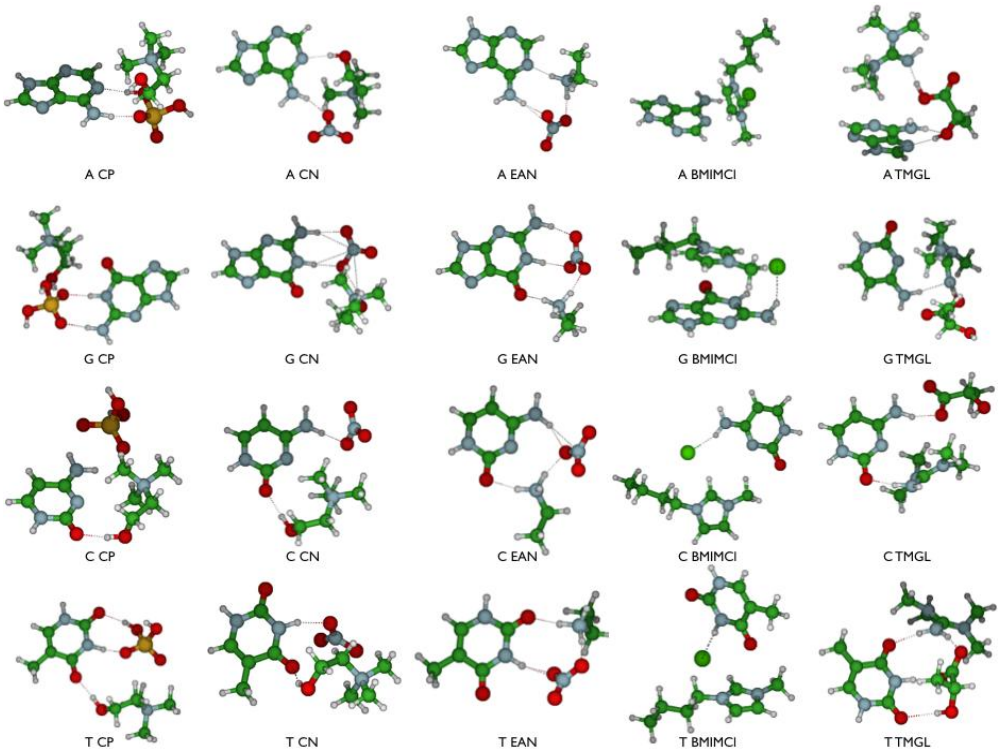
A CP
A CN
A EAN
A BMIMCl
A TMGL
G CP
G CN
G EAN
G BMIMCl
G TMGL
C CP
C CN
C EAN
C BMIMCl
C TMGL
T CP
T CN
T EAN
T BMIMCl
T TMGL

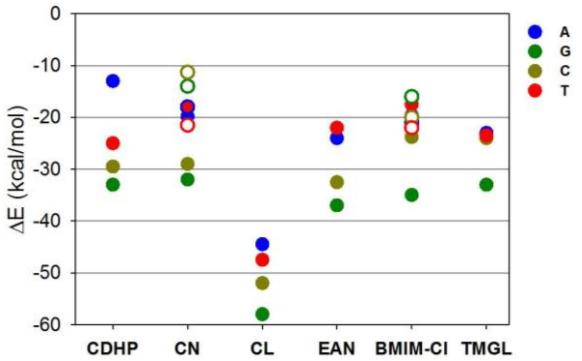

Figure 5.2. Affinity of the different ILs for the bases of DNA adenine (A), guanine (G), cytosine (C), and thymine (T). Solid symbols denote gas phase calculations, hollow symbols consider solvent effects.

characteristics of each IL may not play a significant role, and the interaction relies in a more general property of the ILs, this is, their charged nature. Hence, ruling out that this could be the main source of the experimental behavior observed in **Figure 5.1**.

A similar study was carried out for an insight into the interactions of the IL cations considered experimentally with the DNA-phosphate. In this case, the model included just the cation of the IL, and very similar degrees of affinity were determined, arising mainly from the strong Coulomb interactions taking place between the positively charged cation and negatively charged phosphate. Additionally, each cation can establish one H-bond with one of the oxygen atoms of

the phosphate (**Figure 5.3**). The situation changes, however, when a second cation is introduced: while the overall affinity energy increases for all the cations, as expected, we could observe that some of the cations, namely TMG^+ and $BMIM^+$, suffered significant steric hindrance preventing them from interacting efficiently with the phosphates, as reflected in the H-bond lengths in the complexes. While EA and choline cations maintained the H-bond lengths established with one cation and were able to establish H-bonds of similar length with each phosphate, the bulkier cations $BMIM^+$ and TMG^+ underwent

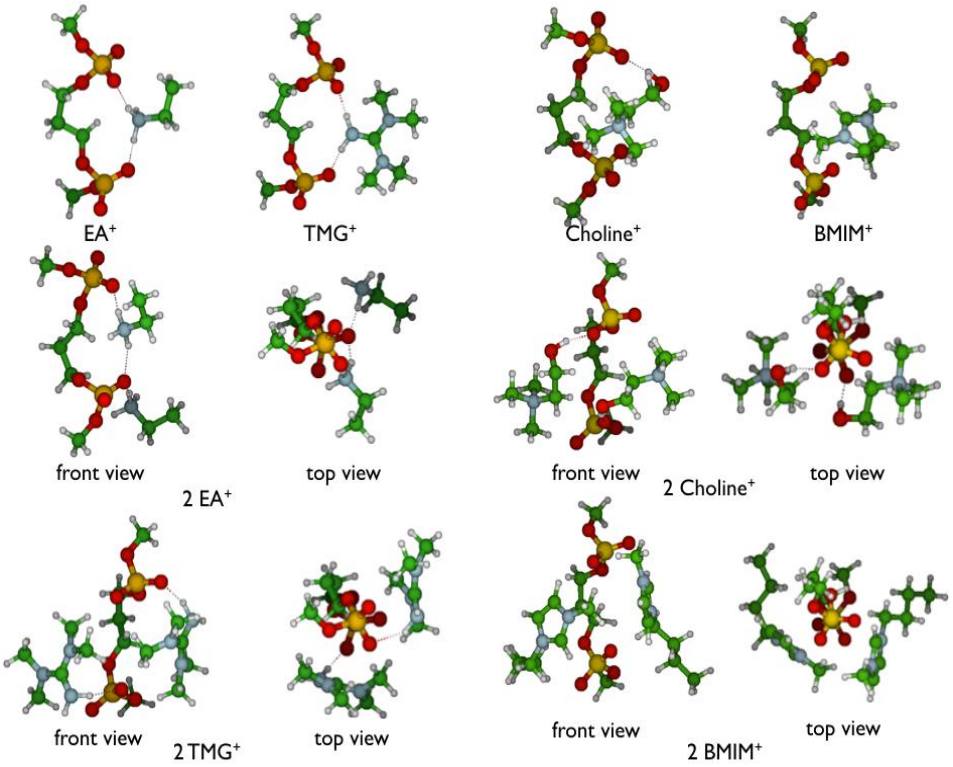

Figure 5.3. Simulation of the interaction of one or two cations with two phosphates of the DNA backbone.

a significant increase of the H-bond lengths formed in the complexes with two cations, pointing out, therefore, to less efficient interactions. Furthermore, these H-bonds were significantly different amongst them (2.567 Å and 2.020 Å, respectively, in the two $BMIM^+$ complex; 2.043 and 1.689 Å, respectively, in the case of TMG^+, see **Table 5.2**). This suggests that in

Table 5.2. Affinity energies and H-bond lengths estimated theoretically when the DNA-phosphates interact with one or two cations of the ILs used.

	ΔE (kcal/mol)		H-bond length (Å)		
Number of cations	**1**	**2**	**1**	**2**	
$BMIM^+$	-172,9	-275,9	1,770	2,567	2,020
$Choline^+$	-166,6	-281,7	1,651	1,642	1,688
TMG^+	-180,1	-254,3	1,677	2,043	1,689
EA^+	-202,6	-298,8	1,577	1,522	1,503

this case, the space between two DNA-phosphates is too small to accommodate both cations. As a consequence, the double helix would be better stabilized by smaller cations rather than the bulkier ones, such as TMG^+ and $BMIM^+$. This confirms, hence, the experimental result that high concentrations of TMGL and BMIM-Cl favour the presence of ssDNA rather than dsDNA, preventing therefore the hybridization.

Our observations were corroborated by the determination of the melting

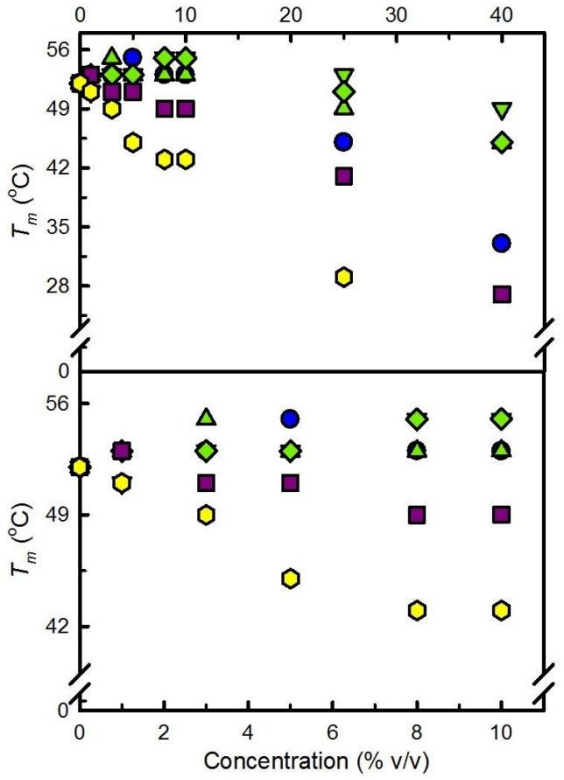

Figure 5.4. Graphic representation of the melting temperature of DNA oligomers, T_m, as function of the increase concentration of EAN (circles), CN (triangles), CDHP (inverted triangles), CL (diamonds), TMGL (squares), BMIM-Cl (hexagons) in TBS solution. The standard deviation here is ±0.5 °C for all samples.

temperature (T_m) of dsDNA formed in presence of ILs. As previously observed for the amount of dsDNA formed, for concentrations up to 10% (v/v), EAN and the choline-based ILs preserved the stability of the formed dsDNA as revealed by a nearly constant melting temperature (**Figure 5.4**). Between 10 and 40% v/v, the general

trend of all ILs was to decrease T_m, however, with this tendency being more pronounced for BMIM-Cl and TMGL, and to a lesser degree also EAN. The Tm of BMIM-Cl and TMGL nearly reaches room temperature at 25% v/v and 40% v/v of the respective IL in solution (T_m = 28 and 27 ^{o}C, respectively). Our results partially contradict results reported by Chandran et al. stating that in an aqueous solution of even very high concentrations (80% w/w) of BMIM-Cl, dsDNA retains its B-conformation, while choline cations due to its bulky tetrahedral headgroup tend to destabilize more the dsDNA structure.[25] We observed that if the duplex is formed already in presence of choline ILs and BMIM-Cl, choline-based ILs widely preserved the dsDNA (T_m = 47 ^{o}C ± 2 ^{o}C) while for high concentrations of BMIM-Cl (40% v/v), the hybridization was no longer occurring.

We made an attempt to compare these observations with those for common salts, well known to affect properties of biological macromolecules such as their structural stability, solubility and biological activity.[30,32,34,37] Bearing in mind the hypothesis that the IL cations are responsible of the stability of DNA, we studied the hybridization and DNA-stability substituting the cations of the ILs by a sodium cation while maintaining the respective anions. In this way we also expected to shed light on the role of the IL anions during interaction with DNA.

As observed for ILs, we found that in presence of concentrations up to 10% v/v of these sodium salts, the amount of DNA hybridized and their stability were maintained when compared to the pure buffer solution (compare **Figure 5.1** and **Figure 5.5 A**). Solutions of sodium dihydrogen phosphate (NaDHP) were only measured until 8% v/v in solution due to its strong tendency to alter the pH, which was also very difficult to adjust. Increasing concentrations up to 40% v/v in solution, a slight decrease of the dsDNA formed was observed when using sodium nitrate and sodium lactate. However, an amount of nearly 90% of dsDNA was still reached, while sodium chloride (NaCl) maintained the amount of hybridized DNA at 100% with increasing concentration in solution.

This apparently indicated that the anions played a minor role for DNA hybridization. However, when determining the melting temperature of the dsDNA formed, a significant difference was observed between the salts studied (**Figure 5.5 B**): while in presence of up to 10% v/v NaCl, NaLac and $NaNO_3$ the stability of dsDNA was maintained, it gradually decreased for concentrations up to 40% v/v of the latter two, reaching a Tm of 35 ^{o}C and 33 ^{o}C, respectively. On the contrary, a

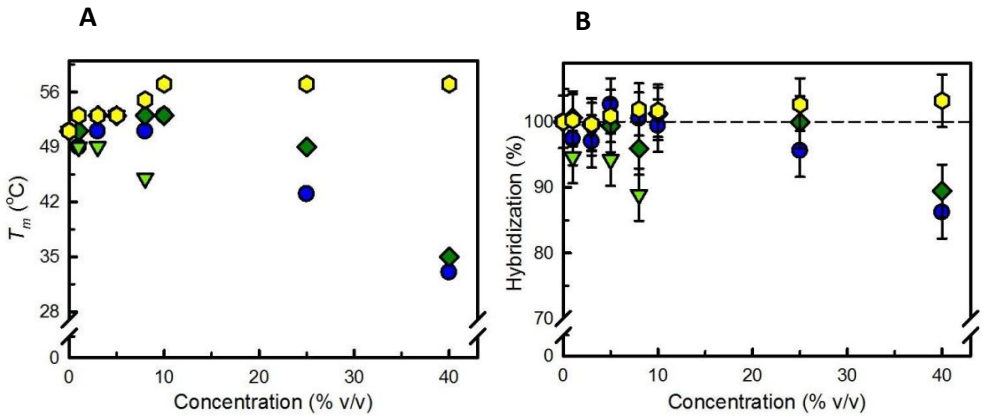

Figure 5.5 Graphical representation of the **A)** amount of DNA hybridized, in percentage (%) and of the **B)** melting temperature of DNA oligos, *Tm*, as function of the increase concentration of $NaNO_3$ (circles), NaDHP (inverted triangles), NaLac (diamonds) and NaCl (hexagons) in TBS solution. The standard deviation *Tm* is ±0.5 °C for all samples.

concentration as high as 40% v/v of NaCl did not provoke any dsDNA instability, which is in line with literature stating that the electrostatic contributions of NaCl present in the buffer for DNA phosphate backbone neutralization are "not saturated".[32,38] This is known as the "screening" of the DNA negative charge resulting in a "cloud" of positive counter-ions.[39] However, since the concentration of DNA in this work was of eight to nine orders of magnitude lower than the concentration of ions in solution, this phenomenon is assumed to have negligible influence. For NaDHP we observed that with 8% v/v in solution the melting temperature of dsDNA was already lower than in pure buffer, T_m = 45 °C (**Figure 5.5 B**). NaDHP destabilized

dsDNA further than other salts and more than its homologue choline DHP. The only similarity between an IL and its sodium salt homologue as regards Tm was found for $NaNO_3$ and EAN (**Figures 5.4 and 5.5 B**).

As a note of caution, when the IL solutions were prepared with the TBS buffer, the buffering capacity was maintained when using EAN, CN and BMIM-Cl, but the pH decreased when mixing CL, CDHP and TMGL. Necessary amounts of NaOH were then added to adjust the pH of the samples to the same as the buffer (pH 8.0) (**Table 2.2** - **Chapter 2**). The additional presence of sodium cation in the solutions may contribute, together with the 138 mM of NaCl already present in the TBS buffer, to the DNA stability by increasing its melting temperature, then influencing the ILs results. However, when the common salt NaCl was added to the buffer solution, the increase in the DNA melting temperature only started to be observed from 8% v/v of NaCl in solution (**Figure 5.5 B**), corresponding to ≈540 mM of a total concentration of Na^+ in solution. Here, for CL and TMGL, with the highest concentrations of NaOH added to the solution we reached final concentrations of sodium cation of 305 mM and 291 mM, respectively, lower than the obtained for 5% v/v of NaCl, 388 mM. The exception was for CDHP that with the highest concentration of NaOH added corresponds to a total sodium concentration in solution of 805 mM, corresponding

to ≈15 % v/v of NaCl. In this case, the influence of the additional sodium in solution might explain the slightly higher Tm registered for CDHP comparing with the other choline ILs used (inverted triangles - **Figure 5.4**).

These results indicate that for one and the same cation, the anion does indeed play a role as regards to the stability of dsDNA formed in presence of ILs, possibly because being smaller than cations and due to charge effects, anions will certainly interact strongly with the bulk. Thus the major direct influence on the DNA structure is through the IL cation. Thus, dsDNA hybridization and subsequent stability in an IL strongly depends on the IL structure and must therefore not be generalized, neither can it be inferred from observations made with respective homologues of common salts.

With regard to possible effects on the bulk of the solution, we are aware of the possible interference of the ILs with the hydrogen-bonded water which then could indirectly affect the dsDNA stability. The ions may be classified as kosmotropes ('order maker') or on the contrary as chaotropes ('disorder maker') in terms of their effect on the hydrogen-bonded network of water, beyond the DNA solvation shell. With the exception of $BMIM^+$ which is considered a kosmotrope, the majority of the ions of the ILs used in this study are chaotropic.[40] The chaotropes tend to interact

less with water molecules than water with itself. It is commonly stated for proteins and enzymes that kosmotropic anions stabilize their native structure, while kosmotropic cations destabilize their native structure.[40–42] Thus, kosmotropic anions and cations evidence opposite effects on the hydration network. With the IL cations in our study being the main responsible for direct interaction with DNA and being here mostly chaotropic, one can thus infer that they should stabilize the dsDNA, which we actually partly observed for the tetraalkylammonium cholines. Being $BMIM^+$ kosmotrope, the opposite effect was expected and was indeed observed. However, studying the mobility of different DNA sequences through capillary electrophoresis, Stellwagen E. et al. found that the mobility differences for dsDNA could not be attributed to the effect of different cations on the hydrogen-bonded structure of water.[34] This is in agreement with what has been stated above that anions have a greater effect on water structure than the cations, and whilst differences between monovalent cations are generally less significant than the differences between the monovalent anions.[32] The Hofmeister series for anions, from the most to the least proteins stabilizer is the following: $SO_4^{2-} > HPO_4^{2-} > CH_3COO^- > Cl^- > Br^- > NO_3^- > I^- > ClO_4^- > SCN^-$.[42] Based on our results on dsDNA stability in presence of different ILs, one would expect the order of stabilizing anions to be:

$H_2PO_4^{2-} > NO_3^- > CH_3CH_2OCOO^- > Cl^-$, which is not exactly the relation arising from the Hofmeister series. Pegram L. M. et al. made similar observations; in accordance with their predictions no salt investigated in their work presented a stabilizing Hofmeister effect on DNA helix formation.[41] They also state that the various effects of different ions on water structure (bulk and/or local), although potentially of interest, are not the direct origins of thermodynamic effects on biomolecular processes. Instead, non-uniform ion distributions (accumulation and exclusion) near biomolecules surfaces are supposed to be responsible for the thermodynamic effects of salts in aqueous solutions.[41] This indirectly confirms our experimental and theoretical results on how IL cations interact with the negatively charged DNA-phosphates.

Functional DNA such as a DNA-aptamer hairpin structure undergo a reversible denaturing and annealing, respectively, upon recognition or absence of a molecular target. It might therefore be argued that the formation or denaturing of the hairpin stem depends on whether the IL is present during annealing or added once the dsDNA is already formed. Indeed, literature reports have so far not discerned between both situations which do not necessarily have to yield same experimental results. We therefore studied the stability of dsDNA, previously formed in a pure aqueous buffer, upon addition of increasing concentrations of ILs. Considering as a

reference dsDNA formed in absence of ILs ([IL] = 0M), **Figure 5.6** represents the amount of DNA that remained hybridized while the IL concentration was increased in each sample. For IL concentrations up to 10% v/v, the amount of dsDNA remained virtually constant. However, when the IL concentration was increased up to 40% v/v, the amount of dsDNA suffered just a slight decrease in the case of choline based ILs and EAN (80% of dsDNA at 40% v/v of EAN) while for TMGL or BMIM-Cl, a significant or total melting of the dsDNA was observed: with 40% v/v (≈2M) of TMGL in solution only 40% of DNA was still in its duplex form, while for BMIM-Cl at the same concentration all dsDNA had denatured. These results are in good agreement with the preceding observations when the dsDNA was formed in presence of IL. Therefore, for the ILs under study, no difference in stability could be observed between dsDNA formed in buffer and to which ILs were subsequently added, or dsDNA formed in ILs (**Figure 5.7**). Hence, this should warrant a functioning of a DNA-aptamer hairpin structure also in presence of ILs.

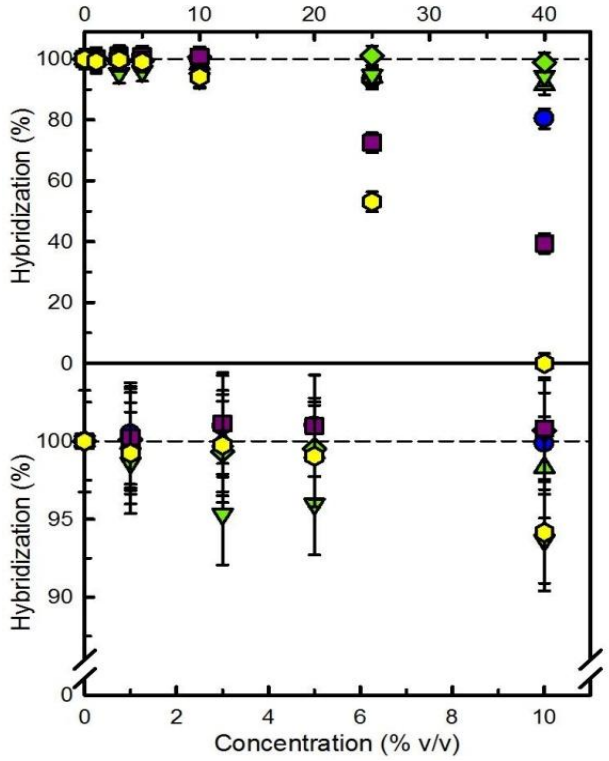

Figure 5.6. Amount of DNA that remained hybridized with the addition of increasing concentrations of EAN (circles), CN (triangles), CDHP (inverted triangles), CL (diamonds), TMGL (squares) and BMIM-Cl (hexagons), with the zoom until 10% v/v (bottom), to the TBS solution containing the previous formed dsDNA. The concentration of the oligomers was 17 nM.

5.2.2. Influence of ILs on the structure of dsDNA

Other than the disrupting or impeding the formation of a dsDNA, ILs may cause perturbations on the DNA secondary structure which in turn could impede or at least deteriorate the target recognition capacity of a DNA-

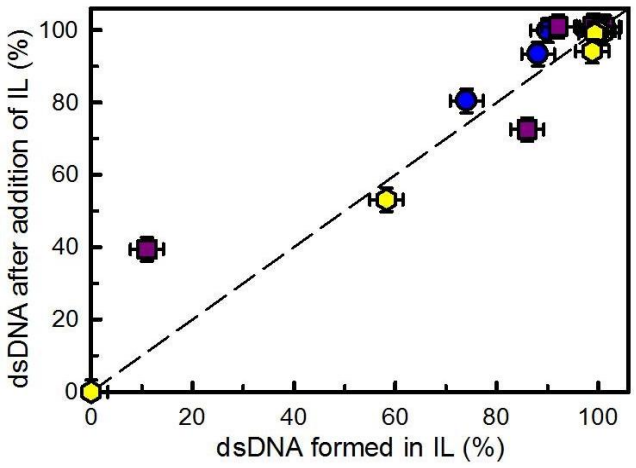

Figure 5.7. Correlation between the amount of DNA hybridized in presence of ILs and the DNA that remained hybridized after the addition of increasing concentrations of EAN (circles), TMGL (squares) and BMIM-Cl (hexagons). For illustration purposes the data of choline ILs were not included since they practically do not alter the duplex formation in IL presence neither the duplex formed before IL addition.

aptamer. We have therefore investigated by circular dichroism the structure of dsDNA formed by the two complementary oligomers, in this case with no dyes attached. The double-stranded DNA formed in TBS buffer exhibits the two characteristic conservative CD peaks above 220 nm with approximately equal positive and negative components of the basic arrangement of dsDNA, the B-conformation (**Figure 5.8**): one positive band around 270 nm corresponding to π-π stacking of the bases that are positioned in parallel between them and

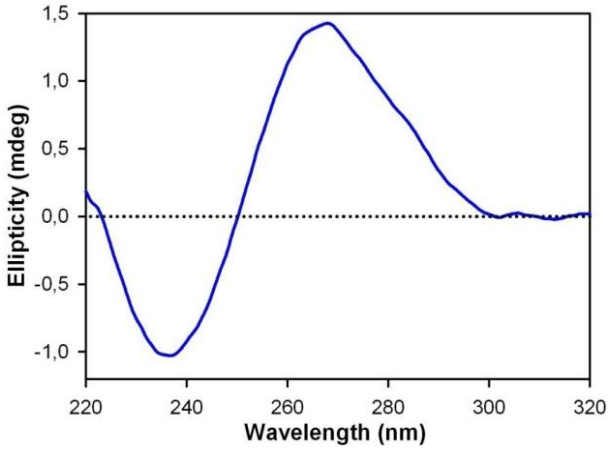

Figure 5.8. Circular dichroism spectrum of the dsDNA formed by oligomer 1 and oligomer 2 in TBS, with no dyes attached. The concentration of the oligos here was 5 μM.

perpendicular to the double-helix axis; and a negative band, around 240 nm corresponding to the helicity of the whole structure.[25,43]

CD measurements in presence of ILs are facing the obstacle that the ILs may present chiral structures,[44] detected in the same wavelength range of a typical dsDNA spectrum and thereby create a signal overlap. With exception for CDHP and BMIM-Cl for low concentrations, we found that for the other ILs the negative band of dsDNA, around 240 nm, disappeared by the overlap of a band corresponding to the increasing concentration of IL introduced in the TBS solution. Therefore, with exception of CDHP and BMIM-Cl, we only examined the influence of ILs on the base stacking of DNA secondary structure represented by the positive band (**Figure 5.9 A**), which admittedly limits the space for accurate conclusions. However, the information provided by the positive band should be enough to verify whether the DNA structure undergoes changes with the concentration of ILs, also because, CD of nucleic acids is considered to be mainly dependent on the stacking geometry of the bases.[45] As an example, by adding conventional salts to a solution containing DNA from a bacteriophage, Baase W. A. et al., observed that the transfer from low to high concentrations of a same salt or from one salt to increasing concentrations of another salt in solution caused a significant decrease of the positive CD band,

keeping the negative band substantially intact.[46] Consequently, they only took into account the change of the intensity of the positive CD band (≈ 275 nm), determining in this way also the number of base pairs per helix turn.[46] Similar observations were made by Kypr J. et al.[43]

Until 40% v/v of CN and CDHP or until 25% v/v of EAN and CL, the dsDNA maintained the stacking of the bases, meaning that the B-conformation remained practically unchanged (**Figure 5.9 B**). For CDHP, the helicity of the dsDNA was also practically maintained even if half of the total volume of the solution was composed of this IL as we only observed a slight decrease of the respective dichroic signal. Tateishi-Karimata H. and Sugimoto N., observed similar results for a 10-mer sequence of dsDNA.[19] They assert that until 4M of CDHP in solution dsDNA did not change "drastically" its structure which is in line with our observation at a final concentration of around 3M of CDHP in solution. At the highest concentration of EAN, at 40% v/v, some alteration of the CD signal was detected indicating a possible interference with the DNA structure and which would be in line with stated in **Chapter 3**. Still, results from fluorescence measurements had shown that at this concentration 80% of DNA was still hybridized (**Figure 5.1**) although with a decreased Tm of 33 ^{o}C (**Figure 5.4**).

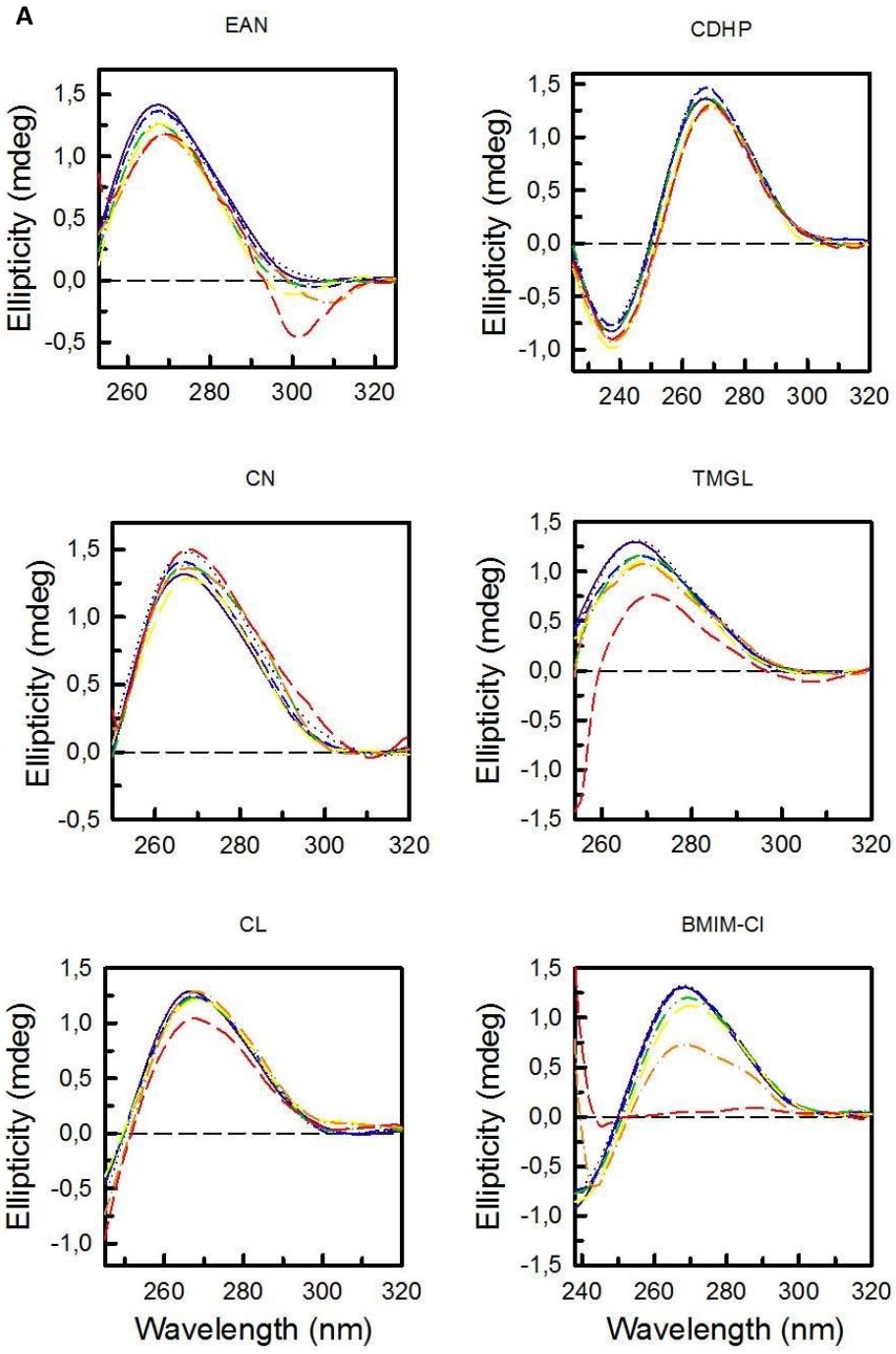
A
EAN
CDHP
CN
TMGL
CL
BMIM-Cl
Ellipticity (mdeg)
Wavelength (nm)

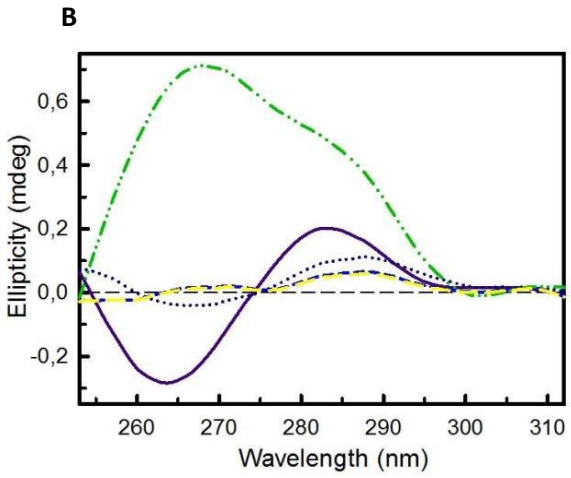

Figure 5.9. A) Circular dichroism spectra of the dsDNA formed by oligomer 1 and oligomer 2, with no dyes attached, with the addition of 0% (solid line – purple), 1% (dotted line – dark blue), 5% (short dash line – blue), 10% (dash-dot-dot line – green), 18% (long dash line – yellow), 25% (dash-dot line – orange) and 40% v/v (medium dash line – red) of the different ILs into the TBS solution. **B)** Circular dichroism spectra of the ssDNA oligomer 1, with no dyes attached, with the addition of 0% (solid line – purple), 25% (dotted line – dark blue) and 40% (short dash line - blue) v/v of BMIM-Cl comparing with the dsDNA with the addition of 25% (dash-dot-dot line – green) and 40% (long dash line – yellow) v/v of BMIM-Cl. The concentration of the oligos here was 5 mM.

On the other hand, the ILs with the biggest cations BMIM-Cl and TMGL again exhibited an opposing trend (**Figure 5.9 A**). Structural changes and the consequent melting of the dsDNA were detected by a decreasing CD peak intensity and a slight red-shift of the positive band when 40% v/v of TMGL were in solution. For BMIM-Cl,

these results are in total agreement with the fluorescence measurements since with 40% v/v of BMIM-Cl in solution, the intensity of the positive band of ssDNA and dsDNA are very similar between them (**Figure 5.9 B short dash line - blue and long dash line - yellow**), hence, the dsDNA denatures completely.

Cholines, EAN and BMIM-Cl caused no shift of the positive band, keeping always the wavelength around 270 nm, thus indicating that the observed changes were occurring only to the B-form of DNA without inducing any conformational change. This also proves that no competition between the ILs and water on DNA surface was occurring as occurs with organic solvents such as ethanol.[47]

Recently, somewhat contradictory results have been reported by different authors on CD measurements for studying the influence of different concentrations of imidazolium ILs on the structure of calf thymus DNA.[3,23,25] Using BMIM-Cl Chandran A. et al. found that DNA maintained its B-form conformation, despite the slight decrease of the positive band with the addition of the IL even at a maximum concentration of 80 wt-% which corresponds to about 57% v/v, opposing then our findings.[25] Changing an alkyl chain and the anion, Jumbri K. et al. used C_4BIM-Br between 25 and 75 wt-% and found similar results as Chandran A. et al.[3] On the other hand, Ding Y. et al., reported for a maximum of 1 mol/L (ca. 17,5% v/v) of

BMIM-Cl in solution an increase both in the positive and in the negative bands.[23] It must be noted that these literature reports used calf thymus DNA which might be more entangled than the 12-mer DNA used in our studies. This may explain the differences in the experimental results.

5.2.3. Hybridization rate (k_h)

The rate at which a hairpin opens and closes in presence or absence, respectively, of the target is important for sensing and gating applications.[16,48] Being aware of the thermodynamic differences between a DNA-hairpin and a DNA duplex without the loop, we studied the hybridization rate, kh, between the two oligomers in solution, considering that's the rate limiting step for the functioning of a DNA-hairpin. Using the selected ILs in concentrations of up to 3-4 M in TBS buffer solution, we determined the rate of hybridization of the oligomers in comparison with pure TBS solution (see **Chapter 2** for calculations). Up to 10 % v/v (≈ 1M) all ILs except EAN increased the rate of duplex formation to a similar degree, i.e. about two-fold, EAN even almost four-fold (**Figure 5.10**). For higher concentrations, all choline-based ILs followed strictly the same pattern not exceeding a 2,5-fold increase of kh even at 40% v/v. Again, BMIM-Cl and TMGL deviated from this trend,

but also EAN; in presence of 25% v/v of BMIM-Cl, *kh* increased 8,5-fold, at 40% v/v of TMGL and EAN six-fold. It appears that the hybridization rate inversely follows the

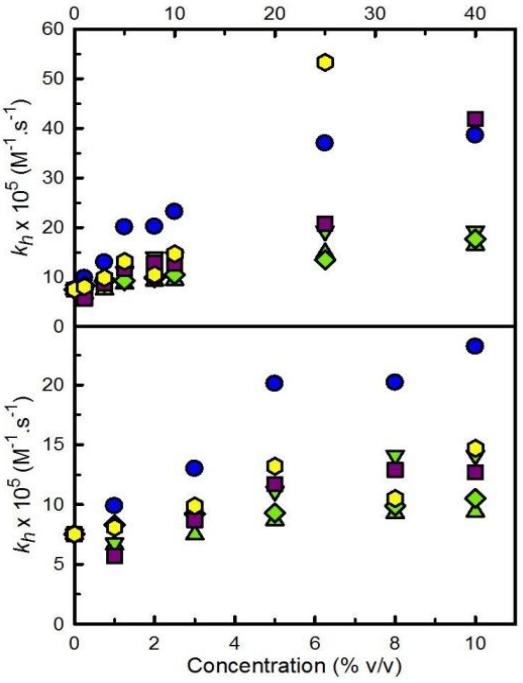

Figure 5.10. Graphic representation of the rate of DNA hybridization, k_h, as function of the increase concentration of EAN (circles), CN (triangles), CDHP (inverted triangles), CL (diamonds), TMGL (squares) and BMIM-Cl (hexagons), with the zoom until 10% v/v (bottom). The standard deviations here range from 0.012 to 1.8 (x 10^5), being the error bar smaller than the symbols.

melting temperature: ILs that with increasing concentration lower the melting temperature seem, on the other hand, to increase the hybridization rate accordingly. In order to verify any correlation between the ILs, we calculated kh/Tm for all ILs studied and represented them versus EAN as an arbitrary reference (**Figure 5.11**).

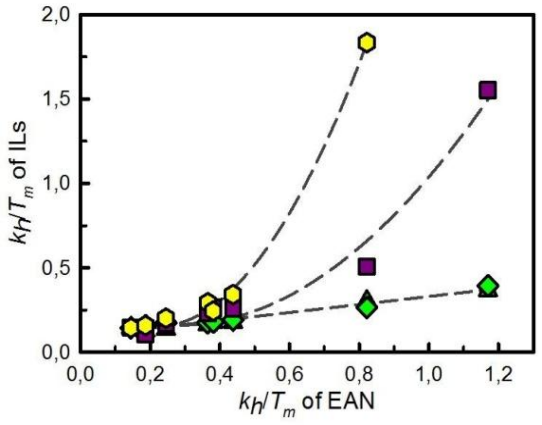

Figure 5.11. Correlation between the specific for EAN, as an arbitrary reference. The symbols correspond to CN (triangles hybridization rate and the melting temperature (k_h/T_m) of the ILs used respect to the same correlation), CL (diamonds), TMGL (squares) and BMIM-Cl (hexagons). The long-dashed lines correspond to the fitting of the data.

It becomes evident that while CN, CL and EAN exhibit a clear linear correlation over the whole range of hybridization rates and melting temperatures, it is again

BMIM-Cl and TMGL that strongly deviate at higher concentrations of these ILs in solution, increasing the hybridization rate four to six-fold in comparison with CN and CL.

This faster formation of dsDNA can be explained by the bulkiness of these IL cations. Bulky cations need more space than available in the dsDNA to interact individually with the phosphate moieties. This steric hindrance during their distribution around the phosphates makes the DNA chain subject to stretching and to enlarge it stiffness in order to accommodate these bulky cations as much as possible. The DNA strand then loses mobility, forcing its alignment, which in turn fosters the hybridization to occur faster. A similar conclusion was also drawn by Zhang Y., et al., through modeling studies.[49] While hybridization takes place faster, it should be recalled that the absolute amount hybridized actually decreased at higher concentration of ILs in comparison with pure TBS in solution. Still, for a DNA-aptamer beacon whose function relies on a rapid and reversible dynamic response, the increase in hybridization rate is considered advantageous.

Given that the hybridization rate is a kinetic parameter, one might argue that it might be affected by viscosity changes of the medium upon addition of ILs. In fact, we determined that a solution of 80 wt-% of TMGL in water presented a viscosity of

nearly 80 mPa·s, being the most viscous of all IL solutions (water viscosity at 25 ^{o}C ≈1 mPa·s, see **Table 4.1 - Chapter 4**). On the other hand, BMIM-Cl, which significantly increased the hybridization rate such as TMGL, yielded a viscosity of about 20 mPa·s when a solution of 75 wt-% in water was measured, similar to that of CN and CL which affected the hybridization rate to a considerably lesser extent. The viscosity of the solution therefore seemed to be of no relevance in this context.

5.2.4. Molecular recognition in presence of different ILs

Taking as reference the results detailed above and on **Chapter 3**,[31] we subsequently performed the study of the function and selectivity of the ATP-molecular aptamer beacon for the AMP target in aqueous solution with 2M of each IL used here. We observed that this concentration, which is already relatively high, the system still worked but with less efficiency than in a pure buffer solution.

Figure 5.12 illustrates the normalized fluorescence data obtained from the AMP recognition by the ATP-aptamer beacon both in pure TBS buffer solution and in TBS with 2M of each IL, corresponding to a volume concentration between 30 and 40% depending on the IL used. We observed that in presence of 2M of choline lactate

(**Figure 5.12 A**) and nitrate (**Figure 5.12 B**) the ATP-molecular aptamer beacon maintained its capacity to recognize the AMP target. As previously observed with EAN in **Chapter 3**, also in presence of 2M of CL and CN the aptamer decreased its sensitivity for AMP presenting dissociation constants (K_d) of 3866 μM and 1144 μM, respectively, compared to a K_d of 700 μM in pure TBS solution.

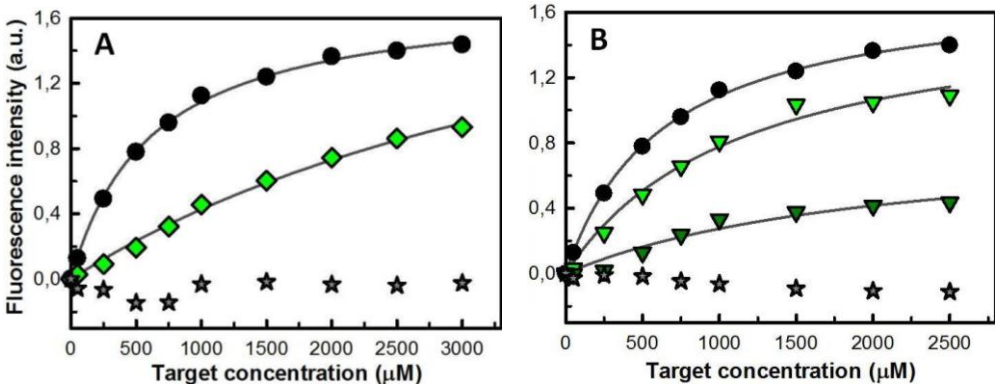

Figure 5.12. Normalized fluorescence obtained by the recognition of ATP-molecular aptamer beacon of increasing concentrations of AMP in **A)** 0M (circles) and 2M (diamonds) of CL and in **B)** 0M (circles), 2M (inverted triangles – green) and 4M (inverted triangles – dark green) of CN; and increasing concentrations of GMP in **A)** 2M of CL (stars) and **B)** 4M of CN (stars) in TBS solution at 25 ^{o}C. The lines represent the model used to calculate the *Kd* values obtained from the SigmaPlot curve-fitting algorithm of one-site ligand binding.

However, we should note that such as in **Chapter 3** also here we used the ATP-aptamer selected by SELEX in Tris-HCl buffer solution and in a total absence of any of the ILs used herein.[31,50] Comparing between CL or CN we verified that with 2M of CN in TBS solution the aptamer works better, as reflected by the lower K_d. Subsequently, we tested the ATP-aptamer sensitivity to recognize the AMP in presence of 4M CN, as an 'extreme' situation. Surprisingly, despite the substantial decrease in the normalized fluorescence and in turn a considerable increase of the dissociation constant, the ATP-molecular aptamer beacon was still able to recognize the AMP target (**Figure 5.12 B**). For CL the same experiment was carried out, but in this case the molecular beacon was no longer functional at this concentration. Considering the significant perturbation of the standard working conditions by introducing in the system this huge concentration of CN, the high capability of the aptamer to maintain its function is remarkable.

At 2M of the other ILs in solution, CDHP, TMGL and BMIM-Cl, no significant increase of the normalized fluorescence was observed for any of them, hence, the MB was not functioning (therefore, data are not shown). For the ILs with large cations this result could be expected because at this concentration BMIM-Cl and TMGL denatured the duplex DNA stem, as noted in the previous sections. Once

introducing the beacon in solution with 2M of TMGL and BMIM-Cl these will immediately cause the opening of the stem of the hairpin structure, causing the separation of fluorophore and quencher and the consequent maximum increase in the fluorescence emission, even in total absence of AMP. Then, when the AMP is introduced into the solution and even if the aptamer is capable to still recognize it, the structural changes that may occur will not be detected since the stem of the beacon probe is already 'open' (melted) by these ILs (**Figure 5.1**, **Figure 5.4** and **Figure 5.6**). With CDHP, however, based on the previous results we expected that as for the other cholines the aptamer would remain functional. It remained unclear what could have been affecting the system such as to not function.

One site where ILs could interfere with the recognition process and which has so far been not been considered is the DNA binding pocket which is responsible for AMP recognition (see **Figures 2.1 - Chapter 2** and Scheme **3.1 - Chapter 3**). As explained in Chapters 2 and 3, the binding pocket in the particular case of the ATP-aptamer consists of a guanine rich region of the sequence.[50,51] From quantum chemistry calculations, even being a simulation and a basic approximation to the real system, we determined above and in accordance with literature[19,52,53] that all IL cations present a good affinity for the DNA bases, and especially for guanine in

ssDNA (**Figure 5.2**). Indeed, Sugimoto et al. also demonstrated by molecular dynamics calculations that choline ions of CDHP bind preferentially to G or C rich regions.[19,52,53] However, unlike results from the hybridization studies, here we observed that the ILs of the choline family do not all cause the same response in the MB. This means that even though the IL cation may have a principal influence on the DNA structure, in this case affecting the MB functionality, the anion also needs to be taken into account when choosing the most adequate IL for a DNA-system.

The decrease in the performance of the MB in presence of these ILs may also be related with the interaction between the charged AMP target and the ILs themselves, preventing the recognition of the AMP by the binding pocket. We therefore determined the ^{31}P-NMR spectra of the AMP molecule in solution with 2M of TMGL, CN, CL and BMIM-Cl (**Figure 5.13**). CDHP was discarded due the phosphate anion. Determining the reference spectrum of AMP in solution with pure buffer a single peak at 4.3 ppm was obtained, corresponding to the single phosphate of AMP. Considering that the phosphates are not involved in the recognition process, we used AMP by containing the lowest number of phosphates.[51,54] No shift in the AMP-peak was observed when CN and BMIM-Cl were in solution. However, when TMGL or CL were in solution, a shielding occurred as observed by an upfield shift to 0.95

ppm. Performing mobility tests, Stellwagen E., et al., found that 5'-adenosine triphosphate (ATP), 5'-adenosine diphosphate (ADP), and 5'-adenosine monophosphate (AMP) bind to different small monovalent cations (Li^+, Na^+, K^+, NH_4^+ and $Tris^+$), but present a very low binding to quaternary ammonium ions.[34] Thus, considering our different results obtained here between the choline based ILs, which are quaternary ammonium ions, and the similar NMR upfield shift when using CL

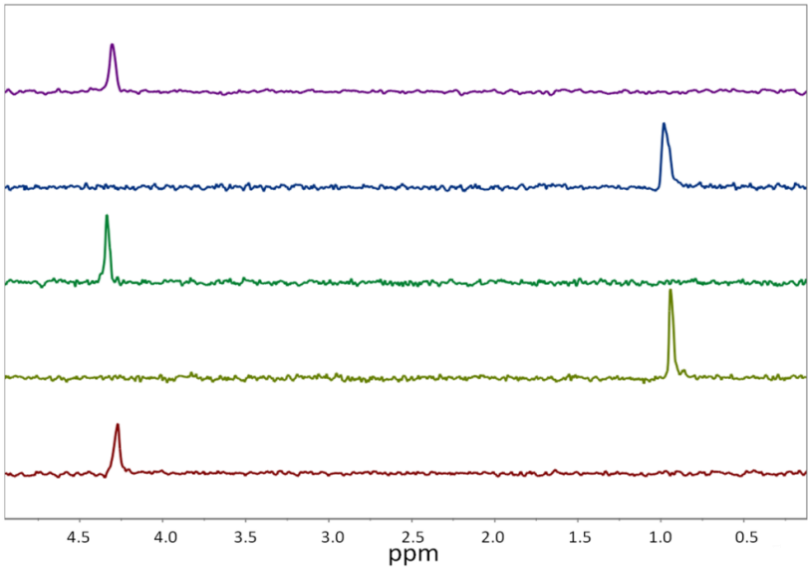

Figure 5.13. ^{31}P-NMR spectra of free AMP in TBS solution (upper spectrum – purple) and with the addition of 2M of TMGL (blue), CN (dark green), CL (green) or BMIM-Cl (bottom spectrum – red).

and TMGL in solution sharing the same anion, apparently here the common anion of the ILs is the responsible of the upfield shift of the spectrum rather than the cation. From here we can deduce that while CN does not affect the recognition of AMP by the molecular beacon, CL does interact with the phosphate of the AMP target, hindering the recognition of AMP by the MB at 2M CL and impeding it entirely at 4M of CL. TMGL both interacts with the target AMP and causes melting of the stem of the beacon, thus preventing the recognition of the AMP by the aptamer beacon. For BMIM-Cl, apparently, the melting of the stem seems to be the main factor interfering with the recognition process, or at least with its detection. Finally, wee verified the specificity of the MB for the AMP target molecule. For that we used guanosine monophosphate (GMP) which is structurally very similar to AMP but known to not be recognized in buffer conditions. As can be seen in **Figure 5.12**, the non-increase of the normalized fluorescence means that with 2M CL and even with 4M CN in solution the ATP-aptamer did not interact with GMP preserving in this way its specificity for the AMP.

5.3. Conclusions

To summarize our study, we can assert that:

- ILs sharing the same cation, such as the cholines, caused similar effects on the hybridization and stability of DNA; from this we may deduce that the cation plays an important role in the interaction with DNA via the negatively charged phosphate backbone of the latter. The effect of the anions seems less significant at first sight but may also have an important role on the MB function.

- In accordance with literature we also observed that the size of the cations is an important factor in the stability and hybridization of DNA. We observed that for higher concentrations the larger cations such as $BMIM^+$ and TMG^+ interact with ssDNA preventing almost all the DNA population to hybridize and shifting the helix-coil equilibrium toward the coil conformation. Due to their large size, these cations interact less efficiently with the phosphates in dsDNA, and therefore favour ssDNA, possibly causing also a stretching of the structure which then may facilitate hybridization kinetics.

- In buffer solution, Na^+ interacting with the DNA is gradually displaced by IL owing to a higher concentration (at some point the concentration of IL in solution is

much higher than Na^+) and due to the ILs interacting not only electrostatically but also establishing multiple H-bonds and dispersion interactions.

- The effect of an IL on dsDNA hybridization and subsequent stability strongly depends on the IL structure and must therefore not be generalized, neither can it be inferred from observations made with respective homologues of common salts.

- TMGL and BMIM-Cl proved to be potent denaturing agents of the 12-mer double-strand DNA.

- The influence of the ILs on the MB function cannot directly be inferred from their effect on a dsDNA structure, although the latter forms the stem of the MB hairpin. While the stem of the hairpin molecular beacon structure warrants its dynamic function, the principle part of the molecular aptamer beacon structure is the recognition pocket with which the IL should preferably interact as little as possible.

- CL, CN and EAN (from the previous Chapter) proved to be suitable ILs for being used with the ATP-aptamer beacon even with the latter being selected in pure buffer.

- ILs are not all equally suitable for nanodevices involving DNA. Depending on the requirements of the system the ILs must be tuned according to the needs which can be achieved by choosing ILs with adequate physico-chemical properties.

5.4. References

(1) Privé, G. G.; Yanagi, K.; Dickerson, R. E. Structure of the B-DNA Decamer C-C-A-A-C-G-T-T-G-G and Comparison with Isomorphous Decamers C-C-A-A-G-A-T-T-G-G and C-C-A-G-G-C-C-T-G-G. *J. Mol. Biol.* **1991**, *217* (1), 177–199.

(2) Cavalieri, E.; Saeed, M.; Zahid, M.; Cassada, D.; Snow, D.; Miljkovic, M.; Rogan, E. Mechanism of DNA Depurination by Carcinogens in Relation to Cancer Initiation. *IUBMB Life* **2012**, *64* (2), 169–179.

(3) Jumbri, K.; Abdul Rahman, M. B.; Abdulmalek, E.; Ahmad, H.; Micaelo, N. M. An Insight into Structure and Stability of DNA in ILs from Molecular Dynamics Simulation and Experimental Studies. *Phys. Chem. Chem. Phys.* **2014**, *16* (27), 14036–14046.

(4) Neddermann, P.; Gallinari, P.; Lettieri, T.; Schmid, D.; Truong, O.; Hsuan, J. J.; Wiebauer, K.; Jiricny, J. Cloning and Expression of Human G / T Mismatch-Specific Thymine-DNA Glycosylase * the Formation of G / T Mismatches . We Have Shown Previ-. **1996**, *271* (22), 12767–12774.

(5) Klibanov, A. M. Enzymatic Catalysis in Anhydrous Organic Solvents. *Trends in Biochemical Sciences*. **1989**, pp 141–144.

(6) Zaks, a.; Klibanov, a. M. Enzyme-Catalyzed Processes in Organic Solvents. *Proc. Natl. Acad. Sci. U. S. A.* **1985**, *82* (10), 3192–3196.

(7) Griebenow, K.; Klibanov, A. M. On Protein Denaturation in Aqueous-Organic Mixtures but Not in Pure Organic Solvents. *J. Am. Chem. Soc.* **1996**, *118* (47), 11695–11700.

(8) Schmitke, J. L.; Stern, L. J.; Klibanov, a M. The Crystal Structure of Subtilisin Carlsberg in Anhydrous Dioxane and Its Comparison with Those in Water and Acetonitrile. *Proc. Natl. Acad.*

Sci. U. S. A. **1997**, *94* (9), 4250–4255.

(9) Lai, J.-Q.; Li, Z.; Lü, Y.-H.; Yang, Z. Specific Ion Effects of ILs on Enzyme Activity and Stability. *Green Chem.* **2011**, *13* (7), 1860.

(10) Van Rantwijk, F.; Lau, R. M.; Sheldon, R. A. Biocatalytic Transformations in ILs. *Trends in Biotechnology*. 2003, pp 131–138.

(11) Weingärtner, H.; Cabrele, C.; Herrmann, C. How ILs Can Help to Stabilize Native Proteins. *Phys. Chem. Chem. Phys.* **2012**, *14* (2), 415–426.

(12) Krishnan, Y.; Simmel, F. C. Nucleic Acid Based Molecular Devices. *Angew. Chemie - Int. Ed.* **2011**, *50* (14), 3124–3156.

(13) Ellington, a D.; Szostak, J. W. In Vitro Selection of RNA Molecules That Bind Specific Ligands. *Nature* **1990**, *346* (6287), 818–822.

(14) Tuerk, C.; Gold, L. Systematic Evolution of Ligands by Exponential Enrichment: RNA Ligands to Bacteriophage T4 DNA Polymerase. *Science* **1990**, *249* (4968), 505–510.

(15) Hernandez, F. J.; Hernandez, L. I.; Pinto, A.; Schafer, T.; Ozalp, V. C. Targeting Cancer Cells with Controlled Release Nanocapsules Based on a Single Aptamer. *Chem Commun* **2013**, *49* (13), 1285–1287.

(16) Serrano-Santos, M. B.; Llobet, E.; Özalp, V. C.; Schäfer, T. Characterization of Structural Changes in Aptamer Films for Controlled Release Nanodevices. *Chem. Commun. (Camb).* **2012**, *48* (81), 10087–10089.

(17) Schafer, T.; Ozalp, V. C. DNA-Aptamer Gating Membranes. *Chem. Commun.* **2015**, *51* (25), 5471–5474.

(18) Marusic, M.; Tateishi-Karimata, H.; Sugimoto, N.; Plavec, J. Structural Foundation for DNA Behavior in Hydrated IL: An NMR Study. *Biochimie* **2015**, *108*, 169–177.

(19) Tateishi-Karimata, H.; Sugimoto, N. A-T Base Pairs Are More Stable than G-C Base Pairs in a Hydrated IL. *Angew. Chemie - Int. Ed.* **2012**, *51* (6), 1416–1419.

(20) Vijayaraghavan, R.; Izgorodin, A.; Ganesh, V.; Surianarayanan, M.; MacFarlane, D. R. Long-Term Structural and Chemical Stability of DNA in Hydrated ILs. *Angew. Chemie - Int. Ed.* **2010**, *49* (9), 1631–1633.

(21) Mazid, R. R.; Cooper, A.; Zhang, Y.; Vijayaraghavan, R.; MacFarlane, D. R.; Cortez-Jugo, C.; Cheng, W. Enhanced Enzymatic Degradation Resistance of Plasmid DNA in ILs. *RSC Adv.* **2015**, *5*

(54), 43839–43844.

(22) Sharma M., Mondal D., Singh N., Trivedi N., B. J. and P. K. High Concentration DNA Solubility in Bio ILs with Long Lasting Chemical and Structural Stability at Room Temperature. *RSC Adv.* **2015**, *5*, 40546–40551.

(23) Ding, Y.; Zhang, L.; Xie, J.; Guo, R. Binding Characteristics and Molecular Mechanism of Interaction between IL and DNA. *J. Phys. Chem. B* **2010**, *114* (5), 2033–2043.

(24) Wang, H.; Wang, J.; Zhang, S. Binding Gibbs Energy of ILs to Calf Thymus DNA: A Fluorescence Spectroscopy Study. *Phys. Chem. Chem. Phys.* **2011**, *13*, 3906–3910.

(25) Chandran, A.; Ghoshdastidar, D.; Senapati, S. Groove Binding Mechanism of ILs : A Key Factor in Long- Term Stability of DNA in Hydrated ILs ? *J. Am. Chem. Soc.* **2012**, *134*, 20330–20339.

(26) Tyagi, S.; Kramer, F. R. Molecular Beacon Probes That Fluoresce on Hybridiztion. *Nat. Publ. Gr.* **1996**, *14*, 303–308.

(27) Hernandez, L. I.; Machado, I.; Schäfer, T.; Hernandez, F. J. Aptamers Overview : Selection , Features and Applications. **2015**.

(28) Huang, J.; Wu, J.; Li, Z. Biosensing Using Hairpin DNA Probes. *Reviews in Analytical Chemistry*. 2015, pp 1–27.

(29) Smestad, J.; James Maher, L. Ion-Dependent Conformational Switching by a DNA Aptamer That Induces Remyelination in a Mouse Model of Multiple Sclerosis. *Nucleic Acids Res.* **2013**, *41* (2), 1329–1342.

(30) Stellwagen, E.; Muse, J. M.; Stellwagen, N. C. Monovalent Cation Size and DNA Conformational Stability. **2011**, 3084–3094.

(31) Machado, I.; Özalp, V. C.; Rezabal, E.; Schäfer, T. DNA Aptamers Are Functional Molecular Recognition Sensors in Protic ILs. *Chemistry* **2014**, *20* (37), 11820–11825.

(32) Tomac, S.; Sarkar, M.; Ratilainen, T.; Wittung, P.; Nielsen, P. E.; Norde, B.; Gra, A.; Nordén, B.; Gräslund, a. Ionic Effects on the Stability and Conformation of Peptide Nucleic Acid Complexes. *J. Am. Chem. Soc.* **1996**, *118* (96), 5544–5552.

(33) Li, T.; Joshi, M. D.; Ronning, D. R.; Anderson, J. L. ILs as Solvents for in Situ Dispersive Liquid-Liquid Microextraction of DNA. *J. Chromatogr. A* **2013**, *1272*, 8–14.

(34) Stellwagen, E.; Dong, Q.; Stellwagen, N. C. Quantitative Analysis of Monovalent Counterion Binding to Random-Sequence , Double-Stranded DNA Using the Replacement Ion Method †.

2007, 2050–2058.

(35) Rezabal, E.; Schäfer, T. First Principle Approach to Solvation by Methylimidazolium-Based ILs. *J. Phys. Chem. B* **2013**, *117* (2), 553–562.

(36) Rezabal, E.; Schäfer, T. ILs as Solvents of Polar and Non-Polar Solutes: Affinity and Coordination. *Phys. Chem. Chem. Phys.* **2015**, *17*, 14588–14597.

(37) Stellwagen, E.; Stellwagen, N. C. Monovalent Cations Affect the Free Solution Mobility of DNA by Perturbing the Hydrogen- Bonded Structure of Water. **2005**, 62–68.

(38) Tan, Z.-J.; Chen, S.-J. Ion-Mediated Nucleic Acid Helix-Helix Interactions. *Biophys. J.* **2006**, *91* (2), 518–536.

(39) Phillips, R.; Kondev, J.; Theriot, J.; Garcia, H. G.; Orme, N. *Physical Biology of the Cell*; 2013.

(40) Zhao, H.; Olubajo, O.; Song, Z.; Sims, A. L.; Person, T. E.; Lawal, R. A.; Holley, L. A. Effect of Kosmotropicity of ILs on the Enzyme Stability in Aqueous Solutions. *Bioorg. Chem.* **2006**, *34* (1), 15–25.

(41) Pegram, L. M.; Wendorff, T.; Erdmann, R.; Shkel, I.; Bellissimo, D.; Felitsky, D. J.; Record, M. T. Why Hofmeister Effects of Many Salts Favor Protein Folding but Not DNA Helix Formation. *Proc. Natl. Acad. Sci. U. S. A.* **2010**, *107* (17), 7716–7721.

(42) Yang, Z. Hofmeister Effects: An Explanation for the Impact of ILs on Biocatalysis. *Journal of Biotechnology*. 2009, pp 12–22.

(43) Kypr, J.; Kejnovská, I.; Renčiuk, D.; Vorlíčková, M. Circular Dichroism and Conformational Polymorphism of DNA. *Nucleic Acids Research*. 2009, pp 1713–1725.

(44) Baudequin, C.; Brégeon, D.; Levillain, J.; Guillen, F.; Plaquevent, J. C.; Gaumont, A. C. Chiral ILs, a Renewal for the Chemistry of Chiral Solvents? Design, Synthesis and Applications for Chiral Recognition and Asymmetric Synthesis. *Tetrahedron Asymmetry*. 2005, pp 3921–3945.

(45) Bloomfield, V. A.; Crothers, D. M.; Tinoco Jr., I. *Nucleic Acids: Structures, Properties, and Functions*; 2000.

(46) Baase, W. A.; Johnson, W. C. Circular Dichroism and DNA Secondary Structure. *Nucleic Acids Res.* **1979**, *6* (2), 797–814.

(47) Piskur, J.; Rupprechtb, A. Aggregated DNA in Ethanol Solution. **1995**, *375*.

(48) Bonnet, G.; Krichevsky, O.; Libchaber, A. Kinetics of Conformational Fluctuations in DNA Hairpin Loops. *Proc. Natl. Acad. Sci. U. S. A.* **1998**, *95* (July), 8602–8606.

(49) Zhang, Y.; Zhou, H.; Ou-Yang, Z. C. Stretching Single-Stranded DNA: Interplay of Electrostatic, Base-Pairing, and Base-Pair Stacking Interactions. *Biophys. J.* **2001**, *81* (2), 1133–1143.

(50) Huizenga, D. E.; Szostak, J. W. A DNA Aptamer That Binds Adenosine and ATP. *Biochemistry* **1995**, *34* (2), 656–665.

(51) Lin, C. H.; Patel, D. J. Structural Basis of DNA Folding and Recognition in an AMP-DNA Aptamer Complex: Distinct Architectures but Common Recognition Motifs for DNA and RNA Aptamers Complexed to AMP. *Chem. Biol.* **1997**, *4* (11), 817–832.

(52) Nakano, M.; Tateishi-Karimata, H.; Tanaka, S.; Sugimoto, N. Choline Ion Interactions with DNA Atoms Explain Unique Stabilization of A-T Base Pairs in DNA Duplexes: A Microscopic View. *J. Phys. Chem. B* **2014**, *118* (2), 379–389.

(53) Tateishi-Karimata, H.; Nakano, M.; Sugimoto, N. Comparable Stability of Hoogsteen and Watson-Crick Base Pairs in IL Choline Dihydrogen Phosphate. *Sci. Rep.* **2014**, *4*, 3593.

(54) Nielsen, L. J.; Olsen, L. F.; Ozalp, V. C. Aptamers Embedded in Polyacrylamide Nanoparticles: A Tool for in Vivo Metabolite Sensing. *ACS Nano* **2010**, *4* (8), 4361–4370.

CHAPTER 6

Selection of single-strand DNA Aptamers in Unconventional Ionic Liquid Solution

6.1 Introduction

The degree to which DNA hybridizes, changes its conformation, preserves it structural stability or performs its function is directly related with its aqueous solvation medium, since this should represent the physiological conditions of *in vivo* systems. However, owing to its unique characteristics and chemical structure which can easily be synthesized and modified, DNA may also possibly be used in presence of organic solvents or non-conventional solvents such as ionic liquids or deep eutetic solvents (DES).[1–3] This makes DNA a very useful functional element in nanotechnology applications. It was already proven that DNA maintains its functionality in solution with different concentrations of ionic liquids presenting different physico-chemical properties: in the previous chapters it was proven that a DNA with a molecular recognition capability, a DNA-aptamer, recognized a molecule as small as ATP in presence of 2M and even 4M of different ionic liquids.[4,5] However, despite of maintaining its functionality in presence of the ILs, we observed that the ATP-aptamer lost some affinity compared with the aptamer recognizing the ATP only in buffer. This was not at all surprising, given that the molecular recognition functionality of this DNA sequence was selected in aqueous buffer, but not in presence of an ionic liquid. On the other hand, and in part as a surprise, the aptamer

remained specific even in presence of that amount of ionic liquids discerning between AMP and GMP which are two structurally similar molecules.

The selectivity of DNA-aptamers is based on a molecular recognition process. This process consists in the ability of binding to a molecular target in presence of competing molecules. Thus, selectivity is only achieved if a large number of functional groups of the two molecules contribute co-operatively to a sufficient number of corresponding non-covalent bonds, more favorable than the ones established with the competing molecules. In literature, this principle is often called complementarity.[6] Naturally, the less functional groups can contribute to this interaction, as is the case for small molecular targets such as ATP, the more difficult it seems to achieve a highly selective molecular recognition.

Thus, we wondered in how far we could improve the specificity of the DNA ATP-aptamer in presence of ionic liquids if we select it in an IL environment from the very beginning.

6.1.1. Concept of SELEX

In order to identify the aptamer sequences of interest, nucleic acid libraries undergo an *in vitro* selection procedure, called Systematic Evolution by Ligand Exponential Enrichment (SELEX), described for the first time in 1990 simultaneously by the three groups already mentioned in *section 1.2.2* of **Chapter 1**.

The SELEX method has proven to be a useful platform for selecting a large number of aptamers for a wide variety of targets, including small ions, small molecules, proteins, organelles, viruses and whole cells.[7–10] **Figure 1.4** shows a standard general SELEX procedure. After the design of the DNA library, this procedure involves the following steps: **1)** incubation and interaction between the mixture of candidates with the target molecule, **2)** partitioning of the mixture of candidates with high and low affinity to the target molecule, **3)** elution of the bound DNA candidates from the target, **4)** amplification of the bound members. Steps 1-4 are repeated in each round of selection in order to achieve a more and more selective sample of bound DNA candidates. When after several rounds of selection the desired enrichment is achieved, the final step **5),** cloning and sequencing, is performed.

The critical steps during SELEX are the separation of nucleic acids unbound and bound to the target molecule (partitioning), and the elution of the bound sequences from the target molecules, as during these steps potential DNA candidates can be lost.

SELEX is, hence, a very efficient method, which is an advantage considering the wide application of aptamers, such as biosensors,[11] drug delivery based on switchable nanovalves,[12–14] or as therapeutic and diagnostic probes in medicine.[15–18]

In the following sub-sections a general SELEX, as it was used in this work, is explained in detail.

6.1.2. Target molecules

There are several reports in the literature about aptamers with high-affinity against over 150 different targets[19,20] including targets with different features such as inorganic components, small organic molecules, nucleotides and derivates, cofactors, amino acids, carbohydrates, antibiotics, peptides and proteins, and complex structures have been classified. The previous confirms the versatility of nucleic acids and the universal application of SELEX for a wide range of molecules. Usually, aptamers are developed for therapeutic applications. For example,

pegaptanib has already been approved by Food and Drug Administration (FDA) for the treatment of neovascular (wet) age-related macular degeneration (AMD).[21,22]

6.1.3. Design of the oligonucleotide library

SELEX starts with the library design. Up to 10^{15} random sequences are synthesized by solid phase nucleic acid synthesis. Each member of the library consists of a randomized internal region (20 to 80 nucleotides) that is flanked by two primer regions at the 3' and 5' ends. In addition, two primer sequences are designed according to the library template that are used as primer-binding sites for PCR amplification[23] of the library and subsequent selected sub-populations. The libraries should be designed such as to incorporate generic features which permit, if needed, immobilization and transduction. Efforts have been made to achieve these properties involving the incorporation of complementary regions that allow immobilizing the library members on the surface of magnetic beads,[24] or the post selection modifications for generic transduction in biosensor development.[25]

The following headers are in line with what is denote in the **figure 6.1** to make easier to follow a general SELEX procedure.

6.1.4. Interaction between library members and target molecule (Incubation)

The main goal of SELEX is to obtain library members with high-affinity to the target molecule. So the latter has to be exposed somehow to the DNA library with the possibility of a subsequent separation of the bound DNA. For this purpose, two main strategies have been reported.[26] One involves a carrier matrix (e.g., affinity tags, column matrices) on which the target is immobilized and then contacted with the DNA library in the liquid phase. The other involves a purely liquid, matrix-free interaction (e.g. capillary electrophoresis). In both the target is exposed directly to millions of library members with a specific incubation period. While the principal advantage of the former is an easier separation, the principal advantage of the latter is that the target is not immobilized and can, hence, freely interact with the DNA as would be the case in a possible final application.

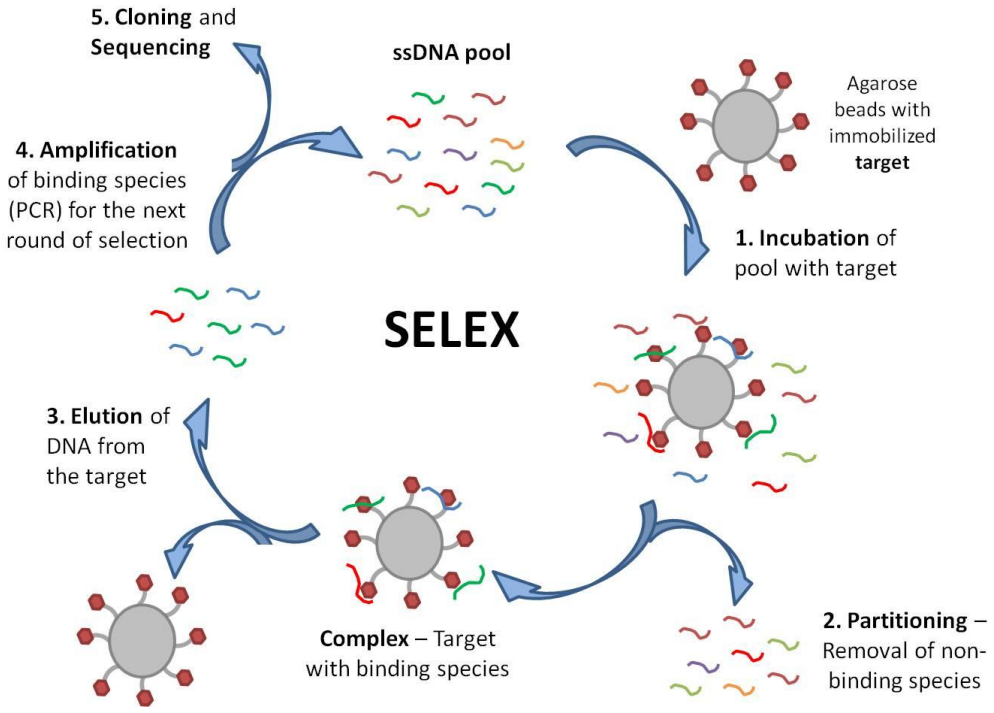

Figure 6.1. Selection scheme describing the main steps of the SELEX procedure. The rounds are repeated until an enrichment is reached. Then after step 4, the sequences are cloned and sequenced.

When an immobilized target is being used a counter selection or negative selection is typically introduced in order to improve the efficiency of the selection procedure. Hereby, the library is initially incubated with a substrate (e.g. magnetic beads, nitrocellulose membrane or protein tag) in the absence of the target. This way the oligonucleotide sequences that bind non-specifically to the target substrate

are eliminated from the library, therefore increasing the selectivity and specificity of the aptamers. A competitor consisting in random large sequences of DNA (e.g. salmon sperm) may also be introduced to saturate the unspecific binding sites and this way favor the specific binding of designed library.[27] A negative selection is usually introduced for whole-cells or complex targets in order to eliminate sequences that bind to common or ubiquitous, non specific regions of a complex target. Aptamers obtained from this type of selection were found to have an enhanced selectivity for the target and are usually intended for therapeutic applications.

In this work, DNA from salmon sperm was used as a competitor and introduced in the solvent matrix together with the ionic liquid.

6.1.5. Partitioning

After an incubation period, the so-called "partitioning step" has the objective to separate library members that are unbound from those that bound to the target molecule forming a complex aptamer-target.[28] This step is crucial in the success of the SELEX method and several strategies have been developed such as:

nitrocellulose membrane filtration,[29] affinity surfaces,[30] affinity tags,[31] column matrices,[32] gel electrophoresis,[33] centrifugation,[34] surface plasmon resonance,[35] flow cytometry,[36] and capillary electrophoresis.[37] The optimum partitioning strategy depends mainly on the physico-chemical properties of the target. Currently, there is no method that generically could be suited for partitioning when small molecules are used as targets. Capillary electrophoresis (CE) is probably a real advance in SELEX technology.[38,39] However, partitioning is based on size and charge parameters, and thus small molecules are not the best target candidates for this system, since the difference in the molecular weight or charge of the complex compared to the aptamer alone may be very little.

For the purpose of this work, and since the used target was a small molecule, it was immobilized on a gel-agarose matrix and chromatography columns were used for facilitating the incubation and the subsequent separation of the unbound DNA sequences.

6.1.6. Elution and Amplification

The next steps in SELEX include the elution of the binding DNA sequences from the target and the consecutive polymerase chain reaction (PCR) amplification.

Regarding elution, since the interactions established in the molecular recognition by the binding sequences with the target are weak and noncovalent, mild conditions can be applied to separate the two species. Elution can then be performed using heat, high concentrations of the target molecule, as a competition method, or chaotropic agents, such as urea, can be performed. The strength of the molecular interactions within the DNA-target complex will dictate the conditions required for the elution.[40,41] Especially when the target is a small molecule, as occurs in this work, the target is usually immobilized on magnetic or agarose beads to allow an easier separation of the bound DNA candidates after the complex formation.[42]

Once separated from the target, the few binding DNA sequences obtained are amplified by PCR to yield enough amount of sample to use in the next SELEX round.[40] The primer regions that flank the library members are used in order to enrich the specifically binding DNA by PCR. A simple PCR step is sufficient for binding member population enrichment. For RNA libraries, the process of enrichment involves reverse transcription PCR (RT-PCR) which produces complementary DNA (cDNA) and finally, a standard PCR to increase the library population.[30]

6.1.7. Conditioning

Conditioning is the preparation of the library after amplification and prior to a new round of SELEX. For DNA libraries, the PCR product is double-stranded DNA which has to be separated into single-stranded DNA for the next round. Several strategies using the streptavidin/biotin system have been reported.[43,44] The modification with biotin of the unwanted strand and the separation of the dsDNA strands by contact or by pass through a column with streptavidin coated-beads has been successfully performed. Denaturing is then induced under alkaline conditions such that the unmodified strand (the desired strand) can be recovered in the supernatant.[44]

Yet another method which already was demonstrated to be advantageous over others[45,46] and which has ben used in this work was the lambda exonuclease digestion of the undesired strand. The lambda (λ) exonuclease is a highly processive 5´ -> 3´ exodeoxyribonuclease that selectively and consecutively digests the 5´-phosphorylated strand of a dsDNA without releasing it. For this purpose, a 5´-phosphate group is introduced into one strand of dsDNA by performing PCR where only one of the two primers is 5´-phoshorylated. The phosphorylated strand is then removed by digestion with lambda exonuclease.[47]

Other strategies, such as asymmetric PCR can also be used where one of the primers is in excess in order to amplify mostly the desired strand.[48] For RNA, the conditioning procedure consists of the *in vivo* transcription of DNA template by T7 RNA polymerase and then use one of the methods for DNA.[49,50]

Typically, the first rounds of SELEX have low stringencies which increases as the selection progresses (e.g. decreasing incubation time or target concentration, changing washing conditions, varying pH and/or increasing ionic strength of the buffer) such as to obtain high affinity binding sequences. When a significant increase in the binding of the sequences to the target is observed compared to the first round, an enrichment of the pool is reached. Different strategies can be used to test whether the enrichment is occurring or not during SELEX such as: SPR;[51,52] radioactive labeling;[30,53,54] fluorescence spectroscopy;[55–57] or the most recent method of next generation sequencing (NGS).[58] When the enrichment is achieved, the final pool is cloned and sequenced in order to identify the sequence or sequences which specifically recognize the target of interest.

6.1.8. Cloning and Sequencing

After several rounds of SELEX (6 to 20) and when the affinity of the enriched library can no longer be increased, the process is completed by the cloning and sequencing procedure.[23] , The number of library members in the last round can vary between 1 and 1.000.000 elements, depending on parameters such as: nature of the target; target concentration; or SELEX method chosen. The main goal of the cloning procedure is to split up the library members into single members. For that purpose, the final pool is cloned into a bacterial vector and individual colonies with single-members are obtained.[59,60] Subsequently, the extraction of the plasmid is performed for the sequencing method that produces the sequence that offers high-affinity against the target molecule. All the isolated sequences (usually 20 to 50) are analyzed to find consensus motifs between them. The consensus motifs derived from this selection process will become the final aptamer-candidates.

6.1.9. Analysis of consensus sequences

Bioinformatic tools are necessary for the analysis of the sequences obtained by SELEX. In order to find the consensus sequence, the alignment of all sequences is a requirement to complete the SELEX method. Bioinformatic programs available

online like Multiple Sequence Comparison by Lon-Expectation (MUSCLE, *http://www.ebi.ac.uk/Tools/msa/muscle/*) or Multiple Alignment using Fast Fourier Transform (MAFFT, *http://mafft.cbrc.jp/alignment/software/*), which substituted CLUSTAL W, are frequently used for the DNA alignment performance. The analysis of the alignment data is based on finding the concordance in practically the entire sequence, differing only by the position of single nucleotides, or at least in some specific identical motif(s) between the different sequences. These motif regions are often involved in the specific target binding and are so-called "binding pockets".[61] This way the similar sequences can be grouped based on homology identification, and non-consensus sequences can be discarded. When performing a complete SELEX method, the expected positive outcome is consensus sequences between different library members.

The secondary structure analysis of the aptamer sequences candidates provides further information about the binding pocket. Commonly, *mfold* (*http://unafold.rna.albany.edu/?q=mfold*) is used for such analysis, calculating the possible configuration of the single-stranded nucleic acids by energy minimizing method considering the formation of stems, loops or bulges.[23]

6.1.10. Binding studies

Following the determination of consensus sequences, the binding studies determining the specificity and affinity of the selected aptamers is the subsequent step. The binding studies are a very important part of aptamer selection. Viable future applications of aptamers depend on matching the expected specificity and affinity to the target molecule. In this context, the determination of the affinity constant (dissociation constant K_d), is of major importance. The lower the K_d-value, the higher the affinity between aptamer and target. To measure K_d, a constant concentration of either the aptamer or target is titrated with an increasing concentration of the other component to yield a binding isotherm. The technique to use depend on the target size and it physico-chemical properties and can, for instance, be based on: spectroscopy (fluorescence intensity, CD, NMR),[62–64] mass-sensitive surface based (SPR, QCM or QCM-D),[65,66] separation (HPLC, CE, equilibrium dialysis, affinity chromatography)[40,67–69] and other methods such as ITC.[63,70]

6.2. Results and Discussion

During SELEX, DNA changes between the single-strand and double-strand form: first, when the DNA pool is incubated with ATP in each SELEX round, it has to be single-stranded. However, in order to subsequently amplify the sequences that bound to the target, in each SELEX round a PCR is carried out for increasing the concentration of the binding sequences such that they can be used in the next round (**Figure 6.1** - step 4). During PCR, the DNA becomes double-stranded. The PCR procedure involves a "cocktail" of reagents mixing the DNA template sequences with the primers, the dNTPs and the polymerase enzyme. As a consequence, contaminations may occur or undesired secondary products may form with the primers, affecting in this way the amplification and formation of dsDNA. The presence of residual ionic liquid might even aggravate this. We therefore ensured first that the double-stranded DNA formed properly in presence of an ionic liquid by running an agarose electrophoresis gel with EtBr incorporated after each PCR procedure. **Figure 6.2** represents one of these gels as an example. Lane 1 represents the DNA ladder (L) as a reference. It is a molecular-weight size marker with bands ranging from 300 base pairs (bp) on top to 10 bp at the bottom with the most intense band representing 50 bp. The bands of lanes 3 and 4 correspond to the

samples incubated in buffer, "b", and in the ionic liquid choline lactate, "CL", respectively. It can be seen that no by-products had formed since we observe only a single band corresponding to the dsDNA bands expected. These bands appeared between the reference bands of 75 and 100 bp which is in line with the length of the sequence employed which was 80 bp. The bands at the bottom of lanes 2, 3 and 4 correspond to the excess of primers that remained in solution and that were not used in the amplification process. Lane 2 depicts the negative control when PCR was conducted without any DNA template. No band can be observed confirming that no contamination or side-product formation took place in the PCR medium. This preliminary finding was utmost important as it confirmed that the SELEX procedure could be conducted in presence of the ionic liquid choline lactate without interference by the latter with the PCR. This is in fact in line with the work of Shi Y. et al., 2012.[71]

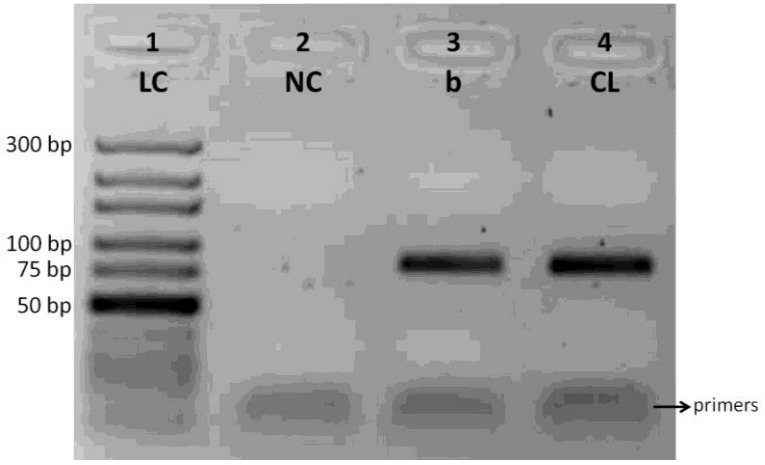

Figure 6.2. Agarose gel 4% after electrophoresis for the dsDNA pool amplified by PCR during a SELEX round. Staining is achieved using EtBr which emits only when it intercalates in between the nucleotides.

After each PCR, the dsDNA needed to be converted into ssDNA again for preparing the pool for the next round, using λ-exonuclease. The successful conversion was confirmed by agarose electrophoresis gels. **Figure 6.3** shows a representative gel made during the exonuclease digestion. The DNA ladder used here was the same as depicted in **Figure 6.2.** The bands of lanes 2 and 3 correspond to the samples incubated in buffer and in choline lactate, respectively. In each lane, one single band was detected and the bands appear at a lower level than the previous ones for dsDNA, validating in this way the complete transformation of

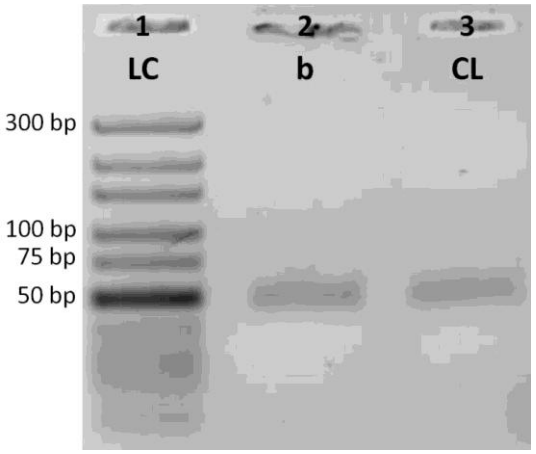

Figure 6.3. Agarose electrophoresis gel after λ-exonuclease digestion of the dsDNA into ssDNA.

dsDNA into ssDNA. The bands here appear brighter because EtBr only intercalates in the possibly formed secondary structures of the more flexible ssDNA structure (e.g. helical regions), mimicking the dsDNA environment conditions which allow the EtBr to emit.

Based on the experience of Huizenga and Szostak,[72] eight selection rounds were expected to yield enrichment of the DNA sequences that would be expected to bind specifically to ATP. In order to prove whether any enrichment had been obtained in our studies,

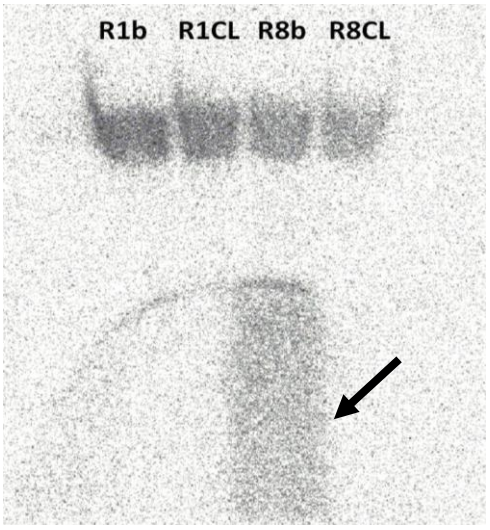

Figure 6.4. PAGE gel after the kinasation to verify if the ssDNA samples of R1 and R8 in buffer and in buffer with 2M CL were well labelled with γ-^{32}P.

the sequences of the first round (R1) as the negative control and of the last round (R8) were labelled with γ-^{32}P-ATP and measured by LSC, both for buffer and buffer with 2M of CL, respectively. The successful labelling was previously verified with a polyacrylamide gel (PAGE) depicted in **Figure 6.4**.

Here, the two first bands that appear in the PAGE gel represent the samples of the first round of buffer (R1b) and choline lactate (R1CL), respectively. The other two bands represent the samples of round 8 of SELEX, again for buffer (R8b) and choline lactate (R8CL), respectively. According to **Figure 6.4**, it can be seen that all four

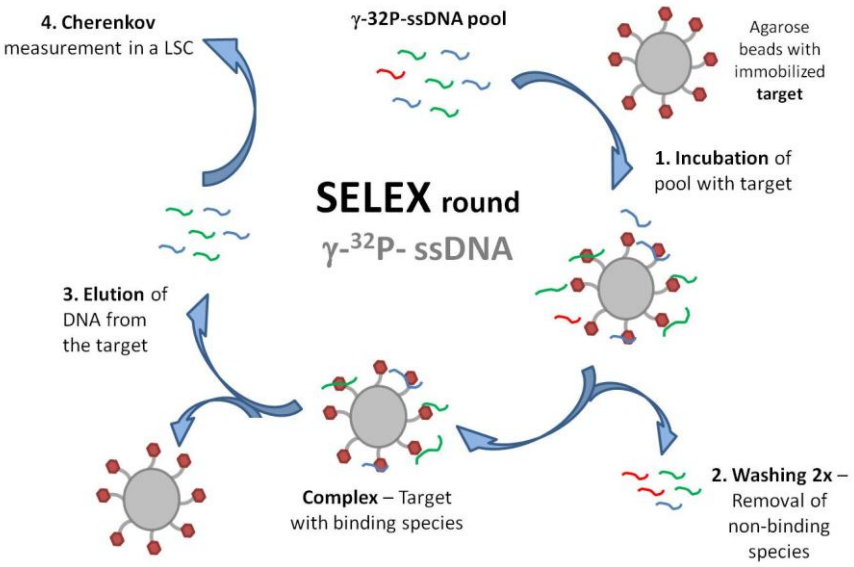

Figure 6.5. Incubation of the labelled pool with the ATP-target subsequent recovered samples for the Cherenkov measurement in the LSC. This procedure resembles a single round of SELEX.

samples were properly labelled with γ-^{32}P. The scattered band below the R8b band (pointed with an arrow - **Figure 6.4**) is probably due to a not totally efficient purification of this sample, with some free γ-^{32}P-ATP remaining in solution.

For determining the evolution, these labelled pools were incubated with the ATP target, resembling a SELEX round. During the round, the supernatants from: incubation; washing; elution; and beads; (**Figure 6.5**) were stored in order to

determine the fraction of labelled DNA in each sample. In the elution supernatant we expected to find the sequences that specifically bound to the target, hence, the enrichment of the pool from the first to the last round of SELEX. On the other hand, any radioactivity measured from the beads with the ATP immobilized would indicate either binding of selective sequences to the ATP target that could not be efficiently eluted, or indicate unspecific binding to the agarose beads. The preliminary step of incubating the DNA library with the agarose beads without the immobilized target, to eliminate the unspecific binders of the library, was not carried out here and must be taken into consideration in a future similar procedure.

The results from the analysis of the different supernatants are depicted in **Figure 6.6** for buffer (left) and for choline lactate (right). The two first bars of **Figure 6.6** (≈ 40% for R1, ≈ 65% for R8 with buffer; ≈ 30% for R1 and R8, respectively, with CL) suggested that a high amount of DNA had not bound to the target but apparently been removed during the elimination of the supernatant just after incubation.

Surprisingly, the binding to the beads was very high, as can be seen from the two last bars of **Figure 6.6**, reaching values that in the case of the CL solution were even higher than for the incubation supernatant (≈ 50% for R1, ≈ 10% for R8 with

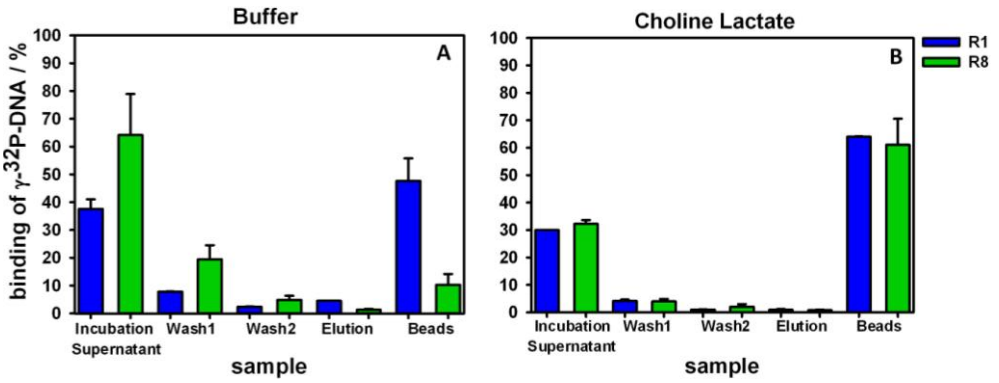

Figure 6.6. Percentages of γ-^{32}P-DNA present in the different solutions collected in each step of the binding assay of round 1 and round 8 for **A)** buffer and **B)** CL as solvents. The bars on top of the columns represent the error bar. Every sample was measured in duplicate.

buffer; ≈ 65% for R1 and ≈ 60% R8, respectively, with CL). These results reveal that a significant binding of the DNA sequences to the beads had occurred. Although hardly any sequences were found in the elution, this would in principle be a desirable result; however, the strikingly high binding values observed for the beads already after round one – when indeed no real enrichment is expected to be observed, yet – hinted at the possibility of an unspecific binding taking place.

In order to overcome what we considered to be a very high degree of unspecific binding to the beads, the use of a competitor for the DNA-aptamer was mandatory. The function of the competitor is to easily establish interactions with the

beads, allowing merely the DNA sequences of interest to interact with the ATP-target immobilized on the beads. The competitor used here was salmon sperm DNA with a concentration of 10 mg/ml. This DNA has an average size of ≤ 2000 bp and is commonly used precisely to reduce the non-specific binding of nucleic acids during hybridization occurring for instance on a filter surface.

With the purpose to check whether our counter-measure was successful, we repeated the procedure of **Figure 6.5** using the same samples but adding 1 mg/ml of salmon sperm DNA. Indeed, we observed a significant decrease of the γ-^{32}P-DNA population that bound to the beads, both in buffer solution and in buffer solution containing 2M of CL (**Figure 6.7**). Henceforth the use of salmon sperm DNA competitor had become essential. In order to verify what concentration of salmon sperm DNA would be most efficient, we repeated the above procedure but only with the rounds of buffer to decrease the amount of samples. Into these we introduced 0,1 mg/ml and 1 mg/ml, respectively, of salmon sperm DNA in the initial solution containing the pools of round 1 and round 8. Incubating the solution with the ATP-target we could determine which of the two

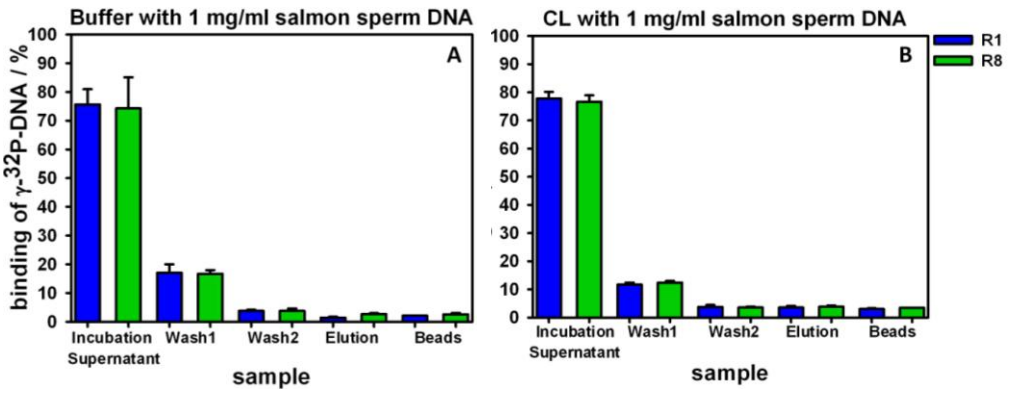

Figure 6.7. Percentages of γ-^{32}P-DNA present in the different solutions collected in each step of the binding assay of round 1 and round 8 for **A)** buffer and **B)** buffer with 2M CL as solvents, each with the addition of 1 mg/ml of salmon sperm DNA. The bars on top of the columns represent the error bar. Every sample was measured in duplicate.

concentrations worked better avoiding that the γ-^{32}P-DNA pools interacted non-specifically with the beads. We found that with 1 mg/ml of salmon sperm DNA in the initial solution much less γ-^{32}P-DNA bound to the beads (≈ 3% for R1 and R8 with buffer) compared to the solution with 0,1 mg/ml of salmon sperm DNA (≈ 10% for R1 and R8 with buffer), **Figure 6.8**.

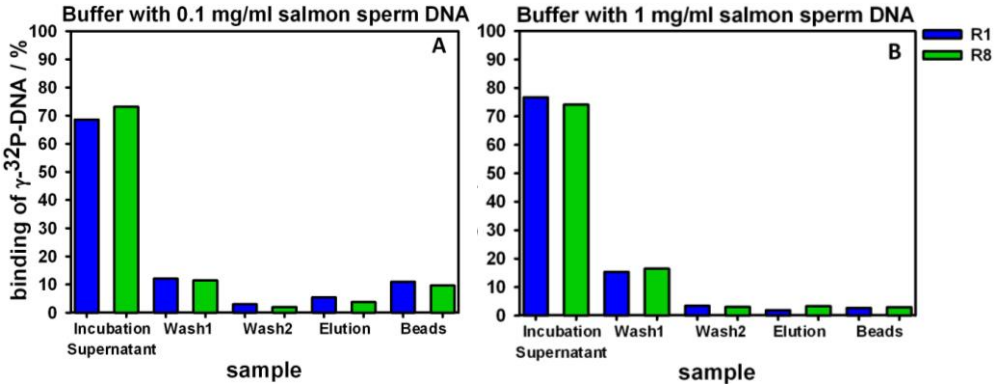

Figure 6.8. Percentages of γ-^{32}P-DNA present in the different solutions collected in each step of the binding assay only with the round 1 and round 8 of buffer solution with the addition of **A)** 0,1 mg/ml and **B)** 1 mg/ml of salmon sperm DNA.

Based on these observations, a second SELEX ("SELEX II") was initiated using 1 mg/ml of salmon sperm DNA in each round. As starting DNA library, we used the one we obtained after the second round of the previous SELEX procedure ("SELEX I"), taking advantage of starting with a first "enrichment" or "filter" of the initial pool, although still in absence of salmon sperm.

Table 6.1. Overview of experiments carried out and sample assignation in SELEX I and SELEX II with the presence of salmon sperm in the SELEX rounds.

SELEX I		**SELEX II**	
buffer	**CL**	**buffer**	**CL**
no salmon sperm		**1 mg/ml salmon sperm**	
R1	R1		
R2	**R2**		
R3	R3	**R3'**	**R3'**
R4	R4	R4'	R4'
R5	R5	R5'	R5'
R6	R6	R6'	R6'
R7	R7	R7'	R7'
R8	R8	R8'	R8'
			R9'
			R10'
			R11'
			R12'
8 rounds	8 rounds	8 rounds	12 rounds

SELEX II was also made for the solutions using the Tris-HCl buffer and Tris-HCl buffer with 2M of choline lactate as solvents, respectively. These new round numbers were denoted with an apostrophe. **Table 6.1** details the samples nomenclature used in SELEX I and in SELEX II.

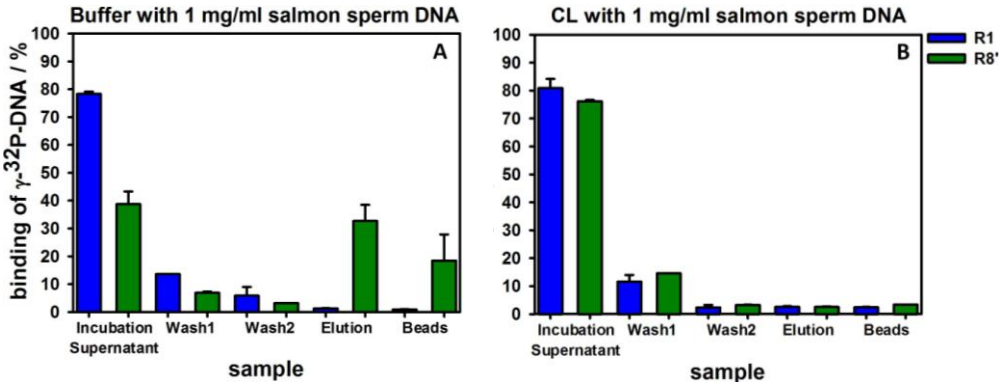

Figure 6.9. Percentages of γ-^{32}P-DNA present in the different solutions collected in each step of the binding assay of round 1 of SELEX I and round 8' of SELEX II for **A)** buffer and **B)** buffer with 2M CL as solvents, each with the addition of 1 mg/ml of salmon sperm DNA. The bars on top of the columns represent the error bar of the measurements. Each sample was analyzed in duplicate.

After six further rounds of selection in presence of salmon sperm DNA, we verified the degree of enrichment by repeating the kinasation and the measurement by LSC. We hereby compared the last round of SELEX II in presence of salmon sperm DNA (R8') with the first round of SELEX I in absence of it (R1). The results are depicted in **Figure 6.9 A**. In buffer solution, we can confirm a considerable increase of supposedly specific DNA sequences in the elution sample of R8' (≈ 33%), as compared to the original sample R1 (≈ 1,5%) in absence of salmon sperm DNA. The bars for the samples of the beads (R1: ≈ 1%; R8': ≈ 18%) follow a similar trend,

meaning that also here we may have increased the specificity of the binding, but the sequences could not be eluted from the target. So if we consider the whole amount of binding in R8' with the elution and with the beads in buffer solution, we obtained around 51% of specific binding. Repeating the Cherenkov measurement for R1, R4', and R8' (**Figure 6.10 A**), we observed also the reproducibility of the procedure when comparing these with the results of **Figure 6.9 A**. Thus, the selection procedure with pure Tris-HCl as solvent could be stopped after R8'. This observation is in good agreement with the that obtained by Huizenga and Szostak who found that in Tris-HCl buffer solution eight rounds of selection are required to yield a pool of sequences that specifically recognize the ATP target.[72]

During SELEX II in presence of 2M of choline lactate, however, no such increase in specificity was observed until R8' (**Figure 6.9 B**). Most γ-^{32}P-DNA did not bind to the ATP-target, being removed, as before, with the incubation supernatant and the washing steps and in this way leaving almost no γ-^{32}P-DNA in the elution and on beads samples.

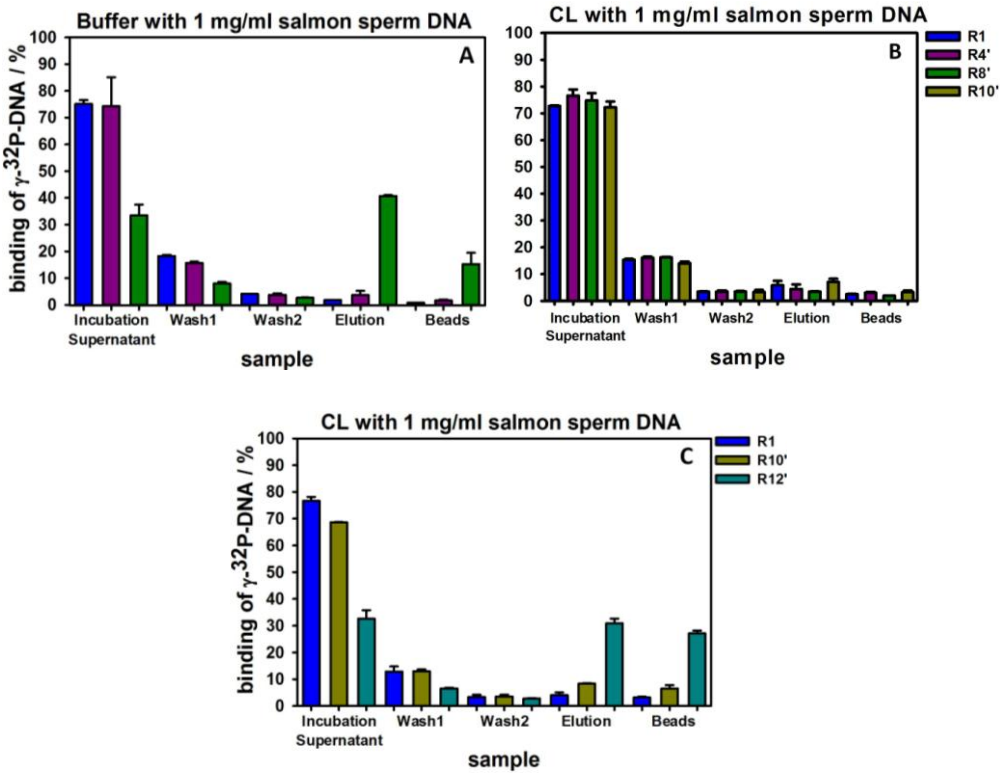

Figure 6.10. Percentages of γ-^{32}P-DNA present in the different solutions collected in each step of the binding assay of **A)** R1, R4' and R8' for buffer, of **B)** R1, R4', R8' and R10' and **C)** R1, R10' and R12' for buffer with 2M CL as solvents, each with the addition of 1 mg/ml of salmon sperm DNA. The bars on top of the columns represent the error bar of the measurements. Each sample was analyzed in duplicate.

The aim was, hence, to find out whether additional rounds of SELEX would result in an enrichment also for the IL-containing buffer solution. For this purpose, four more rounds were conducted in SELEX II containing 2M CL in Tris-HCl (R8' –

R12'), with a simultaneous control of the enrichment during the SELEX process (**Figure 6.10 B** and **C**). The new Cherenkov assays proved that while until R10' a slight increase in the binding was observed (**Figure 6.10 B**), we reached at R12' a significant enrichment based on the analysis of the elution and beads samples of R1, R10' and R12', respectively, as is shown in **Figure 6.10 C**. Considering again the sum of the samples of elution and beads, R12' yielded around 58% (≈ 31% elution + ≈ 27% beads) of binding of the γ-^{32}P-DNA to the ATP target in buffer solution containing 2M of choline lactate.

This validated our working protocol. In presence of 2M of choline lactate, four more rounds were needed (12 rounds in total), but eventually enrichment was also achieved and the percentage of binding was even higher than that observed in pure buffer solution. Hence, the selection of the ATP-binding DNA aptamer takes more rounds in presence of 2M of CL, but it is absolutely feasible. To the best of our knowledge, this is the first time that a DNA-aptamer was successfully selected in presence of an ionic liquid. The fact that more rounds are needed as opposed to pure buffer solutions is in good agreement with the results obtained in our previous work (**Chapter 5**) where we proved that the ATP-aptamer selected in buffer solution lost some specificity to the ATP molecule when in presence of 2M of choline lactate.

In order to isolate an aptamer for each solvent used, the pools obtained in round 8' for buffer and in round 12' for CL were then cloned and sequenced (see **Chapter 2** for experimental details). The obtained sequences, already without the primers, were then aligned and analysed using the bioinformatic software MUSCLE in order to compare the random region of the library members obtained (**Figure 6.11**). Taking into account the sequence of the ATP-aptamer selected by Huizenga and Szostak as reference, we could find similarities in the structures regarding the G-rich "binding pocket" of the ATP-aptamer (**Figure 2.1 - Chapter 2**) with the motif responsible for the ATP recognition being based on the following parts of the aptamer sequence: GGGGGA and GGAGGA. All the sequences obtained in buffer solution contained these two motifs, revealing on one hand that

A)

```
B01 ------------------CGGGGGAGAGC------------TTTTTTGGCGCGGCGGAGTTCCTAAGGATTAA------
B02 GCGGCTATG---------TGGAGGAGGTT------------TTCGCTATACCGGGGGAATATA----------------
B03 ---GATAAGCTTCTATACCGGTGGAGGAA-----------------TATAATGGGGGAGCCGA----------------
B04 --------GCGCCCATTATGGGGGAGGTA---------------CCATTACCGGAGGAATATTGTG-------------
B05 ACTTAGACAAGTATACAACGCGGGGGAAC---------------CTGTTCGTGGAGGA--------------------
B06 ---------------CATCGGGGGAGTTA-----------TAGTGTAATGGCGGAGAGGTTGACAGAAG----------
B07 -------------GTAGACGGGGGAGAAA----------TTTATCAAATTTCGGAGGAGTTACCTAC------------
B09 -----------------CCGGGGGAGGATATCCCCCAGATTCTGGGATTTCCGGAGGAGG-------------------
B10 ---------------ACGCGGGGGAGGGC-------------TAAGACGCCTGGAGGAGCTTTGCTAGATC--------
B11 -GGGATATAATGCACAACCGGGGGAAGCA---------------------ATGGAGGAGGTTGCG--------------
B13 -----------TCAGTACCGGGGGGAGGT-----------------TAGGCGGAGGGAGGGACTAAGGATC-------
B16 ------------------CGGGGGAGAAC-----------------TAATCGGAGGAGGGGCATAAGTTTGAGGATAC
                      *  **                        ** *
```

B)

```
I22 --------------------CAGTCGGGGGAGG----------------TACGGAGGAGACGTATTTACACTAGAAGCA
I23 ------------CTGCAACCAAGTCGGAGGAGATTC-------------ATCGGGGGAGACCTGTGTC------------
I24 --------------ATGCAACAACCGGAGGAGCG---------------CGCGGGGGAGGGTATTGTCGAGT--------
I27 --------------TTACATCTTCGGGAGGAGTATTTTAG---------ACGGGAGGAGAAGATTT--------------
I28 GGACGTCACCGAAAGATCATGTGCCGGAGGAGG----------------GACGGGGGAG--------------------
I29 ----------CTCCCGTTGTGGCTCGGGGGAGAGGA-------------TTCGGAGGAGAGCCGAG--------------
I30 --------------------AGTCGGAGGAGGCTGTAGTAACCTACACACCGGGGGAGAATTA----------------
I31 --------------TCATCCATATTCAAGGTGACTCCAGC--------CCTCGGCGGTGTTGTGA---------------
I32 ----------------------GCGGGGGAGCCCAAGGT---------GGCGGAGGAG----CTCGCAAGGGGATCAA
I33 --------------------TTGCGGAGGAGAGTA-------------CTCGGGGGAG--CAATTCCACGTAAGTCGA
I36 ----------------------ACAGAAGAGCAGT-------------CGCGGGGGAGTAGCCTTTGCGGACGGAGGA
I37 -ATCTGCGACGAAGATACATGCCGCGGGGGAGAGA--------------CTCGGAGGA----------------------
                                  * *                  ** **
```

C)

```
I21 ------------------------TACATCTATCCTTCTACTCTCACTTTTTAAGGGACCCCAAGTG-------------
I25 ---------------GGTGGAGTCA-------GTCGCATCAGTCACTTTAGGAAGTTAC--------------------
I26 GATGTAAGCATAGTGAATAGAAACCACGTTGAGGACGCGGCGC-------------------------------------
I38 ------------TGACTCCAAGCCAGGGTGTTGCCGTAGTCGGCGCGTGTGAAAT-----------------------
                           *
```

Figure 6.11. Alignments made by the bioinformatic software MUSCLE of the sequences obtained when using **A)** Tris-HCl buffer and **B)** - **C)** Tris-HCl buffer with 2M of choline lactate as solvents. The asterisk below the sequences represent the only nucleotides which are common for all the sequences in the groups.

undoubtedly, in solution with Tris-HCl buffer these motifs are essential for the ATP recognition (**Figure 6.11 A**), and on the other hand confirming that the SELEX procedure had been working properly. However, while in the solution containing 2M of the ionic liquid choline lactate the majority of the sequences also presented these two motifs in their structure (**Figure 6.11 B**), four of them were in fact completely

different and without any of these motifs (**Figure 6.11 C**). The later might be an indication for the evolution of the sequences that recognize ATP when in presence of choline lactate.

Using choline dihydrogen phosphate, Sugimoto N. and co-workers found that when DNA is in single-strand, as occurs during the incubation step of SELEX process, choline ions bind preferentially to G bases rather than to the other 3 bases.[73–75] This may hinder the recognition of ATP by sequences with the characteristic G-rich motifs, forcing other sequences to bind to ATP which in part could explain the presence of sequences that bound to ATP without the G-rich motifs identified in pure buffer solution. On the other hand, we proved in **Chapter 5** that the presence of choline lactate in solution does not interfere significantly with the DNA structure, stability and function. Besides, we determined a coordination flexibility of choline cations around DNA nucleobases and phosphate backbone by theoretical calculations, which may facilitate the binding of the sequences presenting the G-rich motifs to the target ATP even in presence of choline lactate. These evidences may explain the variety of the sequences obtained in presence of 2M of CL in solution. As the case may be, it was shown that ATP-binding aptamer sequences can in principle be selected in presence of an ionic liquid such as choline lactate. An important next

step would be the analysis of the newly selected sequences as for their recognition of the ATP-target and determine whether their binding constant (K_d) is more favourable in solutions of choline lactate than that of the aptamer selected in pure buffer.. Unfortunately, due to a lack of time at the end of this doctoral thesis, we did not have the opportunity to determine and compare the binding affinity of the determined sequences in buffer and in buffer with 2M CL. This will certainly be part of future work of the NanoBioSeparations Group..

6.3. Conclusions

The study described here has compared the process of selection of a DNA sequence that recognizes the ATP molecule in presence of buffer and in presence of buffer with 2M of the ionic liquid choline lactate. It was determined that with Tris-HCl buffer as solvent, eight rounds of selection were needed to obtain enrichment, confirming literature date. All the sequences of the control SELEX with Tris-HCl buffer presented the motif responsible for the recognition determined by Huizenga and Szostak, which indicates the high specificity of these sequences for the recognition of the ATP in pure buffer solution. On the other hand, when we introduced 2M of choline lactate to the Tris-HCl solution, 12 rounds of selection

were needed to obtain enrichment. Some of the sequences obtained presented the same motif as the sequences obtained in buffer, but others were completely different. The fact that we obtained enrichment, even though with 4 rounds more than in buffer, is a great success considering that – to the best of our best knowledge - until now no aptamer was ever selected under these conditions.

These new findings already prove the high potential of DNA to maintain its functionality in such different environments, increasing the "degree of freedom" of the SELEX process as well as the application fields of aptamers selected.

6.4. References

(1) Ke, F.; Luu, Y. K.; Hadjiargyrou, M.; Liang, D. Characterizing DNA Condensation and Conformational Changes in Organic Solvents. **2010**, *5* (10), 1–8.

(2) Chandran, A.; Ghoshdastidar, D.; Senapati, S. Groove Binding Mechanism of Ionic Liquids: A Key Factor in Long-Term Stability of DNA in Hydrated Ionic Liquids? *J. Am. Chem. Soc.* **2012**, *134* (50), 20330–20339.

(3) Lannan, F. M.; Mamajanov, I.; Hud, N. V. Human Telomere Sequence DNA in Water-Free and High-Viscosity Solvents: G-Quadruplex Folding Governed by Kramers Rate Theory. *J. Am. Chem. Soc.* **2012**, *134* (37), 15324–15330.

(4) Machado, I.; Özalp, V. C.; Rezabal, E.; Schäfer, T. DNA Aptamers Are Functional Molecular Recognition Sensors in Protic Ionic Liquids. *Chemistry* **2014**, *20* (37), 11820–11825.

(5) Machado, I. Non Published Results - Chapter 5.

(6) Pauling, L.; Delbrück, M. The Nature of the Intermolecular Forces Operative in Biological

Processes. *Science* **1940**, *92* (2378), 77–79.

(7) Gopinath, S. C. B. Antiviral Aptamers. *Archives of Virology*. **2007**, pp 2137–2157.

(8) Gold, L.; Polisky, B.; Uhlenbeck, O.; Yarus, M. Diversity of Oligonucleotide Functions. *Annu. Rev. Biochem.* **1995**, *64*, 763–797.

(9) Osborne, S. E.; Ellington, A. D. Nucleic Acid Selection and the Challenge of Combinatorial Chemistry. *Chem. Rev. (Washington, D. C.)* **1997**, *97* (2), 349–370.

(10) Wilson, D. S.; Szostak, J. W. *In Vitro* Selection of Functional Nucleic Acids. *Annu. Rev. Biochem.* **1999**, *68*, 611–647.

(11) Song, S.; Wang, L.; Li, J.; Fan, C.; Zhao, J. Aptamer-Based Biosensors. *TrAC - Trends Anal. Chem.* **2008**, *27* (2), 108–117.

(12) Özalp, V. C.; Pinto, A.; Nikulina, E.; Chuvilin, A.; Schäfer, T. In Situ Monitoring of DNA-Aptavalve Gating Function on Mesoporous Silica Nanoparticles. *Part. Part. Syst. Charact.* **2014**, *31* (1), 161–167.

(13) Hernandez, F. J.; Hernandez, L. I.; Pinto, A.; Schafer, T.; Ozalp, V. C. Targeting Cancer Cells with Controlled Release Nanocapsules Based on a Single Aptamer. *Chem Commun* **2013**, *49* (13), 1285–1287.

(14) Özalp, V. C.; Schäfer, T. Aptamer-Based Switchable Nanovalves for Stimuli-Responsive Drug Delivery. *Chem. - A Eur. J.* **2011**, *17* (36), 9893–9896.

(15) Famulok, M.; Hartig, J. S.; Mayer, G. Functional Aptamers and Aptazymes in Biotechnology, Diagnostics, and Therapy. *Chem. Rev.* **2007**, *107* (9), 3715–3743.

(16) Brody, E. N.; Gold, L. Aptamers as Therapeutic and Diagnostic Agents. *J. Biotechnol.* **2000**, *74* (1), 5–13.

(17) Tan, W.; Wang, H.; Chen, Y.; Zhang, X.; Zhu, H.; Yang, C.; Yang, R.; Liu, C. Molecular Aptamers for Drug Delivery. *Trends in Biotechnology*. **2011**, 634–640.

(18) Wu, X.; Chen, J.; Wu, M.; Zhao, J. X. Aptamers: Active Targeting Ligands for Cancer Diagnosis and Therapy. *Theranostics*. **2015**, 322–344.

(19) Shamah, S. M.; Healy, J. M.; Cload, S. T. Complex Target SELEX. *Acc. Chem. Res.* **2008**, *41* (1), 130–138.

(20) Hernandez, L. I.; Machado, I.; Schäfer, T.; Hernandez, F. J. Aptamers Overview : Selection , Features and Applications. **2015**.

(21) Chapman, J. A.; Beckey, C. Pegaptanib: A Novel Approach to Ocular Neovascularization. *Annals of Pharmacotherapy*. **2006**, 1322–1326.

(22) Ng, E. W. M.; Shima, D. T.; Calias, P.; Cunningham, E. T.; Guyer, D. R.; Adamis, A. P. Pegaptanib, a Targeted Anti-VEGF Aptamer for Ocular Vascular Disease. *Nat. Rev. Drug Discov.* **2006**, *5* (2), 123–132.

(23) Stoltenburg, R.; Reinemann, C.; Strehlitz, B. SELEX-A (R)evolutionary Method to Generate High-Affinity Nucleic Acid Ligands. *Biomolecular Engineering*. **2007**, 381–403.

(24) Nutiu, R.; Li, Y. In Vitro Selection of Structure-Switching Signaling Aptamers. *Angew. Chemie - Int. Ed.* **2005**, *44* (7), 1061–1065.

(25) Tang, Z.; Mallikaratchy, P.; Yang, R.; Kim, Y.; Zhu, Z.; Wang, H.; Tan, W. Aptamer Switch Probe Based on Intramolecular Displacement. *J. Am. Chem. Soc.* **2008**, *130* (34), 11268–11269.

(26) Gopinath, S. C. B. Methods Developed for SELEX. *Anal. Bioanal. Chem.* **2007**, *387* (1), 171–182.

(27) Mayer, G.; Ahmed, M.-S. L. M.; Dolf, A.; Endl, E.; Knolle, P. a; Famulok, M. Fluorescence-Activated Cell Sorting for Aptamer SELEX with Cell Mixtures. *Nat. Protoc.* **2010**, *5* (12), 1993–2004.

(28) Jenison, R.; Gill, S.; Pardi, A.; Polisky, B. High-Resolution Molecular Discrimination by RNA. *Science (80-.).* **1994**, *263* (5152), 1425–1429.

(29) Přistoupil, T. I.; Kramlová, M. Membrane Chromatography of Dyes on Nitricellulose Filters. *J. Chromatogr. A* **1968**, *34* (C), 21–25.

(30) Ellington, a D.; Szostak, J. W. In Vitro Selection of RNA Molecules That Bind Specific Ligands. *Nature* **1990**, *346* (6287), 818–822.

(31) Dobbelstein, M.; Shenk, T. In Vitro Selection of RNA Ligands for the Ribosomal L22 Protein Associated with Epstein-Barr Virus-Expressed RNA by Using Randomized and cDNA-Derived RNA Libraries. *J. Virol.* **1995**, *69* (12), 8027–8034.

(32) Ciesiolka, J.; Gorski, J.; Yarus, M. Selection of an RNA Domain That Binds Zn2+. *RNA* **1995**, *1* (5), 538–550.

(33) Smith, D.; Kirschenheuter, G. P.; Charlton, J.; Guidot, D. M.; Repine, J. E. In Vitro Selection of RNA-Based Irreversible Inhibitors of Human Neutrophil Elastase. *Chem Biol* **1995**, *2* (11), 741–750.

(34) Zhang, F.; Anderson, D. In Vitro Selection of Bacteriophage ϕ29 Prohead RNA Aptamers for

Prohead Binding. *J. Biol. Chem.* **1998**, *273* (5), 2947–2953.

(35) Katsamba, P. S.; Park, S.; Laird-Offringa, I. A. Kinetic Studies of RNA-Protein Interactions Using Surface Plasmon Resonance. *Methods* **2002**, *26* (2), 95–104.

(36) Blank, M.; Weinschenk, T.; Priemer, M.; Schluesener, H. Systematic Evolution of a DNA Aptamer Binding to Rat Brain Tumor Microvessels: Selective Targeting of Endothelial Regulatory Protein Pigpen. *J. Biol. Chem.* **2001**, *276* (19), 16464–16468.

(37) Drabovich, A. P.; Berezovski, M.; Okhonin, V.; Krylov, S. N. Selection of Smart Aptamers by Methods of Kinetic Capillary Electrophoresis. *Anal. Chem.* **2006**, *78* (9), 3171–3178.

(38) Berezovski, M.; Berezovski, M.; Musheev, M.; Musheev, M.; Drabovich, A.; Drabovich, A.; Jitkova, J.; Jitkova, J.; Krylov, S.; Krylov, S. Non-SELEX: Selection of Aptamers without Intermediate Amplification of Candidate Oligonucleotides. *Nat Protoc* **2006**, *1* (3), 1359–1369.

(39) Mosing, R. K.; Mendonsa, S. D.; Bowser, M. T. Capillary Electrophoresis-SELEX Selection of Aptamers with Affinity for HIV-1 Reverse Transcriptase. *Anal. Chem.* **2005**, *77* (19), 6107–6112.

(40) McKeague, M.; Bradley, C. R.; de Girolamo, A.; Visconti, A.; David Miller, J.; de Rosa, M. C. Screening and Initial Binding Assessment of Fumonisin B 1 Aptamers. *Int. J. Mol. Sci.* **2010**, *11* (12), 4864–4881.

(41) McKeague, M.; Derosa, M. C. Challenges and Opportunities for Small Molecule Aptamer Development. *Journal of Nucleic Acids*. **2012**.

(42) Vant-Hull, B.; Gold, L.; Zichi, D. a. Theoretical Principles of in Vitro Selection Using Combinatorial Nucleic Acid Libraries. *Curr. Protoc. Nucleic Acid Chem.* **2000**, *Chapter 9*, Unit 9.1.

(43) Sefah, K.; Shangguan, D.; Xiong, X.; O'Donoghue, M. B.; Tan, W. Development of DNA Aptamers Using Cell-SELEX. *Nat. Protoc.* **2010**, *5* (6), 1169–1185.

(44) Naimuddin, M.; Kitamura, K.; Kinoshita, Y.; Honda-Takahashi, Y.; Murakami, M.; Ito, M.; Yamamoto, K.; Hanada, K.; Husimi, Y.; Nishigaki, K. Selection-by-Function: Efficient Enrichment of Cathepsin E Inhibitors from a DNA Library. *J. Mol. Recognit.* **2007**, *20* (1), 58–68.

(45) Paul, A.; Avci-Adali, M.; Ziemer, G.; Wendel, H. P. Streptavidin-Coated Magnetic Beads for DNA Strand Separation Implicate a Multitude of Problems During Cell-SELEX. *Oligonucleotides* **2009**, *19* (3), 243–254.

(46) Citartan, M.; Tang, T. H.; Tan, S. C.; Gopinath, S. C. B. Conditions Optimized for the Preparation

of Single-Stranded DNA (ssDNA) Employing Lambda Exonuclease Digestion in Generating DNA Aptamer. *World J. Microbiol. Biotechnol.* **2011**, *27* (5), 1167–1173.

(47) Avci-Adali, M.; Paul, A.; Wilhelm, N.; Ziemer, G.; Wendel, H. P. Upgrading SELEX Technology by Using Lambda Exonuclease Digestion for Single-Stranded DNA Generation. *Molecules* **2010**, *15* (1), 1–11.

(48) Tang, J.; Xie, J.; Shao, N.; Yan, Y. The DNA Aptamers That Specifically Recognize Ricin Toxin Are Selected by Two in Vitro Selection Methods. *Electrophoresis* **2006**, *27* (7), 1303–1311.

(49) Thiel, W. H.; Bair, T.; Wyatt Thiel, K.; Dassie, J. P.; Rockey, W. M.; Howell, C. A.; Liu, X. Y.; Dupuy, A. J.; Huang, L.; Owczarzy, R.; et al. Nucleotide Bias Observed with a Short SELEX RNA Aptamer Library. *Nucleic Acid Ther.* **2011**, *21* (4), 253–263.

(50) Svobodova, M.; Pinto, A.; Nadal, P.; O' Sullivan, C. K. Comparison of Different Methods for Generation of Single-Stranded DNA for SELEX Processes. *Analytical and Bioanalytical Chemistry*. **2012**, 1–8.

(51) Schier, R.; Marks, J. D. Efficient in Vitro Affinity Maturation of Phage Antibodies Using BIAcore Guided Selections. *Hum Antibodies Hybridomas* **1996**, *7* (3), 97–105.

(52) Pileur, F.; Andreola, M. L.; Dausse, E.; Michel, J.; Moreau, S.; Yamada, H.; Gaidamakov, S. A.; Crouch, R. J.; Toulmé, J. J.; Cazenave, C. Selective Inhibitory DNA Aptamers of the Human RNase H1. *Nucleic Acids Res.* **2003**, *31* (19), 5776–5788.

(53) Shi, H.; Fan, X.; Ni, Z.; Lis, J. T. Evolutionary Dynamics and Population Control during in Vitro Selection and Amplification with Multiple Targets. *RNA* **2002**, *8* (11), 1461–1470.

(54) Beinoraviciūte-Kellner, R.; Lipps, G.; Krauss, G. In Vitro Selection of DNA Binding Sites for ABF1 Protein from Saccharomyces Cerevisiae. *FEBS Lett.* **2005**, *579* (20), 4535–4540.

(55) Stoltenburg, R.; Reinemann, C.; Strehlitz, B. FluMag-SELEX as an Advantageous Method for DNA Aptamer Selection. *Anal. Bioanal. Chem.* **2005**, *383* (1), 83–91.

(56) Niazi, J. H.; Lee, S. J.; Gu, M. B. Single-Stranded DNA Aptamers Specific for Antibiotics Tetracyclines. *Bioorganic Med. Chem.* **2008**, *16* (15), 7245–7253.

(57) Kim, Y. S.; Hyun, C. J.; Kim, I. A.; Gu, M. B. Isolation and Characterization of Enantioselective DNA Aptamers for Ibuprofen. *Bioorganic Med. Chem.* **2010**, *18* (10), 3467–3473.

(58) Beier, R.; Boschke, E.; Labudde, D. New Strategies for Evaluation and Analysis of SELEX Experiments. *Biomed Res. Int.* **2014**, *2014*.

(59) Shuman, S. Recombination Mediated by Vaccinia Virus DNA Topoisomerase I in Escherichia Coli Is Sequence Specific. *Proc Natl Acad Sci U S A* **1991**, *88* (22), 10104–10108.

(60) Shuman, S. Novel Approach to Molecular Cloning and Polynucleotide Synthesis Using Vaccinia DNA Topoisomerase. *J. Biol. Chem.* **1994**, *269* (51), 32678–32684.

(61) Ellington, A. D.; Chen, X.; Robertson, M.; Syrett, A. Evolutionary Origins and Directed Evolution of RNA. *International Journal of Biochemistry and Cell Biology*. **2009**, 254–265.

(62) Flinders, J.; DeFina, S. C.; Brackett, D. M.; Baugh, C.; Wilson, C.; Dieckmann, T. Recognition of Planar and Nonplanar Ligands in the Malachite Green - RNA Aptamer Complex. *ChemBioChem* **2004**, *5* (1), 62–72.

(63) Lin, P.-H.; Chen, R.-H.; Lee, C.-H.; Chang, Y.; Chen, C.-S.; Chen, W.-Y. Studies of the Binding Mechanism between Aptamers and Thrombin by Circular Dichroism, Surface Plasmon Resonance and Isothermal Titration Calorimetry. *Colloids Surfaces B Biointerfaces* **2011**, *88* (2), 552–558.

(64) Lee, J.-H.; Canny, M. D.; De Erkenez, A.; Krilleke, D.; Ng, Y.-S.; Shima, D. T.; Pardi, A.; Jucker, F. A Therapeutic Aptamer Inhibits Angiogenesis by Specifically Targeting the Heparin Binding Domain of VEGF165. *Proc. Natl. Acad. Sci. U. S. A.* **2005**, *102* (52), 18902–18907.

(65) Win, M. N.; Klein, J. S.; Smolke, C. D. Codeine-Binding RNA Aptamers and Rapid Determination of Their Binding Constants Using a Direct Coupling Surface Plasmon Resonance Assay. *Nucleic Acids Res.* **2006**, *34* (19), 5670–5682.

(66) Sultan, Y.; Walsh, R.; Monreal, C.; DeRosa, M. C. Preparation of Functional Aptamer Films Using Layer-by-Layer Self-Assembly. *Biomacromolecules* **2009**, *10* (5), 1149–1154.

(67) Deng, Q.; German, I.; Buchanan, D.; Kennedy, R. T. Retention and Separation of Adenosine and Analogues by Affinity Chromatography with an Aptamer Stationary Phase. *Anal. Chem.* **2001**, *73* (22), 5415–5421.

(68) Hu, J. M.; Easley, C. J. A Simple and Rapid Approach for Measurement of Dissociation Constants of DNA Aptamers against Proteins and Small Molecules via Automated Microchip Electrophoresis. *Analyst* **2011**, *136* (17), 3461–3468.

(69) Cruz-Aguado, J. A.; Penner, G. Determination of Ochratoxin A with a DNA Aptamer. *J. Agric. Food Chem.* **2008**, *56* (22), 10456–10461.

(70) Potty, A. S. R.; Kourentzi, K.; Fang, H.; Jackson, G. W.; Zhang, X.; Legge, G. B.; Willson, R. C.

Biophysical Characterization of DNA Aptamer Interactions with Vascular Endothelial Growth Factor. *Biopolymers* **2009**, *91* (2), 145–156.

(71) Shi, Y.; Liu, Y.-L.; Lai, P.-Y.; Tseng, M.-J. M.-C.; Tseng, M.-J. M.-C.; Li, Y.; Chu, Y.-H. Ionic Liquids Promote PCR Amplification of DNA. *Chem. Commun.* **2012**, *48* (43), 5325.

(72) Huizenga, D. E.; Szostak, J. W. A DNA Aptamer That Binds Adenosine and ATP. *Biochemistry* **1995**, *34* (2), 656–665.

(73) Tateishi-Karimata, H.; Sugimoto, N. A-T Base Pairs Are More Stable than G-C Base Pairs in a Hydrated Ionic Liquid. *Angew. Chemie - Int. Ed.* **2012**, *51* (6), 1416–1419.

(74) Nakano, M.; Tateishi-Karimata, H.; Tanaka, S.; Sugimoto, N. Choline Ion Interactions with DNA Atoms Explain Unique Stabilization of A-T Base Pairs in DNA Duplexes: A Microscopic View. *J. Phys. Chem. B* **2014**, *118* (2), 379–389.

(75) Tateishi-Karimata, H.; Sugimoto, N. Structure, Stability and Behaviour of Nucleic Acids in Ionic Liquids. *Nucleic Acids Research*. **2014**, 8831–8844.

General Conclusions and Outlook

The main propose of this thesis was the study of the interactions of DNA and the function of a DNA-aptamer in presence of ILs with different physico-chemical properties, and it was mostly achieved.

As general conclusions, this research enabled to determine that the DNA structure was maintained and that a DNA-aptamer remained functional in the presence of a non-physiological environment containing ionic liquid.

The ILs sharing the same cation caused similar effects on the hybridization and stability of DNA, thus is the cation which plays the key role in the interaction with DNA via the negatively charged phosphate backbone of the latter. We also observed that the size of the cation is an important factor in the stability and hybridization of DNA. However, it was not possible to determine a pattern of interaction between the ionic liquids used and the DNA-aptamer beacon. Therefore the influence of the ILs on the MB function cannot directly be inferred from their effect on a dsDNA structure. Although the latter forms the stem of the MB hairpin, responsible for its dynamic function, the recognition pocket must be taken into account by being the main responsible for the recognition of the target. Consequently, it was concluded

that each system must be characterized independently, even if the ILs have common cations or anions.

It was determined that whether fluorescence is used as experimental method, based in a fluorophore-quencher system, the presence of ionic liquids in solution only affects the fluorescence emission when the fluorophore is free is solution. When the fluorophore is attached to a DNA sequence, the fluorescence remains constant independently on the IL and on the IL concentration used in solution. Thus we concluded that when a molecular beacon is used in an IL solution, as here, the fluorescence changes will only be due to the DNA structural changes.

Regarding SELEX, new DNA-aptamer sequences were obtained in presence of CL in solution showing that in principle this selection procedure might be also employed with non-conventional solution.

Thus, ILs are not all equally suitable for nanodevices involving DNA. Depending on the requirements of the system the ILs must be tuned according to the needs which can be achieved by choosing ILs with adequate physico-chemical properties.

The future perspectives for this work should start with the identification of the first ATP-aptamer selected in presence of CL (IL-aptamer) and its binding affinity

to ATP comparing with the aptamer selected in pure buffer. These binding studies could be performed by different techniques. However, since the use of ILs with techniques such as SPR or thermophoresis are not yet well established, we concluded that the most recommended method would be the radioactivity labeling, as used during the SELEX procedure. It would be also interesting to compare the binding behavior of the obtained DNA pools under cross over condition, meaning CL SELEX pool in buffer and buffer SELEX pool in CL solution. Depending on the results obtained from here, different procedures can be subsequently performed: use the final selected aptamer in systems with the presence of the ionic liquid CL; select new IL-aptamers specific for other targets in presence of CL; select new IL-aptamers specific for other targets in presence of ILs presenting other physico-chemical properties. This could bring advantages to select aptamers for targets with low buffer solubility and that its solubility increases with the presence of ILs in solution. The use of a pure IL solution is also a challenge for future research.

Annex

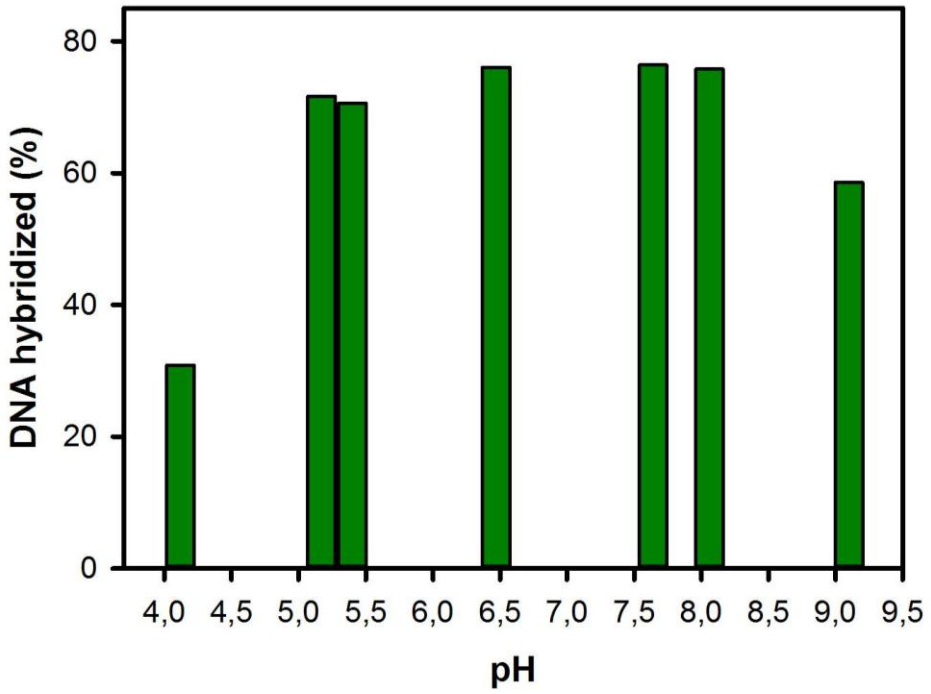

Figure A1. Amount of DNA hybridized in buffer solutions presenting different pH.

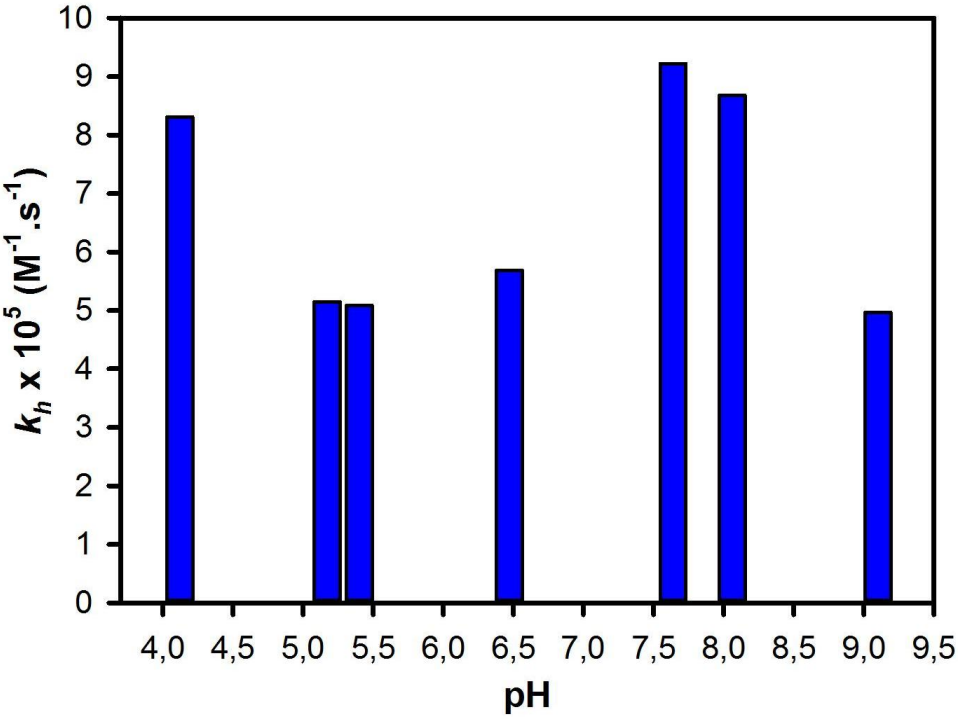

Figure A2. Hybridization rate of dsDNA formation in buffer solutions with different pH.